Traction Kite Testing and Aerodynamics

A thesis
submitted in partial fulfilment
of the requirements for the Degree
of
Doctor of Philosophy in Mechanical Engineering
in the
University of Canterbury

by

J.C. Stevenson, B.E.(Honours)

University of Canterbury
2003

ERING
ARY
59
847
2003

Abstract

A Traction kite is a controllable high performance kite used to pull other objects in a desired direction. In recent years Traction kites have been used for Kite Surfing and Kite Buggying, generating significant sales revenue. In conjunction with Peter Lynn Kites Ltd, this aim of this project was to develop testing methods to determine Traction kite performance. An additional aim was to lay the fundamental groundwork of kite theory to enable further research on kites.

The original testing method used a car-based test rig, in which kites were flown from the roof of the car while driving down a beach. By measuring each kite's line angle and tension under various conditions, the performance of each kite could be determined. Despite extensive development this method was only moderately successful. In particular, the tangent relationship between a kite's line angle and Lift to Drag ratio caused large experimental errors.

In light of the difficulties, a circular testing method was developed for testing Traction kites. It was found that if a kite was flown indoors, in a horizontal circle around the flyer, the performance of the kite was related to the geometry of the test setup. This method was far less sensitive to measurement erro 1 provided very good kite performance results. Unfortunately, this method is limited by the size of the required test site.

Investigations of kite theory determined that the stable flying location of a kite could be predicted and this led to other key flight characteristics. In particular, the structural requirements of a kite can be addressed and the initial turning properties of a kite can be determined.

18 NOV 2003

To Deborah

Acknowledgements

I would like to thank Dr Keith Alexander for supervising this project, and reading the draft of this thesis. His aid and direction during the course of the project were invaluable. I would also like to thank Dr Tony Bowen for his role as co-supervisor and for his help, especially with experimental work.

I would like to thank Peter Lynn Kites Ltd, and the staff working there, for running the project as a joint effort. Without the money, time, resources and experience they provided, this project would have been impossible. I would particularly like to thank Peter and Elwyn Lynn for having me stay in their home, their stimulating conversation, and gracing me with their hospitality.

I am very grateful to staff within the Department of Mechanical Engineering for helping me with the construction of various test rigs, and help with testing. In particular Paul Wells, Julian Phillips, Julian Murphy, Andy Cree, Eric Cox and Graeme Harris, Scott Amies and Ken Brown.

I am extremely grateful for the support given to me by all the members of my family during the course of this project. It has been fantastic.

Along with these people there are a large number of friends who have been a great help to me especially in the relaxation department. Thank you very much for the support that you have given over the years.

Contents

List of Figures and Tables

Figures

Tables

Symbols and Abbreviations

Note concerning subscripts – General subscripts have been outlined at the end of this section. However, for the purposes of clarity, some symbols with subscripts have been included in the main symbols list.

A	Wing area (m^2)
A_k	Nominal kite area (m^2)
AOA	Angle of attack
AR	Aspect Ratio
BL_f	Back-line force (N)
BL_{ang}	Back-line angle
BL%	Percentage back-line load
c	Chord length (m)
CD	Drag coefficient
CF	Lines' centrifugal force in circular testing
CL	Lift coefficient
COM	Centre of mass
COP	Centre of pressure
CT	Tension coefficient
CT_gVar	Variation in Tension coefficient
CX'	Force coefficient in X' direction
CY'	Force coefficient in Y' direction
CZ'	Force coefficient in Z' direction
D	Drag force (N)
D_g/D_k	Modifying factor for line load on car rig
D_{line}	Drag force on line in circular testing (N)

ds	Line segment (m)
D_t/D	Modifying factor for line load in circular testing
E, E'	Variables in line drag model
F	Force on kite (N)
F_d	Force driving vehicle forward (N)
$F_{x,y,z}$	Wing force in X, Y or Z direction (N)
$F_\perp$	Force perpendicular to line in circular testing (N)
FL_f	Front-line force (N)
FL_{ang}	Front-line angle
g	Gravity (m/s^2)
h	Height above the ground (m)
i	Unit vector in X direction
I_o	Rotational inertia around centre of mass
j	Unit vector in Y direction
J	Chapter 9 - construction vector Appendix IV - constant
k	Distance to line's inflexion point as a fraction of the line length
K	Construction vector
$K(\theta)$	Line drag perpendicular to line (N)
$K'(\theta)$	Line drag parallel to line (N)
L	Lift force (N)
L/D	Lift to Drag ratio of wing

L/L_h	Lift to Drag ratio modifying factor in circular testing, to adjust for mass of kite
(L-Mg)/D	Lift to Drag ratio of kite with mass in lift direction
(L-Mg)/L	Lift to Drag ratio modifying factor in circular testing, to put mass in direction of lift force
L_c/D	Lift to Drag ratio in circular testing, with line forces removed
L_c/L_t	Lift to Drag ratio modifying factor in circular testing, to adjust for line forces in 'lift' direction
L_h/D	Lift to Drag ratio in circular testing, with kite centrifugal force removed
L_h/L_c	Lift to Drag ratio modifying factor in circular testing, to adjust for kite's centrifugal force
L_{line}	Lift force on line in circular testing (N)
L_n	Construction vector
LTD	Lift to Drag ratio
L_t/D_t	Lift to Drag ratio from circular testing
m	Mass (kg)
M	Moment (Nm)
m_{line}	Line weight per unit length (kg/m)
MX', MY', MZ'	Moments at the kite's centre of mass around kite axes.
n	Number of lines Chapt 9 - normal vector
O	Constant
P	Chapt 9 - end point of structural member Appendix IV - angular acceleration matrix
R	Kite's flying radius in circular testing (m)
R_{ds}	Radius of line segment in circular testing (m)

r	Walking, or rig, radius in circular testing (m)
	Chapt 8 – radius between bridle and force (m)
	Chapt 9 - distance of disk elements from origin (m)
	Appendix IV - radius of centre of mass from bridle point (m)
r'	Modified r in circular testing with wind effects (m)
r_{cop}	Radius from disk's centre to force (m)
r_{wind}	'Radius' of wind in circular testing (m)
S	Line length (m)
	Chapt 9 – structural member of disk wing
S_{ds}	Line length to line segment (m)
T	Line tension (N)
T_c	Line tension in circular testing with line effects removed (N)
T_h	Line tension in circular testing with kite's centrifugal force removed (N)
T/T_h	Line tension modifying factor in circular testing for mass of kite
T_c/T_t	Line tension modifying factor in circular testing for line forces
T_h/T_c	Line tension modifying factor in circular testing for kite centrifugal force
T_k/T_h	Line tension modifying factor to put mass in lift direction
U	Construction vector
U_1, U_2	Line effect ratios
V	Wind velocity (m/s)
V_a	Apparent/relative wind speed (m/s)
V_{anem}	Natural wind velocity at the anemometer (m/s)
V_{ds}	Velocity at line segment (m/s)
V_f	Natural wind velocity at car as a fraction of car speed
V_{hk}	Natural wind speed at height of kite (m/s)

V_k	Velocity of the kite (m/s)
$V_{measure\text{-}rotating}$	Wind speed measured on rotating car test rig (m/s)
$V_{measure\text{-}nonrotating}$	Wind speed measured on non-rotating car test rig (m/s)
V_{mg}	Velocity made good (m/s)
V_w	Speed of circular test rig (m/s)
V_{wind}	Natural wind speed during circular testing (m/s)
V_∞	Natural wind speed beyond the boundary layer (m/s)
$V_\perp$	Velocity of the kite perpendicular to the line in circular testing (m/s)
w	Width (m)
W_1, W_2	Circular test rig geometry (m)
wt	Weight of line per unit length (N)
X	Cartesian co-ordinate
x	Chapt 1 - distance to centre of pressure from wing's leading edge (m)
	Chapt 6 - rig dimensions (m)
	Chapt 8 - bridle point location in X direction (m)
	Chapt 10 - X' distance of bridle from centre of kite (m)
X'	Wing co-ordinate
$x_1 \ldots x_6$	Force locations in X direction relative to the bridle point, in stability point analysis (m)
Y	Cartesian co-ordinate
y	Chapt 6 - rig dimensions (m)
	Chapt 8 - bridle point location (m)
Y'	Wing co-ordinate
$y_1 \ldots y_6$	Force locations in Y direction relative to the bridle point, in stability point analysis (m)
Z	Cartesian co-ordinate
Z'	Wing co-ordinate

α	Angle of attack
α_{sj}	Angle of attack of j^{th} structural member
α_v	Angle of attack of moving kite relative to V
β	Kite's performance angle
β_v	Angle between V_k and $V_\perp$ in wind affected circular testing models
ϕ	Line diameter (m)
	Appendix IV – angle of line from the kite's bridle point to its centre of mass relative to wind
γ	Vehicle direction relative to the wind
	Chapt 7 – Angle of kite line to Y axis in walking circular test model
φ	Wing's dihedral angle
λ	Line angle of kite relative to r during circular testing
λ'	Line angle of kite relative to r' during wind affected circular testing
μ	Angle of wind to the ground
θ	Line angle of kite, and wing forces, relative to wind direction
θ_{LTD}	Angle forces acting on kite wing relative to wind direction (Chapt 8)
θ_{COP_LTD}	Angle of line between bridle and wing's COP to wind direction (Chapt 8)
θ_x, θ_z, θ_z	Wing angle rotations around Cartesian axes
$\theta_1 \ldots \theta_8$	Chapt 6 – circular rig geometry
	Chapt 7 – wind affected circular testing geometry
ρ	Density (kg/m^3)
σ	Chapt 1 – angle between kite line and vehicle direction
	Chapt 2 – degree of twist in kite lines
ω	Angle between line and wind
ω_{ds}	Angle of line segment in circular testing
ψ	Angle between R and r in circular testing
Δt	Time interval (s)

Subscripts

anem	Anemometer properties
cent	Lines' centrifugal force component during circular testing
h	Properties at a distance h above the ground
n,i,j	Index
x,y,z	Properties in Cartesian co-ordinates
x',y',z'	Properties in kite co-ordinates
g	Kite properties at the ground
k	Kite properties at the bridle point
l	Line properties
m	Measured values
min	Minimum values
max	Maximum values
t	Circular testing properties
tot	Total properties
v	Craft or vehicle properties

1. Introduction

1.1 Introduction to Kites

Although kites have a relatively long history, they have been used in only a limited number of applications. Kites were invented in the east approximately fifteen hundred years ago and the idea was introduced to the west via the trade routes between the two regions (Hobbs, 1989). Despite their early invention kites have remained largely a leisure activity without being developed for other uses. Over the last three hundred years kites have been used in some research applications as shown in Table 1 (Hobbs, 1986) but the kites themselves generally had a role secondary to the research objectives. Typically kites were used to provide a stable aerial platform with which to do atmospheric experiments, so their performance, beyond stability, was relatively unimportant. The lack of practical applications means that the academic community has largely ignored kites as a valid research topic. However, the last thirty years has seen significant developments in the design of kites, and the need for research is becoming increasingly important.

Table 1 Kites as Research Tools

1740's	Alexander Wilson, England, uses a train of paper kites. In 1749 he uses them to lift thermometers for experiments.
1752	Benjamin Franklin, USA, uses a kite to show that lightning is electrical (taking sensible precautions).
1753	De Romas (France) performs electrical experiments with kites.
1762	Peter van Musschenbroek (Dutch physicist) publishes brief mathematical description of kite flight, having done several experiments.
1822	Sir William Parry and Rev. George Fisher uses kites to lift thermometers for measuring the temperature profile in the Artic – no temperature gradient is found.
1825-6	George Pocock uses steerable kites to tow carriages and for man-lifting. He publishes The Aeropleustic Art describing his work.
1835	Franklin Kite Club formed in Philadelphia, USA, to perform electrical experiments.
1841	J.P. Espy (Franklin Kite Club) publishes "The Philosophy of Storms", with kites used as an important tool for studying columnar clouds.
1847	W.R. Birt uses hexagonal kites at Kew Observatory to carry meteorological instruments.
1860-70's	Cleveland Abbe and Charles du Hauvel experiment with instrument carrying kites.

1883	E.D. Archibald introduces the use of steel piano wire for the kite line, and in 1887 he flies kites in tandem up to 1500 ft to carry anemometers, cameras, etc.
1885	Alexander McAdie carries out kite experiments at Blue Hill, USA. Under Lawrence Rotch, the Blue Hill Observatory becomes an important centre of meteorological research. Maillot man-lifting kite. France.
1888	Arthur Batut (France) starts using kites for aerial photography.
1891	William Eddy (USA) develops his bow kite, similar to the Malay.
1892	Lawrence Hargrave (Australia) introduces the Box Kite.
1895-6	Blue Hill Observatory and US Weather Bureau start using Hargrave kites.
1898	S.F. Cody starts work on kites, eventually developing the Cody War kite, and a reliable man-lifting system.
1898-1908	Alexander Graham Bell uses kites as the basis of his work to build an aeroplane; introduces the Tetrahedral kite.
1906	S.F. Cody appointed to post of Chief Kite Instructor at Farnborough.
1938-42	Royal Aircraft Establishment and National Physical Laboratory perform experiments into kite performance and stability to develop a kite barrage.
1940's	Paul Garber's Target kite in use by the US Navy.
1948	Francis Rogallo patents the Flexible kite, related to his parawing.
1950	William Allison patents the Sled, later improved by Frank Scott who added slots.
1964	Domina Jalbert introduces the parafoil design.
1976	Ray Meny and Andrew Jones first show the Flexifoil in public. C.F.Woodhouse and Ray Holland start using the TALA kite anemometer system.
1982	Jacob's Ladder captures the World Speed Sailing record in C class with 25.03 kt using kite traction.

Hobbs (1986)

The development of high performance Traction kites has significantly increased the scope of kite use. The flying location of a Traction kite can be controlled in order to pull another object in a desired direction. The Flexifoil, developed by Woodhouse and Holland (Hobbs 1986) was the first kite of this type. In the beginning Traction kites were primarily ram air structures, although recent kite designs utilise permanently inflated structures. For control purposes these kites have multiple lines, which can also be used to adjust the flying characteristics of the wing. Modern Traction kites were first used in high speed sailing applications but land-based activities developed where kites powered small three-wheeled buggies capable of speeds in excess of 100 km/h (Figure 1:1 (a)). At this point Traction kites began to gain popularity, with significant sales revenue generated from kites and their accessories. The most recent development has been the invention of Kite Surfing. In this sport a person uses a kite to power them on the water with a planing board attached to their feet as shown in Figure 1:1(b). Not only are Kite Surfers capable

of high speeds, but the ability of controllable kites to increase their apparent wind (see section 1.9) enables flyers to perform spectacular aerial manoeuvres. Kite surfing has been very successful and has enticed large numbers of new participants. Consequently, the Traction kite market is large and attracts numerous kite manufacturers with different kite designs.

(a) (b)

Figure 1:1 Kite Buggying and Kite Surfing

1.2 Research Goals

This research project has been run in conjunction with a New Zealand-based kite manufacturer, Peter Lynn Kites Ltd. Being able to effectively test kite performance is an important aspect of their research and development programme. Prior to this study it was difficult to accurately gauge the effect of design changes and a more analytical approach was needed to determine kite performance. The main task of this project was to develop testing methods suitable for a research and development operation of the scale of Peter Lynn Kites Ltd.

Kite flying is not limited to Traction kites but has broader appeal. Large kite festivals occur frequently worldwide, attracting large numbers of spectators and kite makers. This project aimed to contribute to the recreational use of kites by considering some of the fundamental characteristics of kites. It is hoped that this will enable kite flyers to better understand some of the crucial aspects of their kites' designs.

It is possible that kites will have uses beyond recreational. Possible applications vary from towing devices for ships, to providing stable platforms in the jet stream, on which electricity can be generated (i.e., Geola, 1979. Fletcher, 1983. Fletcher, Honan & Supuppo, 1983. Fletcher & Roberts, 1979. Riegler, Riedler & Horvath, 1983). Although, many of the suggested uses are far fetched, some of them are potentially useful applications. It is hoped that this project will provide some useful tools for broader kite development.

1.3 Definition of Kites

The following is a typical definition of a kite taken from the Merriam-Webster online dictionary (http://www.m-w.com/cgi-bin/dictionary).

[1]kite

Pronunciation: 'kIt

...

3 : a light frame covered usually with paper or cloth, often provided with a stabilizing tail, and designed to be flown in the air at the end of a long string

...

Compared to other dictionaries this is a fairly good definition as it identifies some of the physical characteristics of the kite, most notably the line. Unfortunately it is not rigorous enough to adequately define a kite.

For the purposes of this study, for an object to be called a kite it must have the following characteristics.

1. The object must have a tether that connects it to a stable platform. In most cases the tether is a string or line and the platform is the ground. However, the tether could also be a solid rod with three degrees of freedom at each end. Also, the 'stable platform' could equally be another moving vehicle such as a boat.

2. The object must have a lift force acting on it that pulls it away from the stable platform. In most cases this force is an aerodynamic lift force to pull the structure into the air. Buoyancy forces will also apply and in the case of an inverted kite, gravity forces will act in this way.

3. The object must be immersed in a moving fluid and therefore have a drag force acting on it. The fluid in this case is usually air.

The most important characteristic is the existence of the tether. This puts kites into a separate category from planes and free-flying gliders. Most authors have identified the tether as making kite dynamics both different and more difficult to analyse than planes (Bryant, Brown & Sweeting (1950), De Laurier (1970) and Hobbs (1985)) so the tether is what distinguishes a kite from other flying objects. Gliders under towing conditions would be defined as a kite.

1.4 Previous Research

The following is a brief summary of the past work on kites relating to this research topic. A more complete outline of past research on kites from Hobbs (1986) has been included in Appendix I as there has been very little addition since this time. Most of the research that has already been done is in areas beyond the scope of this thesis but those parts that are relevant are included in this section.

As already stated, the academic community has largely ignored kites due to the lack of practical applications. The little attention given can be divided into a few key areas. These areas are: kite hobbyist literature, stability calculations, anemometry and Parafoil design.

There is a wealth of books by kite hobbyists and enthusiasts but most of this is not of an academic nature. Books such as the Penguin Book of Kites (Pelham, 1976), while sometimes containing a brief section on some of the very basic physics involved, are more concerned with how to make kites. The advent of Traction kites has seen a few more books on the physics relating to high speed sailing (e.g., Van Veen, 1996) and much relevant analysis of this area can be found in sailing texts such as Marchaj (1979). The most academic work that looks at kite flying for its own sake is the work by Toshio Ito and Komura (1983) which outlines most of the key theory as well as trying to solve some of the more interesting kite flying issues. However, the text focuses on the centre of pressure migration of different wing surfaces, to the detriment of other characteristics, most notably the Lift to Drag ratio of the kite. It therefore fails to identify some of the key characteristics of kites but is still the most complete kite text at this point.

There is a large body of research focused on determining whether a kite will fly in a stable manner and therefore independently. The driving force behind this is the desire to use kites as a stable platform above the earth's surface. In particular, stable platforms are required to do atmospheric research (Hobbs, 1986, 1989) although there have been other uses. World War II and the need to defend British airspace saw research into kites (Bryant, Brown, Sweeting, 1942) and towed gliders. These studies determined the equations of motion of a kite and the conditions for a kite to be stable. They made some disturbing conclusions. The existence of the tether in kites adds an extra degree to the stability equations that govern planes, making kites more difficult to analyse. In general it was found that kites display the same modes of motion as planes and that these remain stable. However, the new modes introduced by the line are unstable. Unfortunately this problem increases in kites with higher Lift to Drag ratios therefore undermining attempts

to make a stable high performance kite. The discovery that the line is the main determinant of stability in a kite has dominated kite research since (De Laurier, 1972a,b and Kalikov, Nekrasov & Ordanovich, 1974).

Hobbs (1986) carried out the latest work that concentrated solely on kites. His research involved determining the best kite design for tasks such as kite anemometry. Along with this he also outlined how changes in the setup of the kite will alter its performance. Notably he outlined how a change in the bridle point will alter the height at which a kite will fly. Unfortunately he made some incorrect assumptions about the relationship between the line angle and the angle of attack which detracted from his results.

Although this previous work was mathematically complete it is not directly relevant to this research. Whereas this previous work focused on making the kite a stable platform so it could fly independently, Traction kites are controlled by the flyer and are therefore relatively immune to the necessity of long term stability. The other difficulty with the research to date is that it provides very few guidelines to kite designers on how to improve the performance of their kites. Much of the work is virtually impossible to apply in any concrete manner and well beyond the abilities of most, if not all, kite designers to understand.

The use of ram air structure in parachuting and paragliding applications has produced some interesting work that does relate to this research. Nicolaides and Tragarz (1971) performed some tests on the first ram air airfoils used for parachuting. Along with free flying drop tests they also towed the parachutes behind a vehicle in much the same way as was originally visualised for this testing procedure (see Chapter 2). Cook and Kilkenny (date unsure) used a car test rig for hanglider tests but these were not free flying. Paragliding has also seen attempts at analysis such as those performed by Babinsky (1999).

Despite the research outlined, kites, particularly homemade and high performance recreational kites have been largely unstudied. It is essential that the basics of kite theory are studied and communicated in a way that is relevant to the industry.

1.5 Aerodynamic Principals

Despite the distinction between kites and planes, kite aerodynamics rest heavily on classic aerodynamic definitions. In most cases kites have at least a vague aerodynamic shape and therefore are amenable to the use of traditional definitions. The following section outlines some of the basic aerodynamics necessary to understand kites. It will cover the geometry, orientation, and forces on different shapes immersed in a moving fluid. Figure 1:2 shows a typical aerofoil shape to aid this explanation.

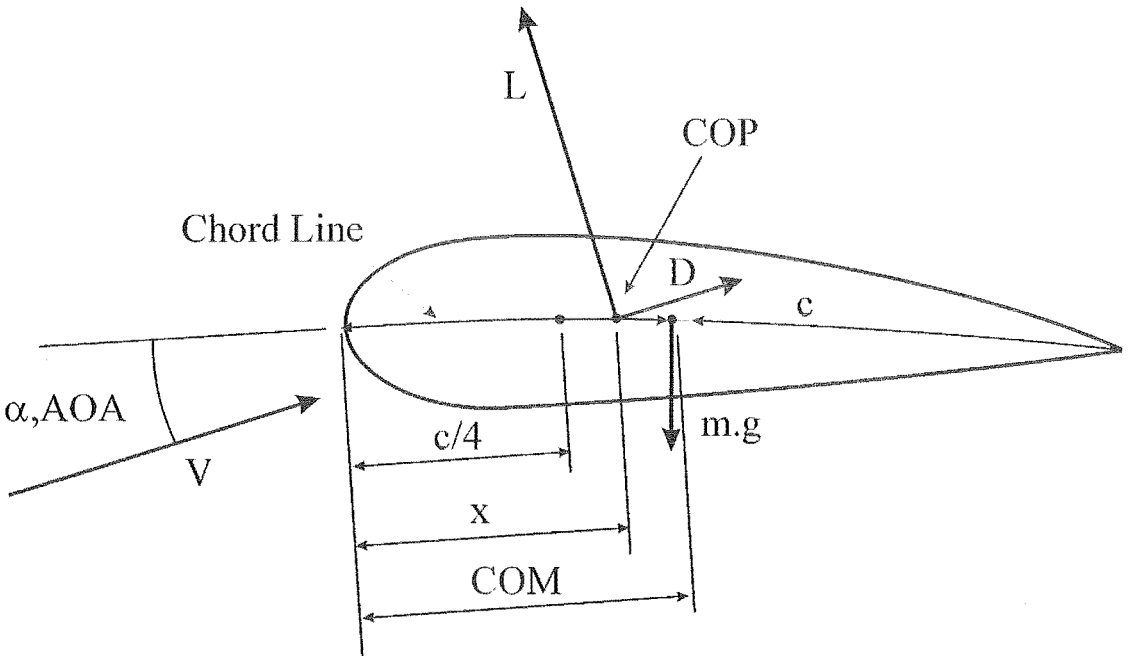

Figure 1:2 Aerofoil geometry and forces

First, the size of the wing is physically defined by its chord (c) and span (w). The chord is the distance from the front of the wing to the trailing edge. Along with this dimension a chord line is defined. The location of this line is arbitrary but conventionally it is located

equally between both the upper and lower surfaces of the aerofoil. One of the chord line's uses is to locate where the resultant lift and drag forces act along the wing and to provide a reference point for how their position changes. The other important dimension is the width, or span, (w) of the wing. This is used in conjunction with the chord to determine the area (A) and the aspect ratio (AR) of the wing.

The area of the wing affects the magnitude of the forces that act on it. Usually the projected area is required to determine the forces. If the wing is rectangular this area is defined as

$$A = c.w \qquad \textbf{Eq 1:1}$$

In most cases the wing is tapered so therefore more complicated methods are used to determine the projected area.

The aspect ratio is a ratio of the breadth to the chord length of the wing. To take into account the variability of the chord length along a wing's length, it is defined as

$$AR = \frac{w^2}{A} \qquad \textbf{Eq 1:2}$$

Varying the aspect ratio of the wing varies the performance that can be obtained. Due to end effects, a longer (high AR) wing will usually perform better than a shorter (low AR) wing with similar profiles. Therefore simply knowing the two-dimensional characteristics of an aerofoil is not sufficient to determine the performance of a three-dimensional wing.

Secondly, the aerofoil is orientated at an angle relative to the direction of the fluid that is moving over it. This is called the Angle of Attack (AOA or α) and is usually defined as between the wind and the chord line.

Thirdly, there are two aerodynamic forces, D and L, which act on the aerofoil both parallel and perpendicular to the airflow. These are called the Drag and Lift forces respectively and the magnitude and location of these forces depends on the AOA. The mechanisms through which these forces occur are beyond the scope of this research but are outlined in any good aerodynamics text. However, it is worth noting that these forces are a distributed load over the surface of the object and are presented as single forces for simplicity.

The magnitude of the force is a function of the area of the wing, fluid density (ρ), speed of the wing (V), and AOA. Using non dimensional analysis both the Lift and Drag values are converted to non dimensional Lift and Drag Coefficients (CL and CD) by the following formulas.

$$CL = \frac{L}{\frac{1}{2}\rho A V^2} \qquad \textbf{Eq 1:3}$$

and

$$CD = \frac{D}{\frac{1}{2}\rho A V^2} \qquad \textbf{Eq 1:4}$$

Note that the Lift and Drag forces are directly proportional to the velocity squared. Also in some cases the area in this formula appears as a chord dimension. This assumes that the breadth is only 1m and therefore is equivalent to above.

Along with a magnitude, these forces have a location at which they act on the aerodynamic surface. As already mentioned the chord line is arbitrarily created to help locate the forces. Where the forces act is called the centre of pressure (COP) and its location is expressed as a fraction of the chord.

$$COP = \frac{x}{c} \qquad \textbf{Eq 1:5}$$

As the AOA of the wing varies so will the COP.

The design of planes is more concerned with the moment caused by the combination of the magnitude and the location of the forces. A coefficient of moment (CM) is defined in a similar way to the definitions of CL and CD above.

$$CM = \frac{M}{\frac{1}{2}\rho A V^2 c} \qquad \textbf{Eq 1:6}$$

This method assumes that the Lift and Drag forces are located at the quarter chord (ie c/4) and to compensate for the COP migration, a moment (M) has to be applied at this point. Although this is a valid approach to take with kites, the location of the COP is important for describing many characteristics of kites, so it is used in this thesis.

Fifthly, all objects have a mass force (mg) acting on the wing. This force acts through the Centre of Mass (COM), which does not change location.

Another important aspect of a wing is its Lift to Drag ratio. The Lift to Drag ratio is defined as: the forces acting perpendicular to the wind divided by the forces acting parallel to the wind. Since the Lift and Drag coefficients vary with AOA the Lift to Drag ratio also varies. It will be shown in the following sections that the Lift to Drag ratio is effectively a measure of the performance of a kite.

1.6 Kite Geometry

Figure 1:3 shows a simplified kite structure that will be used extensively throughout this thesis. Kites vary from this form but most contain the key features shown.

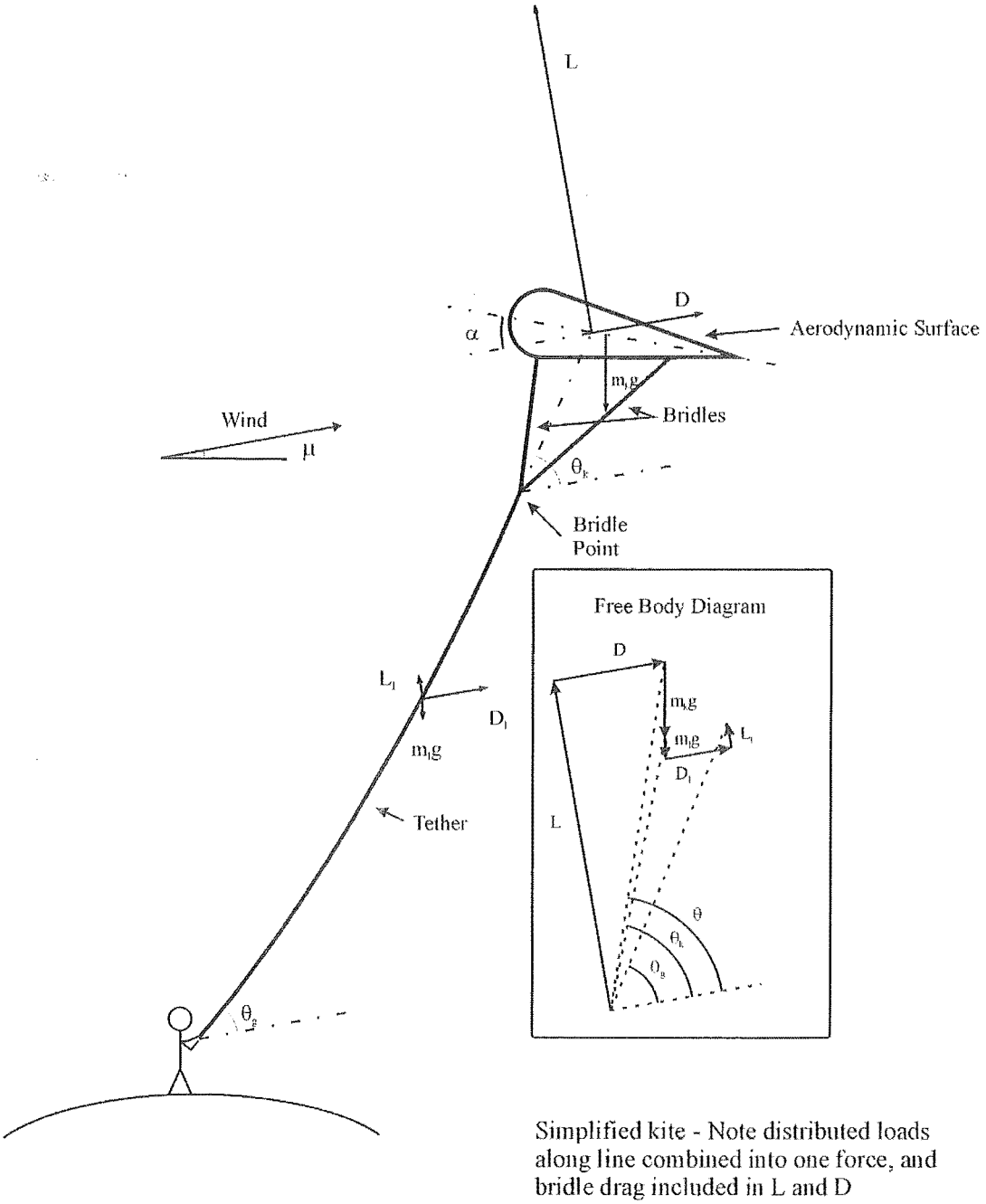

Figure 1:3 Basic kite structure

A kite must have a lifting surface of some kind. This lifting surface, or wing, must have all the components described in the previous section. Note that in Figure 1:3 the wind is at an angle μ to the ground. This can happen, particularly when flying a kite near trees or buildings. The distinction is important because the performance of the kite is determined

relative to the wind rather than to the ground. In most cases the difference between the two measurements will be insignificant.

The wing is attached to the tether through the bridle point. The location of the bridle point relative to the wing has a large influence on the flight of the kite. To be a bridle point, it must be used by the wing structure as a point of rotation when changing angle of attack, so must be suitably restrained so that this can happen.

The bridle lines run from the bridle point to the kite. These can be included as part of the aerodynamic surface or as separate entities. Each line has lift, drag and weight forces acting as a distributed load along its length. These contribute, usually in a negative way, to the performance of the kite. The bridle lines are also important in that they carry the forces on the kite to the tether. As traction kites become more developed, bridle lines are being eliminated with the loads being transferred to the tether through the structure of the kite.

The tether or kite line is a very important part of the kite. Like bridle lines the tether also has lift, drag and weight (L_l, D_l, $m_l g$) components acting along its length, and therefore affects the performance of the kite. The number of lines varies. Traditional kites usually have one line while most traction kites use four. Controllable kites use at least two lines with two-line stunt kites being particularly popular.

There are a number of important angles associated with kite physics. The Angle of Attack (AOA) of the wing has already been mentioned. This is the angle between the wind and the chord line and affects the performance of the kite. In practice this angle is difficult to measure when a kite is flying.

The Lift to Drag ratio is the most important measurement in kite flying and this ratio is related to some of the angles shown in Figure 1:3. In any kite there are at least three different measurements of Lift to Drag ratio. The first of these is the aerodynamic Lift to Drag and is defined as

$$\frac{L}{D} = \frac{CL}{CD} = \frac{Lift}{Drag} \qquad \textbf{Eq 1:7}$$

This corresponds to an angle θ, shown in the free body diagram in Figure 1:3, measured from the direction of the wind by the formula

$$\theta = \tan^{-1}\left(L/D\right) \qquad \textbf{Eq 1:8}$$

This is the aerodynamic Lift to Drag ratio of the wing surface only. This ratio is relatively unimportant in kites as it is not the ratio that flyers experience. It is also difficult to measure.

A more important Lift to Drag ratio is the Lift to Drag ratio of the kite (LTD_k) which is defined as

$$LTD_k = \frac{\sum Lift - \left(\sum m \cdot g\right)\cos(\mu)}{\sum Drag + \left(\sum m \cdot g\right)\sin(\mu)} \qquad \textbf{Eq 1:9}$$

When the direction of the wind is perpendicular to the earth's gravitational field this equation can be simplified to

$$LTD_k = \frac{\sum Lift - mg}{\sum Drag} \qquad \textbf{Eq 1:10}$$

This ratio only considers the forces above the bridle point. This is the Lift to Drag ratio of the kite if it is held at the bridle point or is flown on very short lines. This corresponds to angle θ_k by the formula

$$\theta_k = \tan^{-1}\left(LTD_k\right) \qquad \textbf{Eq 1:11}$$

If the kite was flown on very short lines θ_k is the angle that these lines would form with the wind. Unlike the L/D ratio this ratio changes with wind speed since the weight force is independent of wind speed.

Kites usually have a tethers of kite lines so another ratio that takes these into account must be defined. This is the Lift to Drag ratio at the ground (LTD_g) and is the easiest ratio to obtain by experimentation. It is defined in the same way as Eq 1:9 above except that now the force components include those of the tether. Likewise an angle of the tether to the wind θ_g can be found by the same formula as equation Eq 1:11 above.

1.7 Lift to Drag Ratio and High Speed Sailing

To understand the importance of the Lift to Drag ratio for determining kite performance it is necessary to demonstrate the relationship between kites and traditional sailing theory. Of particular interest is high speed sailing both in land and water based applications. This theory demonstrates the importance of the Lift to Drag ratio in limiting the maximum speeds that can be achieved by craft in any sailing direction. The following analysis has been taken from Marchaj (1976) but has been adapted to Traction kite applications.

Figure 1:3 and Eq 1:11 show that the azimuth angle (θ_g) that the line forms with the wind is directly related to the Lift to Drag ratio of the kite. When a kite is flying directly above the ground as in Figure 1:3, and is stable, the resultant force acts directly along the string. If the kite is controllable it can be manoeuvred so that it is flying parallel to the ground and positioned to the side of where the flyer is facing. Despite this reorientation the kite is effectively in the same configuration as before and the kite line still has the same angle to the wind[1]. A kite is not restricted to these two locations but can be positioned at any point on an arc around the flyer as shown in Figure 1:4. Adjusting the

[1] This is not absolutely correct as the mass of the kite acts in a different plane to the aerodynamic forces and therefore changing the kites Lift to Drag ratio slightly.

location of the kite on this arc varies the magnitude of the force that acts in the horizontal direction. This horizontal force can be used to propel a vehicle in the same way that a sail does.

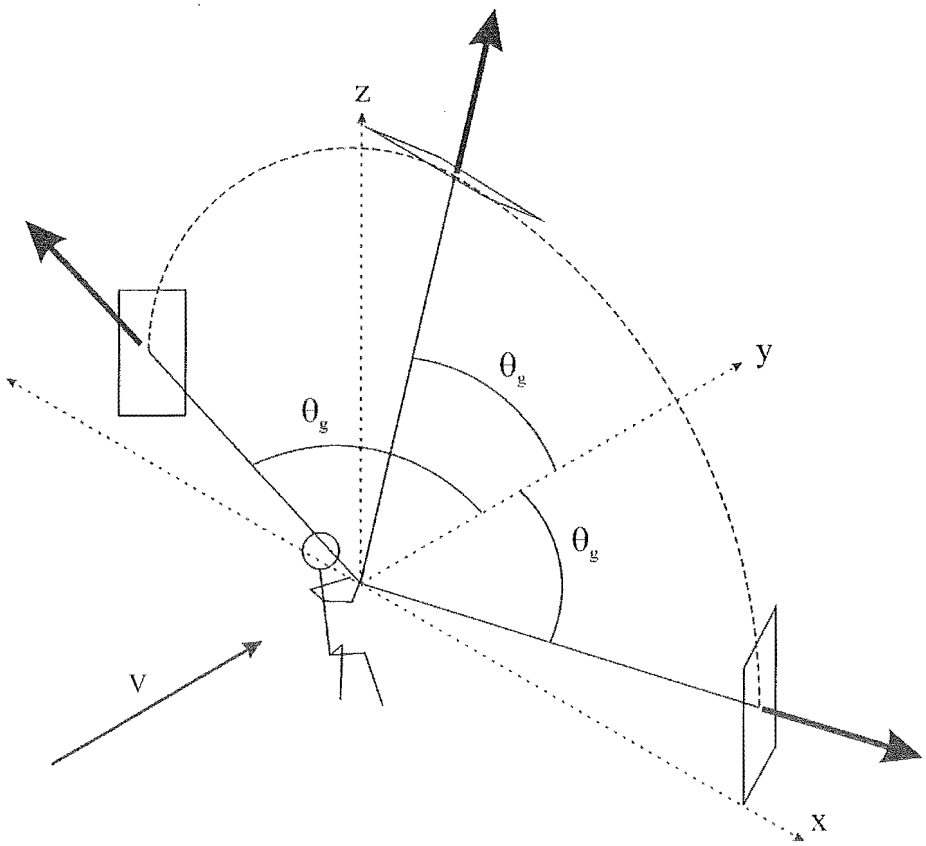

Figure 1:4 Stable flying positions of a controllable kite

To illustrate how a kite propels a vehicle, assume that the flyer is in a vehicle that can be directed in a set position and can resist sideways forces. The flyer is holding a kite with a certain performance characteristic so that the line is parallel to the ground. The speed and direction that a flyer can go are dependent on two angles: the angle between the wind and the line, θ, and the angle between the wind and the direction of the vehicle, γ. Figure 1:5 a,b & c illustrates these angles for three kites with different performance characteristics θ_1, θ_2 and θ_3.

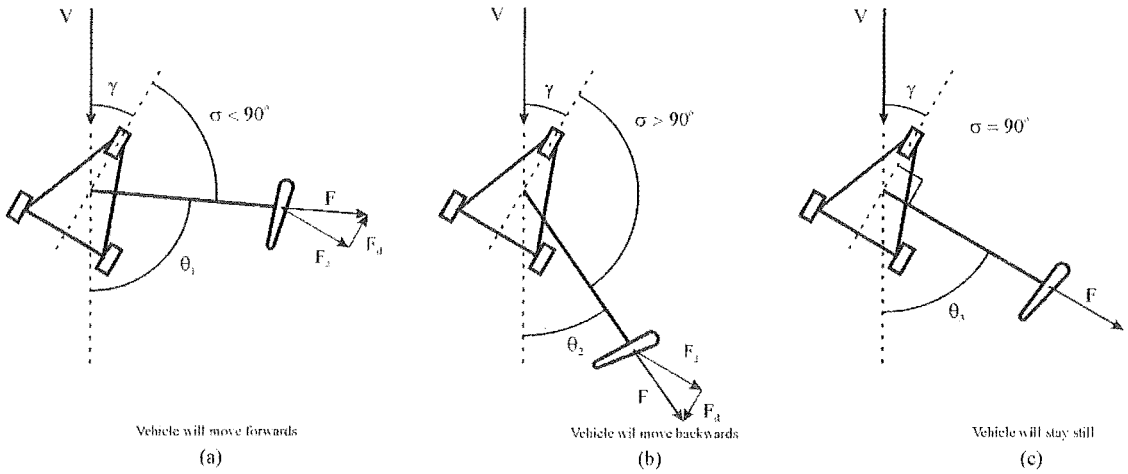

Figure 1:5 Forces acting on a stationary object

If the angle between the course that the flyer wished to go and the kite line (σ), is less than 90 degrees (Figure 1:5(a)) there will be a component of the force from the kite (F) in the direction that the flyer wishes to travel (F_d). Consequently the vehicle will move forward. If σ is greater than 90 degrees (Figure 1:5(b)) the kite will pull the flyer backwards. If σ is equal to 90 degrees the kite will have no effect either way. Therefore the maximum angle into the wind (γ) that the flyer can sail is related to the Lift to Drag ratio and therefore θ_g by the formula

$$\gamma \geq 90 - \theta_g \qquad \textbf{Eq 1:12}$$

Once the vehicle is moving the system is affected by the increase in apparent wind, V_a. Apparent wind is very important in high speed sailing situations as the vehicles being used usually have low drag component, which allows very high velocities to be obtained. Figure 1:6 shows that as the velocity of the craft increases, the magnitude and direction of the wind that the kite sees are affected. The kite has to respond to this change. Since the angle between the kite line and the apparent wind direction, θ, is fixed by the performance characteristics of the kite, the kite must change position relative to the vehicle to maintain this angle. However, the direction of the craft (γ) does not change, so the angle between it and the kite line (σ) moves towards the 90 degree point as the speed

increases. Once this point is reached the vehicle will stop accelerating since there is no force in the direction it wishes to go. This position is stable because if the craft gets accelerated the kite will move further back introducing a force to decelerate the craft, while if it gets slower the kite will move forward and accelerate the craft back to a stable speed.

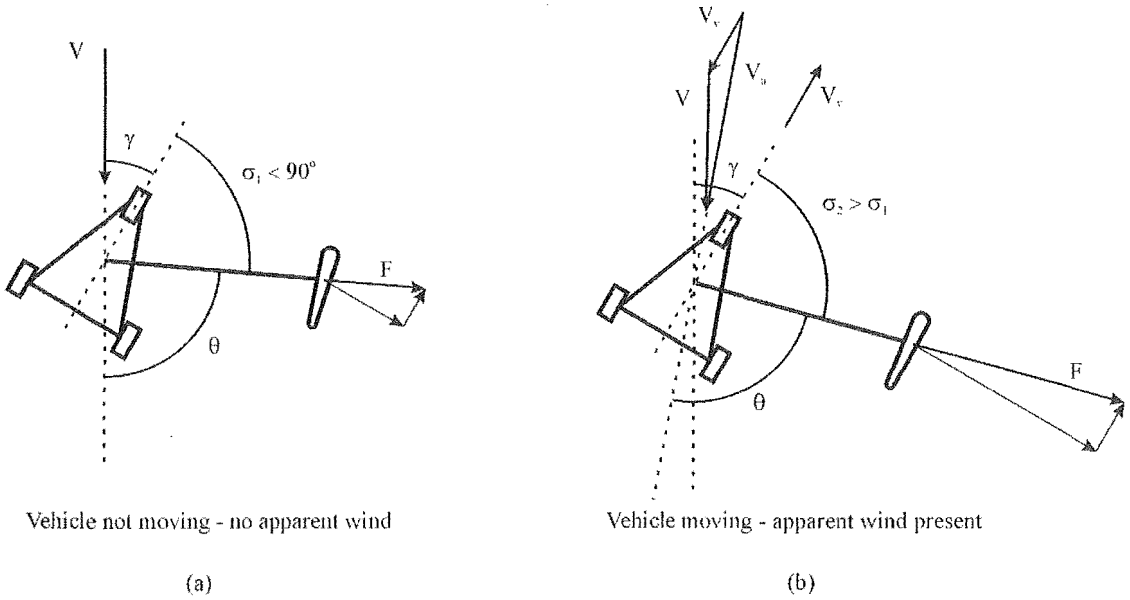

Figure 1:6 Apparent wind effects on sailing course

As the craft accelerates, the apparent wind speed increases, significantly affecting the forces on the kite. Because the aerodynamic force is a function of the velocity squared, these forces increase rapidly as the vehicle gets faster. This requires careful kite selection as the force on the kite may not be great when the vehicle is stationary, but could make resisting side slip and/or holding on to the kite very difficult when moving at high speeds.

Because of the effect of apparent wind, the maximum speed that can be obtained is dependent on the direction that the flyer wishes to go. As with all sailing there are three key directions that need to be determined: the optimal course into the wind, the optimal course downwind and the direction where the maximum speed can be obtained. When dealing with the upwind and downwind directions we are more concerned with the best

direction to sail to maximise the speeds directly into and away from the wind. This is called the velocity made good (V_{mg}) and is easily demonstrated using a polar diagram as in Figure 1:7. This shows the sailing characteristics of a kite/craft combination with a Lift to Drag ratio of 5.

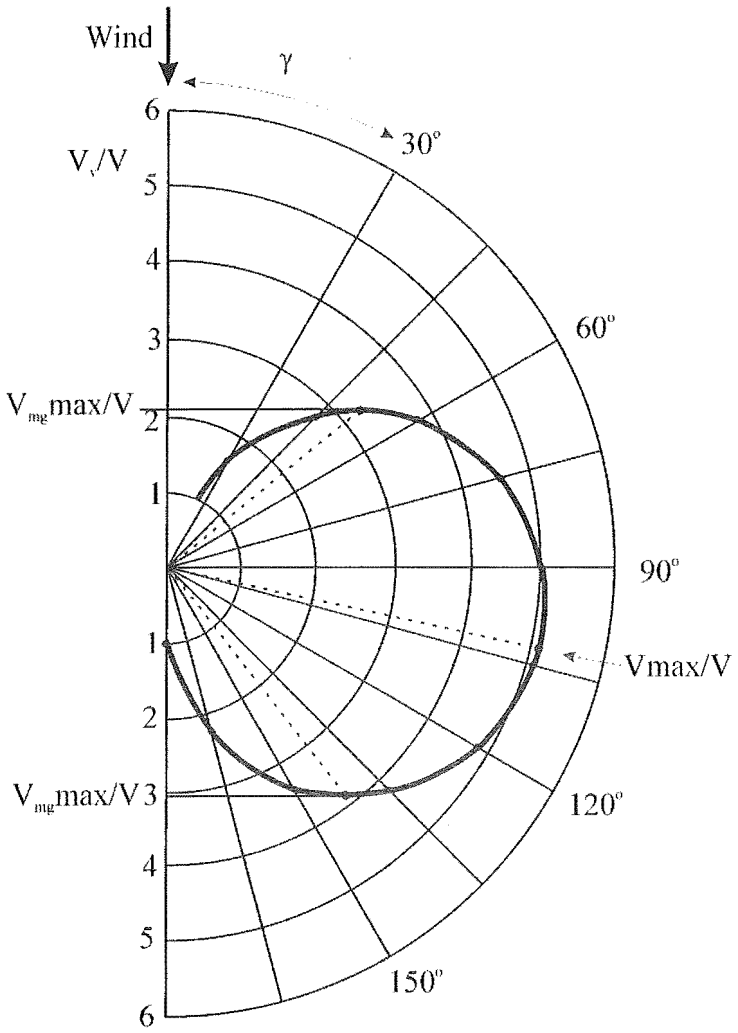

Figure 1:7 Polar diagram showing sailing speed in each direction for a Kite/Craft Lift to Drag ratio of 5

A polar diagram is a very useful tool in sailing as it shows multiple different attributes at once. First, it shows the speed of the craft for all the directions that can be sailed. Although it only shows 180°, the other half is simply a mirror image so is unnecessary.

Secondly, the vertical 0^{o} line is in the direction of the wind, and the speed scale shown on it is the velocity made good divided by the wind speed either upwind or downwind. Thirdly, the speed scale extends all the way around forming an arc so that the absolute speed of the craft as proportion of wind speed in all the sailing directions can be determined. The solid black curve represents this performance characteristic of the vehicle at all angles.

By drawing lines horizontally, tangentially to the curve, the optimal velocity made good upwind and downwind can be read off the vertical scale. By drawing a line from the origin to this tangent point, the sailing courses to obtain this optimal velocity made good can be found. By locating where the curve is furthest away from the origin, the maximum speed and sailing direction at which it occurs can be determined.

These curves, particularly in high speed applications, are primarily a function of the Lift to Drag ratio of the kite and vehicle combined. Although this project is mostly concerned with kites, obtaining optimal speeds is very dependent on the type of vehicle used. To combine the Lift to Drag ratio of the kite and vehicle together another angle, β, needs to be used. β is defined as

$$\beta = 90 - \theta = \tan^{-1}\left(\frac{1}{LTD}\right) \qquad \textbf{Eq 1:13}$$

The angle β for both the kite and the vehicle can then be combined to find the overall Lift to Drag ratio of the kite and craft by

$$\beta_{tot} = \beta_v + \beta_k \qquad \textbf{Eq 1:14}$$

The following is the formula that determines both the optimal speeds and directions as shown in Figure 1:7. The maximum velocity made good into the wind is

$$\frac{V_{mg}\,\max}{V} = \frac{1}{2}\left(\frac{1}{\sin\beta_{tot}} - 1\right) \qquad \textbf{Eq 1:15}$$

And this occurs at

$$\gamma = 45^{0} + \beta_{tot}/2 \qquad \textbf{Eq 1:16}$$

while the maximum velocity made good downwind is

$$\frac{V_{mg}\,\max}{V} = \frac{1}{2}\left(\frac{1}{\sin\beta_{tot}} + 1\right) \qquad \textbf{Eq 1:17}$$

and this occurs at

$$\gamma = 135^{0} + \beta_{tot}/2 \qquad \textbf{Eq 1:18}$$

The maximum speed that can be achieved is

$$\frac{V_{v}}{V_{\max}} = \frac{1}{\sin\beta_{tot}} \qquad \textbf{Eq 1:19}$$

and does not occur at ninety degrees to the wind, as most people assume, but at an angle slightly more than this. The angle is

$$\gamma = 90^{0} + \beta_{tot} \qquad \textbf{Eq 1:20}$$

Since Eq 1:13 to Eq 1:20 are all function of the Lift to Drag ratio they demonstrate why this ratio determines a kite's performance. There are other aspects of a kite which need to be taken into account but the Lift to Drag ratio determines the upper limit of what a kite can achieve.

1.8 Lift Coefficient and Performance

A kite's Lift to Drag ratio is an important performance measurement, but it is also necessary to consider a kite's Lift Coefficient. As outlined in section 1.5 the Lift Coefficient is the amount of wing force acting perpendicular to the wind direction, scaled by the fluid density, wind velocity and the area of the kite. Essentially, the larger the Lift Coefficient is the more 'pull' per unit area can be obtained.

The Lift Coefficient is important in kites for a number of reasons. First, in general, smaller kites are more responsive than larger kites. Therefore, the smaller a kite is for a given 'pull' the more control a flyer will have over how the kite behaves. Secondly, the large increase in apparent wind when using kites requires that the kite 'pull' be carefully selected. It is no use having a kite with a large Lift Coefficient and not being able to restrain it at high speed. Therefore, when measuring the performance of kites both the Lift to Drag ratio and the Lift Coefficient must be measured.

1.9 Why Use Kites?

Based on the previous section it is obvious that sailing speed is a function of the total Lift to Drag ratio of the craft and kite. Since a normal sail has a higher Lift to Drag ratio than a very good kite the obvious question to ask is why a kite would be used over a sail to propel a craft? Apart from the novelty value that kites have there are two main reasons to use a kite

1. The ability to reduce heeling moment on the craft by using a kite
2. Kites apparent wind capabilities.

The major advantage that kites have over sails is that they allow high performance, low drag, craft to be used. Figure 1:8 shows how the heeling force acting on a boat can be reduced by using a kite. With a sail the force acts through a point above the boat requiring either a large weight, in the form of a keel, to keep the boat upright or the use of

multiple hulls. Achieving stability in this way significantly reduces the Lift to Drag ratio of the craft. With a kite the tether can be located so that the force produces no or very little heeling moment. Since the craft no longer needs to resist the heeling moment its appendages can be kept to a minimum significantly increasing the Lift to Drag ratio of the craft. Since the total Lift to Drag ratio is a combination of the 'sail' and the craft the fact that kites have a lower Lift to Drag ratio than sails is more than offset by the increases in performance of the craft.

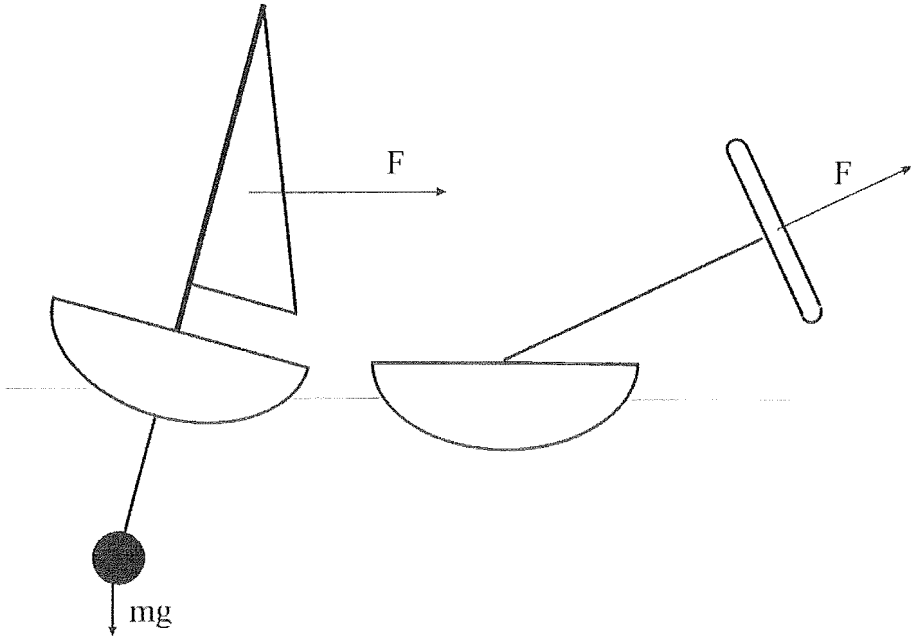

Figure 1:8 Forces acting through sail and kite

The other major advantage that kites have is the ability to increase the apparent wind of the kite independently of the motion of the craft. Since Traction kites can be controlled, they can be flown around in the air thereby increasing their apparent wind and the force they produce. Although the performance of the kite, in the direction the craft wishes to go, is sacrificed when the kite is flown around, the increase in force can have useful purposes. In particular, a large force may be required to get the craft to a speed where planing occurs. A large kite cannot always be used to provide a large initial force since when the craft is at optimal speed the forces on the kite may be too large for the craft to

resist. Instead, by increasing the apparent wind a smaller kite can be used to get the craft going and then the kite can be held steady once the craft is at a suitable velocity. Kite surfers can also use a temporary increase in apparent wind to do jumps. This gives kite surfing an aerial component that other sailing-based sports do not have.

1.10 Outline of Report

This report is divided into two sections.

- The first section covers the two testing methods developed for traction kites. The first of these testing methods is the car based test rig and the development of the rig and the limitations of this method are outlined. The report also presents some of the results that were obtained using this rig. The second testing method is the rotating test rig that was developed in light of the difficulties with the car-mounted test rig. The method is fully described and the preliminary test performed to verify this method are documented.
- The second section outlines some parts of fundamental kite theory developed. The particular areas covered are: determining of a kite's stability point, predicting the properties of complicated kite structures using disks, and the fundamentals of kite turning.

2. Car Test Rig

2.1 Summary

The original design brief for this project was to design and build a car-mounted rig to test the performance of Traction kites. Both the frame and the instrumentation of the initial test rig underwent number of different design iterations. The frame developed from a triangulated, rotational structure mounted on the front of the car to a non-rotational fixed structure mounted on the roof of the car. The most important part of the instrumentation was found to be the angle guides. These went through a number of design changes to improve the reliability of the results.

The repeatability of the results from the test rig was found to be $\pm 0.8^{o}$ on the angle guides and $\pm 15\%$ for the Lift Coefficient. The accuracy of the angle measurement has a large impact on the accuracy of the Lift to Drag ratio measurement due to the tangent relationship between the line angle and the Lift to Drag ratio. This proved to be the major limitation of this testing method. Although the errors in the Lift Coefficient readings were relatively high the test rig was still able to determine trends in this data.

After several modifications it was decided that further improvements of the testing equipment would not significantly alter the accuracy of the measurements. Very accurate readings would be difficult to obtain using this method even in ideal conditions, let alone in an outdoor test performed on a beach.

2.2 Introduction

2.2.1 Test Rig Background

This project began as a Graduate Research in Industry Fellowship (GRIF) Scholarship. The project was a joint research effort between Peter Lynn Kites Ltd based in Ashburton, New Zealand and the Mechanical Engineering department at Canterbury University, Christchurch, New Zealand. Peter Lynn Kites Ltd required a test rig for determining the performance of their traction kites. In particular they wanted to know if design changes they made were beneficial to the performance of their kites.

2.2.2 Performance Measurements

The following are the desired measurements that were either required or would be beneficial for kite design

1. The kite's Lift to Drag ratio. Chapter 1 outlines a number of different Lift to Drag ratio definitions. The Lift to Drag ratio of interest was the LTD_k. It was envisaged that the kites would be flown off short control lines (3-4m) and that the Lift to Drag ratio would be determined by measuring the line angle as shown in Chapter 1.
2. The kite's Lift and Drag Coefficient (CL and CD). This measurement would indicate whether the force of the kite could be varied by the flyer providing some 'Power Control' capabilities. To measure CL and CD the tension in the line was required.
3. Luff Resistance of the kite – or the ability of the kite to respond to variations in wind direction. (see section 2.2.4 for a full description)

2.2.3 Testing Methods in Use

Up until this point Peter Lynn Kites Ltd had no comprehensive method for determining the performance of kites. Testing methods ranged from sighting up the kite line, and determining its angle relative to the wind, to comparing the performance of two flyers of

similar ability in a race. Although these techniques can be effective they did not give a reliable performance characteristic for each kite.

Using a wind tunnel to test kites was not feasible for Peter Lynn Kites Ltd for a number of reasons. First, a kite's performance is related to both the shape and the dynamic response of the kite's surface in the wind. As kites are scaled in size these dynamics change considerably, and the kite will not necessarily perform in the same way. Secondly, modern Traction kites need to be flown on lines so that they will have the correct shape. Only having the wing in the wind tunnel would not take into account the variation in the width of the bridle point with different conditions. Since Traction kites can be up to $20m^2$ and fly on lines greater than 10m in length, these two characteristics require a very large wind tunnel to test kites. Facilities of this kind were beyond the capabilities of Peter Lynn Kites Ltd.

2.2.4 Initial Design Requirements

It was envisaged that the test rig would be attached to a car or some other powered vehicle. This car would then be driven to a suitable site and the kite flown above it. By measuring the angle of the lines relative to the wind the, Lift to Drag ratio of the kite could be obtained. If the line load could also be measured, the aerodynamic coefficients could be determined. Varying the speed of the car would indicate how these characteristics changed with wind speed.

Determining the Luff Resistance of a kite was considered a more difficult proposition than the first two performance measurements. Luff Resistance is a measure of a kite's ability to fly while experiencing rapid changes in the direction of the wind. Of particular importance is the kite's ability to recover and keep flying if the angle of attack is less than 0^{o}. Finding a method to test this is difficult especially when the other two performance measurements are taken at the same time. Eventually it was decided that the initial design would concentrate on determining the Lift to Drag ratio and the aerodynamic coefficients of the kite and that determining Luff Resistance would be re-evaluated after reliable data in these areas could be obtained.

The following is a list of key requirements in the design of the test rig

1. The rig must obtain accurate measurements of the kites Lift to Drag ratio , CL and CD.
2. The test rig must test at speeds up to 100km/h.
3. The test rig must be able to withstand a peak load of 300kg. which was anticipated to occur if a kite breaks at full speed.
4. The maximum width between the kite line attachment points must be 6m while the maximum distance between the front and the back lines must be 2m.
5. The test rig must rotate to face into the direction of the natural wind.
6. The test rig must be able to test 2 line and 4 line kites.
7. The rig must be able to be attached to a car and be able to be removed quickly when required.
8. One person must be able to perform the test.
9. The kite must be controllable while flying.
10. The testing method must be repeatable.
11. The testing method must be quick and as straightforward as possible.
12. The rig must be made of stainless steel to avoid corrosion.
13. The test rig must use as few load cells as possible, as they are expensive.
14. Appropriate data collection and transfer systems must be installed.
15. The method used must be achievable for an operation the size of the Ashburton facilities.

2.3 Initial Design Solution

The initial design solution focused on two main problems. First, how to take the require measurements while the kite was flying, and secondly, how to build the rig strong enough while having the rig rotate under the design loads at wide attachment points? At the beginning of the project it was unclear what the major difficulties would be during the

tests. It was decided to build a usable rig and simplify it later after experience was obtained in the testing procedure.

The crucial step in resolving the first problem was determining how to obtain the required measurements with the least number of instruments. In particular the number of load cells needed to be kept to a minimum due to their high expense. There were also only eight data collection channels available in the data acquisition system (see section 2.7.1), restricting the total number of measurements that could be taken.

A schematic of the angle and load measurement system and the control mechanism used in the test rig is shown in Figure 2:1. For simplicity it was decided that only two lines would be used to adjust the kite during a test. In the case of four-line kites only the back lines would be controlled. The rig was primarily based around four-line kites rather than two because traction kite design had moved away from two-line kites toward four line kites in the time that project started. Because of this it was not anticipated that there would be a great demand for two-line testing.

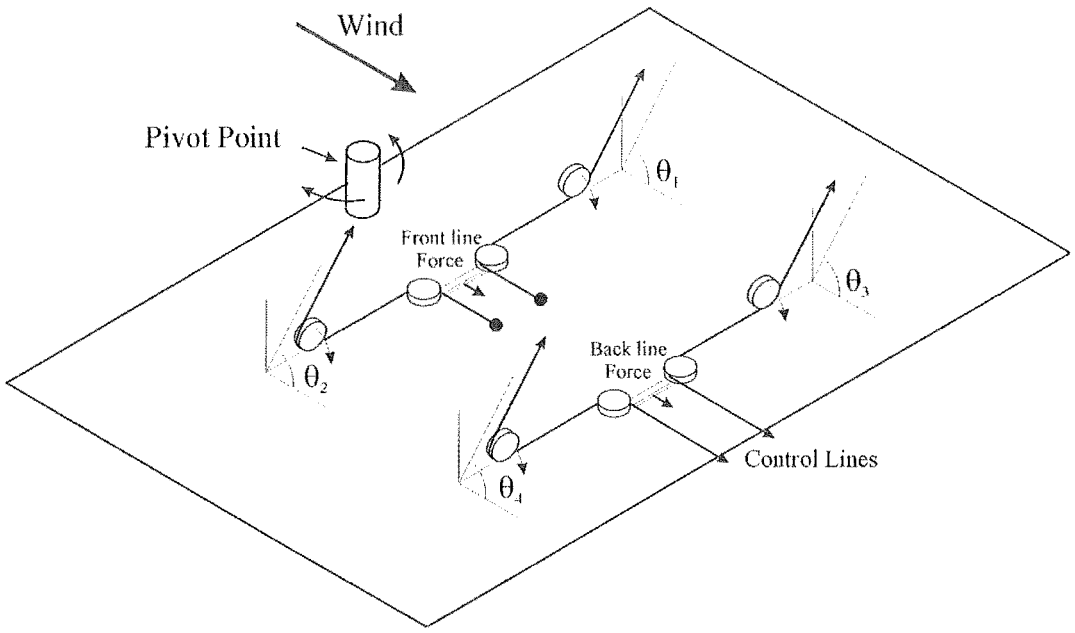

Figure 2:1 Measurement schematic

This essence of this method for obtaining the measurements worked well and was largely retained throughout the further developments.

To obtain the required measurements each line goes through two pulleys. Once the line has left the kite, the line goes though the first pulley and makes a 90^{o} turn perpendicular to the wind direction. This pulley is hinged so it can rotate to allow the line angle , θ, to be measured. This measurement is found by attaching a variable resistance potentiometer to the pulley shaft. The line then heads to another pulley where it goes through another 90^{o} bend. This pulley is attached to a pivoted arm along with the corresponding pulley from the opposing line. This arm is then attached to a load cell to record the tension in both lines. The front lines then go to a termination point while the back lines go to the inside of the car for control purposes. In the case of two line kites only the 'back lines' are used.

The second problem was to design a frame strong enough to withstand the forces from the kite. The main concern was designing the frame to rotate while withstanding the design loads occurring at the wide attachment points. The solution was to make the frame triangulated to restrict the bending forces on the frame components. A schematic of the frame is shown in Figure 2:2.

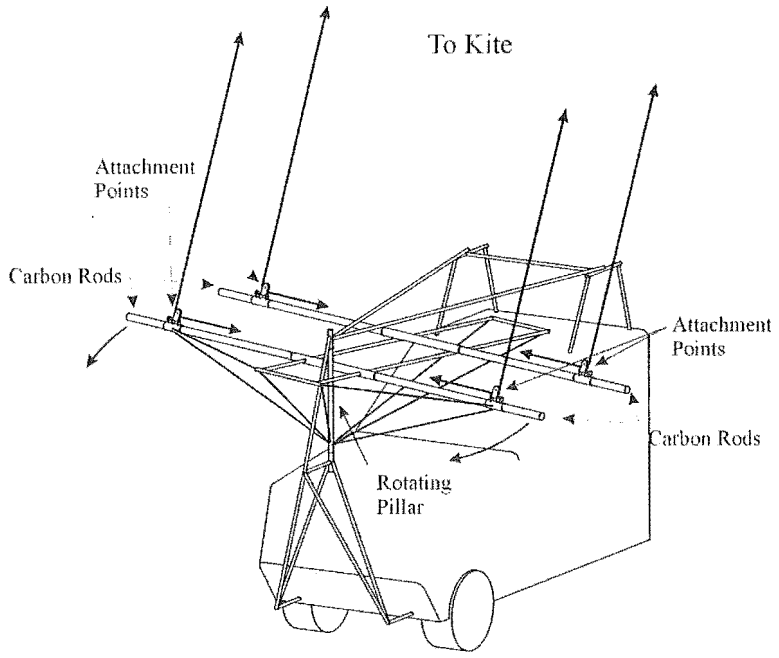

Figure 2:2 First test rig

The central part of the frame is a rotating pillar located near the front of the frame. This pillar is located by bearings at each end that allow it to rotate. These bearings are kept in place by a triangulated structure which transmits the loads on this pillar from the kite to mounting lugs underneath the front of the car and to the roof. Attached to this rotating pillar is a cross piece into which carbon fibre rods are inserted, and a set of rails onto which the attachment for the back line rods are located. The attachment points can be moved along these carbon fibre rods to vary the bridle width. The rails are used to vary the distance between the front and back lines. Rigging was used on the front attachment points to transfer the load directly to the bearing housing thereby keeping the front carbon fibre rods in compression rather than bending.

2.3.1 Testing Location

A suitable location to perform the tests was found at Pines Beach, 30km north of Christchurch. This sand-based beach is over 20km long and often has conditions suitable for the kite testing.

2.4 Theoretical Limitations of Method and Changes to Initial Design Solution

Once this rig was completed significant experience was obtained in the testing process and areas for improvement identified. This led to a comprehensive re-working of some areas and a step by step development of others. It also became apparent that there were significant limitations on the results that could be obtained using this testing method. The following is an outline of the key developments and theoretical limitations of the method.

2.4.1 Angle measurements

It became obvious that obtaining an accurate measurement of the line angle was not only important to the viability of the test method but also difficult to do. The accuracy of the angle was important because the Lift to Drag ratio is related to the tangent of the line angle. Because the tangent function is asymptotic near 90°, and good Traction kites fly between 75-85°, any variation in the angle causes a very large change in the Lift to Drag ratio that is measured (see Figure 2:3). Obtaining a reliable and accurate angle measurement on the original rig was virtually impossible, prompting a number of design changes. Section 2.5 describes the design stages to improve the angle guides to the point where a degree of confidence in the results was obtained.

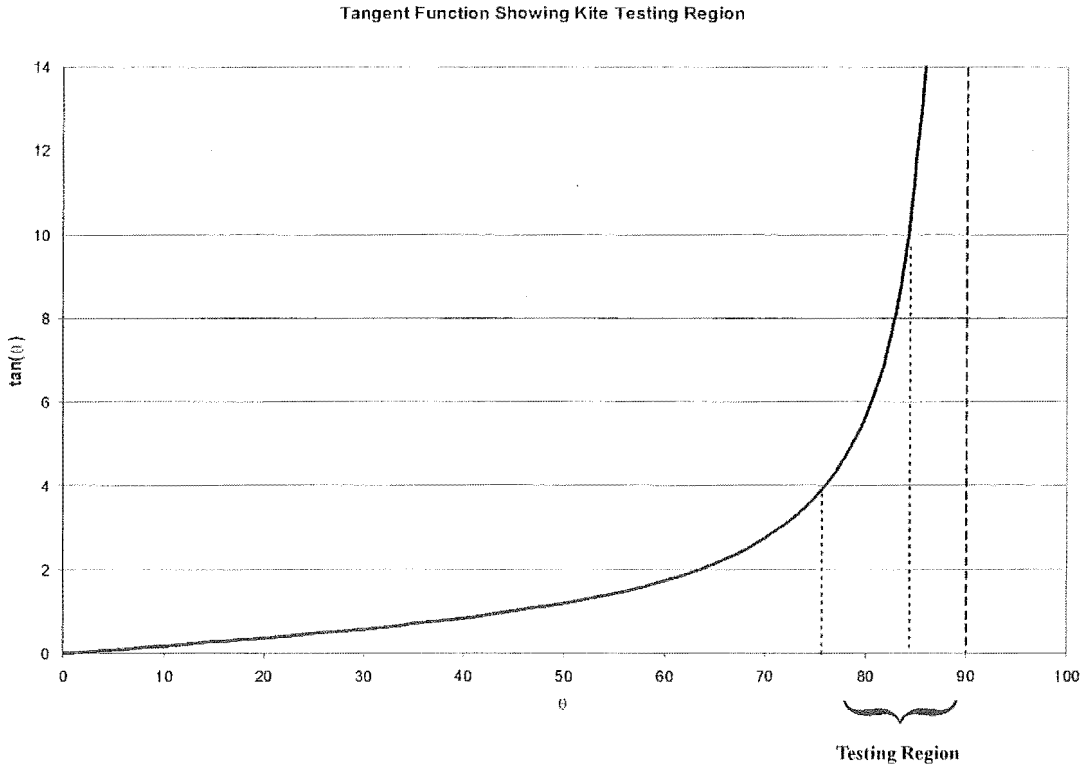

Figure 2:3 Effect of tangent function on measurements

2.4.2 Rotating or Not Rotating

It was originally thought that the rig should be able to rotate, enabling the kite to point into the direction of the apparent wind. Since there will always being some natural wind, the actual direction of the wind the kite sees is not the same as the direction of the test vehicle. However, it was eventually decided that it was best to eliminate the rotating component of the rig for the following reasons.

1. Having the rig rotate made it very difficult to measure the angle of the line with any degree of accuracy. To do this the rotating table would have to be accurately positioned so that it moved in the plane of the car. This is very difficult to do and is virtually impossible when the rig has to be taken on and off the car at regular intervals. Making the structure rigid enough to obtain accurate angle readings was also hard with a rotating rig.

2. Surprisingly, it was more difficult to get the kite to fly in a stable manner when the rig rotated. When the rig was fixed the kite maintained its location far better than when it was able to rotate. This was perhaps the most important reason for eliminating the rotation.
3. Since natural wind increased the errors on the rig and also tended to increase the instability of the kite, testing was only performed when the natural wind speed was less than 15 km/h or a more preferable 10km/h. Low natural wind speeds limited the need for the rig to rotate.
4. Having a rotating rig increased the set up time and made it almost impossible for one person to perform the tests.

It was apparent that eliminating the rotating nature of the rig would make the testing procedure easier and more reliable so a fixed rig was designed. Section 2.6 has a full description of the final rig design.

2.4.3 Errors due to natural wind

It was realised that the presence of natural wind while testing was going to increase the experimental errors. The first source of error was due to the height difference between the kite and the anemometer. Because of the boundary layer effect the natural wind will be stronger at the height of the kite than at the anemometer located at the car. To determine what this error it was assumed that the velocity varies with height according to Blasius's $1/7^{th}$ power law, which is

$$V_h = V_\infty \frac{1}{7} h^{1/3} \qquad \textbf{Eq 2:1}$$

where V_∞ is the natural wind speed beyond the boundary layer, h is the height above the ground, and V_h is the wind speed at height h. Therefore if we know the natural wind speed at the height of the anemometer (V_{anem}), the wind speed at the height of the kite (V_{hk}) is approximately

$$V_{hk} = \frac{V_{anem}}{(h_{anem})^{1/3}} \cdot h_k^{1/3} \qquad \textbf{Eq 2:2}$$

Figure 2:4 shows the effect that this velocity profile has on the measurement taken when the natural wind is coming from an angle γ to the direction of the car.

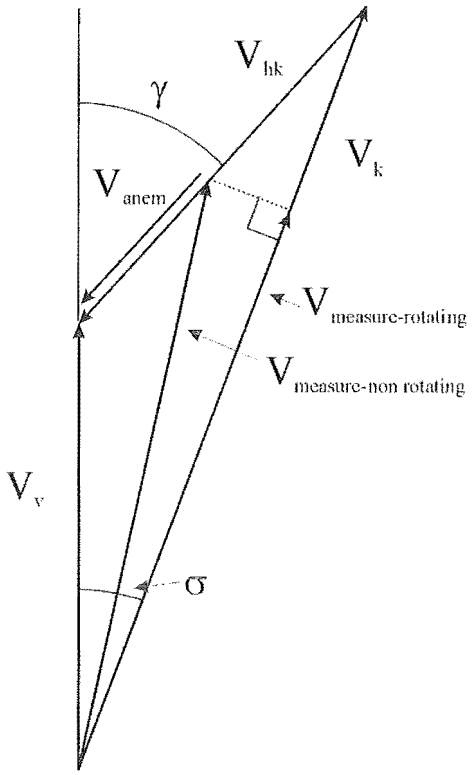

Figure 2:4 Natural wind effects on measurements

Two velocity measurements are shown in Figure 2:4. $V_{measure\text{-}rotating}$ is the anemometer reading at the height of the car if the anemometer is directionally dependent and is attached to the rotating part of the rig. $V_{measure\text{-}non\ rotating}$ is the anemometer reading if the anemometer is not directionally dependent. Since it was decided to remove the rotating nature of the rig the effect of the natural wind using $V_{measure\text{-}non\ rotating}$ will be shown.

The error in the wind speed measurement can be found as a function of the wind speed at the height of the car (V_{anem}) as a proportion of car speed (V_v). This ratio is defined as

$$V_f = \frac{V_{anem}}{V_v} \qquad \textbf{Eq 2:3}$$

From Figure 2:4 and using Eq 2:2 and Eq 2:3, using the cosine rule, the ratio between the wind speed at the kite (V_k) and the measured wind speed (V_m) is

$$\frac{V_k}{V_m} = \frac{\sqrt{1+\left(\frac{(V_f)h_k^{1/3}}{h_{anem}^{1/3}}\right)^2 - 2\frac{(V_f)h_k^{1/3}}{h_{anem}^{1/3}}\cos(180-\gamma)}}{\sqrt{1+(V_f)^2 - 2(V_f)\cos(180-\gamma)}} \qquad \textbf{Eq 2:4}$$

Using this formula the measurement error can be estimated for varying wind angles (γ) and V_f. Figure 2:5 shows the variation in the error with direction and strength for a kite on 10m lines and the anemometer at 2m.

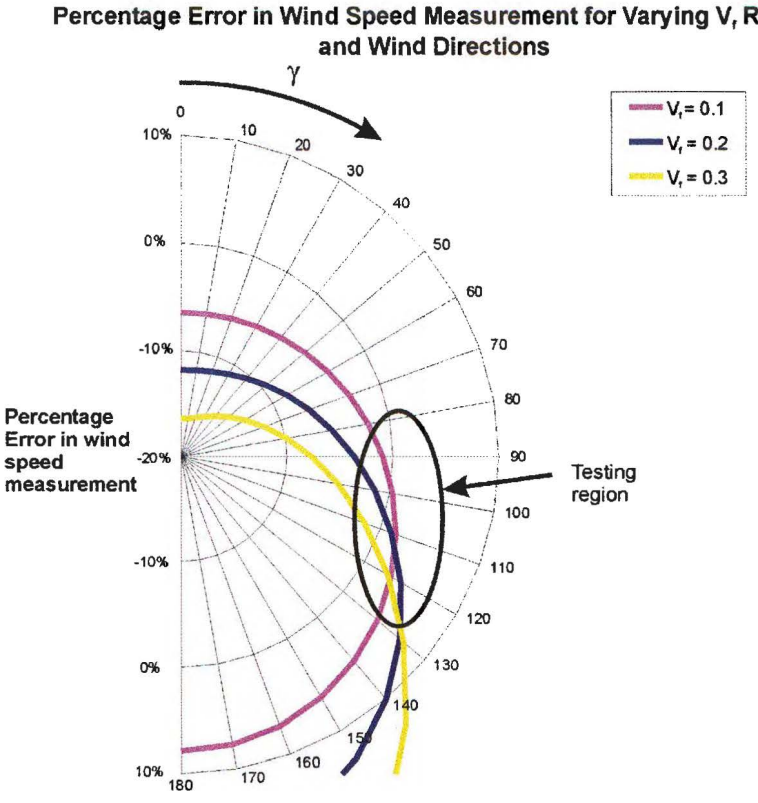

Figure 2:5 Errors in wind measurements due to natural wind

The best direction for the wind to come from is approximately 90° to the direction of the car as the error is close to zero at this point. In the location that the tests were performed the wind is smoothest when it comes off the sea and therefore at this site testing only happened when the wind was in the region of 90° to the direction of the car.

With the first rig design the error was slightly different to this since the rig was able to rotate into the direction of the wind **at the kite** and the anemometer used on this rig was directional dependent. As shown in Figure 2:4 the measured speed in the rotational case is slightly different than with a non-directional anemometer.

With a non-rotating test rig natural wind also introduces the problem of twist. Since the rig does not rotate, the kite is pointing in a different direction than the car by an angle σ. As the twist increases, the relationship between the Lift to Drag ratio and the measured line angle is reduced. The amount of twist depends on the direction and the magnitude of

the wind speed. Although the error in the recorded wind speed is lowest at 90°, Figure 2:6 shows that the twist in the lines is peaking at this point. There is an inevitable measurement error due to twist. Although measuring all of the line angles reduces the error, it will never be eliminated

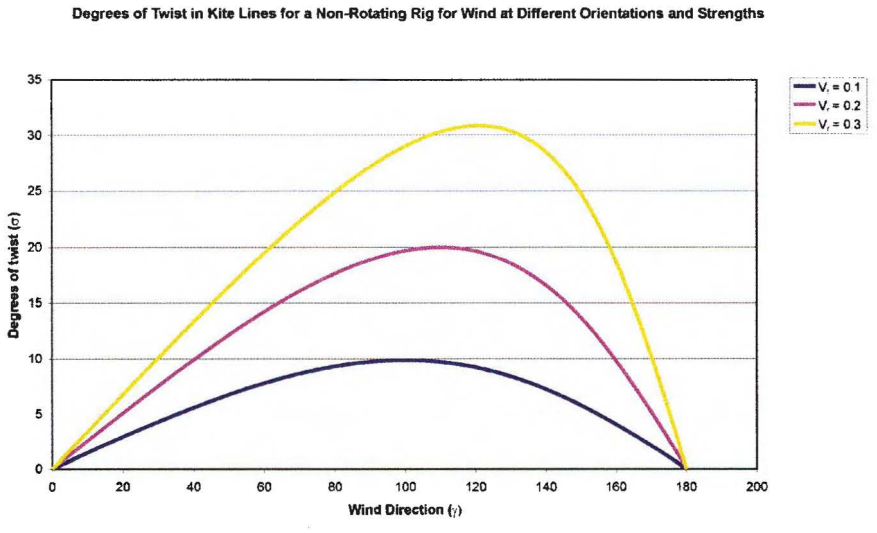

Figure 2:6 Twist in kite lines due to natural wind

What is clear from these graphs is that the accuracy of the testing procedure was affected by the presence of natural wind. High winds increase both the errors in the wind measurement (and therefore CL and CD) and the twist in the lines. Because of this, tests were only performed when the natural wind speed was below 15km/h but it was preferable if they were below 10km/h. This reduced the number of days that testing could be performed.

2.4.4 Line length

On the original rig the line length used was only 4 metres. This was enough to enable the kite to launch and keep it above any interference from the car, and yet not too high to increase the natural wind component. It also reduced the line drag component. However, it was decided to increase the line length to at least 10m for a number of reasons. First the kite flew better with longer lines, secondly, the kite was easier to launch off longer lines,

and thirdly, the testing required that the natural wind was at low levels so that there was not a large difference in wind speed between the car and the kite. The issue of line drag still remained. It was felt that line drag was a minor problem because:

1. Kites are flown on lines and therefore users will consider lines, and line drag, as part of the kite's overall performance.
2. If there is consistency in the line length a comparison between kites can still be made.
3. There are ways to estimate the effect of line drag and lift on the performance measure obtained, as shown in Chapter 4.

The decision to use longer lines meant that the rig no longer measured LTD_k but rather it measured LTD_g and CL_g as defined in Chapter 1.

2.4.5 Attachment points

The original specification for the attachment point width of 6m was unrealistically large. When the kite is on short lines the attachment points on the rig need to be the same as the distance between the bridle points. In most cases the required width was closer to 1m rather than 6m. Coupled with the fact that longer lines were being used it was decided to bring the attachment points closer together for all kites, similar to how a kite is usually flown. The final width of the attachment points was 0.6m with 0.4m between the front and back lines. A test rig this size could be permanently mounted to the roof of the car. This simplified the calibration of the rig and measuring the line angles, as the attachment points no longer had to be moved. .

2.4.6 Line load

The original brief indicated that the test rig should be able to withstand loads of up to 300kg. After gaining testing experience it was decided that loads this high were very unlikely for a number of reasons. First, it was found that loads greater than 100kg made the testing process rather hair-raising. Therefore, 100kg was the natural limit of the test.

Secondly, launching the kite did produce high loads but seldom greater than 150kg. Thirdly, although kite breakages did occur at times, and could cause high loads, testing to loads of only 100kg made breakages infrequent. Due to these considerations the design loads were reduced when the rig was redesigned.

2.4.7 Wind angle relative to the ground

There was uncertainty about the necessity of measuring the angle of the wind relative to the car in the vertical plane as illustrated in Figure 2:7. Due to the shape of the beach and the presence of natural wind it was thought that calibrating the angles relative to the car would not be sufficient to obtain accurate angle measurements. Attempts were made to measure the wind angle without much success. However, in the end it was deemed unnecessary as

1. Tests were only performed on days when there was very little natural wind and therefore the direction of the car predominantly determined the direction of the wind at the kite.
2. Although obtaining the direction of the wind may have made the angle measurement more accurate, the measurements taken indicated that the difference in the wind angle from the car was minor compared to the accuracy that could be obtained by any instrumentation.

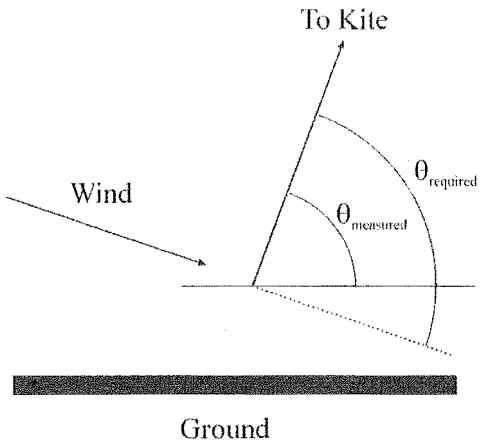

Figure 2:7 Wind angle effects

2.4.8 Set up speed

The rig had to be simplified to increase the set up speed. The first rig took two people 30-40 minutes to setup which did not meet the design requirements. More importantly, it meant that many tests had to be cut short due to conditions deteriorating during the long set up time. Coinciding low tide and still conditions was difficult without also speeding significant amount of time setting up equipment.

2.4.9 Data acquisition program

Originally it was felt that the computer data collection required some graphical display so that testing could be viewed in real time. The original programme had a display of this sort but it was found to be unnecessary. The only information required during the test was the speed, line load and back line load percentage during the test. Graphical displays also slowed the programme down and increased the chance of programme difficulties. A new programme (see section 2.7.1) was written that was basically a data logger and only displayed the data entry by entry.

2.5 Angle Guide Development

Due to the importance of the angle measurements a lot of attention was given to the angle measurement system. The following sections outline the necessary developments in this area to obtain accurate readings.

2.5.1 Angle guide developments

The original system for measuring the line angles was inadequate to achieve the accuracy required. Figure 2:8 shows a diagram of this guide. A potentiometer was attached to the shaft of the pulley which was able to rotate as a line angle changed. This system had many problems but the main one was that the pulley would not always follow the line and when it did it was uncertain if it was doing so with any accuracy.

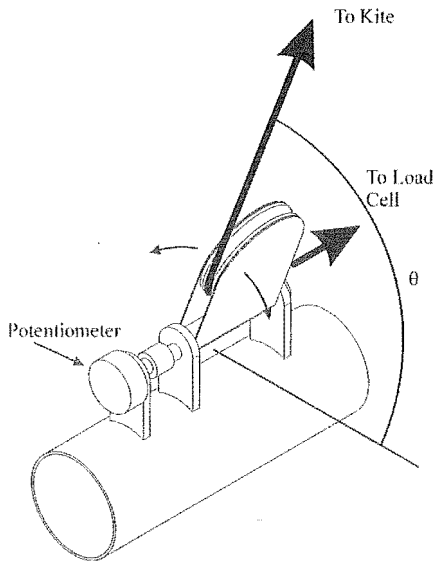

Figure 2:8 First angle guide

The first modification was to attach an arm to the potentiometer with a guide on the end to follow the line as illustrated in Figure 2:9. The potentiometer was also disengaged from the pulley (but not the arm). This showed more signs of success and the principle was used in further improvements.

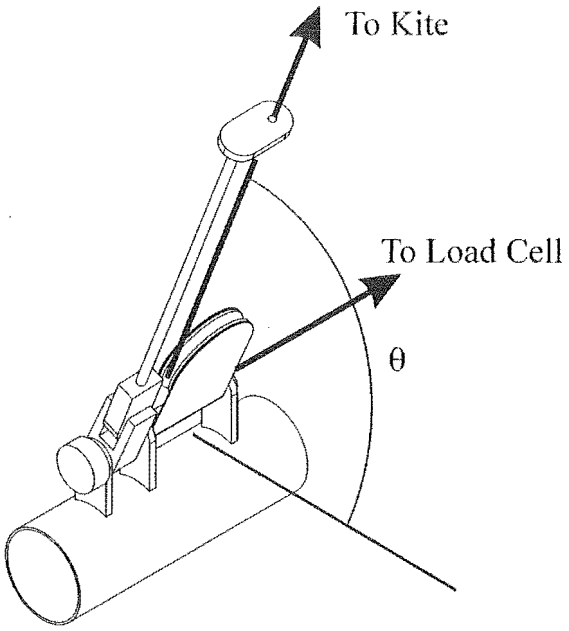

Figure 2:9 Second angle guide

Further modifications were then put on hold while the new frame was built which gave a more rigid and permanent structure on which to mount the angle guides. The first angle measurement mechanism on the new rig was virtually identical to that shown in Figure 2:9, except a flat base was used to mount the guide to the frame rather than a tube.

Eventually it was realised that further improvements in the design of the angle guide were required, to be certain that the line angles were being measured correctly. In the new design the pulley was located so that the kite line out of the pulley was on the axis of rotation, bearings were inserted and the arm mechanism was made more robust which enabled the potentiometer to be directly coupled to the pulley housing. Originally it was thought that nylon bearings would be sufficient but these were later replaced with roller bearings. The final angle guide is shown in Figure 2:10.

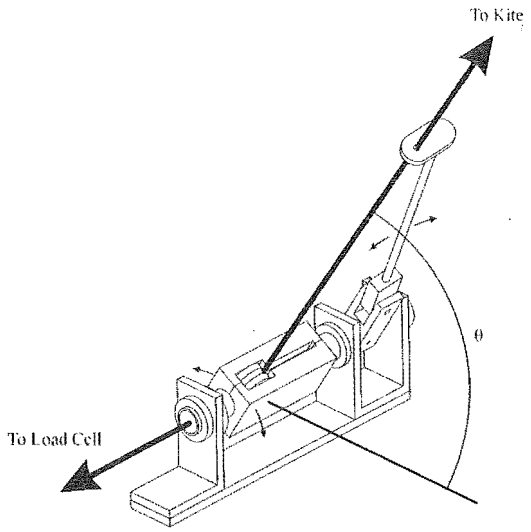

Figure 2:10 Third angle guide

2.5.2 Calibration mechanisms

It was soon realised that the level of accuracy required for the angle measurement made having an accurate calibration mechanism for the potentiometers imperative. To do this an accurate circular table was used to locate a series of pins on a board 2.5° apart on a 250mm radius around an accurately drilled hole as shown in Figure 2:11. By resting each angle guide on these pins a series of voltages from the potentiometer relating to the different angles could be obtained. These were then converted to an angle measurement.

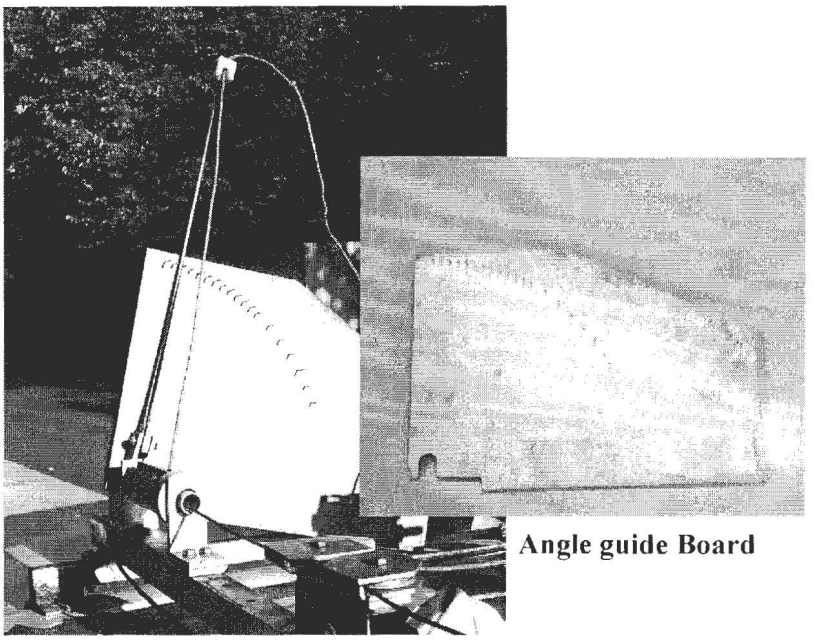

Figure 2:11 Angle calibrating board

Of all the improvements that were made, this device had the greatest impact on the repeatability and accuracy of the rig measurements.

2.5.3 Zeroing the rig

Difficulties were faced when zeroing the rig so that a standard measurement could be taken. A method was required to obtain the potentiometer readings when the lines were perpendicular to the horizon and while the car was on a flat surface. Many methods were attempted, ranging from spirit levels to hot air balloons. Eventually the method shown in Figure 2:12 was used.

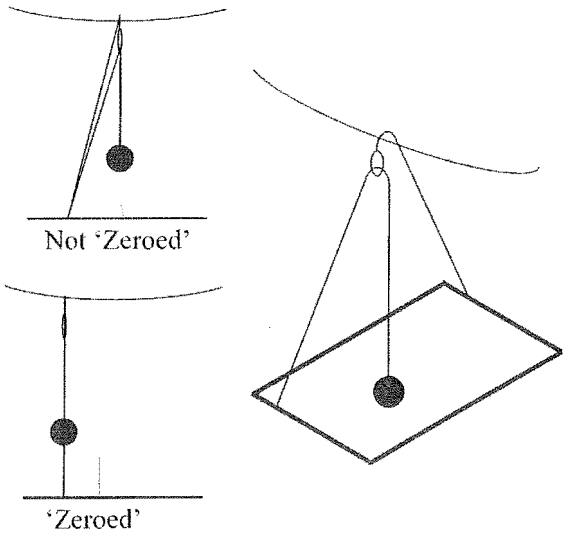

Figure 2:12 "Zeroing" mechanism

In this method a rope is attached to one angle guide and a loop is put in the end. This rope is then put over a rope attached to the roof above the rig. Through this loop passes another rope of which one end is attached to the opposite angle guide while a weight is attached to the other end. This makes three ropes going to one point and this point can be moved until all three ropes align. When they do the two potentiometers will correctly read the angle when they are at 90^{o} to the horizon. This corresponds to them being 90^{o} to the wind produced by the car. This method proved to be very repeatable and had the benefit of calibrating two angles at once. This zeroing process was done before and after the test.

2.6 Final Test Rig Specifications

Figure 2:13 shows a schematic of the final test rig. The rig mounts directly to the roof and the control lines go through the sunroof. The load is obtained in a slightly different way to what was shown in Figure 2:1. Rather than having a pivoting arm which pushes against the load cell, the front lines pull directly on the load cell while the pulleys for the back lines are mounted on a bar, which in turn is attached to the load cell. The change in

direction of the ropes as they go through this pulley allows the back line load to be obtained.

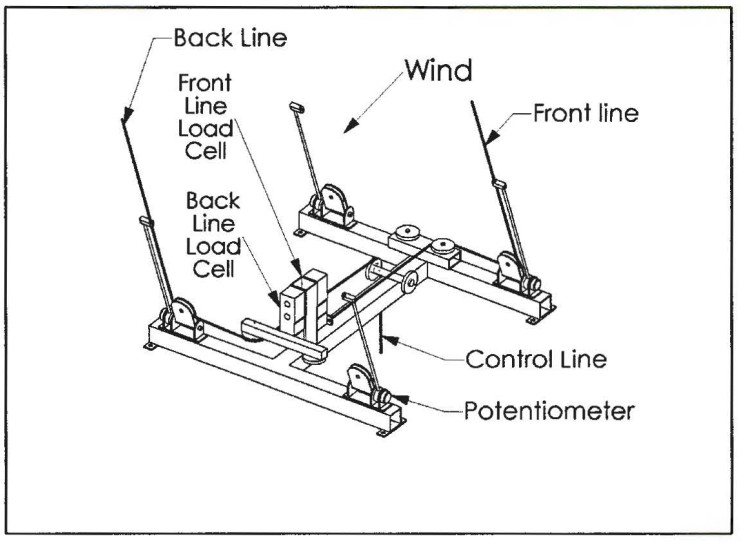

Figure 2:13 Final test rig schematic

Figure 2:14 shows the rig mounted on the car at the test site.

Figure 2:14 Car used in tests with rig and anemometer attached

2.7 Testing Methodology

2.7.1 Data Acquisition System

The data acquisition system was designed by the Mechanical Engineering Department specifically for remote use. It is capable of measuring eight data channels and returning a string of numbers for each recording. A suitable programme for processing these numbers, adjusting the sample rate and displaying and saving the data is the responsibility of the person using this system.

The data required for processing were

1. An index for each measurement, which can be related back to a time by the collection rate.
2. A measurement of the wind speed
3. Both front and back line loads and the total load (FL_f,BL_f,F_{tot})
4. Four line angles

The measurement device returns a voltage proportional to the measurement taken. The data acquisition system then converts this analogue signal into a digital signal. The display programme written for this application then processes this digital signal. This display programme applies appropriate calibration constants to the different digital signals that it receives to obtain the desired measurement.

The display program has two sampling rates. The first is the rate that data is drawn from the data acquisition system. This is set to the fastest rate that Windows 98 will allow which is around 13 times per second. The second sampling rate is simply the rate at which the data is saved to file. The program will collect values at the first sampling rate then average and save them at the second sampling rate.

While the programme is running the user sees the screen as shown in Figure 2:15. There are three main parts to this programme. The top bar contains the controls whereby the program is started, paused, stopped and a new data file created for a different kite. When the program starts, a line is inserted into the program giving the titles of all the data collected. Whenever the program is paused this line is also inserted so that a pause can be identified later. The second sampling rate is also modified in this section.

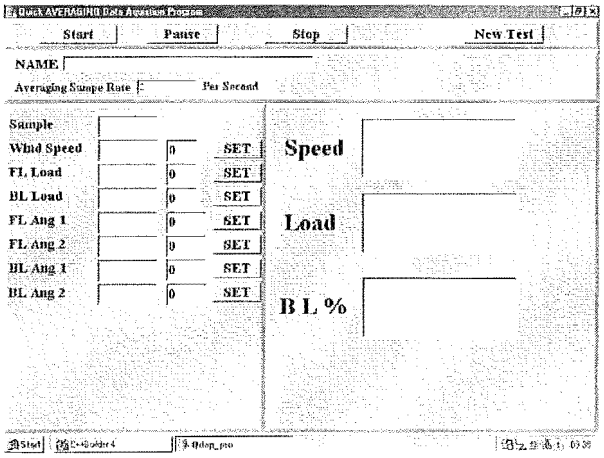

Figure 2:15 Data Acquisition Program

The second part at the left of the screen displays all the data that is being collected. Where required there is also a calibration function. By pressing the set button the data will be modified to read whatever is in the box next to the button. In the end only the front and back line loads were set to zero, as the anemometer did not require this and the angle calibration was applied when the data was processed at a later date.

The third section simply shows an enlargement of the wind speed, the combined load and the back line percentage load. This section is there because the operator requires a large, clear display of this data during the testing process.

All the data is saved to a text file as it is generated. This file is then imported to a spreadsheet for processing once the test is finished. In the data file commas are inserted between values for delimiting purposes.

2.7.2 Kite testing method

After the experience gained with the initial test rig and the subsequent developments the testing process settled into the following routine.

1. Prior to the test all angle guides were calibrated.
2. If conditions were suitable at the testing site, set up of the rig would proceed.
3. The data collection program was started and the load cells were set to read zero load. The data collection rate was usually set within a range of 2-5 times per second.
4. A kite was attached to the lines and positioned behind the car on the ground in manner ready for takeoff. In low winds the kite would normally stay in position until the car could be operated. Different kites required different starting positions, which were determined after experimentation.
5. The car was then driven up to a slow speed to allow kite to reach flying height and fly in a stable manner. With larger kites the car may have to speed up to get the kite to start flying and then slow down again to reduce the magnitude of the relative wind. During take off the relative wind effect can cause very large forces on the rig and kite, which are best avoided.
6. Data was then recorded up and down the beach. With four-line kites the two parameters that were varied were the wind speed and the back line load. To obtain a good range of data two techniques are used to change these variables.

    (a) The back line tension was held relatively constant and the speed was varied. This was repeated for varying back line tensions. This technique was good for getting a wide range of speed-readings.

(b) The speed was held constant and the back line tension was varied. This was repeated for varying speeds. This technique was good for getting a range of back line tensions but the speed tended to fall into fixed bands.

7. The car was brought slowly to a stop to land the kite gently. A new kite was then attached.
8. The angle guides were recalibrated upon returning from the tests and the average 90^{o} reading used in the data processing.

2.7.3 Data analysis

Once testing was completed the data was analysed. Usually 30-40 minutes of testing was performed for each kite producing 3000-6000 lines of data. There were a number of steps to process this data.

1. The data was transferred to a spreadsheet for analysis. Commas had been inserted between measurements in the test file already for de-limiting purposes.
2. The data that was not part of the test was deleted i.e., data collected during the load cell calibration step and sections of data on each side of a turn on the beach.
3. The calibration for the angle guides was inserted in the spreadsheet and the angle guide readings adjusted.
4. The two front angle readings were averaged along with the two back angle readings to obtain FL_{ang} and BL_{ang}.
5. The Lift to Drag ratio was determined using the following formula

$$LTD_g = \frac{FL_f \sin(FL_{ang}) + BL_f \sin(BL_{ang})}{FL_f \cos(FL_{ang}) + BL_f \cos(BL_{ang})} \qquad \textbf{Eq 2:5}$$

This formula takes the lift components of the front and back line tensions and divides them by the drag components. This calculation is necessary as the Lift to Drag ratio is a combination of both the back and the front line forces and angles.

6. The Lift Coefficient was then determined using the following formula

$$CL_g = \frac{1}{2} L \cdot \rho \cdot A \cdot V^2 = \frac{1}{2}\left[FL_f \sin(FL_{ang}) + BL_F \sin(BL_{ang})\right] \rho \cdot A_k \cdot V^2 \qquad \textbf{Eq 2:6}$$

where A_k is the nominal area of the kite. This is the usual definition of a Lift Coefficient. In this case the force used is the combined lift force on the front and back lines.

7. The back line percentage load was then determined using

$$BL\% = \frac{BL_f}{T_{tot}} \times 100 \qquad \textbf{Eq 2:7}$$

After analysing the data of various kites it was found that back line percentage load had the largest influence on the performance of the kites. The variation of this load is also the only control that a flyer has over a kite's performance. Due to this, back line percentage was used as the major parameter to analyse and sort the data obtained in tests.

8. The Lift to Drag ratio found in step 5 was converted to an angle, in order to identify if a particular data point was out of the ordinary (see step 12). The Lift to Drag ratio cannot be used for this purpose because of the asymptotic nature of the tangent function, which makes high angles look more extreme than they are.
9. The data was then copied and put into a new sheet as values rather than equations as this speed up the next steps. The data index was also copied.
10. This data was then sorted by the back line percentage load.
11. Discrete ranges of data at certain back line loads were then analysed for different trends. In this project an interval of 2% ±0.5% back line percentage load was used over the range of loads applied to each kite. The data from each range was then copied into a new worksheet for analysis. Doing this isolates the data for one kite parameter.
12. The data from each range was then sorted by the angle related to the Lift to Drag ratio (see step 8). All the points were then plotted to identify the results that were

obviously higher or lower than the bulk of the results obtained. Any obviously erroneous results were then removed from the data set.

13. General results were then calculated for each set of data. In general mean results of the Lift to Drag ratio and Lift Coefficient were found. The data was also sorted by other variables, such as wind speed, to see if there were any other relationships.
14. The results were then compiled into a separate file with other data from separate tests on the same kite to determine the overall trends.

2.8 Results

2.8.1 Process to verify rig

To verify the repeatability of the rig, one kite was used as a standard kite and was tested on each test day. It was hoped that the results from different test days would be consistent, indicating how reliable the test rig was. If the rig was reliable tests from this kite would also indicate if a particular day's results were out of the ordinary and could not be trusted.

The chosen kite was a 3.2m C-Quad. This is a relatively small kite but it proved to be good for this role. It is strong and does not experience large loads so was not as susceptible to breakage and/or stretching. Figure 2:16 is a picture of a C-Quad type kite

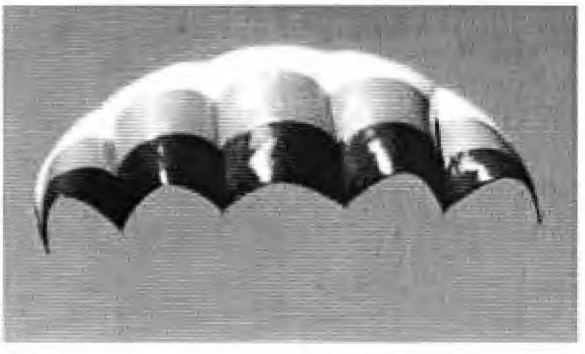

Figure 2:16 C-Quad type kite

2.8.2 3.2 C-Quad Results

Figure 2:17 and Figure 2:18 show the test results for the 3.2 C-Quad's Lift to Drag ratio and Lift Coefficient on different testing days. Error bars are not included in these graphs so that the trend of the data can be easily seen. Errors are outlined in Section 2.8.3.

There is a variation in the results for the Lift to Drag ratio but the data lies in a range between 4 and 5. Likewise, the values for the Lift Coefficient vary between runs but there is a consistent positive trend as the back line load is applied.

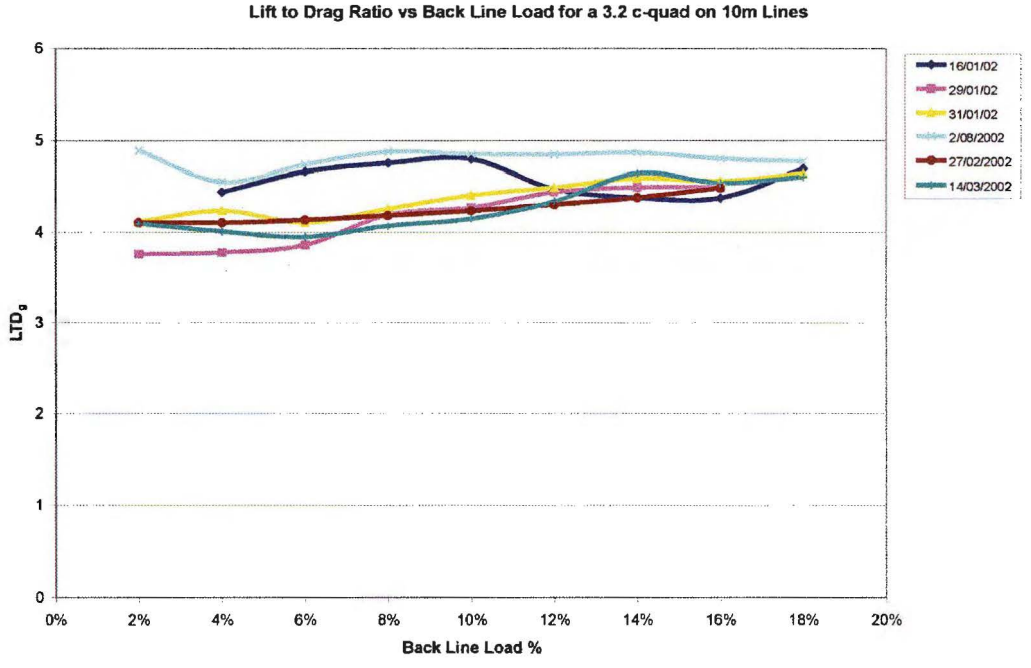

Figure 2:17 3.2 C-Quad Lift to Drag ratio data

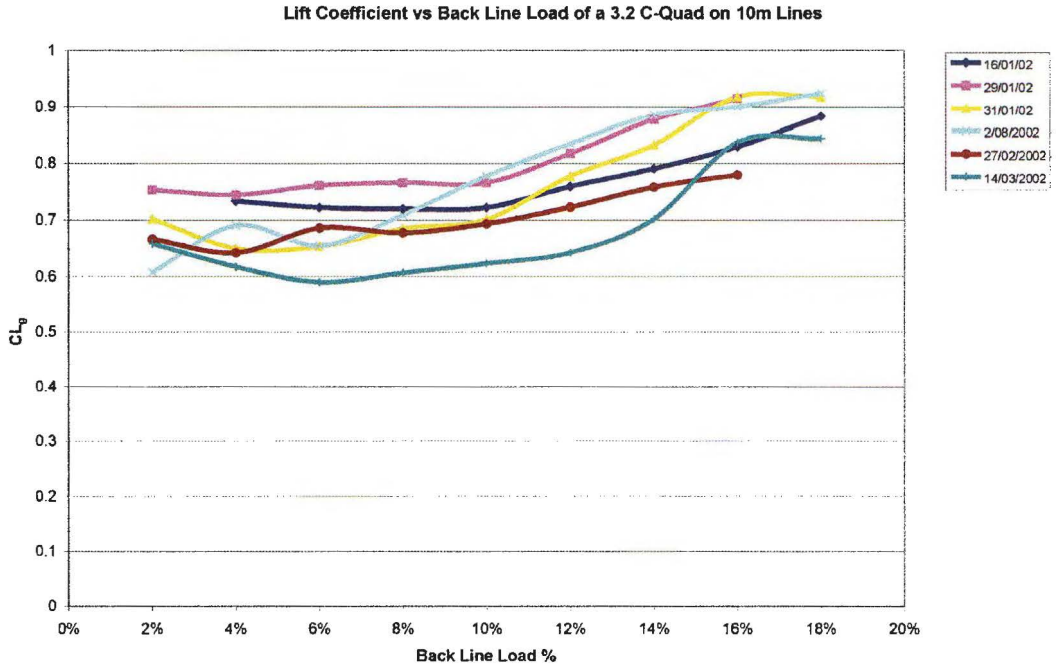

Figure 2:18 3.2 C-Quad Lift Coefficient data

2.8.3 Errors in Test Rig

The following are the estimated errors in the instrumentation and their effect on the results

1. The error in the angle measurement is made up of three parts. First, the potentiometer and angle guides under ideal conditions will read to within ±0.2°. This is the best accuracy that could be obtained with the calibrating board. Secondly, the zeroing method is only accurate to ±0.3°. Finally, as the car changes weight (i.e., with people, fuel loss) the calibration changes by up to 0.2° due to the change in weight on the suspension of the car. Therefore the error on the angle measurement is ±0.7°. Although the car bounces around on its suspension this is largely averaged out during the test. Due to the tangent relationship between line angle and Lift to Drag ratio this error will have a larger effect as kites get better .
2. The Load measurements are accurate to ±5%.

3. The wind measurement has two errors associated with it. First, the instrumentation will read to ±0.5km/h. Secondly, as shown in Figure 2:5 the natural wind introduces an error in wind speed measurement. However, the tests were only performed when the natural wind was below 15km/h and off the sea so the error is within ±10%.

The angle error affects both the Lift to Drag ratio and the aerodynamic coefficients. However, because this relationship is non-linear neither an absolute nor percentage error can be determined for all cases. Figure 2:19 and Figure 2:20 show how these errors vary for kites with different Lift to Drag ratios.

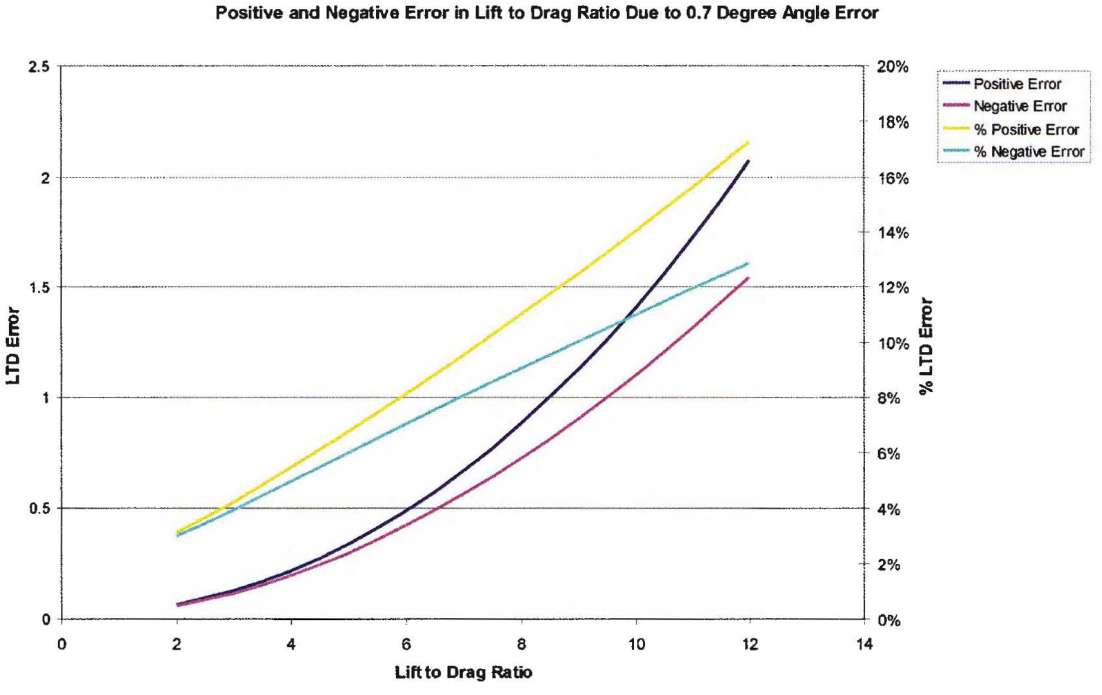

Figure 2:19 Error in Lift to Drag ratio measurement due to angle measurement error

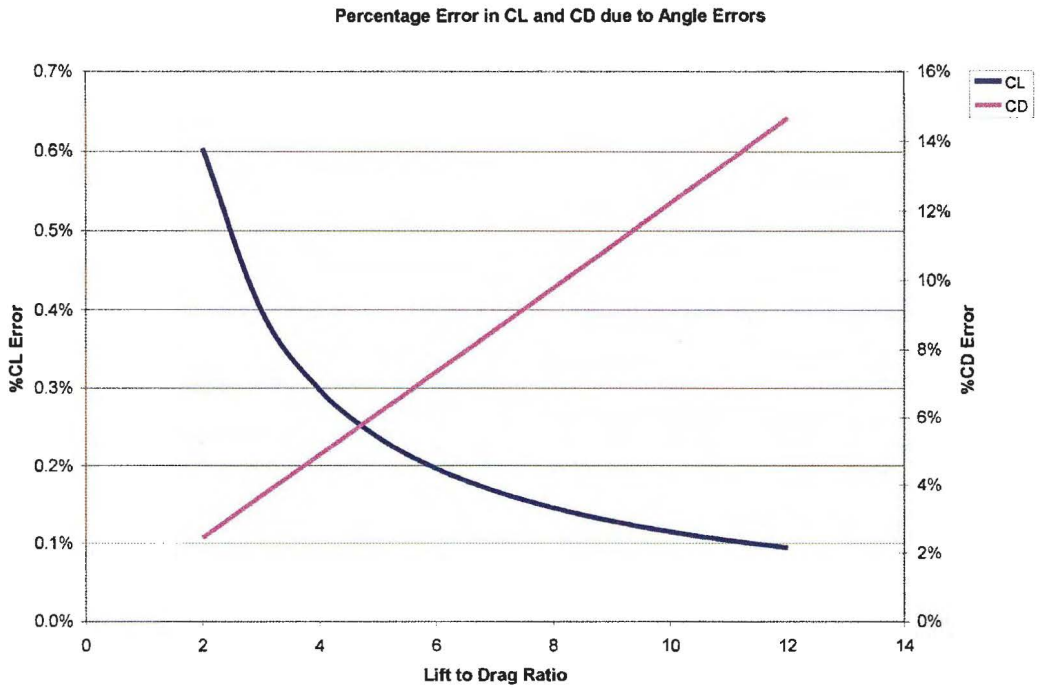

Figure 2:20 Percentage error in CL and CD due to angle measurement error

The errors in the load and wind speed measurements primarily affect the aerodynamic coefficients rather than the Lift to Drag ratio. The most significant of these is the error due to the natural wind since the velocity term is squared. Therefore on the windiest days the error on the wind measurement can cause an inaccuracy of ±20% in the Lift and Drag Coefficients. The total error can be as high as ±25% although this is unlikely as tests are only performed on low wind days. However, according to Figure 2:18 the repeatability of the CL measurement was within ±15%, significantly better than was expected.

2.9 Discussion

2.9.1 Rig Accuracy

The main issue with this rig is how accurate it is and how repeatable the results are. According to Figure 2:17 the Lift to Drag ratio of the 3.2 C-Quad reference kite was between 4-5. However, there is a band of data that falls within a much narrower range

than this. The results for the 16/01/02 and the 2/08/02 are very different to the trend displayed on the other four days. Taking all the data into account the variation in angle corresponding to the upper and lower Lift to Drag readings is ±1.5°. However if these two day's recordings are removed the repeatability of the rig falls to within ±0.5°, which is significantly better. However, based on these results, to obtain this level of accuracy a kite will need to be tested multiple times.

Figure 2:21 shows the Lift to Drag data for a 630 Arc tested on most of the same days as the 3.2 C-Quad. At first glance the two testing days that were out of the ordinary for the C-Quad do not seem to be so out of the ordinary with the Arc. However, with this data included the repeatability of the ARC tests are ±1.5°, similar to above, but if these days are excluded the repeatability is ±0.7°, also similar to above. Unfortunately, if these days are excluded there is not enough data to get a reliable estimate of this kite's performance. This indicates that the error in angle measurements is somewhere between 0.5° and 1.5°. It is also evident that the results for the 3.2 C-Quad on a particular day will not indicate if the results for other kites are high or low, as this trend was not shown in the 630 Arc results.

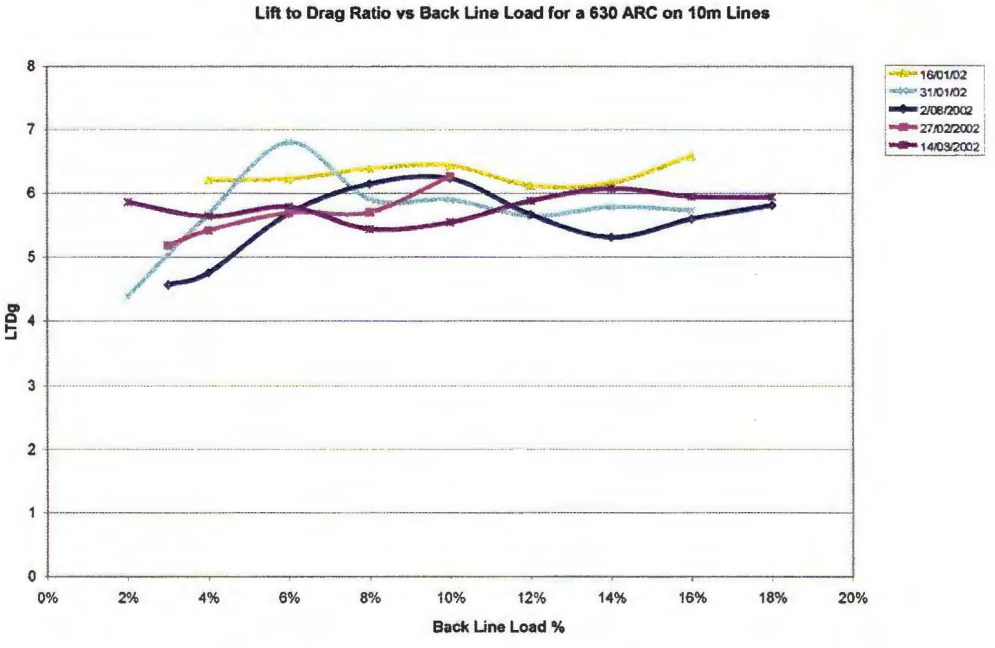

Figure 2:21 630 ARC Lift to Drag ratio data

Is this level of repeatability acceptable? An accuracy of $\pm 0.8^{\circ}$ is good, and realistically is approaching the limit of this method. However, with the tangent relationship between the angle measurement and the Lift to Drag ratio, even this level of repeatability introduces significant uncertainty into the results. This will become even more of a problem as Taction kite performance improves and identifying the difference in performance between kites with similar characteristics will be difficult.

2.9.2 Further Improvements

Further improvements to the accuracy of the test rig will be difficult to achieve for the following reasons:

1. Calibrating the angle guides to a greater accuracy will be very difficult. Even with the use of the calibrating board the potentiometers only read to within $\pm 0.2^{\circ}$.
2. The zeroing mechanism had a similar level of accuracy to the calibration board and any significant improvements are unlikely.
3. The testing surface was not very smooth. The beach has a number of undulations and this will always affect the data.
4. Despite using a relatively robust kite, the kite performance can change between runs making improvements in the readings meaningless.
5. Variations in the weight of the vehicle (ie petrol usage) changed the angle readings by $\pm 0.2^{\circ}$.
6. A small amount of natural wind can vary the results significantly. To perform to a reasonable testing schedule, tests will need to be occur when there is wind.

Overall it is felt that the level of accuracy achieved by the rig is reasonably good. However, even with this accuracy the value of the rig as a viable testing option is questionable. A kite design change that improved performance of a kite by 5% would be very hard to identify with this rig. On the other hand it would give a strong indication of what a kite's performance is compared to another kite design. This would be useful for identifying the general performance capabilities of a kite.

2.9.3 Tides and Weather

Doing these kite tests outside was a significant issue in the testing process. Because the testing could only be done on fine days the number of days suitable for testing was reduced. The requirements for a low tide narrowed the testing times even further. It is possible that these two factors had the greatest impact on the feasibility of the testing process.

2.9.4 Other uses for the test rig

There are other uses for the test rig. Sometimes there are particular kite characteristics that are difficult to reproduce in the windless environment of Ashburton. By having the rig on the car and being able to adjust the wind speed it may be possible to reproduce these characteristics. The test rig is also a good way to fatigue-test the kites. As kites get older and the material stretches, kites will exhibit different flying behaviour. By using the test rig kites can be made into the 'old' condition faster and therefore the effect of age can be determined.

2.10 Conclusion

The final design of the test rig was successful given the conditions that the test was performed in. For a one-off test a kite's line angle can be determined to within $\pm 1.5^{o}$ while with further tests a range of $\pm 0.8^{o}$ can be achieved. A reasonably large error arises with the determination of the aerodynamic coefficients but this is less important than the angle measurements.

However, even this accuracy limits the effectiveness of the rig. Because of the tangent relationship between the Lift to Drag ratio and the line angle a high degree of accuracy is required to obtain good results. This accuracy is unobtainable in this rig due to the characteristics of the testing method and the variable nature of kite's performance. As a results the feasibility of using a test rig such as this for kite development is limited

because the effect of small design changes are difficult to detect. However, the rig is still useful for determining the general performance of a particular kite design.

3. Kite Test Results

3.1 Summary

In the course of commissioning the car based test rig, a number of different kites were tested. Although these tests are not a comprehensive review of all kite designs they do provide some insight into the development of Traction kites. Based on the results it was found that the performance of the kites produced by Peter Lynn Kites Ltd have improved significantly. In particular improvements were made to their kite's Lift to Drag ratios and the ability to vary their aerodynamic coefficients. However, although the test rig can determine several performance characteristics there are other important aspects that it cannot give information about such as luff resistance, turning and the 'feel' of the kite.

3.2 Introduction

In the process of verifying the car test rig a series of kites were tested for their performance. These tests were done primarily to determine the usefulness of the test rig rather than to provide a comprehensive outline of different kites' performance. It was found that kites took a long time to test and designs changed too quickly for test data to reflect the current performance of each kite design. However, the data shown in this section can be utilised to determine the general performance characteristics of kites of various types.

3.3 Method

The kites were tested on the car test rig once all the modifications had been completed. The testing methodology and data analysis method has been outlined in Chapter 2.

3.4 Kite Results

The three different styles of kite that were tested are shown in Figure 3:1.

C-Quad ARC FARC

Figure 3:1 Example of different kite designs tested

The results have been summarised into four key measurements. First, the Lift to Drag ratio $(LTD_g)^2$ is shown along with the Lift Coefficient (CL_g). The Lift coefficient is based on the nominal area of the kite (A_k). On the second graph the magnitude of the lines Tension Coefficient and the percentage change in this value are shown. The Tensions Coefficient is defined as

$$CT_g = \frac{T_g}{\frac{1}{2}\rho A_k V^2} \qquad \textbf{Eq 3:1}$$

where T_g is the tension of the line at the test rig. The percentage change in the line tension (CT_gVar) is found by converting the CT_g values to a percentage. These percentage values are based on each kites CT_g value at its lowest back line tension. Both CT_g and CT_gVar are important because these values indicate the size and the variability of the line forces experienced by the flyer.

---

[2] Note that all the results have a subscript 'g' as they include the line properties.

3.4.1 Kite areas used

In all results the nominal area of the kites, as quoted by the manufacturer, have been used to determine the aerodynamic coefficients. Although it is more correct to use the projected area of the kite, which can differ significantly from the nominal value, obtaining accurate measurements of the projected area is difficult. Using the nominal area is a valid measurement as the trends are still the same as for the projected area. Using the nominal area also keeps the responsibility for measuring kites in the hand of the manufacturer and gives them an indication of how realistic their measurements are.

3.4.2 Error bars

Error bars have been included on the data. These are based on the errors outlined in Chapter 2. They are

- $\pm 0.8^{o}$ error in the line angle measurement.
- $\pm 15\%$ error in the measurement of the aerodynamic coefficients.
- $\pm 1\%$ in the Percentage Back Line Load measurement.

3.4.3 3.2 C-Quad results

Figure 3:2 and Figure 3:3 show the results for a 3.2 C-Quad. The nominal area of this kite is $3.2m^2$.

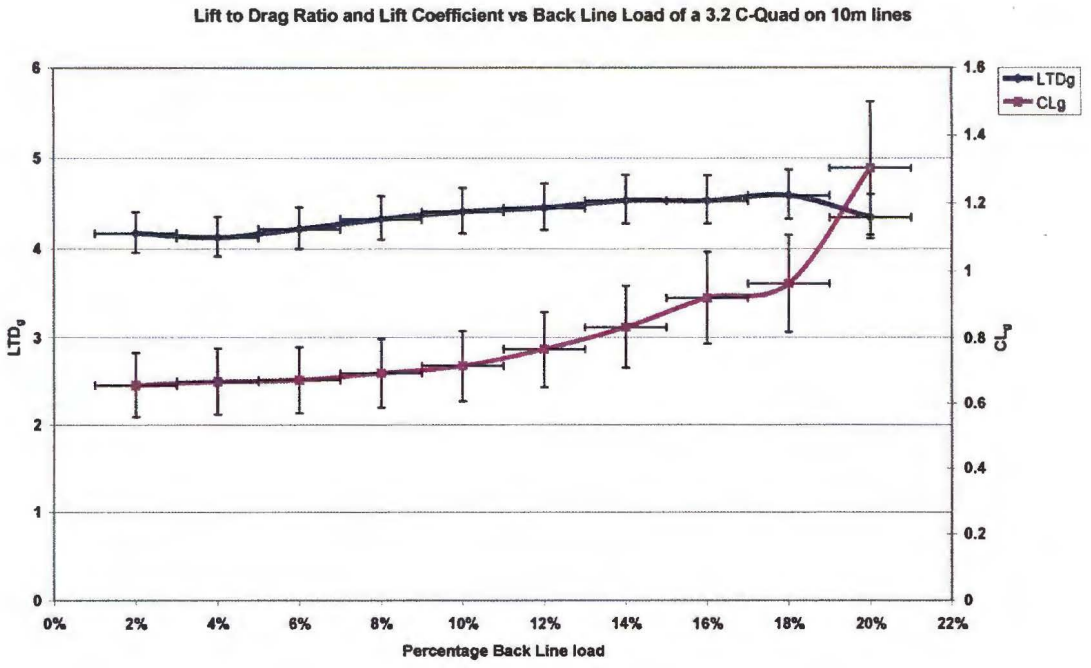

Figure 3:2 LTD_g ratio and CLg results for a 3.2 C-Quad

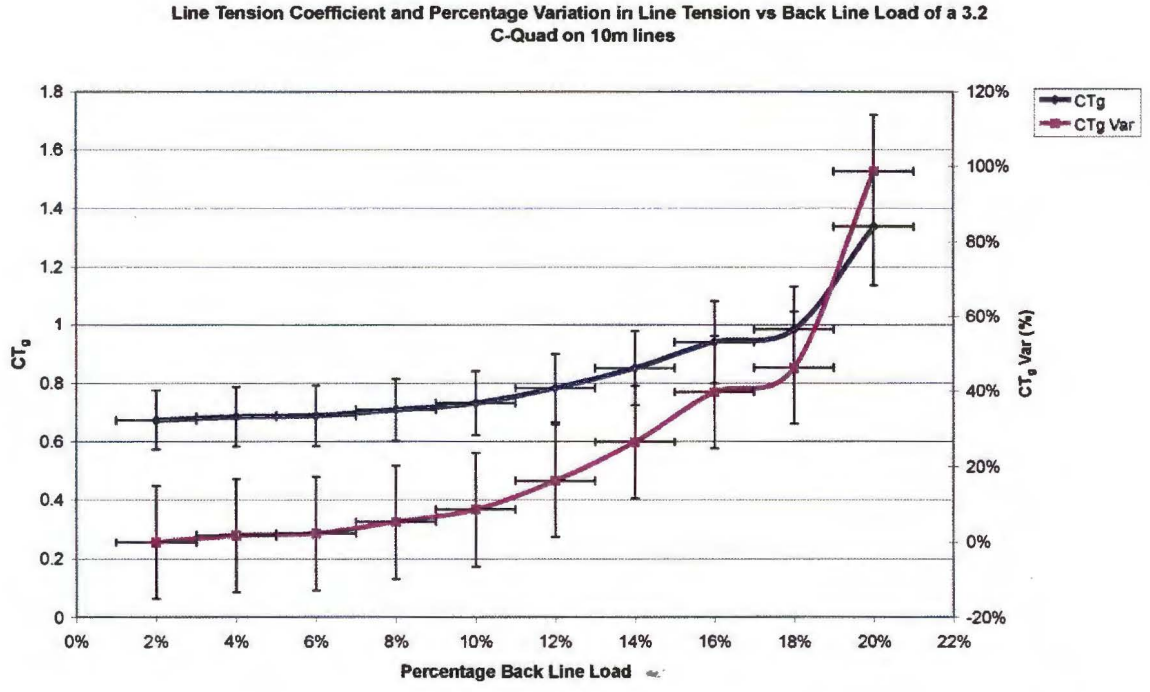

Figure 3:3 CTg and percentage variation in CTg results for a 3.2 C-Quad

Many tests were performed on this kite as it was used to verify the repeatability of the car test rig. This kite displayed the following key characteristics.

- The Lift to Drag ratio peaks at a value of 4.5-4.6 when 18% Back Line Load is applied.
- After this peak Lift to Drag ratio the kite quickly begins to stall at approximately 20% Back Line Load.
- Varying the back line load increases the Lift Coefficient. Due to the onset of stall the Lift Coefficient of 1.3 at 20% back line tension is not a very reliable figure. It is likely that the effective variation in the Lift Coefficient is 0.6-1.
- The variation of the line Tension Coefficient with back line load is relatively smooth

3.4.4 4.2 C-Quad results

Figure 3:4 and Figure 3:5 show the results for a 4.2 C-Quad. The nominal area of this kite is 4.2m^2.

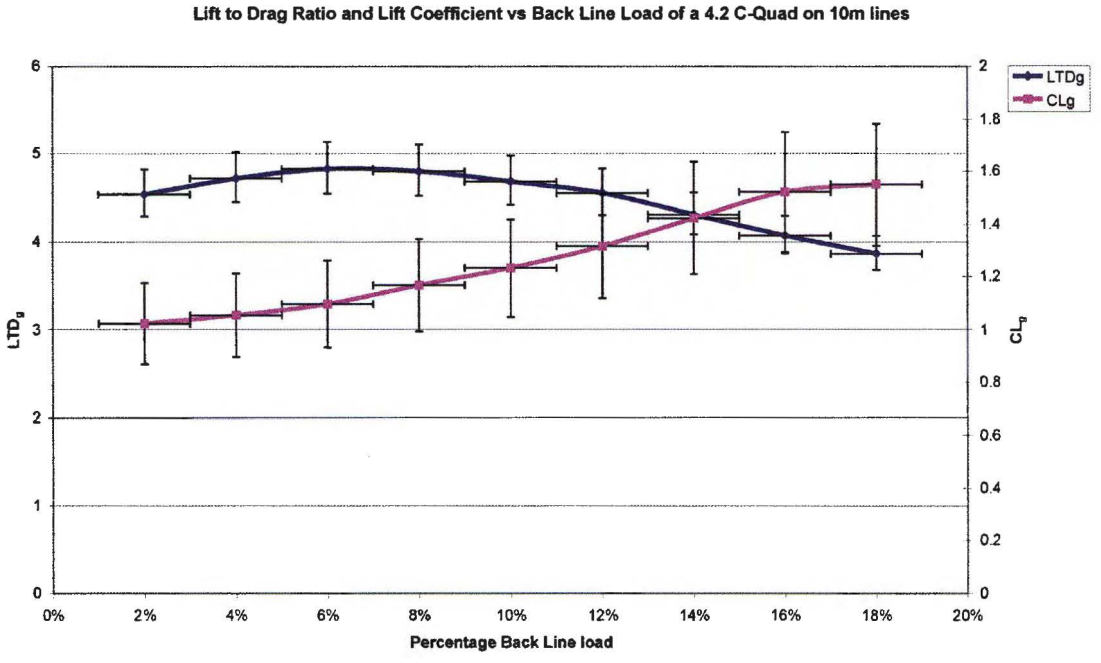

Figure 3:4 LTD_g and CLg results for a 4.2 C-Quad

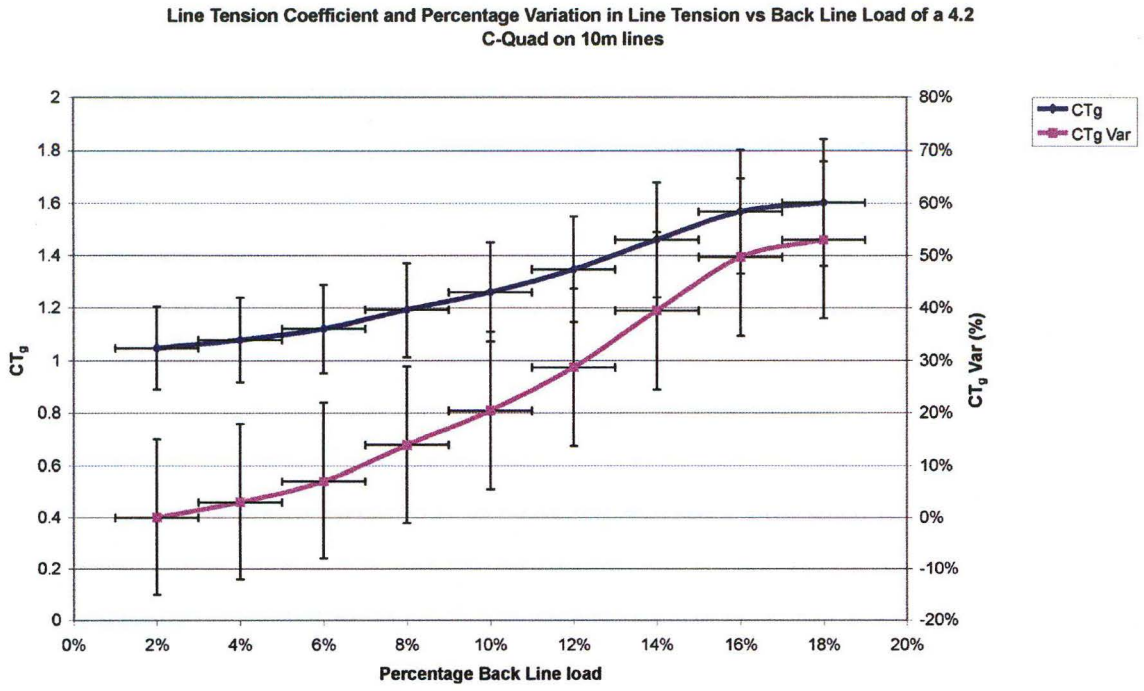

Figure 3:5 CTg and percentage variation in CTg results for a 4.2 C-Quad

The results remained very consistent across the four tests carried out on this kite. The kite displayed the following trends.

- The peak Lift to Drag ratio value of 4.8 is higher than was achieved by the 3.2 C-quad.
- The peak Lift to Drag ratio occurs at a back line tension of 6%, lower than for the 3.2 C-Quad.
- The kite displays a gradual reduction in Lift to Drag ratio until stall occurs at back line tensions above 18%.
- Like the 3.2 C-Quad the Lift Coefficient increased with back line tension. In this case the Lift Coefficient varied between 1-1.6. This is a similar variation to the 3.2 C-Quad although difference in the size of the numbers indicates that there is considerable scope in how the areas of the two kites are defined.
- Like the 3.2 C-Quad the variation in the Tension Coefficient is relatively smooth.

3.4.5 460 ARC results

Figure 3:6 and Figure 3:7 show the results for a 460 ARC kite. The nominal area of this kite is 4.6m^2.

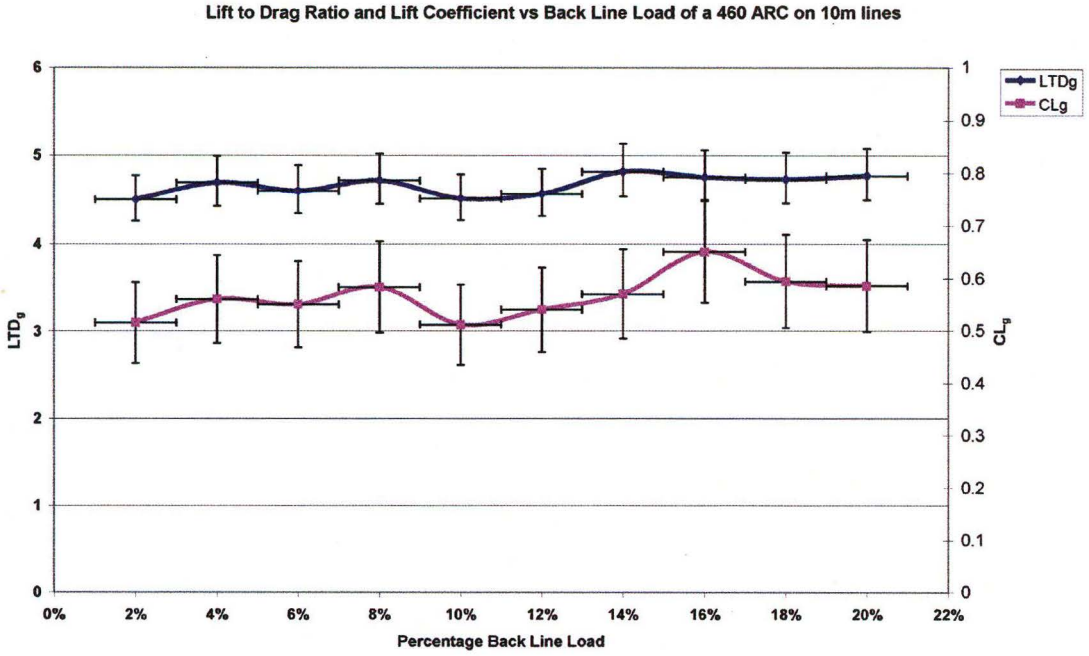

Figure 3:6 LTD_g and CLg results for a 460 ARC

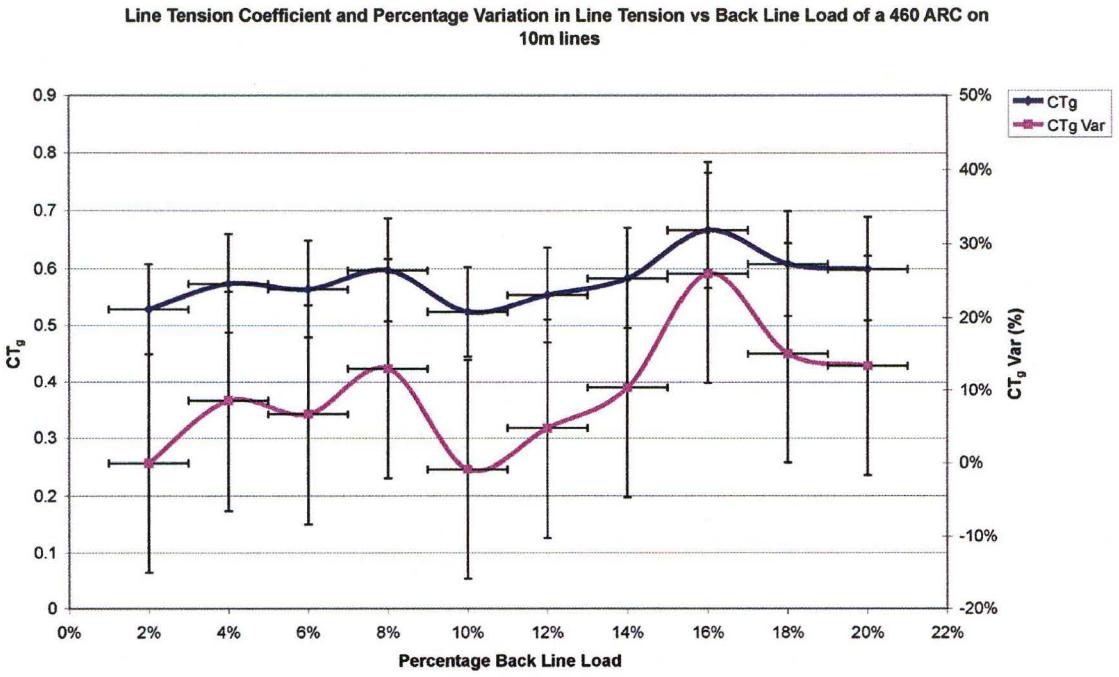

Figure 3:7 CTg and percentage variation in CTg results for a 460 ARC

Only two tests were carried out on this kite so the results shown here are only initial estimates of this kites performance. However, based on these results this kite has the following key characteristics.

- The Lift to Drag ratio of this kite is about 4.8 irrespective of how much back line load is applied.
- The kite's Lift Coefficient varies around 0.55. Although the Lift Coefficient appears to vary with back line load a direct relationship is not apparent.
- The peak percentage variation of line tension of 25% is probably an error in the test results as a sharp peak like this does not appear in other kites with similar designs.
- These findings indicate that the performance of this kite is largely independent of user.

3.4.6 630 ARC results

Figure 3:8 shows the results for a 630 ARC. This kite has a nominal area of $6.3m^2$.

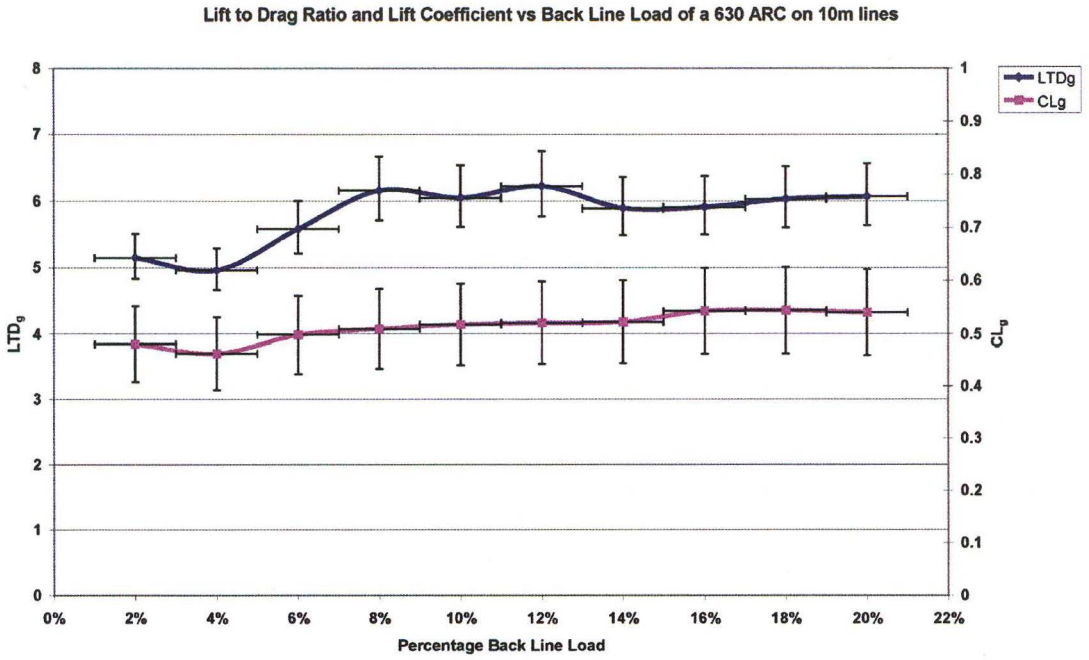

Figure 3:8 LTD_g and CLg results for a 630 ARC

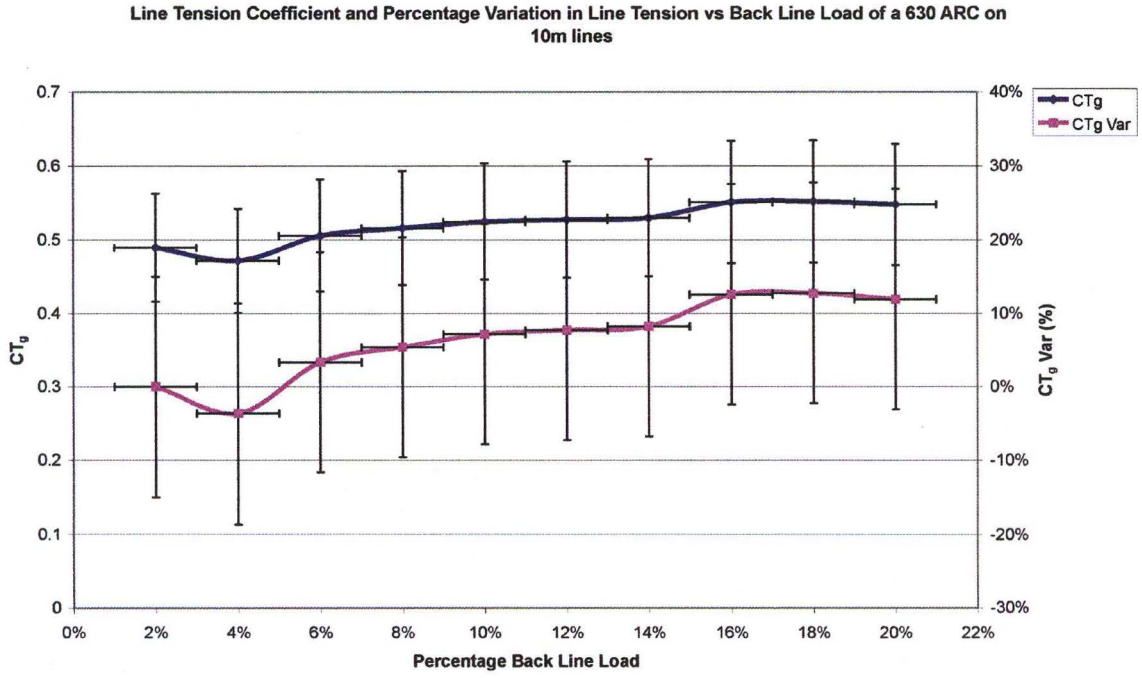

Figure 3:9 CTg and percentage variation in CTg results for a 630 ARC

These results were based on six different test runs. The results show the following key characteristics.

- There is an increase in the kite's Lift to Drag ratio until a plateau of 6 at 8% back line load is reached. This Lift to Drag ratio is considerably higher than for the smaller, 460 ARC.
- Once 8% back line tension is applied the Lift to Drag ratio does not vary.
- There is a slight increase in Lift Coefficient with back line tensions from 0.49-0.55 but this increase is far less noticeable than that achieved by the C-Quad kites.
- Like the 460 ARC this kite's performance is largely independent of back line load.

3.4.7 840 ARC results

Figure 3:10 and Figure 3:11 show the results for the 840 ARC. The nominal area of this kite is 8.4m^2. This particular kite is a later model than the other two ARC style kites tested.

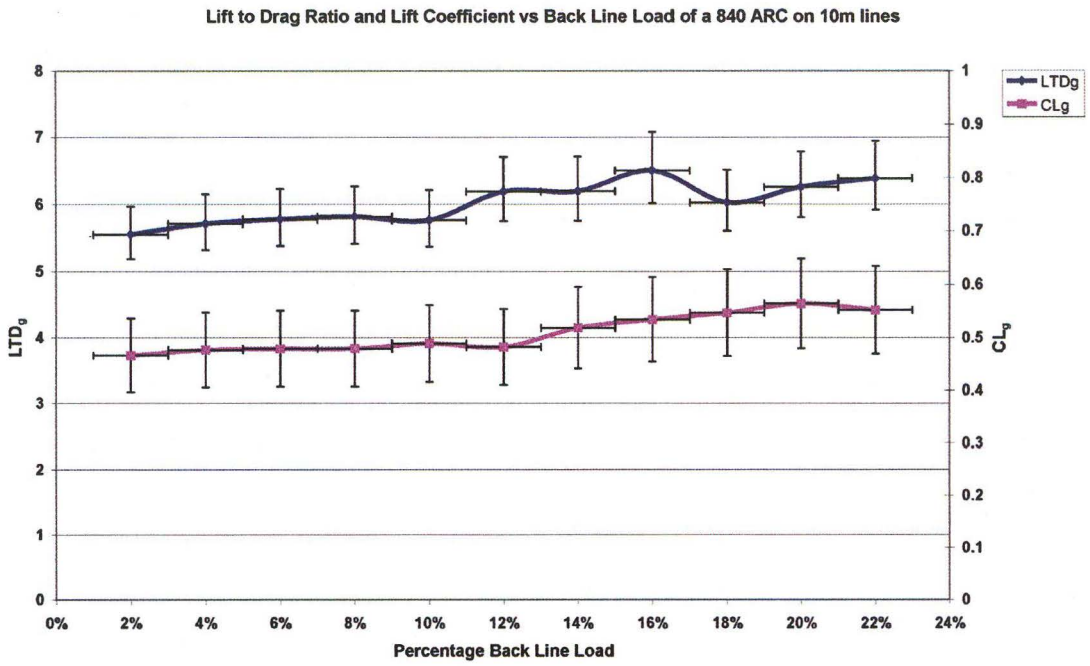

Figure 3:10 LTD_g and CLg results for a 840 ARC

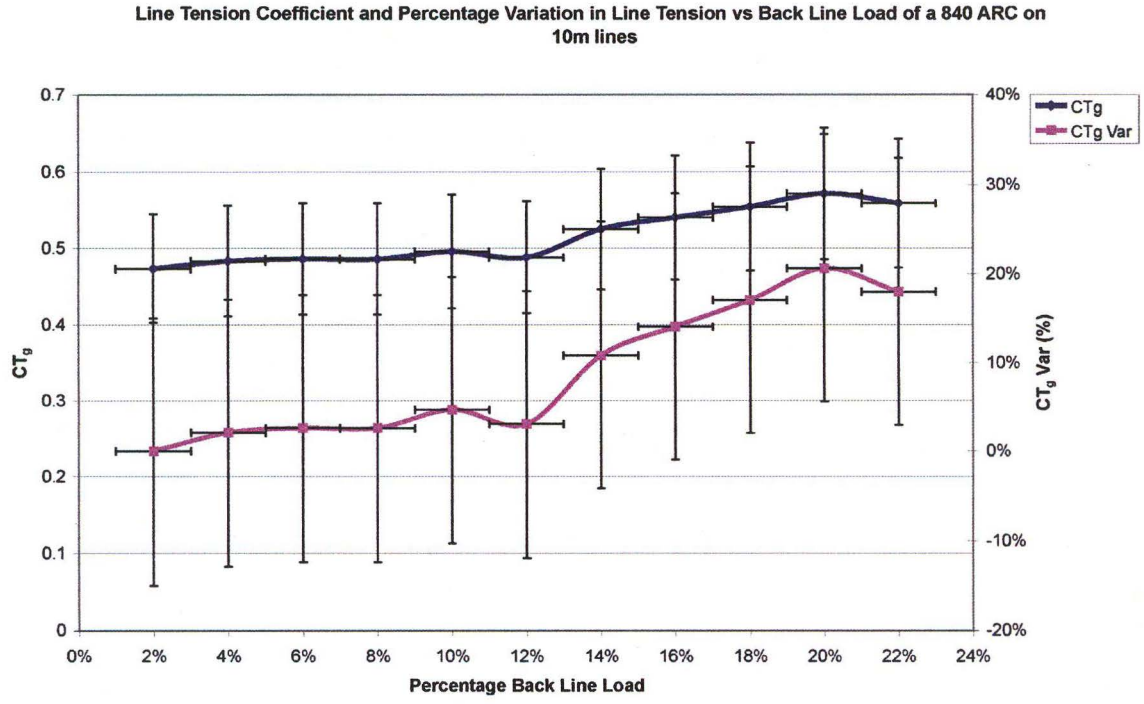

Figure 3:11 CTg and percentage variation in CTg results for a 840 ARC

These results were based on three tests. Based on the findings in Chapter 2 this is the minimum number of tests required to obtain a reasonable estimate of a kite's performance. The kite displayed the following characteristics.

- The peak Lift to Drag ratio of this kite is 6.5, higher than the other two smaller kites of the same design.
- The Lift to Drag ratio varies between 5.5 and 6.5 with back line tension. This kite does not show the plateau that the smaller ARC kites did.
- There is a very noticeable correlation between back line tension and Lift Coefficient. The Lift Coefficient varies between 0.47 and 0.57.
- The onset of stall occurs much later with this kite as a back line tension of 23% could be achieved during tests.

3.4.8 1200 FARC results

Figure 3:12 and Figure 3:13 show the results for a 1200 FARC. The nominal area is $12m^2$.

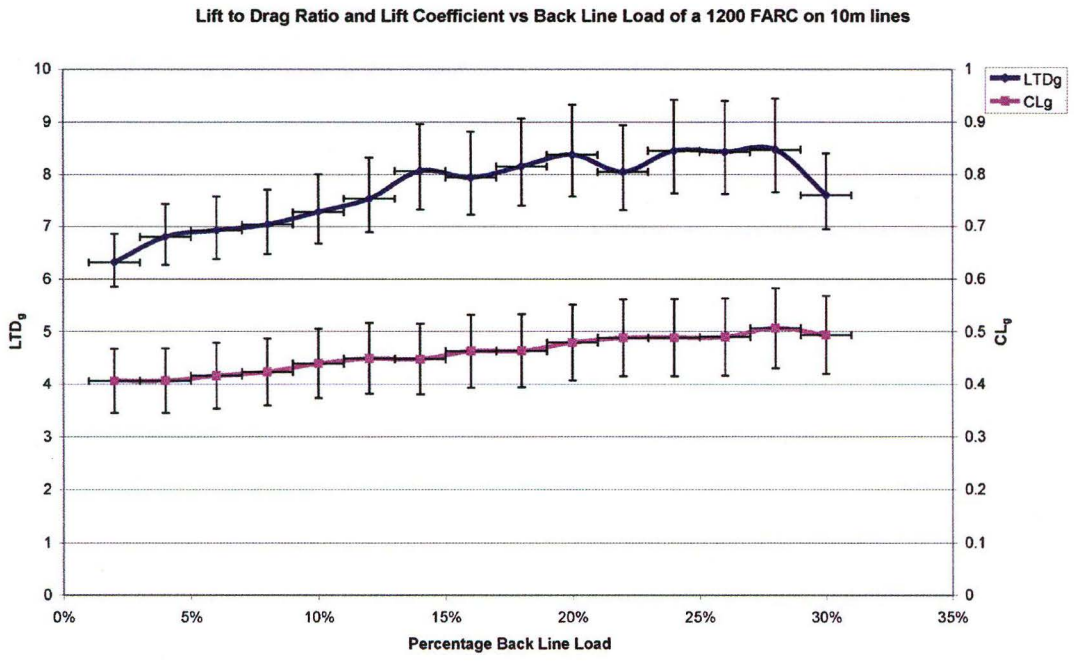

Figure 3:12 LTD_g and CLg results for a 1200 FARC

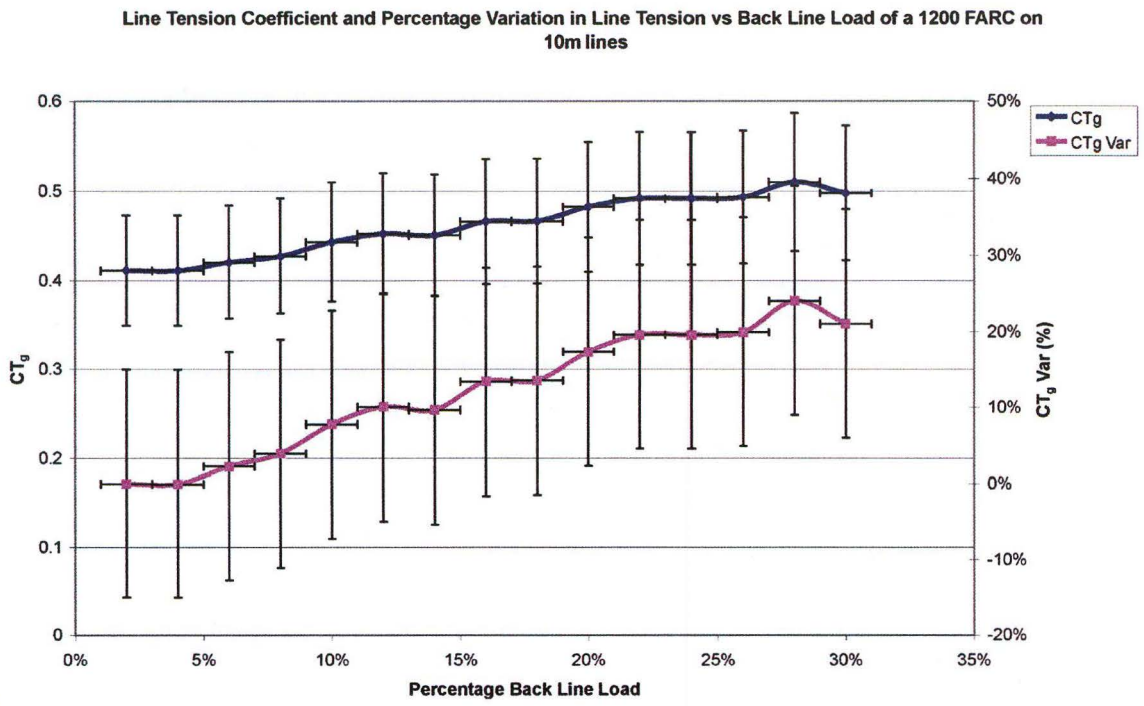

Figure 3:13 CTg and percentage variation in CTg results for a 1200 FARC

These results were based on four test runs. The kite displayed the following key characteristics.

- This kite has the largest Lift to Drag ratio of all the kites tested. The Lift to Drag ratio peaks at 8.5, well above other kites.
- A significant change in the Lift to Drag ratio can be achieved by varying the back line load. This is largely due to the fact that the kite structure tends to flap at back line tensions below 15%.
- A large amount of back line load can be applied before the kite stalls at 28-30% back line load.
- There is a direct relationship between Lift Coefficient and back line load. The Lift Coefficient varies between 0.4 and 0.5 with back line load.
- The variation in the line tension is relatively smooth.

3.5 Discussion

The results shown in the previous section represent six months of testing. Due to the necessity of having very little natural wind during tests, the number of suitable occasions for tests were very limited. The weather coupled with the rapid changes in kite designs that were occurring, meant that it was unrealistic to do a comprehensive test of all kites. Instead the focus was on commissioning the test rig for future use. The results shown here are only a few of the kites produced by Peter Lynn Kites Ltd, but using these results the following observations can be made.

The results are ordered by the age of the kite design and this shows that significant improvements have been achieved over the period of this project. The FARC's Lift to Drag ratio is essentially double that of the C-Quad, which represents a large improvement in kite performance.

Comparing the FARC results to the ARC results it is evident that despite being similar designs, the operator can vary the FARC's performance more than the ARC's. Although the FARC's Lift to Drag ratio is higher and can be varied more than the ARC's, it is perhaps the improvement in the Power Control capabilities, or the ability to change the aerodynamic coefficients, which is most significant. Despite this improvement, the original C-quad design had more power control that the 'ARC' style kites.

Measurements of the aerodynamic coefficients indicate that in some cases the nominal areas of kites are a marketing tool only loosely related to the actual size of the kite. By adjusting the size specification kites can be favourably compared to kites from other manufacturers. This is especially apparent when comparing the two C-Quad designs, that had significantly different Lift Coefficients. However, the reasonably consistent Lift Coefficient values of the ARC and FARC style kites show that for these types of kites a consistent area measurement system has been used.

Although not shown in the results there was little variation in the Lift to Drag performance of any kite with wind speed. At very low wind speeds there was a slight reduction in the performance due to the weight of the kite but this was only small and is largely irrelevant at the wind speeds a which the kite usually operates. It was expected that the performance of the kites would change at higher wind speeds as the increased load on the kite distorted the kite surface. This did not occur, with the kites' performances remaining stable to the peak of their wind range.

In some tests there was a reduction in the Lift Coefficient as the wind speed increased. In light of the stability of the Lift to Drag ratio with wind speed, this trend was not expected. However, this effect is more likely to be due to the presence of natural wind at the kite rather than changes in the kite properties. As shown in Chapter 2 natural wind has a large effect on the wind speed measurements at low speed so the test rig will tend to over-measure the Lift Coefficient at low speeds.

Although the test rig has identified these improvements in Lift to Drag ratio and Power Control it only provides information on a part of the overall performance of kites. The FARC may be the best performing kite of those tested but it is not ideal for all flyers. All the designs have characteristics that have not been shown here. These include turning ability, luff resistance and an element of 'feel' that it is very difficult to analyse. Not only is there room to test these things aspects, but a lot more thought needs to be put into determining what other qualities that need to be measured.

3.6 Conclusion

The test results shown in the chapter indicate that the car test rig can determine general trends in the development of Traction kites. From the results it is apparent that the design process at Peter Lynn Kites Ltd is succeeding at improving the performance of kites.

4. Line Drag Models

4.1 Summary

All of the kites tested using the car test rig were flown on 10m kite lines. In most cases these results are adequate to describe kite performance but in some situations it would be ideal to remove the effect of the lines from the results. This chapter outlines the methods described by Geola, Somu, Abedinzadeh and Vijaykumar (1985) to mathematically determine the effect of lines on kite performance. These methods were then applied to Traction kites for the conditions that they are used in. These results indicated that a simple straight-line method will adequately describe the line component for Traction kites. It is also apparent that the kite lines will have less effect on the performance of larger kites than that of smaller kites.

4.2 Introduction

Throughout the kite testing process kites were tested on 10m lines as long lines made testing easier, as outlined in Chapter 2. In addition, the forces on long lines could be estimated if raw kite data was ever required. This chapter outlines the models used to determine the effect lines have on the car test rig data. This chapter also identifies the major parameters used to generalise the effect of kite lines on kite performance.

4.3 Past Research

In the small amount of literature dedicated to kites much attention has been directed at the line (e.g., Hobbs, 1986. De Laurier, 1972a,b. Bryant, Brown & Sweeting, 1942). Kite lines have received this attention because they contribute more to the stability of the system than any other kite part. Generally these studies have been concerned with the

dynamics of the system and not on the effect of the lines on kite performance. However, the methods for analysing a kite line developed by Geola, Somu, Abedinzadeh and Vijaykumar (1985) are particularly relevant to this research. His methods are relative straightforward as it is assumed that the line is in static equilibrium, which is a valid assumption for Traction kite results from the car test rig. Geola, Somu, Abedinzadeh and Vijaykumar (1985) analysis also identified the factors that determine the impact of the line on the kite.

Geola, Somu, Abedinzadeh and Vijaykumar (1985) methods cannot be understood in isolation, as their working requires equations from Hoerner (1965). The working behind these methods have been reinterpreted in the following section, and then applied to the particular case of Traction kites. Geola, Somu, Abedinzadeh and Vijaykumar (1985) were interested in kites with long lines (>500m) so their results were reworked to be useful to Traction kites, which are flown on relatively short lines.

4.4 Models

Two models to describe the line forces and their impact on a kite are used in this project: a straight line model and a curved line model. The process for applying these models to kite results is outlined and the key parameters identified. In both cases a constant velocity profile has been used. The reasons for this are outlined in section 4.6.5.

4.4.1 Straight Line Model

The straight-line model assumes that the kite line runs directly from the flyer to the kite without any curvature. In real life the kite line does curve but this model assumes that the curve is not large enough to significantly affect the Lift and Drag Coefficients of the line (CL_l and CD_l). The Lift and Drag Coefficients of a line as a function of line angle (θ) have been defined in Hoerner (1965) as

$$CD_l = 1.1\sin^3(\theta) + .02 \qquad \text{Eq 4:1}$$

and

$$CL_l = -1.1\sin^2(\theta)\cos(\theta) \qquad \text{Eq 4:2}$$

If it is assumed that the angle and the tension of the kite line at the ground are known then by using the straight line method, the Lift to Drag ratio at the kite (LTD_k) can be found using the performance equations defined in Chapter 1 (Eq 1:7 to Eq 1:11). To obtain LTD_k, the line forces must be removed from the Lift to Drag ratio definition. Therefore

$$LTD_k = \frac{T_g \sin(\theta) + 1.1\sin^2(\theta)\cos(\theta)\frac{1}{2}\rho S\phi V^2 + m_l g}{T_g \cos(\theta) - (1.1\sin^3(\theta) + .02)\frac{1}{2}\rho S\phi V^2} \qquad \text{Eq 4:3}$$

where S is the line length, ϕ is the line diameter, and

$$\theta = \tan^{-1}(LTD_g) \qquad \text{Eq 4:4}$$

CL_k can also be found by

$$CL_k = \frac{T_g \sin(\theta) + 1.1\sin^2(\theta)\cos(\theta)\frac{1}{2}\rho S\phi V^2 + m_l g}{\frac{1}{2}\rho A_k V^2} \qquad \text{Eq 4:5}$$

These equations are very simple to apply to the kite test results to determine the effect of the kite lines on the kite.

4.4.2 Curved Line Model

There are a few methods of analysing the kite line to allow for curvature. The method described below is directly taken from Geola, Somu, Abedinzadeh and Vijaykumar (1985) as it shows the key variables that affect the line/kite system.

A line segment of length ds is shown in Figure 4:1. The tension (T) and the line angle (θ) vary along its length by dT and dθ respectively. Three separate line forces act on the segment. First there is a weight force per unit length (wt), secondly there is an aerodynamic force acting perpendicular to the line (K(θ))and lastly there is an aerodynamic force acting parallel to the line (K'(θ)). K(θ) and K'(θ) are not in the usual orientation of the aerodynamic forces but this orientation enables further mathematical simplifications.

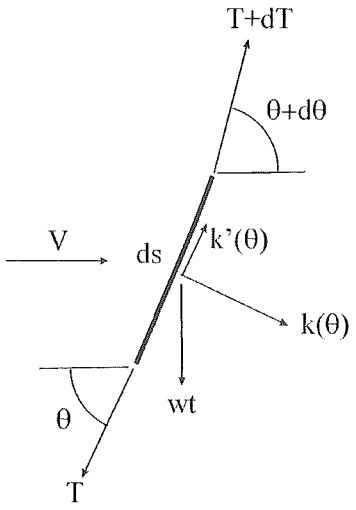

Figure 4:1 Forces acting on line segment ds

The aerodynamic forces k(θ) and k'(θ) are determined by projecting the aerodynamic coefficients defined in Eq 4:1and Eq 4:2 onto perpendicular and parallel directions relative to line. In the perpendicular direction the two coefficients combine to give

$$K(\theta) = \tfrac{1}{2}\rho\phi ds V^2\left(1.1\sin^2(\theta) + 0.02\sin(\theta)\right) \qquad \textbf{Eq 4:6}$$

and in the parallel direction they combine to give

$$K'(\theta) = \tfrac{1}{2}\rho\phi ds V^2 (0.02\cos(\theta)) \qquad \textbf{Eq 4:7}$$

Defining

$$E = 0.55\rho\phi V^2 \qquad \textbf{Eq 4:8}$$

and

$$E' = 0.05\rho\phi V^2 \qquad \textbf{Eq 4:9}$$

then

$$K(\theta) = E\sin^2(\theta) + E'\sin(\theta) \qquad \textbf{Eq 4:10}$$

and

$$K'(\theta) = E'\cos(\theta) \qquad \textbf{Eq 4:11}$$

If the line is in a stable location the forces shown in Figure 4:1 can be resolved in the direction perpendicular and parallel to the line to give

$$\frac{dT}{ds} = wt\sin(\theta) - K'(\theta) \qquad \textbf{Eq 4:12}$$

$$T\frac{d\theta}{ds} = wt\cos(\theta) + K(\theta) \qquad \textbf{Eq 4:13}$$

By dividing the line into several segments the change in angle and tension of the line can be determined using these equations. To solve these equations a boundary condition either at the ground or at the kite needs to be applied. At the ground the boundary condition is the tension and the angle of the line, along with its location. To apply a boundary condition at the kite, the kite's Lift to Drag ratio and Lift Coefficient are required prior to the tests. If they are not known an iterative process must take place. For kite tests the boundary condition at the ground is more appropriate as these are the results obtained by the car test rig.

When these equations are applied the angle of the line at the kite (θ_k) can be determined along with the tension at the kite (T_k). From these values, LTD_k and CL_k can be found by

$$LTD_k = \tan(\theta_k) \qquad \textbf{Eq 4:14}$$

and

$$CL_k = \frac{T_k \cos(\theta_k)}{\frac{1}{2}\rho A_k V^2} \qquad \textbf{Eq 4:15}$$

4.4.3 Important parameters

Geola, Somu, Abedinzadeh and Vijaykumar (1985) identified two major variables to determine the effect that the kite line has on the kite's performance. The first of these relates the tether weight to the line tension by

$$U_1 = \frac{Swt}{T}$$

As U_1 becomes smaller the weight of the kite line will have less effect on the kite.

The second ratio relates the line drag component to the weight of the line by

$$U_2 = \frac{E}{wt}$$

Since E and E' are related, only one ratio that compares the aerodynamic loads and the weight is required. If U_2 is small then the wind loadings can be ignored and a normal catenary model, where only the line weight is important, can be used. When both U_1 and U_2 are small the straight-line model can be used. If both U_1 and U_2 are large a curved line model is required.

4.5 Results

The following figures show how the ratio LTD_k/LTD_g varies for U_1 (Swt/t) and U_2 (E/wt) values appropriate for Traction kite conditions. The ratio LTD_k/LTD_g is determined as it can be used to convert LTD_g into LTD_k by

$$LTD_k = LTD_g \frac{LTD_k}{LTD_g} \qquad \textbf{Eq 4:16}$$

In the following figures, the straight and curved line models are shown. In many cases the two models are identical.

These graphs cover a wider range of conditions than are usually encountered. Typical Traction kite parameters are:

LTD_g = 4-7
S = 30m
wt = 0.02 N/m
T = 100-250 N – Average line tension over four lines
V = 6 – 20 m/s
ϕ - 0.001 m

Therefore

U_1 = 0.006 - .0024

and

U_2 = 1 – 15

For example: a kite is flying on 30m lines (same weight and diameter as above), in a wind of 10m/s, with 200N of line tension, and a LTD_g of 6. Therefore

$U_1 = 30x0.02/200 = 0.003$

$U_2 = 0.55x1.23x0.001x10^2/0.02 = 3.4$

Therefore, as shown in Figure 4:3 both the straight line and curved line models are virtually identical at this point, and LTD_k/LTD_g=1.075. Therefore

LTD_k=6x1.075 = **6.45**

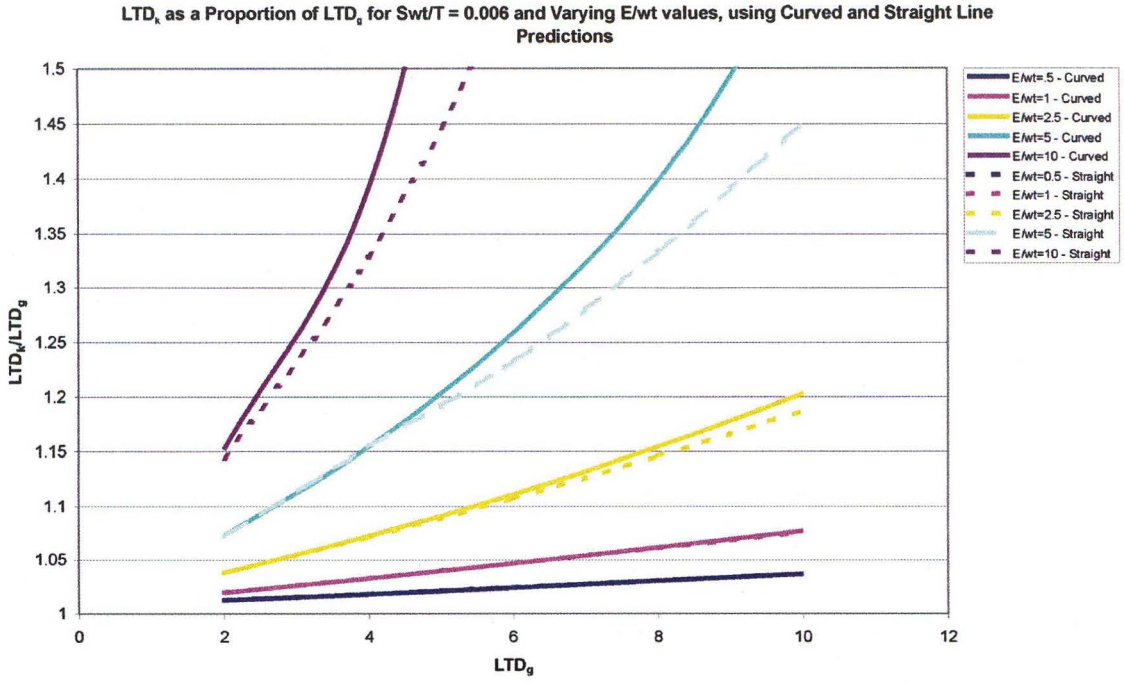

Figure 4:2 LTD$_k$/LTD$_g$ for Swt/T ratio of 0.006

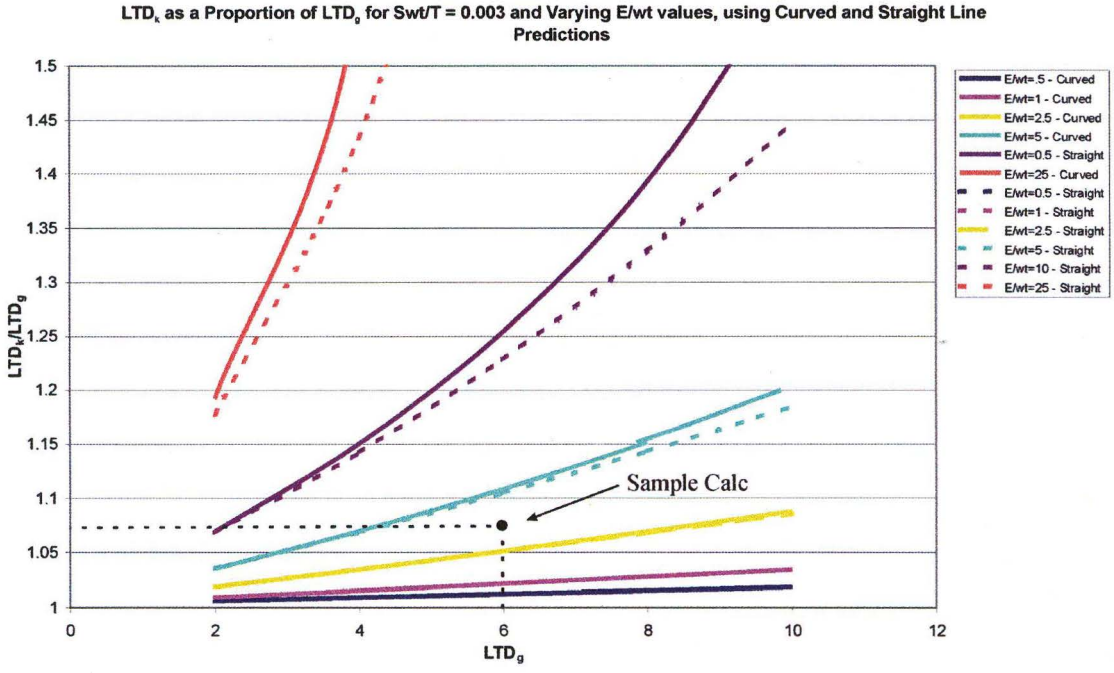

Figure 4:3 LTD$_k$/LTD$_g$ for Swt/T ratio of 0.003

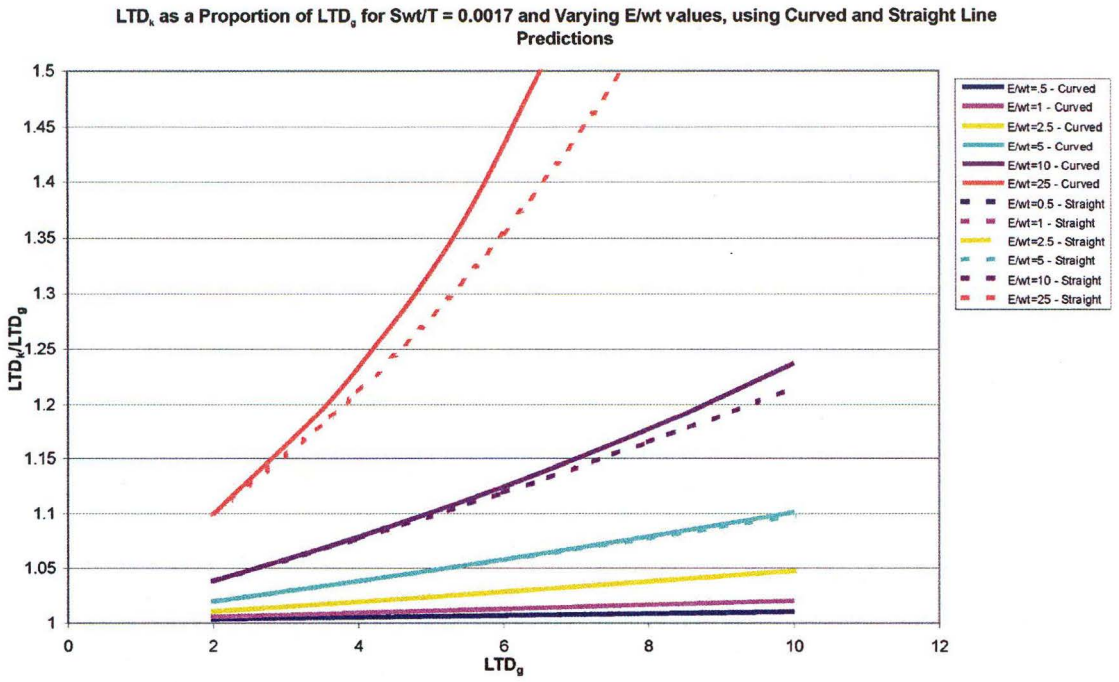

Figure 4:4 LTD_k/LTD_g for Swt/T ratio of 0.0017

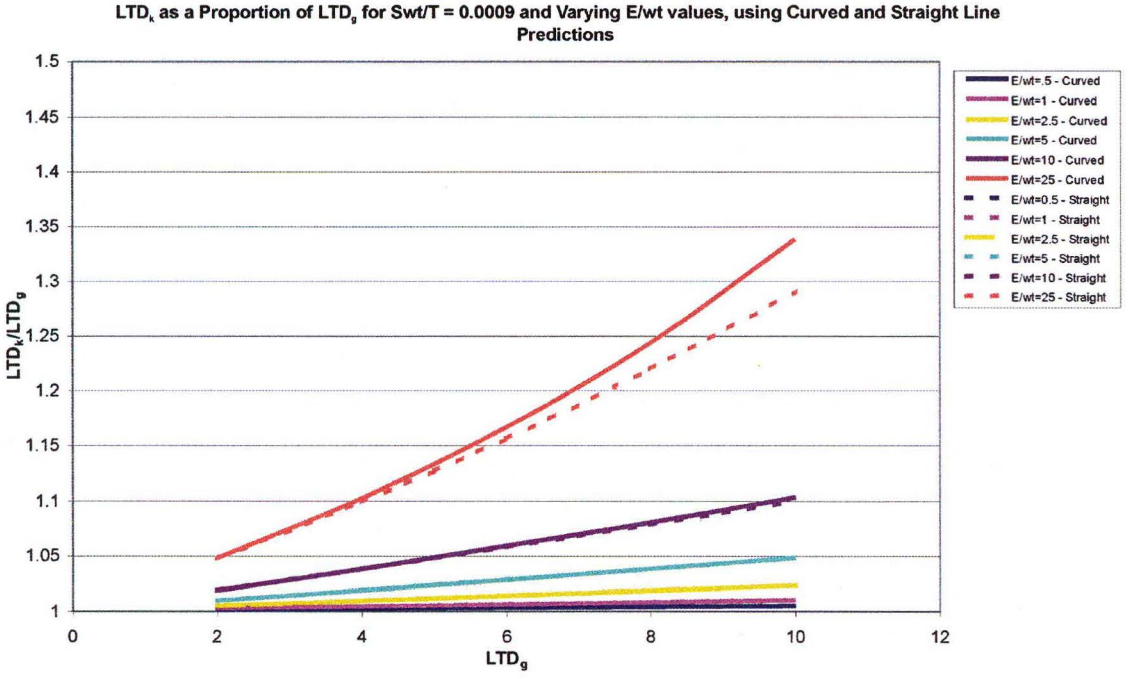

Figure 4:5 LTD_k/LTD_g for Swt/T ratio of 0.0009

4.6 Discussion

4.6.1 Straight Line vs Curved Line Method

Figure 4:2 to Figure 4:5 show that the results from the straight-line method differ from the curved line method when the ratios U_1 (Swt/T) and U_2 (E/wt) are large. However, in most cases the results from the two methods are identical.

When deciding which method to use to estimate the effect of the lines it therefore necessary to considering the relationship between U_1 and U_2. As the wind speed increases the line drag will increase, increasing the ratio U_2. At the same time the line tension will increase, as kite forces are also a function of wind speed, decreasing U_1. Figure 4:2 to Figure 4:5 show that the increased inaccuracy of the straight line method with increasing line drag (increasing U_2) is partially offset by the increase in line tension (reducing U_1).

In most cases the straight line method will be adequate for determining the line drag effect on a Traction kite. At the very least the simplicity of the straight line method is a very strong incentive for using it for a first approximation.

4.6.2 Size of kite, and line drag effect

Assuming that a straight-line method is used, a modifying factor can be determined that converts LTD_g to LTD_k. A modifying factor is a figure that can be directly applied to the data that is obtained from the test rig to convert it to LTD_k. In Figure 4:2 Figure 4:5 a single modifying factor was calculated, but for simplicity this modifying factor has been divided into two. These are calculated in the following way.

$$LTD_k = LTD_m \frac{L_k}{L_g} \frac{D_g}{D_k} \qquad \textbf{Eq 4:17}$$

where

$$\frac{L_k}{L_g} = \frac{CL_g OA_k - CL_L O\phi S + wtS}{CL_g OA_k} = 1 - \frac{CL_L \phi S}{CL_g A_k} + \frac{wtS}{CL_g OA_k} \qquad \textbf{Eq 4:18}$$

and

$$\frac{D_g}{D_k} = \frac{CD_g OA_k}{CD_g OA_k + CD_L O\phi S} = \frac{1}{1 + CD_k \phi S / CD_g A_k} \qquad \textbf{Eq 4:19}$$

if O is defined as equal to $\frac{1}{2}\rho V^2$.

Assuming that the aerodynamic coefficients do not significantly vary between different kites then it is apparent that both L_k/L_g and D_g/D_k are reduced as the area of the kite relative to the lines is increased. Since the same kite lines are used on different sized kites, smaller kites will have a larger line drag penalty than larger kites.

4.6.3 Multiple-Line Kites

Both line drag models analyse the effect of only one line on the kite's performance. These models are therefore adjusted when they are applied to kites with multiple lines. When using the straight-line method it is a matter of multiplying the Lift, Drag and weight forces by the number of lines that are attached to the kite. If the curved line method is used the adjustment for multiple lines is more complicated. The tension force used in Eq 4:12 and Eq 4:13 is the tension in each line rather than the total tension from the kite, requiring a modification in the calculations. With two-line kites the tension force used in Eq 4:12 and Eq 4:13 is simply half the total kite tension. The angle and the tension at the top of the line are then determined and used to calculate the Lift to Drag ratio and the aerodynamic coefficients using Eq 4:14 and Eq 4:15 (remember to double the tension at the kite when calculating the aerodynamic coefficients). Four-line kites make the calculations more complicated due to the difference in line tension between the front and the back lines. To do the calculations it is necessary to determine the angle and tension of each line at the kite. The performance equations, shown in the data analysis

methodology in Chapter 2, are then used to determine the Lift to Drag ratio and aerodynamic coefficients at the kite.

4.6.4 Low line tension

A significant problem occurs with applying these methods when the line tension is very low. This is particularly apparent with four-line kites when very little back line tension is applied. Low line tensions will cause a large amount of curvature in the lines, reducing the accuracy of the straight-line method. If the line tension is so low that the angle of the back lines at the kite is greater than 90^{o} to the wind, then the curved method will not work either, as the line tension is negative. In these cases the straight-line method is really the only option available. Although the straight-line method is not ideal in this case it will still allow a reasonable estimation of the whole kite's performance.

4.6.5 Velocity Profile

In these calculations a constant wind velocity profile with height is used. Primarily this is for simplicity but there are two other reasons. First, kites are generally flown on lines 10-30m so the difference in wind speeds experienced by the kite and the flyer is small. Secondly, the models are of particular use for the car test rig, which is used when there is very little natural wind, so there is only a slight velocity profile.

A velocity profile can be applied to the models in Section 4.4 to determine what the effect of varying wind speed has on the line drag calculations. To do this the height of the line at each segment is found and the velocity profile used in Chapter 2 is used to calculate the wind speed at this height. Once the wind speed is known, the aerodynamic forces acting on each line segment can be found. The calculations will then proceed as outlined.

In general a larger velocity at the kite will tend to reduce the effect of the kite lines, as it will increase the 'size' of the kite in proportion to the lines. The higher wind speed at the kite will increase the Lift and Drag forces on the kite relative to the lines. Section 4.6.2

showed how an increased kite size reduces the effect of the lines on the Lift to Drag measurements.

4.7 Conclusion

Using the line drag models described in this chapter is possible to determine the effect that the kite lines have on the measurement of LTD_k. For Traction kites it is usually adequate to apply the more simple straight-line model to the test data. However, the method used will ultimately depend on the conditions and the nature of the kite.

5. Circular Testing Theory

5.1 Summary

By flying a controllable kite in a horizontal circle a flyer is able to determine the performance of the kite from the geometry of the system. In particular the Lift to Drag ratio is related to the line length, the radius of the circle that the flyer walks in and the angle between the line and this radius. Since the kite is flying horizontally, the measured Lift to Drag ratio and Lift Coefficient differ from their usual definitions. However the results can be manipulated to obtain standard measurements. Despite this, the testing method is far less sensitive to measurement error than other methods, allowing accurate results to be obtained.

5.2 Outline of Method

On a day when there is no wind it is possible to fly a controllable kite by walking backwards in a circle and flying the kite in a horizontal circle. Figure 5:1 illustrates this method. Flying the kite in this manner allows the kite's performance characteristic to be determined, as its Lift to Drag ratio is related to: the radius of the circle the flyer walks (r); the length of the line attached to the kite (S); and the angle between S and r (λ).

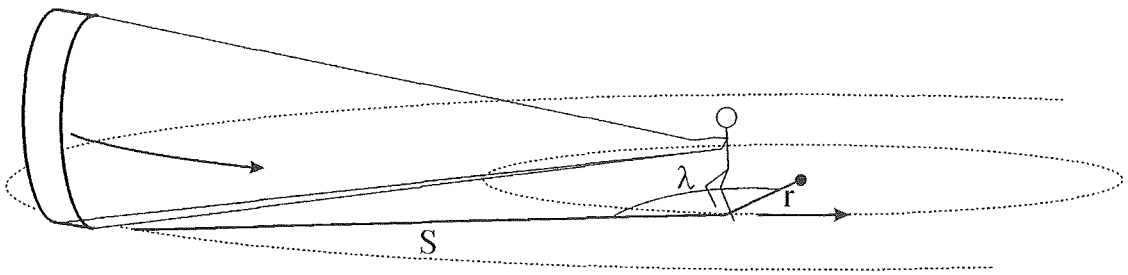

Figure 5:1 Flying a kite in a circle

To illustrate how the Lift to Drag ratio is obtained, assume that during a test the flyer modifies the circle radius (r) until the kite is flying directly in front of them. In this case λ will be 90^{o} as shown in the plan view of the system in Figure 5:2. This is a unique position as in this location three geometrically similar triangles are formed. The first is formed by the physical arrangement of S, r and an imaginary line between the centre of the circle and the kite (R). The velocity vectors at the kite form the second triangle. This is made up of the walking speed of the flyer (V_w), the velocity of the kite tangential to the line, which is equal to

$$V_{\perp} = \frac{S}{r} V_w \qquad \textbf{Eq 5:1}$$

and the resultant velocity (V_k), which is the apparent wind that the kite sees. The forces acting on the kite form the third triangle. The lift force (L_t) acts perpendicular to V_k while the drag force (D_t) acts parallel to V_k. The resultant force (T_t), which is felt as a tension in the line, must act down the line or the kite will move relative to the flyer. Since all these triangles are dimensionally similar the Lift to Drag ratio can be found by

$$\frac{L_t}{D_t} = \frac{S}{r} \qquad \textbf{Eq 5:2}$$

The parameters S and r are relatively simple to obtain making this testing method very attractive for testing kites.

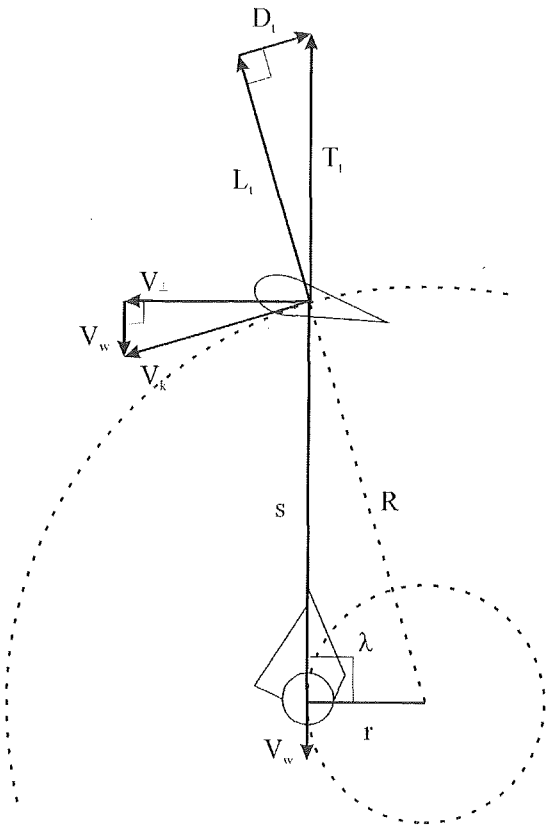

Figure 5:2 Plan view of 90° testing arrangement

The Lift to Drag ratio obtained is defined as L_t/D_t to distinguish it from the usual definitions of the Lift to Drag ratio as defined in Chapter 1. It will be shown how this value relates to the more usual definition in Section 5.4.

Flying the kite directly in front of the flyer is a special case. If the dimensions r and S are fixed, λ will depend on the characteristics of the kite. There are three general positions that the kite can fly: λ equals 90°, as already described; λ greater than 90°, and λ less than 90°. Figure 5:3 illustrates these three positions showing the velocity vectors and force vectors as they apply in each case.

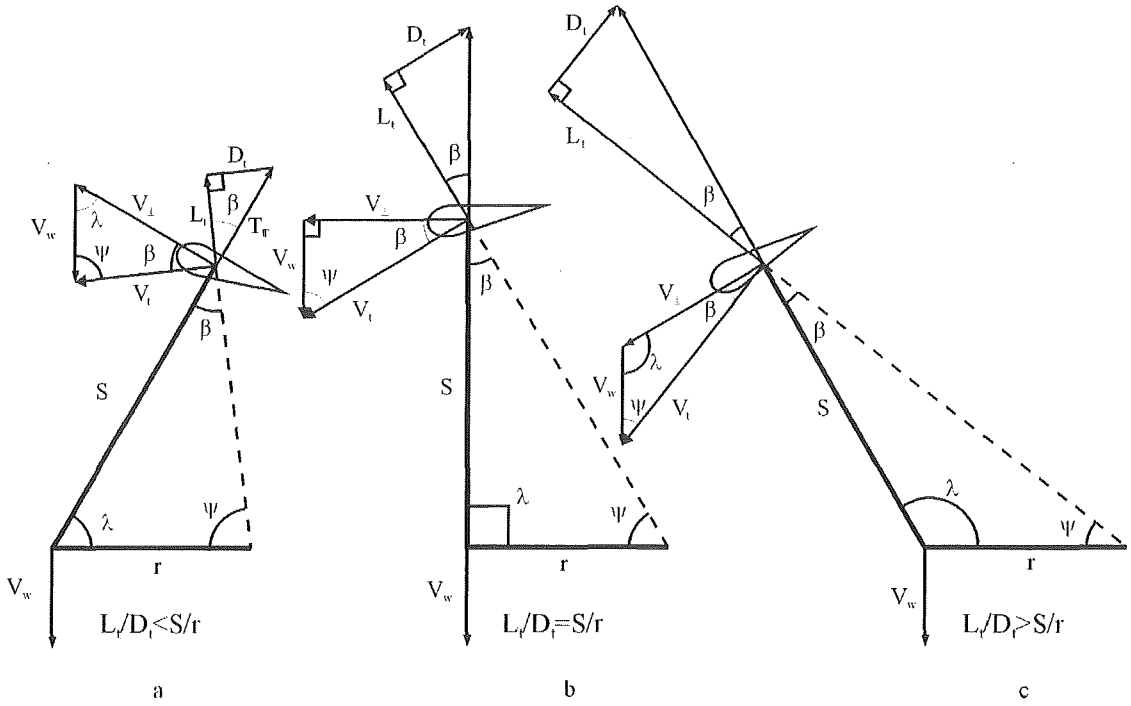

Figure 5:3 General flying positions

The force triangle is only dimensionally similar to the velocity and the physical setup when λ equals 90°. Only in this particular case does Eq 5:2 apply. To determine the Lift to Drag ratio in all cases the angle β must be determined. The Lift to Drag ratio is related to β by the formula

$$\frac{L_t}{D_t} = \frac{1}{\tan(\beta)} \qquad \textbf{Eq 5:3}$$

β can be found by using the following equation

$$\beta = \sin^{-1}\frac{r\sin(\lambda)}{\sqrt{r^2 + S^2 - 2rS\cos(\lambda)}} \qquad \textbf{Eq 5:4}$$

Therefore, to determine the Lift to Drag ratio of the kite the only parameters that are required are the line length, the radius of the walking circle and the angle that the lines form with this radius.

These parameters are relatively easy to obtain indicating that this could be an effective testing method. More importantly, the space required to do this test is less than that for other methods.

5.2.1 Past research on circular testing

No evidence could be found that other researchers have considered using this method to determine the performance of kites.

5.3 Characteristics of this method

5.3.1 Varying Rig Dimensions

By varying the line length (S) and the radius of the circle (r), kites with different performance characteristics can be made to fly at a different angles, λ. Figure 5:3 shows that λ is related to β by the equation

$$\lambda = 180 - \beta - \sin^{-1}\left(\frac{S}{r}\sin(\beta)\right) \qquad \textbf{Eq 5:5}$$

The relationship between the line angle λ and Lift to Drag ratio, for different S/r ratios, is shown in Figure 5:4. This graph was calculated using Eq 5:3 and Eq 5:5. Figure 5:4 indicates that that if S>r (which it normally will be) there is a minimum ratio, $L_t/D_{t\ min}$, that a particular setup can test for. For example, for a setup of S/r=2, the $L_t/D_{t\ min}$ is approximately 1.73. It is impossible for a kite with a lower Lift to Drag ratio to be tested using this setup.

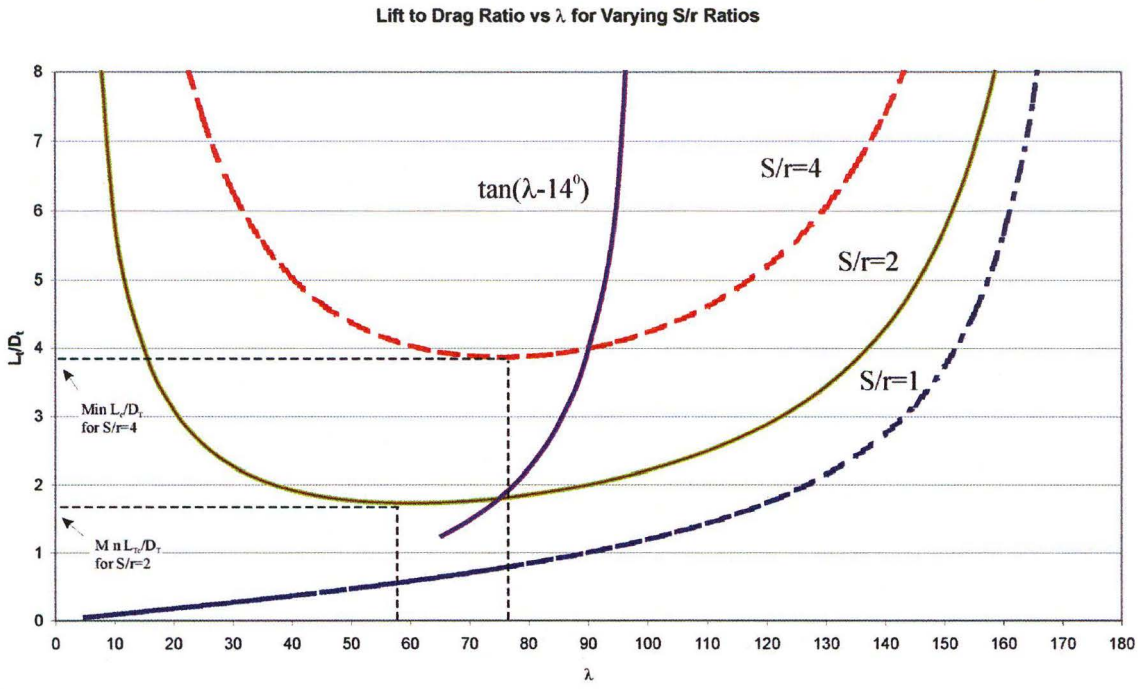

Figure 5:4 Effect of varying S/r ratio

From Figure 5:3 and Eq 5:3 it can be seen that the minimum Lift to Drag value is found when β is at a maximum. From Figure 5:3 and using the sine rule

$$\sin(\beta) = \frac{r\sin(\psi)}{S} \qquad \textbf{Eq 5:6}$$

where ψ is the angle between r and R. From Eq 5:6 the maximum value of β will occur when ψ equals 90° and the minimum Lift to Drag ratio that can be tested is

$$L_t/D_{t\,min} = 1/\tan(\sin^{-1}(r/S)) = \sqrt{S^2 - r^2}/r \qquad \textbf{Eq 5:7}$$

Figure 5:4 indicates that above this minimum Lift to Drag ratio there are two possible angles λ that a kite with a given L_t/D_t can fly. Realistically the kite will only sit at the larger of these two angles, as the lower angle is unstable. This is illustrated in Figure 5:5, which shows the forces on the system when the kite is located so that the line angle,

λ, corresponds to a Lift to Drag ratio measurement greater than the kite's Lift to Drag ratio (i.e., $\beta_k > \beta_t$). As shown in Figure 5:4, for λ's above L_t/D_{tmin}, a measured Lift to Drag ratio above the kite's Lift to Drag ratio corresponds to a line angle, λ, larger than the stable value. In this case the forces on the kite ($F_\perp$) will return it to a stable position. At line angles below L_t/D_{tmin} , a test larger Lift to Drag ratio corresponds to a reduced λ. As shown in Figure 5:5, in this case the kite will tend to reduce λ even further, rather than returning the kite to a stable flying location.

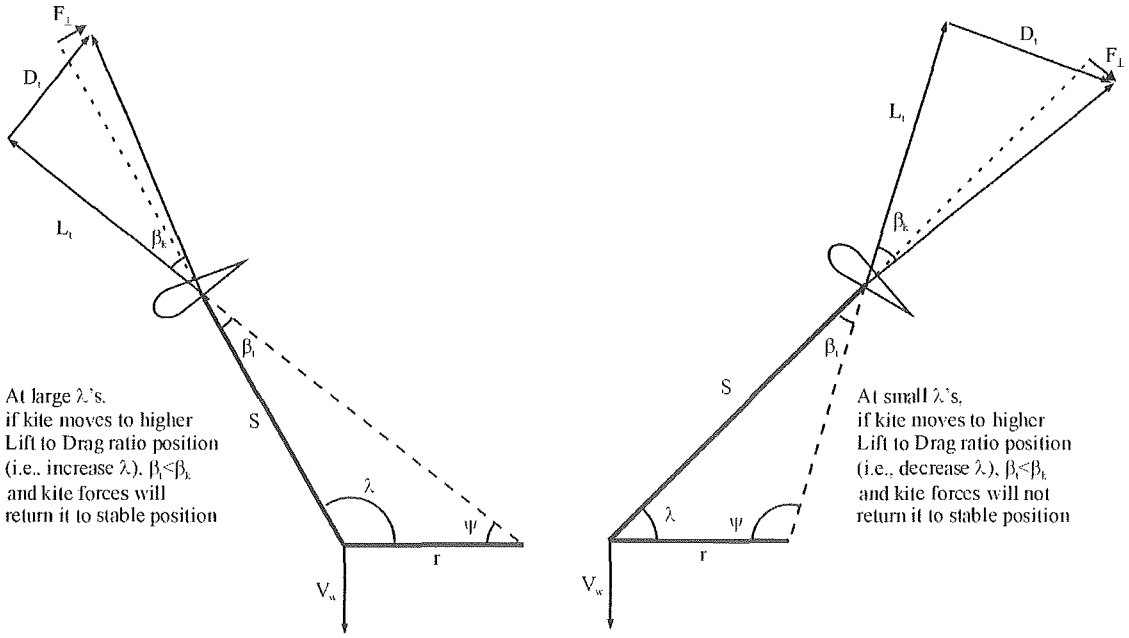

Figure 5:5 Restoring forces on kite due to perturbation in flying location

A minimum L_T/D_T ratio only exists when the line length is greater than the arm length i.e., S>r. If the arm is longer than the lines, it is possible to test for all L_t/D_t ratios. However, with a setup like this it will be difficult to get an accurate result since the measured Lift to Drag ratio will become very sensitive to angle variation, as most kites would fly at a high angle λ.

As shown in Figure 5:4, the Lift to Drag curves in relation to λ are relatively flat near the 90^o point. By adjusting the test setup so that the kite is flying in this location the

sensitivity of this method to the angle measurements can be reduced. Being able to tune the test conditions for each kite in this way gives this testing method an advantage over other testing procedures. Included in Figure 5:4 is a curve showing the variation in Lift to Drag ratio with the line angle for a kite flying directly above the flyer (i.e., as occurs in the car test rig). This curve has been shifted to the right by 14° so a direct comparison with the S/r=4 curve can be made. The flatter slope of the circular testing curve demonstrates that this method is far less sensitive to angle change than the car test rig. This is the main reason why this method is worth pursuing over others as a viable testing method for kites.

5.3.2 Bridle Length

Prior to this point the line length (S) used in equations assumes that the kite does not have any bridles. However, the distance S is actually the distance to the lifting surface so the length of the bridle has to be included as part of the line length, S.

5.3.3 Wing shape

Ideally the lifting surface should be flat so that both the magnitude and direction of the wind that the wing sees is constant over its surface. Increasingly Traction kites have an arc-style profile, which causes there to be a greater variation in wind speed over their lifting surfaces. However, by using long lines (i.e., s>30m) the variation in velocity over the kite will become increasingly insignificant.

5.3.4 Line Tension and CL

If the line tension of the kite can be measured then the Coefficient of Lift can be determined. In this case

$$L_t = \frac{T_t}{\sqrt{1+\left(\frac{1}{L_t/D_t}\right)^2}} = T_t \cos(\beta) \qquad \textbf{Eq 5:8}$$

which can then be converted to a Lift Coefficient using Eq 1:3. To do this the velocity of the kite (V_k) needs to be determined. V_k is related to the geometry of the system by

$$V_k = V_w \frac{R}{r} \qquad \textbf{Eq 5:9}$$

and R can be found by

$$R = \sqrt{r^2 + S^2 - 2rS\cos(\lambda)} \qquad \textbf{Eq 5:10}$$

The line tension is also required to convert the Lift to Drag ratio obtained in this test to the more usual definitions of Lift and Drag ratio as shown in section 5.4.

5.3.5 General comparison with more usual definitions of kite performance

How the kite performance measurements taken from this test method differ from usual performance measurements will be outlined in the next section. However, based on typical kite parameters, the Lift to drag ratio and Lift Coefficients obtained by this type of test method will be within 10% of the kite's performance using usual definitions. If this is not adequate, the following section outlines how these measurements can be adjusted to give a closer comparison.

5.4 Converting L_T/D_T to L/D and (L-mg)/D

The Lift to Drag ratio obtained by applying Eq 5:3 and Eq 5:4 is not the same as the more usual definitions found in Chapter 1. Because the kite is flying in a horizontal circle it is subjected to centrifugal forces and due to its orientation, the mass of the kite acts in a different plane to normal. The aerodynamic forces on the lines are also different to those on a stationary kite and the lines have centrifugal forces acting along their length.

THE LIBRARY
UNIVERSITY OF CANTERBURY
CHRISTCHURCH, N.Z.

Figure 5:6 shows how these forces affect the system while Figure 5:7 is a plan view of the vector diagram used to determine the actual Lift to Drag ratio from the measured value. Modifying factors are used to convert the measured values into the more usual definitions of kite performance.

Throughout this analysis De Lambert's theorem has been used to account for the centrifugal forces rather than Newton's method. This allows the problem to be considered a statics problem, as this is useful for working out the modifying factors.

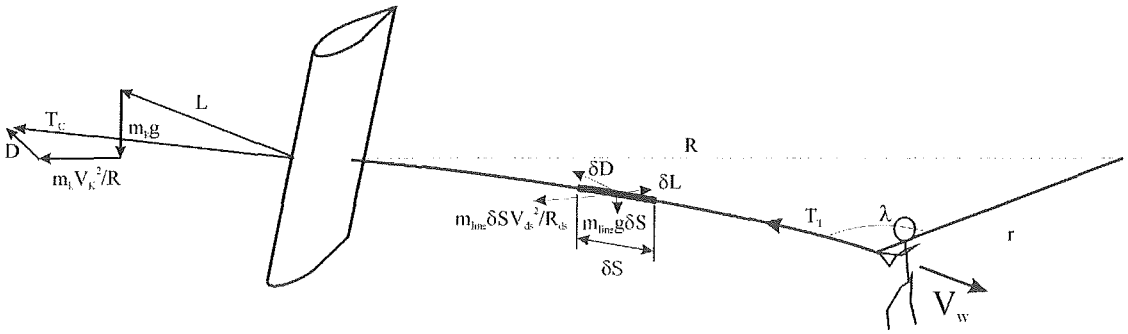

Figure 5:6 Forces on system

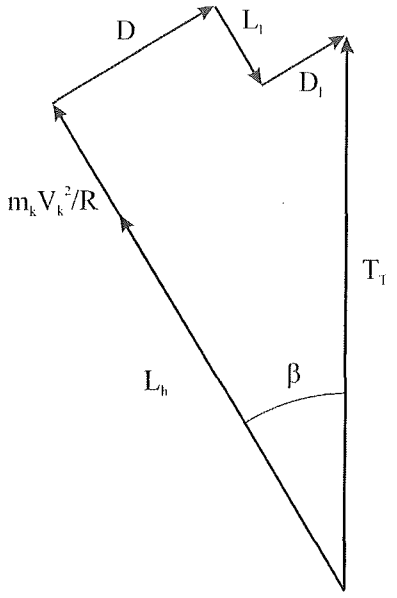

Figure 5:7 Plan view of force vectors

5.4.1 Removing the effects of the Lines

Determining the effect of the lines in this system is more difficult than for a kite being flown in natural wind as shown in Chapter 4. Moving away from the flyer the wind varies both in strength and direction, changing the aerodynamic loads and the centrifugal force on the lines.

One way to determine the modifying factor to remove the effect of the lines is to project the forces on the line so they are orientated in the same direction as the Lift and Drag forces acting on the kite wing. Doing this enables modifying factors to be applied in the following way.

$$\frac{L_c}{D} = \frac{L_t}{D_t} \cdot \frac{L_c}{L_t} \cdot \frac{D_t}{D} \qquad \textbf{Eq 5:11}$$

Where L_c/L_t and D_t/D are the modifying factors to remove the effect of the lines. From Figure 5:7 it can be seen that

$$\frac{L_c}{L_t} = 1 + \frac{L_l}{T_t \cos(\beta)} \qquad \textbf{Eq 5:12}$$

and

$$\frac{D_t}{D} = \frac{1}{1 - D_l / T_t \sin(\beta)} \qquad \textbf{Eq 5:13}$$

where L_l and D_l are the forces on the lines in the direction of the wings lift and drag force. It is also necessary to modify the tension force that is being measured using the following equation.

$$T_c = T_t \cdot \frac{T_c}{T_t} \qquad \textbf{Eq 5:14}$$

where

$$\frac{T_c}{T_t} = \frac{\sqrt{(T_t \sin(\beta) - D_l)^2 + (T_t \cos(\beta) + L_l)^2}}{T_t} \qquad \textbf{Eq 5:15}$$

D_l and L_l can be calculated by finding the forces acting along the length of the line. Figure 5:8 shows the forces acting on a small segment of the line ds.

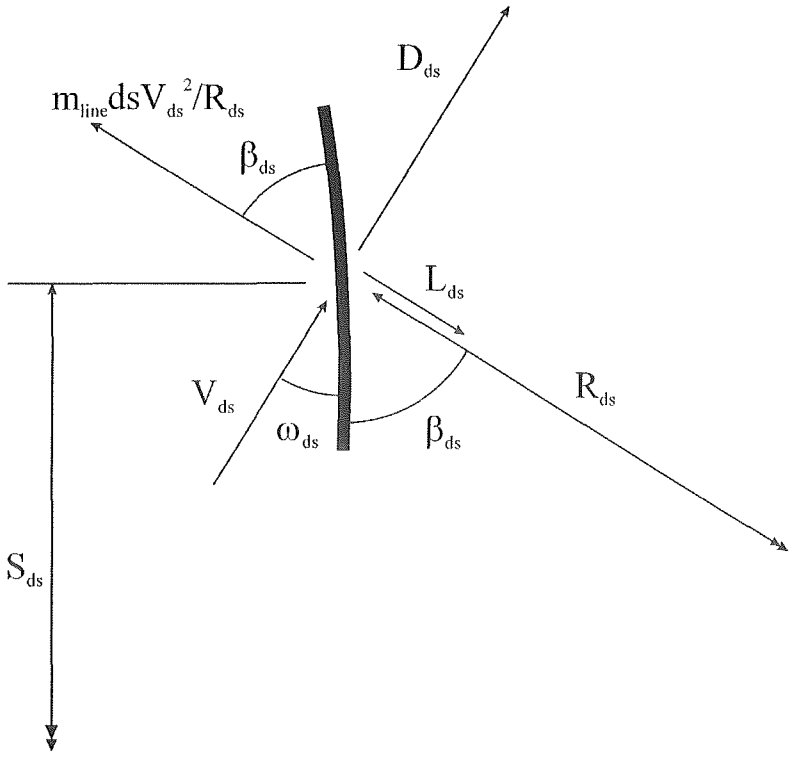

Figure 5:8 Forces on a Line Segment ds

Using equations for line drag and lift from Hoerner (1965), the forces acting on the line are

$$D_{line} = \frac{1}{2}\rho\phi \int_0^S \left(1.1 \sin^3(\omega_{ds}) + .02\right) V_{ds}^2 \, ds \qquad \textbf{Eq 5:16}$$

and

$$L_{line} = \frac{1}{2}\rho\phi\int_0^S \left(1.1\sin^2(\omega_{ds})\cos(\omega_{ds})\right)V_{ds}^2 ds \qquad \textbf{Eq 5:17}$$

Where the positive lift acts towards the flyer. The centrifugal force is

$$CF = \int_0^s \frac{m_{line}V_{ds}^2}{R_{ds}} ds \qquad \textbf{Eq 5:18}$$

Since

$$\omega = f(r, S_{ds}) \qquad \textbf{Eq 5:19}$$

and

$$V = f(r, S_{ds}, \lambda, V_w) \qquad \textbf{Eq 5:20}$$

and

$$R = f(r, S_{ds}, \lambda) \qquad \textbf{Eq 5:21}$$

it is appropriate to divide the line into finite lengths and sum the forces. The analysis that generated the following results assumed that the line was straight. This assumption is realistic as in most cases the line angle only changes marginally along its length (see Chapter 4)

Figure 5:9, Figure 5:10, Figure 5:11 and Figure 5:12 are graphs showing the forces coefficients on the lines in the lift and drag directions from aerodynamic (CL_{line} and CD_{line}) and centrifugal forces (CL_{cent} and CD_{cent}). The values are dimensionless coefficients and to obtain the actual drag and lift values these results need to be modified by

$$D_{line} \ \& \ L_{line} = r\phi\rho V_w^{\ 2} n(CD_{line} \ \& \ CL_{line}) \qquad \textbf{Eq 5:22}$$

while the centrifugal force in the Lift and Drag directions is

$$D_{cent} \ \& \ L_{cent} = m_{line} V_w^{\ 2} n(CD_{cent} \ \& \ CL_{cent}) \qquad \textbf{Eq 5:23}$$

where n is the number of lines attached to the kite. All these coefficients have been worked out based on V_w, as this is the speed that is measured during a test rather than V_k.

D_l and L_l then equal

$$D_l = D_{line} + D_{cent} \qquad \textbf{Eq 5:24}$$

and

$$L_l = L_{line} + L_{cent} \qquad \textbf{Eq 5:25}$$

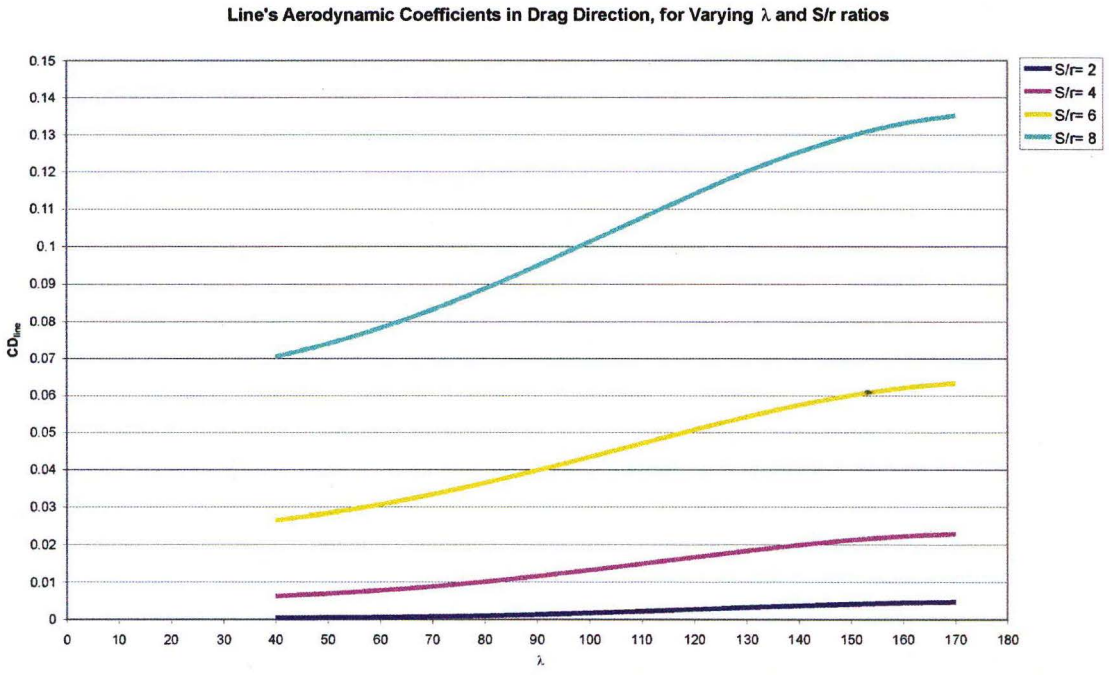

Figure 5:9 Line's aerodynamic coefficient in drag direction

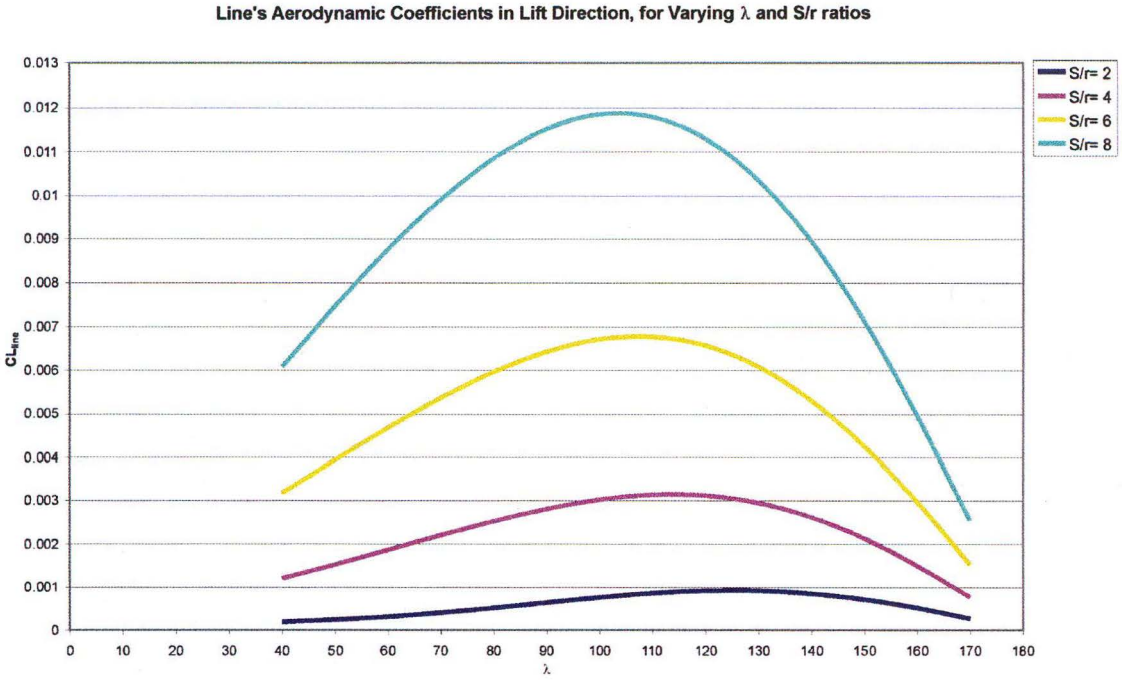

Figure 5:10 Line's aerodynamic coefficient in lift direction

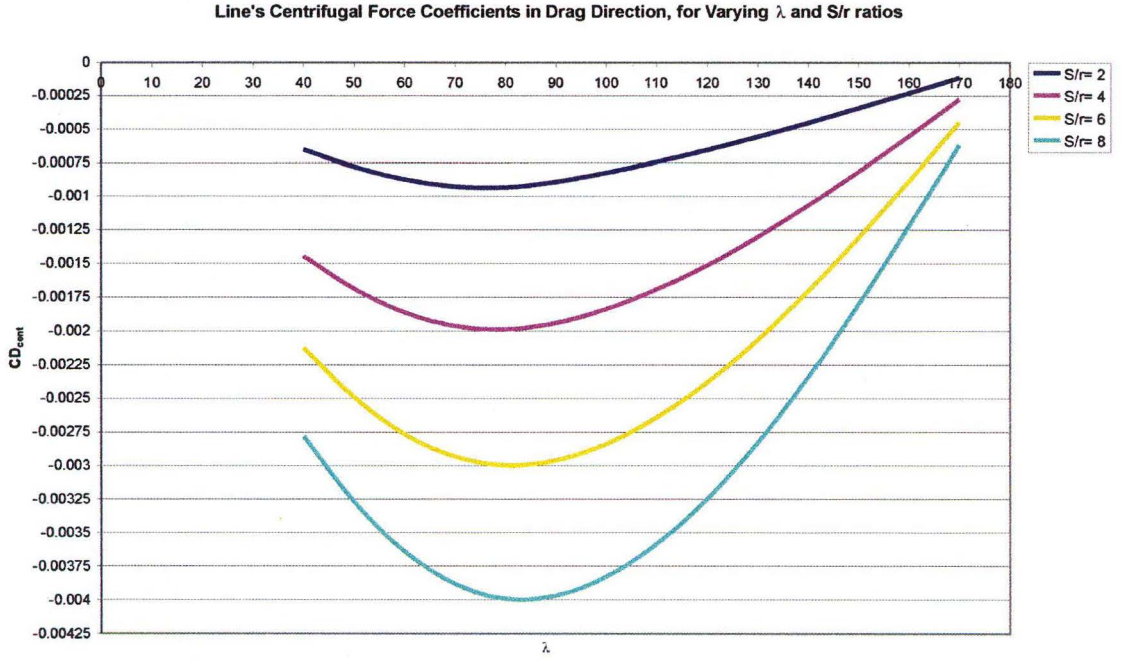

Figure 5:11 Line's centrifugal force coefficient in drag direction

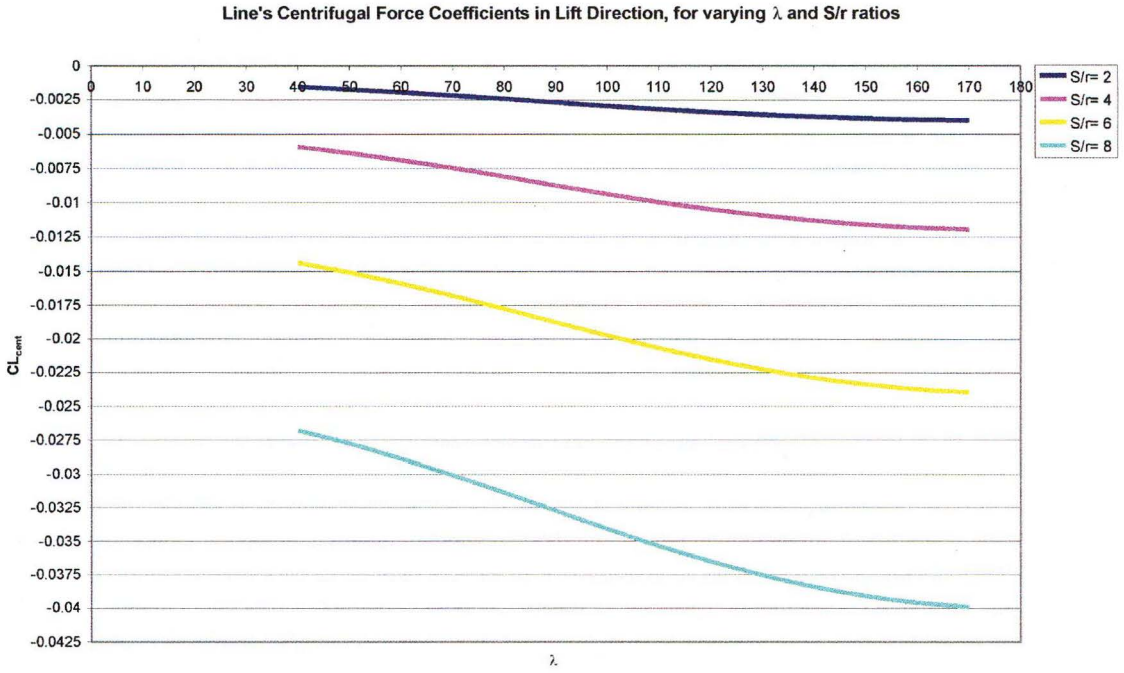

Figure 5:12 Line's centrifugal Force coefficient in lift direction

Once the forces in each direction have been obtained, Eq 5:12, Eq 5:13 and Eq 5:15 can be applied

For example, a kite has the following parameters

S/r=4

r=7.5 m

V_w=2.5 m/s

n=4

ρ=1.23

ϕ=.5

m_{line} = 1.5g/m

In the test the following results were obtained

λ= 105°

T_T=300N

So from Eq 5:4

β=12.77

and from Eq 5:3

L_T/D_T=4.4

Using Figure 5:9, Figure 5:10, Figure 5:11 & Figure 5:12the forces in the lift and drag directions are

D_{line}= 7.5· 0.5· 1.23· 2.5^2· 4·(0.014) =1.61N

L_{line}= 7.5· 0.5· 1.23· 2.5^2· 4·(0.0031)=0.36N

D_{cent}=1.5· 2.5^2· 4· (-0.00185) =-0.07 N

L_{line}=1.5· 2.5^2 4· (-0.0097)=-0.36N

Therefore

D_l= 1.61-.007 = 1.54N

L_l= 0.36 –0.36 = 0N

And from Eq 5:12, Eq 5:1 & Eq 5:15

L_c/L_T = 1

D_T/D = 1/(1-1.54/300sin(12.77))=1.024

T_h/T_T = sqrt((300sin(12.77)-1.54)^2+(300cos(12.77))^2)/300=0.999

Therefore L_c/D of the kite is

L_c/D=4.4· 1.024=**4.51**

which is a 2.4% offset, while

T_C=300· 0.999=299.7N

which is a 0.1% offset.

It should be noted that if the geometry of the test stays constant then the modifying factors will remain constant with speed. Even though the forces on the line increase in proportion to the velocity squared, so too does the forces on the wing.

5.4.2 Removing the Centrifugal force on the kite wing

Because of its mass there is a centrifugal force component acting on the kite as it flies in its circular path. This force acts in the same direction as the aerodynamic lift force. To eliminate the effect of this force, another set of modifying factors are determined[3]. In this case

$$\frac{L_h}{D} = \frac{L_c}{D} \cdot \frac{L_h}{L_c} \qquad \textbf{Eq 5:26}$$

And

$$T_h = T_c \cdot \frac{T_h}{T_c} \qquad \textbf{Eq 5:27}$$

Assuming that the Lift to drag values and the tension values have been modified for line effects then the modifying factors become.

$$\frac{L_h}{L_c} = 1 - \frac{m_k V_k^{\,2}}{R T_c \cos(\beta)} \qquad \textbf{Eq 5:28}$$

$$\frac{T_h}{T_c} = \sqrt{1 - \frac{2 m_k V_k^{\,2} \cos(\beta)}{T_c R} + \frac{m_k^{\,2} V_k^{\,4}}{T_c^{\,2} R^2}} \qquad \textbf{Eq 5:29}$$

[3] See appendix II for complete derivation of modifying factor

Using the same kite as in section 5.4.1, with the values already modified for line effects, and assuming that m_k= 0.5 kg then these modifying factors are calculated as

β = atan(1/4.51) = 12.5

R=sqrt(7.5^2+30^2-2(7.5)(30)cos(105)) = 32.75 m

$$V_k = V_w \frac{S}{r}\sqrt{1+\left(\frac{r}{S}\right)^2 - 2\frac{r}{S}\cos(\lambda)} = 2.5 \cdot 4 \cdot \sqrt{1+\frac{1}{16} - \frac{\cos(105)}{2}} = 10.92 m/s$$

$$\frac{L_h}{L_C} = 1 - \frac{0.5 \cdot 10.92^2}{32.75 \cdot 299.7 \cdot \cos(12.5)} = 0.994$$

$$\frac{T_h}{T_c} = \sqrt{1 - \frac{2 \cdot 0.5 \cdot 10.92^2 \cos(12.5)}{299.7 \cdot 32.75} + \frac{0.5^2 \cdot 10.92^4}{299.7^2 \cdot 32.75^2}} = 0.988$$

Therefore

L_h/D=4.51· 0.994 = **4.48**

T_h=299.7· 0.988 = **296.1**

This is an offset of 0.6% on the Lift to Drag ratio and 1.2% on the line load. As the length of the lines increase, the magnitude of the centrifugal force reduces so its effect will be less. Also, like the line forces, the modifying factors for the kite's centrifugal force should stay constant with speed as long as the geometry does not change, since both the centrifugal force and kite forces are a function of V^2.

5.4.3 Removing the Mass Effect

Because of the direction of the lift force in relation to the mass, a modifying factor is needed to acquire the more usual measures of Lift to Drag ratio. In this case two sets of modifying factors are defined: one to convert L_h/D to L/D and another to convert L_h/D to (L-Mg)/D. In these cases

$$\frac{L}{D} = \frac{L_h}{D} \cdot \frac{L}{L_h} \qquad \textbf{Eq 5:30}$$

$$T = T_h \cdot \frac{T}{T_h} \qquad \textbf{Eq 5:31}$$

$$\frac{L - Mg}{D} = \frac{L_h}{D} \cdot \frac{L - Mg}{L} \qquad \textbf{Eq 5:32}$$

$$T_g = T_h \cdot \frac{T_g}{T_h} \qquad \textbf{Eq 5:33}$$

In this case[4]

$$\frac{L}{L_h} = \sqrt{1 + \frac{(m_k + km_l)^2 g^2}{T_h^2 \cos^2(\beta)}} \qquad \textbf{Eq 5:34}$$

$$\frac{L - Mg}{L_h} = \sqrt{1 + \frac{(m_k + km_l)^2 g^2}{T_h^2 \cos^2(\beta)}} - \frac{(m_k + km_l) g}{T_h \cos(\beta)} \qquad \textbf{Eq 5:35}$$

$$\frac{T}{T_h} = \sqrt{1 + \frac{(m_k + km_l)^2 g^2}{T_h^2}} \qquad \textbf{Eq 5:36}$$

$$\frac{T_k}{T_h} = \sqrt{1 + \frac{2(m_k + km_l)^2 g^2}{T_h^2} - \frac{2(m_k + km_l) g}{T_h^2} \sqrt{T_h^2 \cos^2(\beta) + (m_k + km_l)^2 g^2}} \qquad \textbf{Eq 5:37}$$

---

[4] See appendix II for complete derivations of these modifying factors

The variable k is the proportion of the line mass (m_l) that the kite lifts and is the distance to the inflexion point of the line from the kite as a proportion of the line length. In general this can be approximated as 0.5.

Using the previous kite specifications and the values adjusted for line effects and the kite's centrifugal force

km = 0.5· (1.5· 30· 4)/1000 = 0.09kg

β = atan(1/4.48) = 12.58

$$\frac{L}{L_h} = \sqrt{1 + \frac{(0.5 + 0.09)^2 9.81^2}{296.1^2 \cos^2(12.58)}} = 1.0002$$

$$\frac{L - Mg}{L_h} = \sqrt{1 + \frac{(0.5 + 0.09)^2 9.81^2}{296.1^2 \cos^2(12.58)}} - \frac{(0.5 + 0.09)9.81}{296.1 \cos(12.58)} = 0.9802$$

$$\frac{T}{T_h} = \sqrt{1 + \frac{(0.5 + 0.09)^2 9.81^2}{296.1^2}} = 1.0002$$

$$\frac{T_k}{T_h} = \sqrt{1 + \frac{2(0.5 + 0.09)^2 9.81^2}{296.1^2} - \frac{2(0.5 + 0.09)9.81}{296.1^2}\sqrt{296.1^2 \cos^2(12.58) + (0.5 + 0.09)^2 9.81^2}} = 0.9627$$

Therefore

L/D=4.48· 1.002=4.481

(L-Mg)/D=4.48· 0.9802=4.39

T=296.1· 1.0002=296.15N

T_k=296.1· 09627=285.1

In this case there is a 0.02% offset in acquiring L/D and T, which is very low, while there is just under a 2% offset when converting to (L-mg)/D and just under a 4% offset in acquiring T_k.

5.4.4 Difference between tested results and actual results

The kite used as an example in the above calculations had a Lift to Drag ratio from this test method of 4.4. After applying all the modifying factors, the Lift to Drag ratio of the kite without mass included is 4.48, and with mass added it is 4.39. In both cases this difference is not very significant.

5.4.5 Effect of parameters

To determine the kite performance from this testing method all the parameters need to be applied. For example

$$\frac{L}{D} = \frac{L_T}{D_T} \cdot \frac{L_C}{L_T} \cdot \frac{D_T}{D} \cdot \frac{L_h}{L_C} \cdot \frac{L}{L_h} \qquad \text{Eq 5:38}$$

The magnitude of these modifying factors will depend on the nature of the test. However, the following relationships will apply

1. The modifying factors to adjust for the orientation of the mass are essentially a function of the mass and the line tension. Figure 5:13 shows the four modifying factors as a function of a ratio $(m_k+km_l)/T_h$. Since this ratio is usually less than 0.01 it has a larger effect on the modifying factors that the kite performance angle β. All these ratios will get closer to 1 as V_w^2 increases because this will increase T_h.

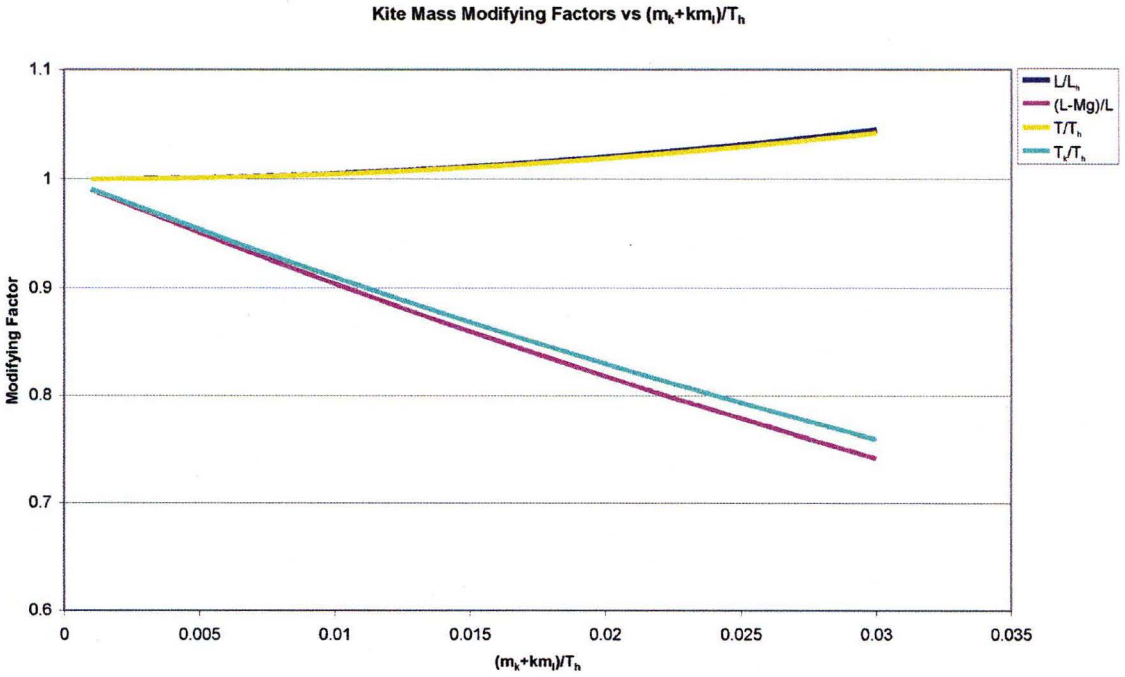

Figure 5:13 Mass modifying factors

2. Figure 5:14 shows L_h/L_c and T_h/T_c as functions of the ratio $m_k V_k^2/RT_c$. The smaller this ratio, the closer these modifying factors will get to 1. These modifying factors are also related to kite performance via the angle β but this influence is a secondary effect

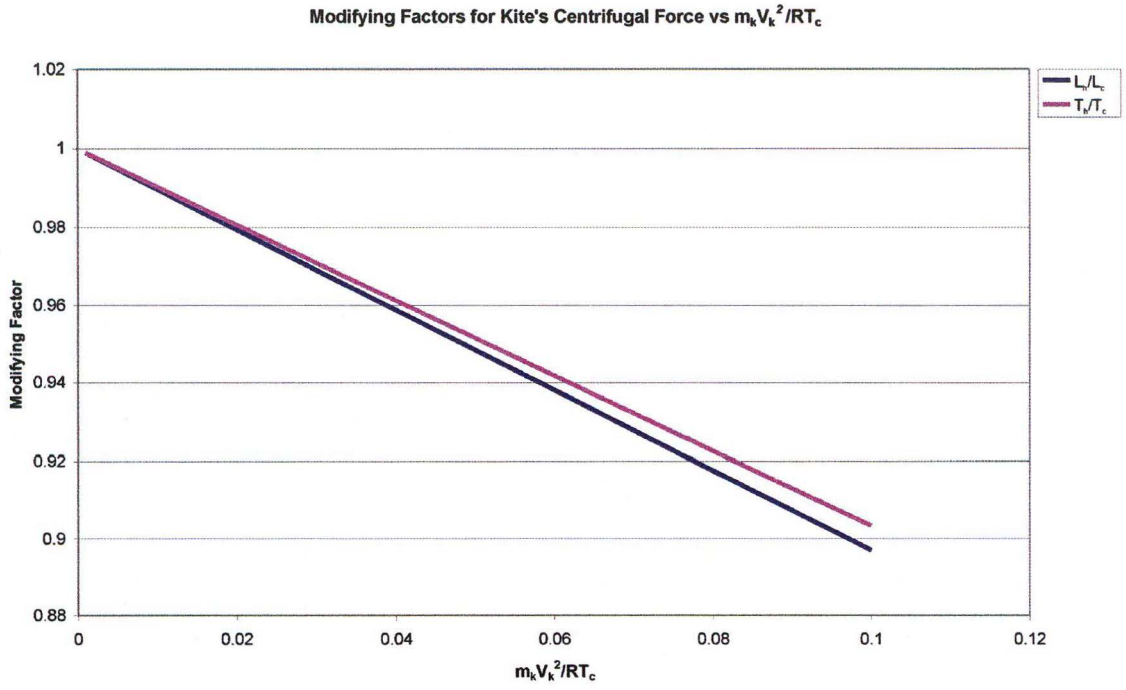

Figure 5:14 Kite's Centrifugal force modifying factors

3. Summarising the modifying factors for the lines is more difficult due to the complexity of the relationships. The variation in D_T/D and L_c/L_T are shown in Figure 5:9, Figure 5:10, Figure 5:11 & Figure 5:12. Varying S/r will vary the effect of the lines both directly and by changing λ. Eq 5:22 & Eq 5:23 show that line effects are directly related to r, ρ, ϕ, m_l, n and V_w^2. Theoretically line effects should be independent of velocity because kite pull is also related to velocity.

5.5 Conclusions

The reduced sensitivity of the measurements using this testing method is its most attractive quality. This testing method can be tuned for each kite, so that the most accurate results are obtained. However, significant mathematical manipulation is required to convert the measurements from this method into a more usable form. The circular nature of the testing procedure introduces forces into the system that are not normally

present in kite measurements. More traditional measurements can be obtained as long as the tension of the lines is recorded during the test.

6. Circular Testing Methodology and Results

6.1 Summary

The circular kite testing method was developed because of difficulties in obtaining accurate results with the car-mounted test rig. Because this method allows the testing arrangement to be adjusted for each kite, the sensitivity the Lift to Drag ratio measurements can be significantly reduced. To verify the theory supporting this method, a rig was designed and built to perform a series of tests on kites with known performance characteristics.

The key findings of these tests were:

1. The sensitivity of the Lift to Drag measurements to angle change was significantly reduced compared to those on the car-mounted test rig.
2. Due to the inaccuracy of the speed-readings of the buggy, the error in the measurement of the aerodynamic coefficients was greater than those obtained with the car-mounted rig.
3. The Lift to Drag ratio and Lift Coefficient measurements were repeatable.
4. Allowing for size effects the results were directly comparable to those using the car-mounted test rig.
5. The accuracy of the results are dependent on the size of the kite in relation to the flight path radius. Further work is required to determine the appropriate test size for each type of kite. Initial estimates indicate that a test site at least 80m in diameter will be required to test large Traction kites

These tests confirmed that circular testing has the ability to provide accurate kite performance results. In particular the reduced sensitivity of the Lift to Drag ratio measurement was very encouraging.

6.2 Introduction

As outlined in Chapter 5, the circular method for testing kite performance can provide accurate results. This is largely due to the ability to tune the test procedure for each kite. The benefit of this is that the sensitivity of the Lift to Drag ratio measurement to line angle change can be kept constant. This is very attractive in light of the issues that arise when measuring line angle using the car test rig as outlined in Chapter 2.

To verify the theory behind Circular Testing, a test rig was built to test kites and compare the results with those from the car rig. A comprehensive test schedule was out of the question as a large enclosed space to do the tests was only available for limited periods. Therefore, the primary goal was to confirm that this is a viable method for testing kites and that the theoretical basis behind it is correct.

The following sections describe the tests performed for this purpose. They outline the test rig that was built, the measurement devices used, the results obtained and conclusions concerning the viability of the method. It is hoped that the experience acquired from doing these tests can be used if a permanent circular testing facility is ever built.

6.3 Performance equations

All the relevant equations used to determine the kite performance using circular testing are outlined in Chapter 5. The following equations have been repeated here as an aid to explaining the measurements in the test.

As shown in Figure 5:3 the Lift to Drag ratio found in this test is determined by

$$\frac{L_t}{D_t} = \frac{1}{\tan(\beta)} \qquad \textbf{Eq 6:1}$$

where

$$\beta = \sin^{-1}\frac{r\sin(\lambda)}{\sqrt{r^2 + S^2 - 2rS\cos(\lambda)}} \qquad \textbf{Eq 6:2}$$

By measuring the tension in the lines the lift force can be determined using

$$L_t = T_t\cos(\beta) \qquad \textbf{Eq 6:3}$$

This force can then be converted into a Lift Coefficient using the usual definition.

$$CL_t = \frac{L_t}{\frac{1}{2}\rho A V_k^2} \qquad \textbf{Eq 6:4}$$

To compare the results from these tests to the kite results from the car rig the measurements were converted to the more usual definitions of Lift to Drag ratio and Lift Coefficient, using the equations in Chapter 5. Since the results from the car rig were for a kite with 10m lines the results were further modified to give LTG_g and CL_g using the line drag predictions from Chapter 4.

6.4 Testing Apparatus

The testing apparatus built needed to meet several criteria for the purposes of this project.

1. The test rig needed to mimic a person flying a kite in a perfect circle.
2. The dimensions S, r and λ needed to be measured.
3. The path of the test rig needed to be automatically maintained, as a person is unable to keep a constant radius.
4. To determine the aerodynamic coefficients and modifying factors the load on the lines were required.

5. A sample rate of at least 5-10Hz was required, as it will only take a few seconds for the kite to complete a full circle.
6. The test rig needed to be easy to move. In this case access to a test location was intermittent so it was essential that the apparatus could be put in place quickly.
7. Due to the time restraints on the tests it was essential that accurate results were obtained immediately. To ensure this, many of the developments made to the instrumentation of the car rig were incorporated into this rig.
8. Only two people could be required to do the tests.
9. Preferably the test rig should be able to be taken apart for easy storage.

The final design solution consists of three parts: The under frame, including the driving components; the kite's control mechanism and the instrumentation used to obtain the results.

6.4.1 Under frame

The under frame of the test rig is shown in Figure 6:1

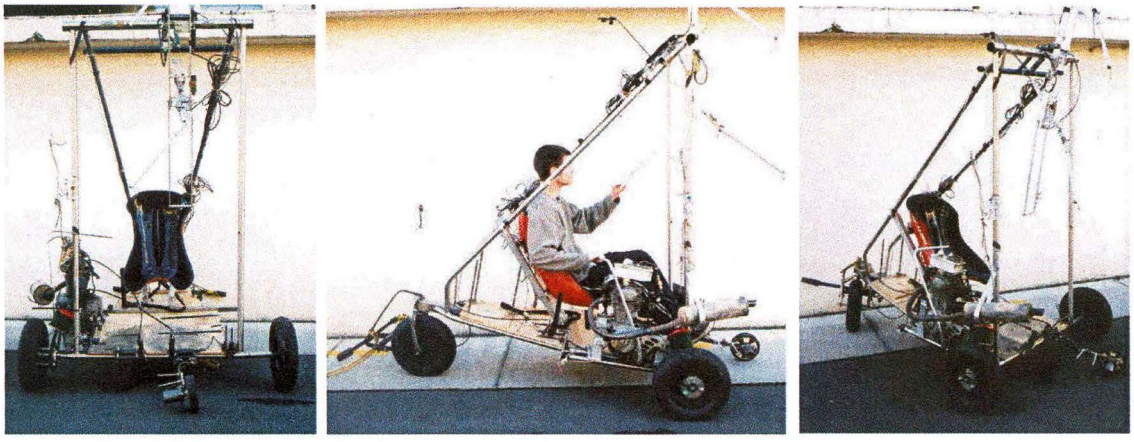

Figure 6:1 Testing frame

The key elements of this testing frame are

1. The testing frame is based around a three-wheeled trolley with steering provided by the front wheel. It is powered by a Honda 125 cc motorbike engine which drives the inside back wheel.
2. During the test the trolley drives around in a circle. To maintain a constant radius the rig has a self-steering mechanism. A rope is attached between the front wheel and the centre of the 'walking circle'. If the radius of the trolley increases, the rope pulls the front wheel towards the centre of the circle. As the trolley moves towards the centre of the circle the rope goes loose and a 'bungee' cord pulls the front wheel outwards.
3. The person controlling the kite sits in the trolley facing backwards while controlling the speed of the trolley.
4. Where possible the testing frame has used a triangulated structure to reduce the stress on each member.
5. The testing frame can be dismantled when not required.

6.4.2 Kite Attachment and Control

The kite controlling mechanism consists of a control bar which pivots at the top of the under frame. This bar is shown in Figure 6:2. The lines of the kite are attached to both ends of the control bar and the kite is controlled by moving the base of the bar in and out. This has two advantages. First, the effective line length (S) stays constant as it is measured to the pivot point not to either end of the bar. Secondly, very little force is required to control the kite as the loads are largely balanced on either side on the bar.

While two-line kites can be directly attached to this mechanism, four-line kites require an adjustment for the back-line load. To do this, lines from each side of the kite are first attached to a handle. These handles pivot on the end of the control bar and the location of the pivot can be varied to adjust the back-line load.

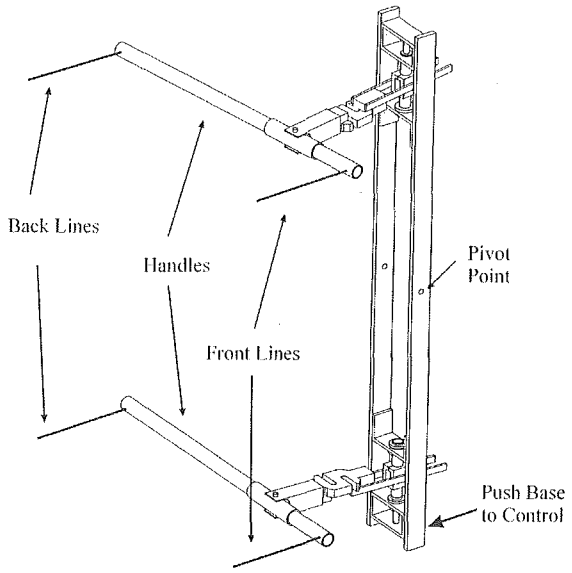

Figure 6:2 Kite control bar

6.4.3 Measurements and Instrumentation

The following measurements are required to obtain the kite's performance characteristics

1. The distance from the control bar pivot to the lifting surface of the kite was measured for each kite. This value is S in Eq 6:2. The error in this measurement was ±0.2m
2. The distance between the inside wheel and the centre of the 'walking circle', r_m, was measured during each test. This was used to obtain the actual radius of the control bar, r, used in Eq 6:2. Unfortunately, the radius of the wheel did vary with speed but error was only ±0.05m.
3. Eq 6:2 requires that the angle of the line, λ, be obtained. The first step in acquiring this value was to measure the angle of the line relative to the control bar, λ_m, during the test. The point where the lines attach to the end of the control bar consists of two arms mounted on vertical shafts. These arms are free to rotate in all directions but two potentiometers measure the angle of the shafts as the kite is flying. One of these mechanisms is shown in Figure 6:3. The two angles obtained are averaged to get a final value of λ_m, which had an accuracy of $\pm 1.0^{o}$.

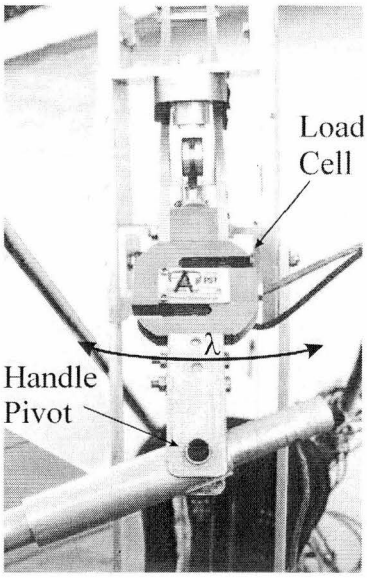

Figure 6:3 Angle measurement device

4. The load on the lines was measured to obtain the aerodynamic coefficients and determine the modifying factors as outlined in Chapter 5. Two designs were used to do this. In the first, the line load was transferred using pulleys to a single load cell mounted in the centre of the control bar. This method was eventually discarded since it was difficult to eliminate hysterisis from the load measurement. Instead a load cell was mounted behind each handle as shown in Figure 6:3. Although the self weight of the handle did effect the results the error was only ±200g.
5. Two devices were used to measure the speed of the buggy. A speedometer was attached to a jocky wheel located directly below the control mechanism and an anemometer was located in front of the control mechanism. Generally the anemometer was used only as a backup to the speedometer. This speed along with the dimension S, r and λ were used to determine the speed of the kite. The accuracy of the speedometer was ±0.15 m/s
6. The angle of the rig in relation to the centre of the circle (θ_m) was measured. Since the axis of the rig does not point directly to the centre of the circle and r_m is measured to the centre of the inside wheel this angle is required to determine the

actual values of r and λ used in Eq 6:2. The angle guide used to measure θ_m is shown in Figure 6:4. The end of the arm was connected with a bungee cord to the centre of the 'walking circle'. This angle measurement was accurate to $\pm 0.5^o$

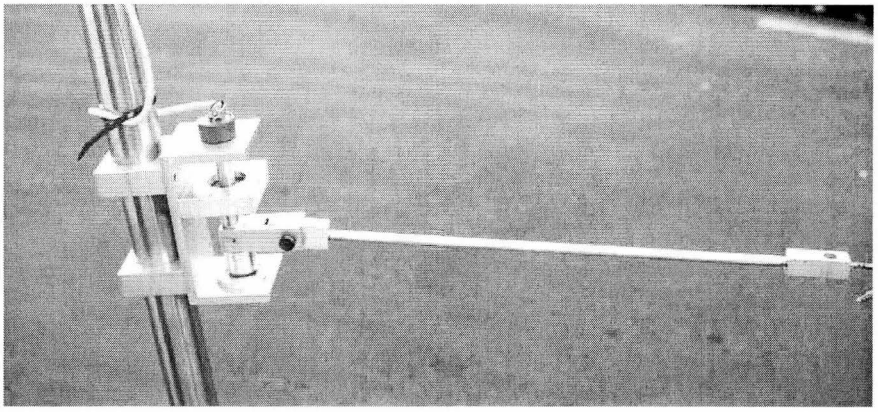

Figure 6:4 Instrument to measure θ_m

The geometry of the rig showing the angles that were measured is shown in Figure 6:5. To obtain λ and r from the measured rig angle (θ_m), the measured line angle (λ_m) and the measured radius of the inside wheel (r_m) the following steps were necessary.

- The dimensions x_1, x_2, y_1 & y_2 were measured from the rig. The dimensions W_1, W_2, θ_1, θ_2 & θ_3 were then calculated.
- θ_4 then equals $\theta_m+90-\theta_1$.
- Using the sine rule θ_5 was obtained and from this θ_6 was determined.
- Using θ_2, θ_3 & θ_6, the angle θ_7 was found. Using this angle and the lengths W_2 & r_m the cosine rule gave the actual radius (r)
- Using the sin rule θ_8 was determined from which the line angle λ was obtained.

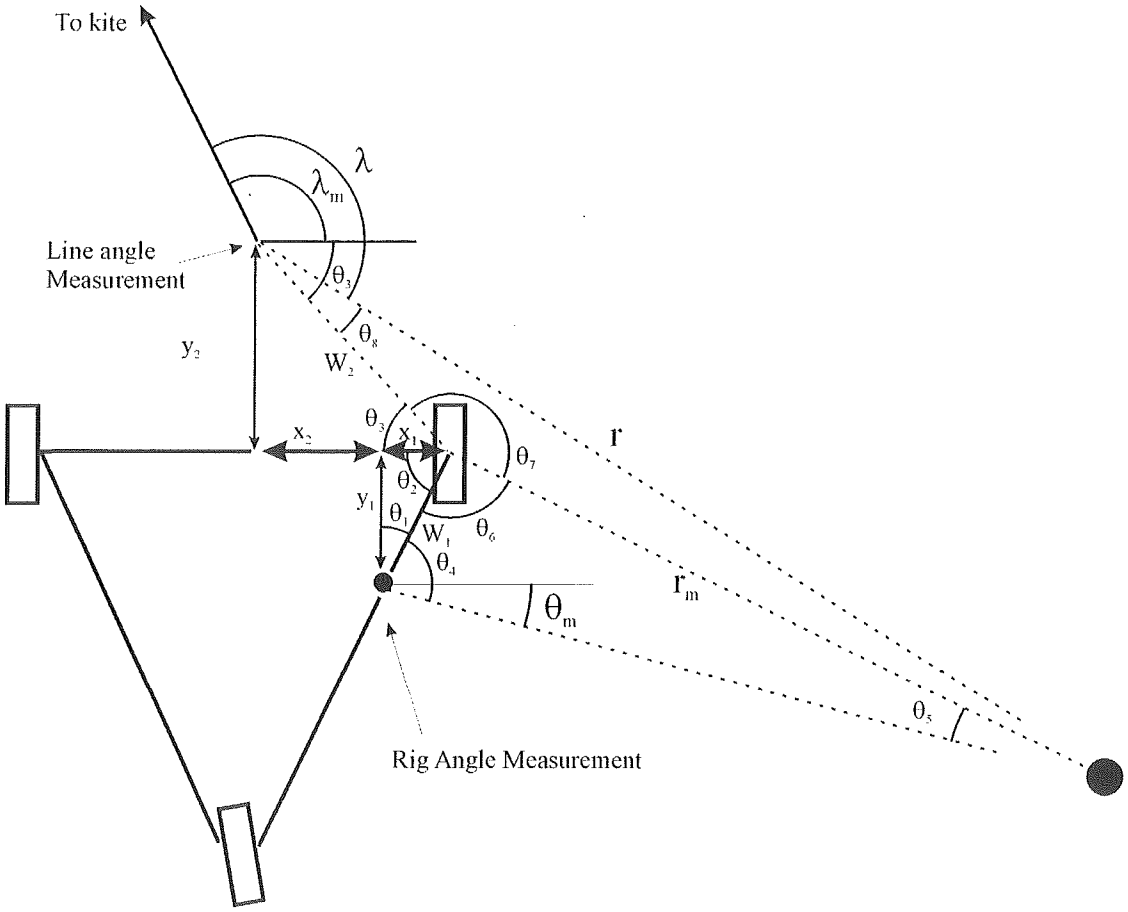

Figure 6:5 Rig Geometry with exaggerated dimensions

7. The weight of the kite was obtained and the dimensions and weight of the kite line. These were required to implement the modifying factors as outlined in Chapter 5.

6.4.4 Data acquisition system

The data acquisition system used in this rig was the same as that used in the car rig. The programme used to process the data and the upfront display was slightly modified to reflect the measurements required for this test. During the test the computer was located on the deck of the under frame.

6.5 Testing Method

6.5.1 Location and conditions

The testing method requires that there is no natural wind present during the test. To obtain these conditions an aircraft hanger was used for the tests. This was large enough for a 13-15m flying radius and tests were performed over three separate days.

The flying radius and the height of the roof meant that only some types of kites could be flown in this environment. Although the 3.2 and 4.2 C-quad could be flown very easily it was virtually impossible to get an ARC to fly. After the results were analysed it was also found that the results for the 4.2 C-quad were significantly lower than expected. Outdoor tests, using a larger radius, were attempted to determine if any size effects were occurring.

Although outdoor tests were attempted on calm, frosty mornings the results were significantly affected by the very small amount of natural wind present. Only a few results could be taken but this was enough to confirm that size effects did occur when a smaller radius was used and that ARC style kites could be tested with a larger setup[5].

6.5.2 Test Procedure

The testing procedure consisted of the following steps

1. The rig was moved to the test location and the apparatus set up.
2. The data acquisition system was initialised and the angles and line load calibrated.
3. The appropriate line length, S, was attached between the rig and the kite.
4. Based on S, the rope attached to the self-steering mechanism was adjusted to an initial estimate of r_m. Ideally the kite should sit at a λ just greater than 90^o. If λ was greater than this r_m needed to be reduced, but if λ was less than r_m was

[5] See Chapter 7 for methods to obtain data from wind affected results

increased. It was better for λ to be slightly greater than 90^{o} because this prevented the kite moving into an unstable position.

5. One person sat in the rig and started the data acquisition system. The other held the kite in position ready to fly. It was best to start the kite at a λ greater than the 90^{o} point.
6. The kite was flown so the lines were as close to the horizontal as possible (See Figure 6:6)
7. A typical test lasted for 4-5 min. During this time the speed of the buggy was varied as smoothly as possible. Ideally the buggy started slow and speed up to the point corresponding to the peak kite load. The rig was then bought back to the slow speed again.
8. The dimensions S and r_m were then measured and applied when the data is processed.
9. The kite's back line load was adjusted and the tests were performed again.

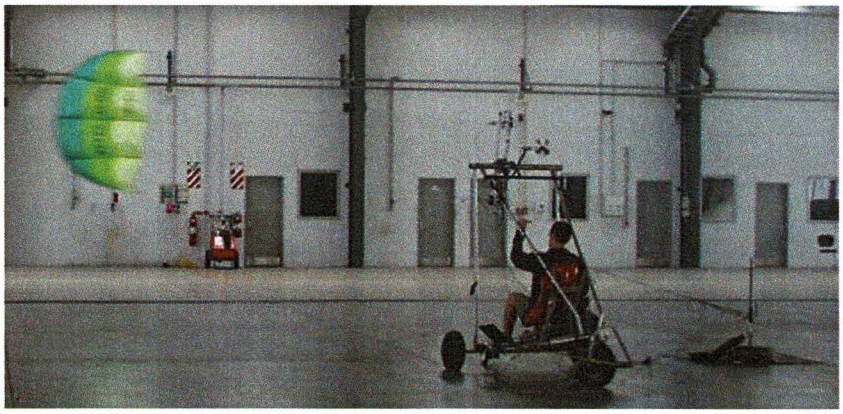

Figure 6:6 Test of a 3.2 C-Quad

6.5.3 Data Analysis

The following is an outline of the steps required to analyse the data obtained during the test

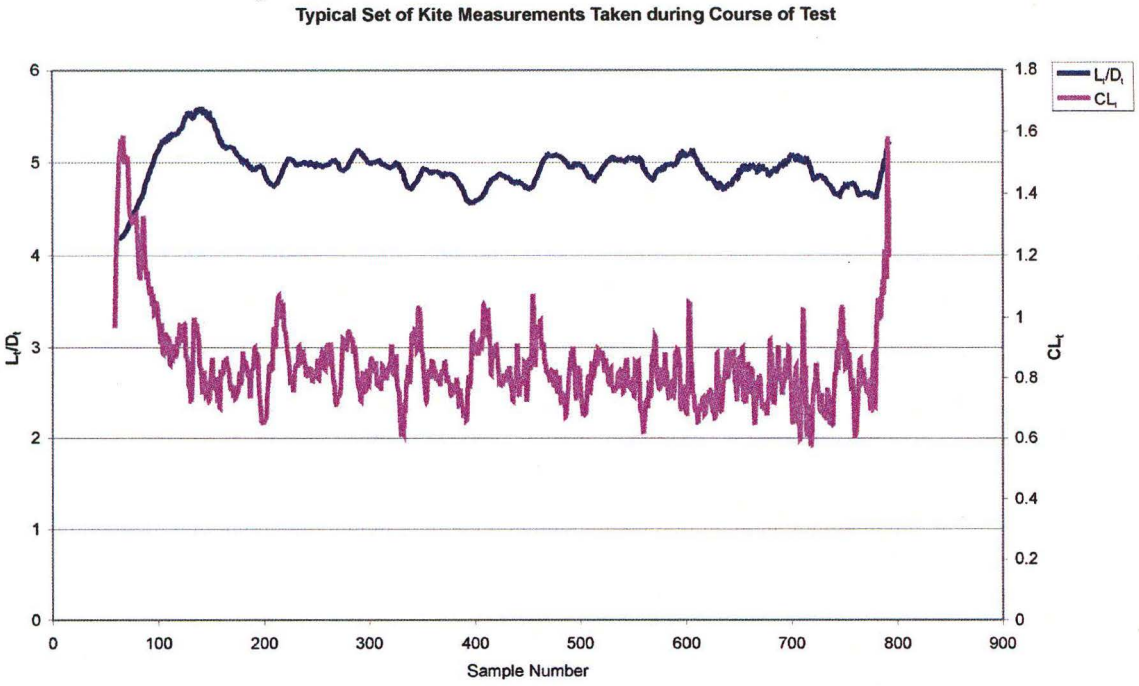

Figure 6:7 Typical test results using circular testing method

The slightly periodic nature of Lift to Drag ratio data is due to interference from the wall of the test site as explained in section 6.7.6.

6.6.2 Repeatability of testing Method

Figure 6:8 and Figure 6:9 show the data obtained for the 3.2 C-quad over a number of days and with varying S/r ratios.

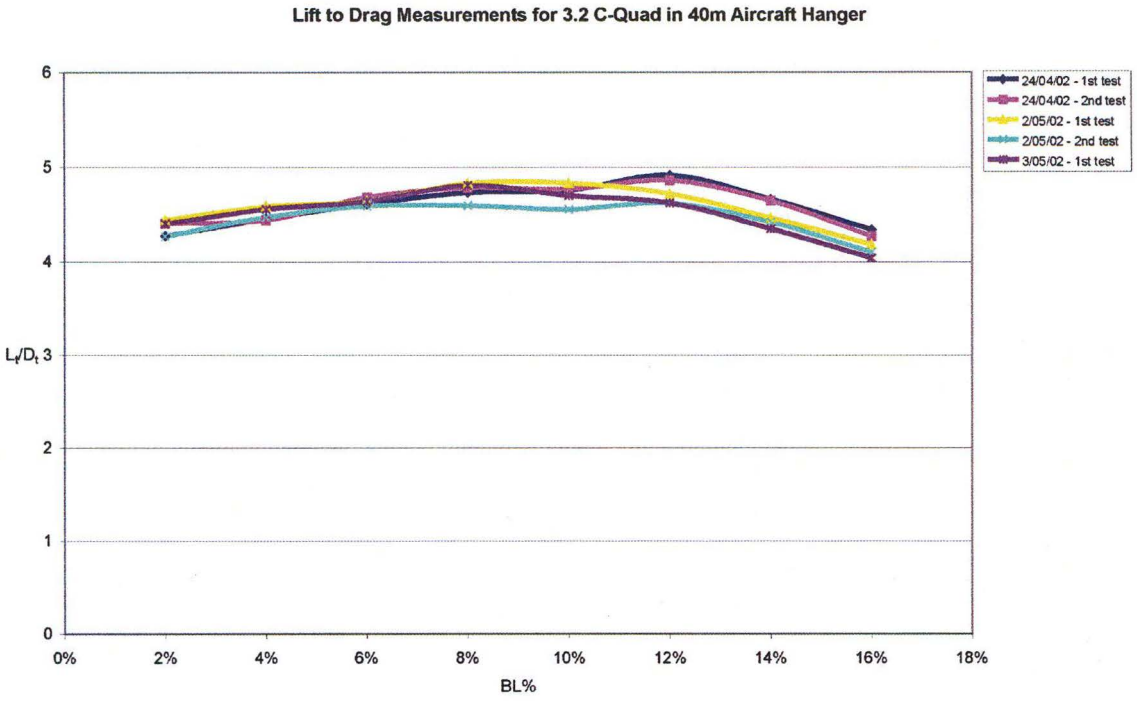

Figure 6:8 3.2 C-Quad Lift to Drag ratio results from aircraft hanger

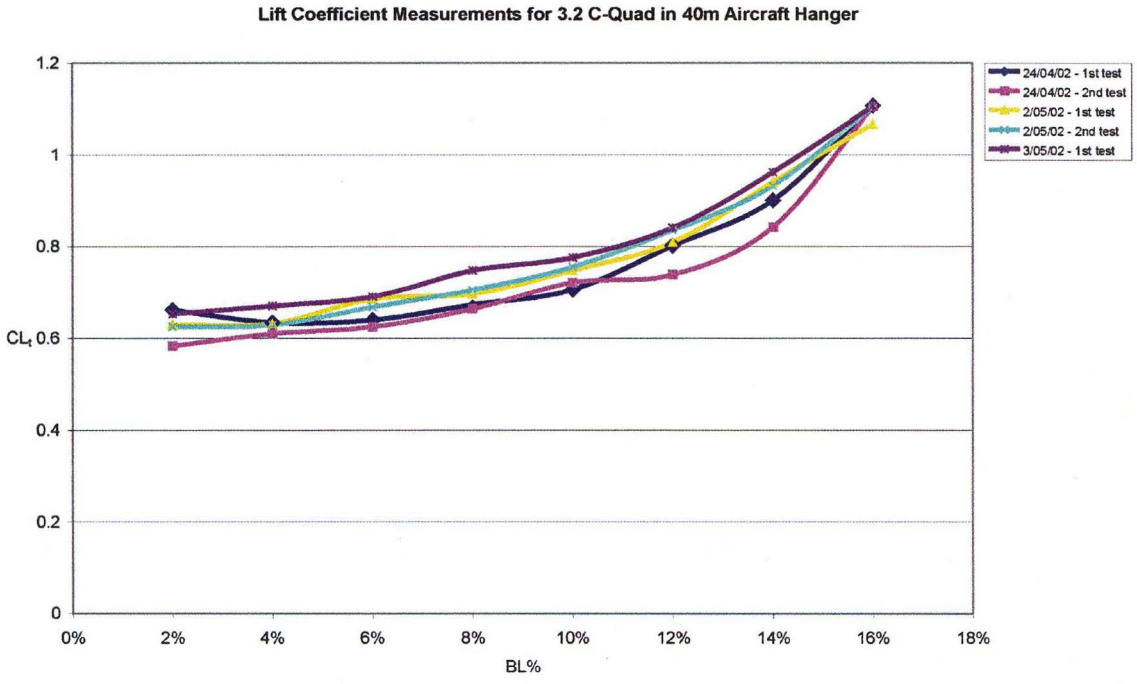

Figure 6:9 3.2 C-Quad Lift Coefficient results from aircraft hanger

6.6.3 Comparison of results with car rig

Figure 6:10 and Figure 6:11 show how the data acquired from this testing method compares to the data obtained from the car test rig for the same kites.

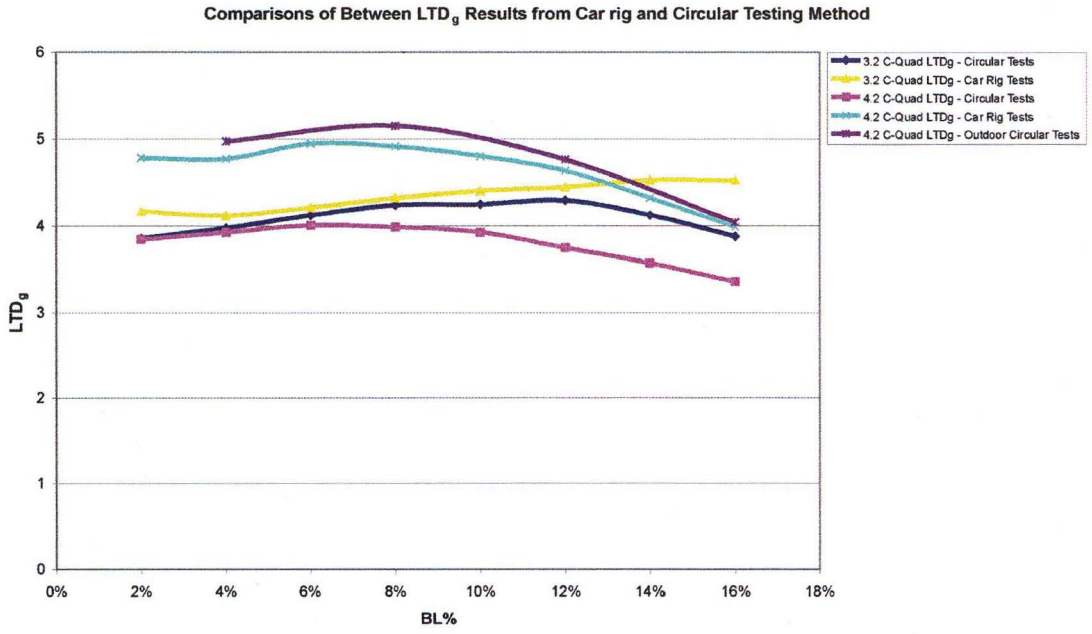

Figure 6:10 Comparative LTD_g data between Car Rig and Circular Test Rig

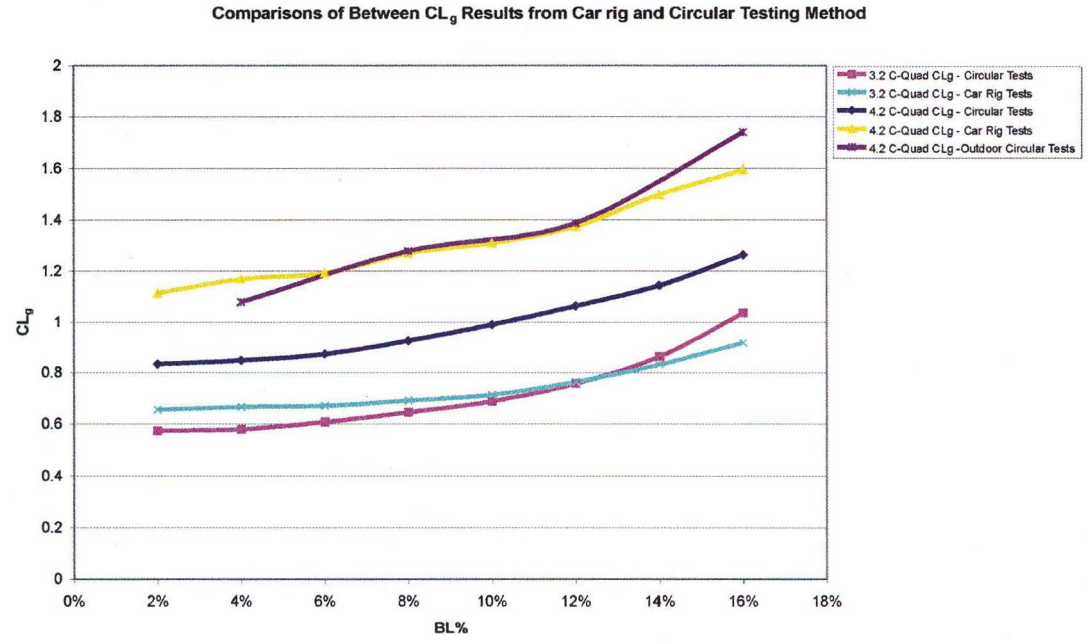

Figure 6:11 Comparative CL_g data between Car Rig and Circular Test Rig

6.7 Discussion

6.7.1 Sensitivity of the Testing Procedure

Figure 6:7 shows the key characteristics of this method. They are:

1 The test results were located around a set value and did not significantly deviate from this

2 The results tended to have a peak at the beginning of the test. This was equivalent to the kite taking off and over flying its stable position.

3 The peak in the Lift Coefficient at the end of the test was because the kite kept flying as the rig came to a stop. The loads on the kite were therefore high compared to the measured speed.

The Lift to Drag ratio measurements obtained using this testing method fell within a relatively narrow band as shown in Figure 6:7. As a comparison Figure 6:12 shows a data set from the car rig for the same kite. As a kite's performance improves this difference will become more pronounced because results from the car rig will become more sensitive to angle variation.

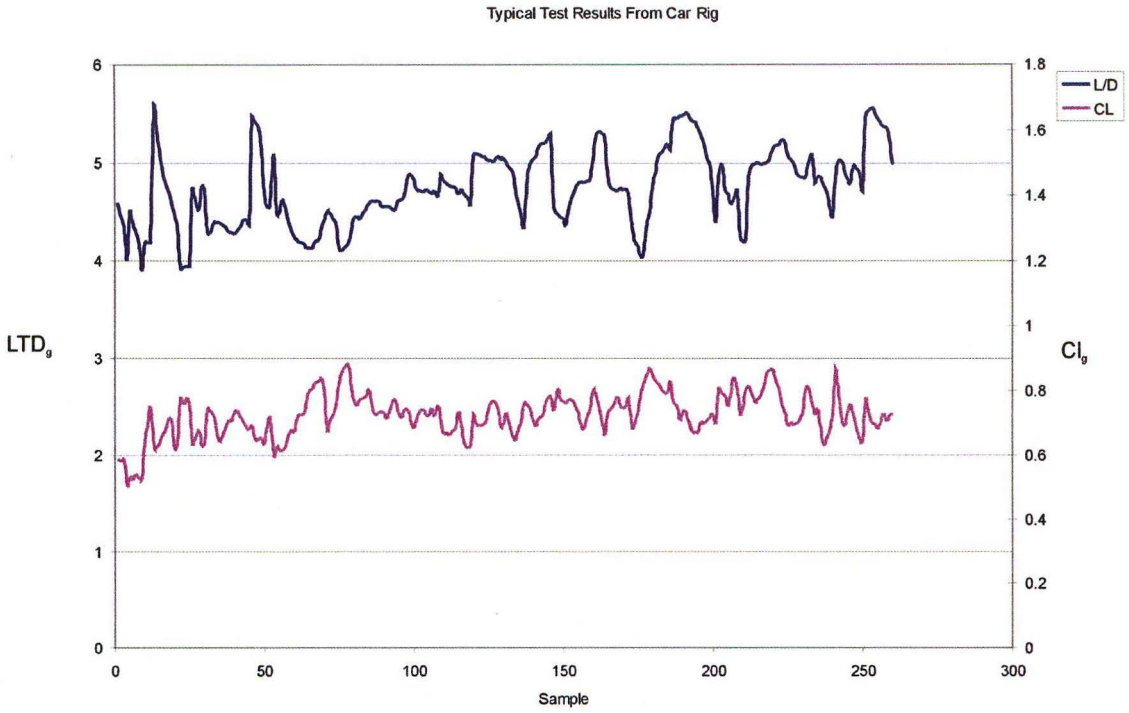

Figure 6:12 Typical test results from Car Rig

The reduced sensitivity of the Lift to Drag ratio measurement was the primary reason for using the circular test method. However, due to the practicalities of testing kites the tests were not performed in their optimal location of $\lambda=90^{o}$. It was found that if the kite was flown in this location the variation in the performance of the kite had a tendency to locate the kite at an angle λ where the kite was unstable (see section 5.4.1) To avoid this the kites were flown at angles greater than 90^{o} thereby slightly increasing the sensitivity of the test.

Although the Lift to Drag ratio measurement was less sensitive, the variation in the Lift Coefficient was greater using the circular test rig than using the car rig. There were two reasons for this. First, the measurement capabilities of the speedometer coupled with the low speed of the buggy caused a large error in the speed-reading. Since the speed of the kite is calculated based on the speed of the buggy, and the lift coefficient is based on V^2, this error had a large effect on the Lift Coefficient. Secondly, a small variation in the

performance of the kite caused a large change in λ as the kite changed position to its new stable point. As the kite moved the relative wind speed at the kite was different to the measured wind speed. This is because the measured wind speeds were based on the kite being stationary. The periods when the kite was changing location had a significant effect on the Lift Coefficient measurements.

Despite the increased sensitivity of Lift Coefficient measurement the average result was still consistent with the results from the car test rig.

6.7.2 Repeatability of the testing procedure

Figure 6:8 and Figure 6:9 demonstrate that this testing procedure gives results that are far more repeatable than those obtained using the car test rig. The maximum variation in the results shown in Figure 6:8 corresponds to an angle variation of $\pm 0.3^{o}$, better than $\pm 0.8^{o}$ obtained with the car rig. However a direct angle comparison has minimal relevance in this case. The circular testing rig setup can be adjusted for each kite so that the repeatability of the Lift to Drag ratio, rather than the angle, will remain constant no matter what the Lift to Drag ratio of the kite is.

6.7.3 Comparison of results with Car test rig

Because some kites could not fly in the aircraft hanger, only a limited comparison with the results from the car rig was possible. From this comparison several issues emerged.

First, the results for the 3.2 C-Quad were the most accurate. However, with this kite the Lift to Drag ratio dropped off more rapidly with back-line load than with the car rig. This was due mainly to the design of the pivot on the attachment handles. Upon completion of the tests it was discovered that, due to the location of the pivot point, the back-line load depended on the angle of the handles. Unfortunately, this meant that the back-line loads measured were only a guide and the proportion depends on the relative lengths of the front and back lines. Based on the results it appeared that the range in back-line loads for the 3.2 C-Quad was greater than the 2-16%, which has been assumed in the results.

The Lift to Drag data obtained from the 4.2 C-Quad was significantly lower with the circular test rig than with the car rig. This trend was not as apparent for the 3.2 C-Quad and indicated that the size of the kite in comparison to the radius of the flight path, affected the performance of the kite. (See section 6.7.5 for a more in depth discussion of this)

When the 4.2 C-Quad was tested outside with a larger setup, a far better comparison with the data from the car test rig was obtained. This is good but implies that a large enclosed testing site is required to obtain good results.

6.7.4 Errors in Results

Due to the presence of non-linear terms in the performance equations determining a general error in the results was problematic. However, a typical set of data from the 3.2 C-quad was analysed in order to obtain an estimate of the inaccuracies of the measurements. The analysis found that the error in the Lift to Drag ratio measurement was ±2%, which corresponds to the range of values obtained. The error in the Lift force measurement was only ±3% but the error in the speed measurement was ±7%. This final error dominated the results and caused an error of ±17% in the Lift Coefficient measurement. As already stated this accounted for the increased sensitivity of this measurement.

The most obvious area for improvement is the instrumentation used to determine the speed of the buggy. Doing this will reduce the variation in the Lift Coefficient measurement. Although improvements can be made to the other measurements they will not significantly improve the overall accuracy significantly.

6.7.5 Larger testing setups and size effects

The brief number of tests that were performed outside highlighted a few key issues. First, to be effective the tests need to be done inside. Small amounts of wind (i.e., >0.3km/h)

severely affect the results making the testing method almost unusable (See Chapter 7 for a full description of wind affected results). Secondly, the tests that were done on the 4.2 C Quad gave Lift to Drag ratio and Lift Coefficient results that were much closer to those obtained in the car rig. Thirdly, ARC style kites are much easier to test with larger setups.

Size effects are a major concern when using short line lengths. Results from the indoor tests on the 4.2 C-quad were significantly different to those obtained on the car rig. However, the results for the smaller 3.2 C-quad compared well with the car test rig results. This is partially due to the kite's chord length. If a kite has a large chord length, and is flown on short lines, the flying radius (and therefore the wind velocity) differs slightly over the kites lifting surface. However, the difference in the chord length between the 4.2 and 3.2 C-quads are not significant enough to account for all the differences between results. Therefore, the area of the kite must have an effect on the results. Exactly what affect different kites areas have is still undetermined, and further work is needed to specify what size test setups are required for each kite. Ideally the test site should be as large as possible, and based on the outdoor tests it is estimated that a flight radius of 40m will be required to obtain accurate results for large Traction kites.

ARC style kites benefit from a larger setup because it allows them more time to inflate. These kites have a much lower performance characteristic when they are only partially inflated. With a small setup the kite does not have enough time to fully inflate before it reaches a position where testing is impossible. As shown Figure 6:13, larger setups give the kite a longer distance, and therefore time, to inflate.

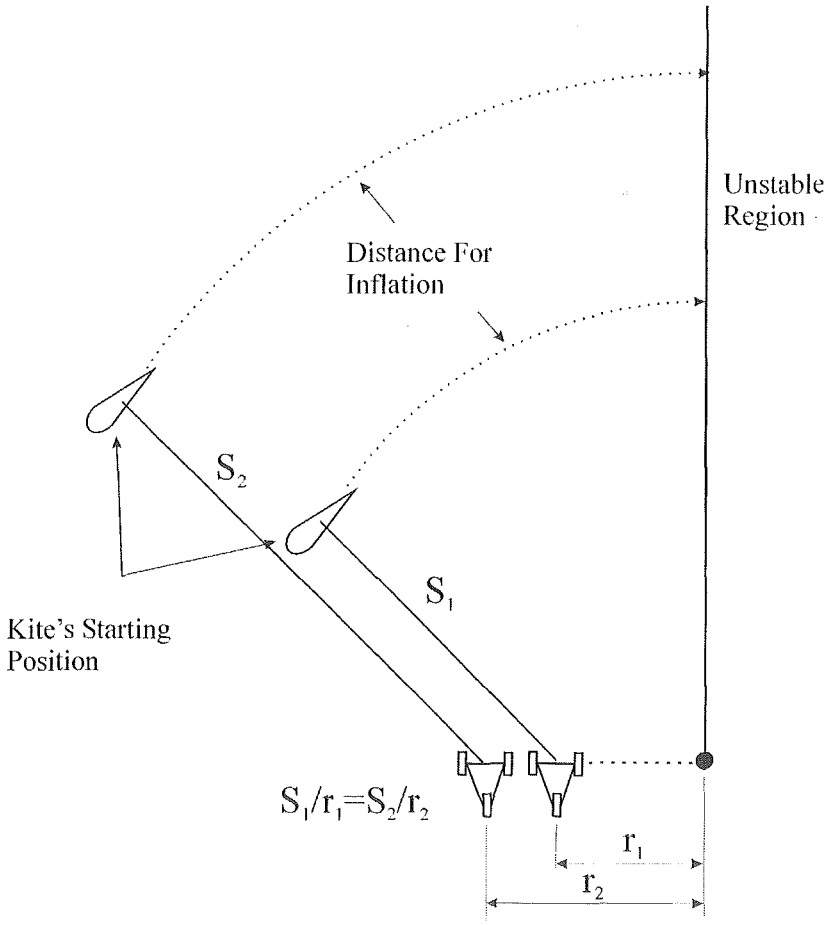

Figure 6:13 Distance for inflation to occur with different setup sizes

6.7.6 Other issues relating to this testing method

Ground effects

If the mounting point for the kite lines on the test rig is low to the ground, and the kite line is kept as horizontal as possible, then the tip of the kite will be close to the ground. This will influence the performance of the kite, as the ground will interfere with the kite's tip vortex. This can be alleviated by either having the mounting point well off the ground or by flying the kite higher up. If the latter is done then it is necessary to determine the angle of the lines to the ground, as this will affect the line length, S, used in the performance measurements.

Wall effects.

If the tests are performed inside it is important that there is a sufficient gap between the wall and the kite surface. If not, the wall will interfere with the pressure distribution over the top surface of the kite and therefore affect its performance. This tends to give slightly periodic results because the kite's performance changes as it passes a wall.

Wake effects

The theoretical basis for the circular test method assumes that as the kite flies in a circle it is always flying in still air. However, during the tests in the aircraft hanger the wake of the kite caused a noticeable airflow within the building. Surprisingly, it is unclear if this airflow had a significant effect on the results.

There are two hypotheses concerning the effects of wake-generated airflow on the test results. In the first hypothesis, the flight path of the kite will locate the airflow in a circular direction. This means that the **direction** of the wind that the kite sees should not vary, but the magnitude will. In the second hypothesis, the measured kite performance will be reduced by wake-generated airflow, as it causes airflow out of the test circle. The Lift to Drag measurements will be affected because the direction of the apparent wind at the kite will be altered.

If the first hypothesis is correct, there should be no variation in the Lift to Drag ratio with time, but the Lift Coefficient should increase as the airflow develops. The second hypothesis predicts a reduction in measured Lift to Drag ratio with time as the airflow increases.

So far, more evidence points to the second theory than the first. Some results show a slight decrease in the Lift to Drag ratio over time. However, over the course of the tests this variation, when it occurred, was well within the error range.

Although there was a noticeable wake-generated airflow in the test site used, as the size of the test area increases there will be a longer time period for the airflow to dissipate. Because of this it is unlikely that wake-generated airflow will be a significant problem.

Control Bar Design

Different kites have different control mechanisms to suit their particular characteristics. The current control bar design and the use of handles is ideally suited for kites that use separate handles for control. Other kites use a single bar with the lines attached at each end and separate mechanisms for adjusting the back-line load. Future designs should take this into account, as different kites require different attachment conditions to obtain optimal control.

Two line kites

Although the data is not shown, this method is very effective at testing two-line kites. They are very easy to control and since they only have one setting they are very quick to test.

6.7.7 Ideal Test Conditions

Since this test procedure was only to verify the feasibility of using circular testing it is worth considering the ideal arrangements if a permanent testing apparatus was built.

1. It is estimated that a building at least 80m in diameter is required to test large kite accurately. This is a very large area and an expensive piece of real estate. To reduce the construction costs a single internal support could be used in the centre of the building. This would also need to be the point that the rig rotated around. A cheaper option may be to buy a forest and cut out a circular area inside it. This would still require netting around it to ensure that wind effects are reduced.
2. Rather than use a self-steering mechanism and be required to measure the angle of the rig to the centre of the circle, it may be more effective to build a solid arm as the radius. A motor could still be mounted on the end so that the stress in the arm would be reduced.

3. It would be ideal if the radius of the rig could be varied during the test. The setup could then be tuned for each kite while it is flying.
4. The flier of the rig did get nauseous going around in a circle for long periods of time. If the controls could be operated remotely this would be ideal. This would also allow the tests to be performed by one person.

Without the large enclosed area this testing method is difficult to use. Of all the requirements this is the most essential element.

6.8 Conclusion

Circular testing has proved to be very effective as a means to test kites. The sensitivity and repeatability of the results obtained make this testing method more effective than other testing procedures. However, the accuracy of the results for large kite are affected by the size of the test area. Further work needs to be done to determine the appropriate test area for each size of kite, but initial estimates are that a building 80m in diameter will be required.

7. Circular Testing and Wind Effects

7.1 Summary

Any natural wind present during a circular test has a significant effect on the results obtained. Despite this, techniques were developed to obtain useful kite performance data from wind-affected results performed outdoors. This was particularly relevant in light of the difficulties in finding a large enclosed area to perform tests.

The most effective method to analyse wind-affected data was to take the average results over a complete cycle. Theoretically, the average result is not quite the same as the actual kite performance but the accuracy that could be obtained using this method was far better than could be obtained using other techniques. The next most effective method was to adjust the parameters in a dynamic model until the model approximated the actual results. However, the insensitivity of this model to input parameters restricted its viability.

Analysing wind-affected data indicated that outdoor tests should only be performed at last resort. Not only does natural wind add uncertainty in the results but even small amounts of wind can make the test impossible to do. This final aspect severely limits the number of days on which tests can be performed.

This chapter also outlines the effect that natural wind will have on walking kite tests. It demonstrates that natural wind tends to make the walking path a spiral rather than a circle. However, the kite performance can still be obtained from this distorted walking path.

7.2 Introduction

To obtain accurate results through circular testing a large enclosed area is required. Unfortunately, a building of the size required is very expensive and it would be more cost-effective to perform tests in an outdoor environment. However, as shown in Figure 7:1 even a small amount of natural wind has a significant effect on the results obtained using circular testing. In this case the wind speed was only 0.3m/s.

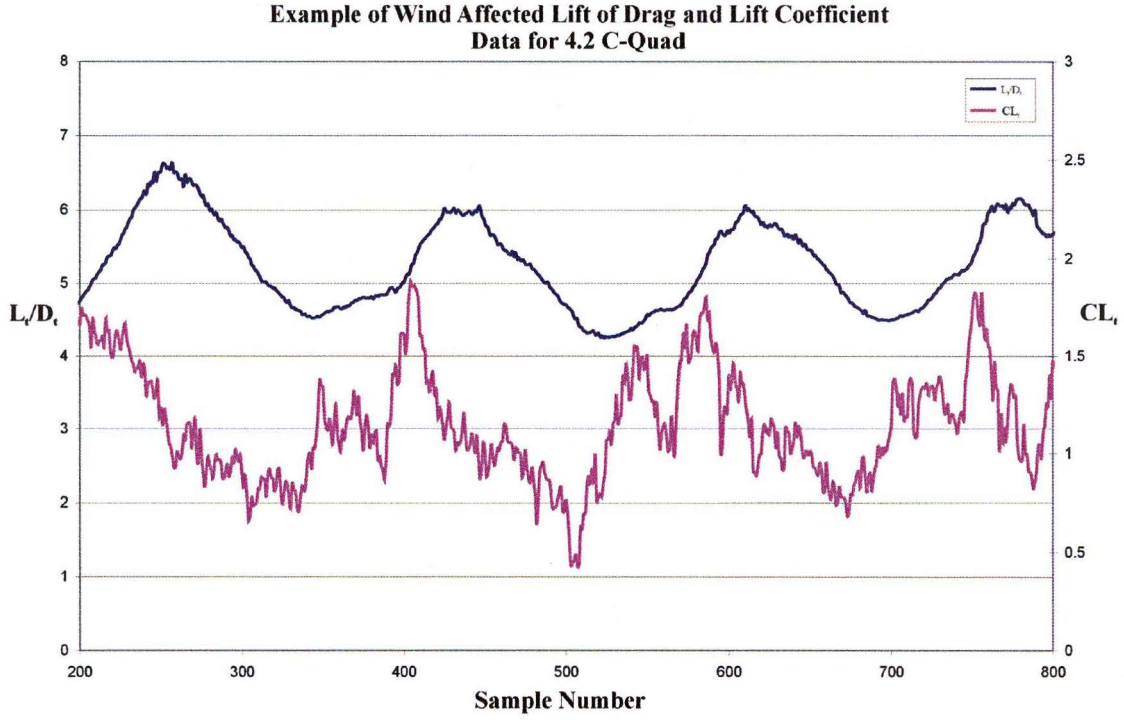

Figure 7:1 Sample of wind-affected circular testing data

Having a kite accelerate during tests is not ideal as there are effects that are very difficult to take into account in measurements. Throughout the course of this project attempts were made to model the motion of a kite as it took off from the ground to a stable flying location (See Appendix IV). Through the course of this modelling it was found that the properties of an accelerating kite are significantly different to that of a stationary kite. Properties that need to be considered are: added mass, rapid changes in angle of attack,

and the time required for the properties of the wind to settle. All these things are present in the wind affected circular test results, making any analysis very difficult. In light of these things, an outdoor test is not a particularly viable option for circular testing.

Despite these difficulties the data from wind affected results still reflects the underlying performance characteristics of the kite. This chapter considers why natural wind affects the data as shown in Figure 7:1, the limitations on outdoor tests, and some of the techniques that were attempted to extract the actual kite performance from these results.

7.3 Theoretical basis and Kite Test Models

Figure 7:2 shows two vector diagrams of a circular test in the presence of natural wind represented by the vector V_{wind}. In Figure 7:2(a) the natural wind causes a resultant force ($F_{\perp}$) that increases the angle λ while in Figure 7:2(b), where the wind is coming from the opposite direction, the resultant force reduces λ. Since during this test the kite follows a circular path the wind will act at all directions to the kite causing it to surge back and forth.

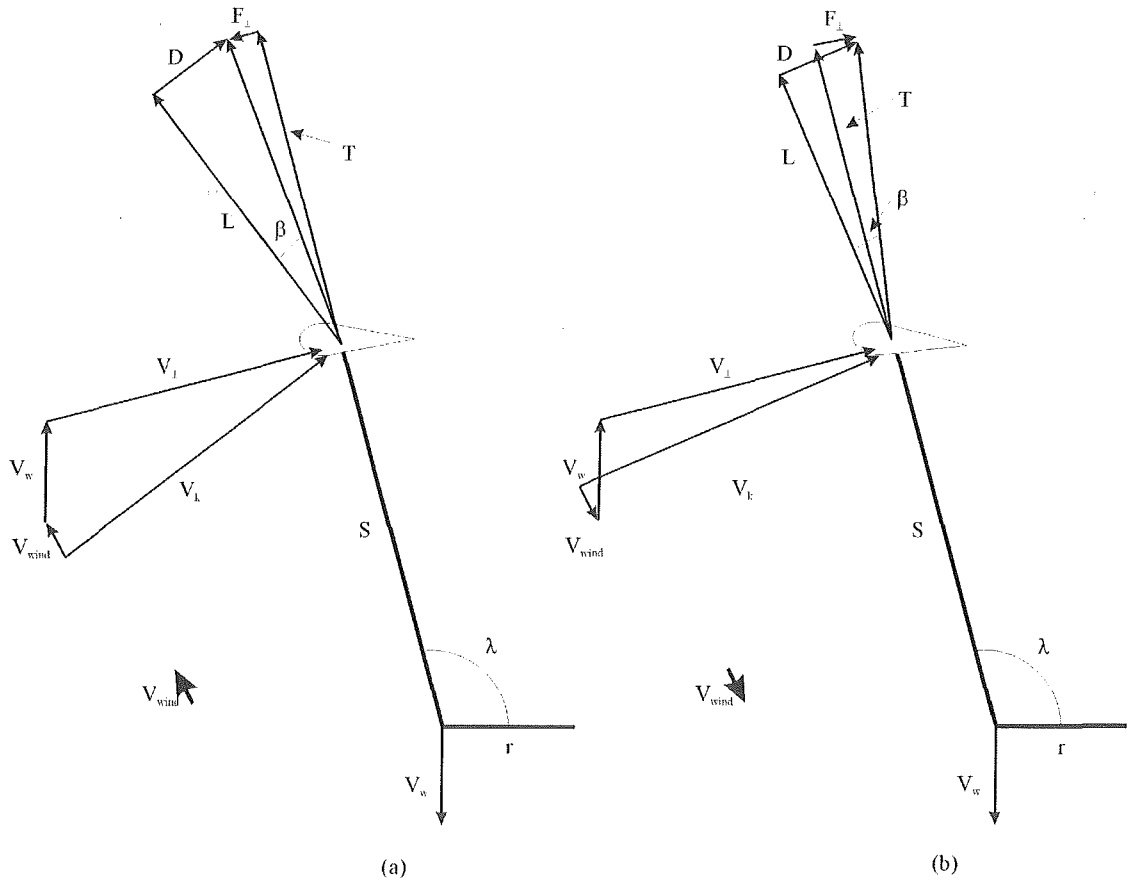

Figure 7:2 Natural wind effects on circular testing

To determine how much natural wind affects the measurements it is necessary to model the kite as it flies in a circle. The following is a description of the models that can be used.

7.3.1 Static Analysis

The simplest analysis ignores the motion of the kite and considers what the angle λ should be at discrete locations in its circular path. This method assumes that the kite is stationary which is not a valid assumption. However, this analysis helps explain the more complicated dynamic model described later.

Up till this point the kite's performance has been determined based on the geometry of the system r, S and λ. This is because the velocity vectors are geometrically similar to the

test setup. Keeping with this theme, one way to analyse the influence of natural wind is to give it a geometric representation. The real geometry can be adjusted by including a 'radius', r_{wind}, which is related to the magnitude and direction of the natural wind. The length of r_{wind} is found by

$$r_{wind} = r\frac{V_{wind}}{V_w} \qquad \textbf{Eq 7:1}$$

and the direction of the vector is 90° anticlockwise to the direction of the wind. Consider the case shown in Figure 7:3. This kite is in a stable position where there is no resultant force varying the line angle λ. By including a 'wind radius', the geometry of the test setup is dimensionally similar to the velocity components at the kite. However, unlike the radius, r, the wind radius does not move. Therefore, as the radius, r, follows its circular path during the test the ratio S/r' varies. According to Figure 5.4 (Chapter 5), varying S/r without changing the Lift to Drag ratio of the kite, will change λ. This will affect the Lift to Drag ratio measurements and the calculation of V_k, which affects the Lift Coefficient measurement.

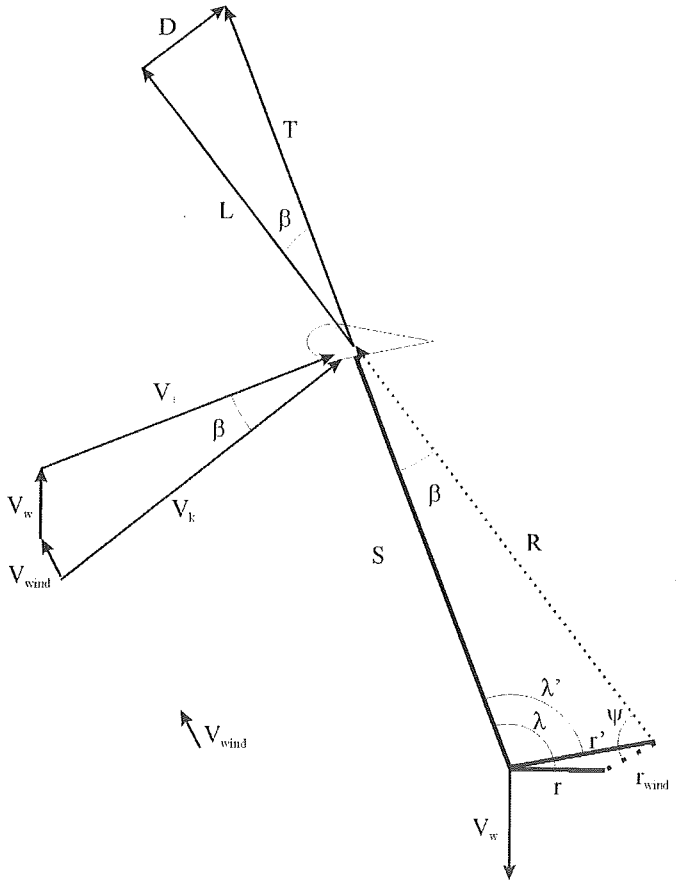

Figure 7:3 'Static' geometry with wind effects

The following steps are used to determine the value of λ at different points.

- First define an angle to represent the angular location of r in respect to r_{wind}.
- Use the dimensions r and r_{wind} and the angle between them to find r' using the cosine rule.
- Use the sine rule to find the angle between r' and R
- Use the sine rule to determine λ'
- Use the sine rule to determine the difference between λ and λ' and therefore determine λ.
- Use the cosine rule to determine R using λ',r' and S.
- Use R to determine V_k using

$$V_k = V_w \frac{R}{r} \qquad \textbf{Eq 7:2}$$

Figure 7:4 shows an example plot of how λ and $(V_k/V_{kmea})^2$ vary with the angular location of the radius r. $(V_k/V_{kmea})^2$ is shown as this indicates how the measured Lift Coefficient varies from the kites actual Lift Coefficient.

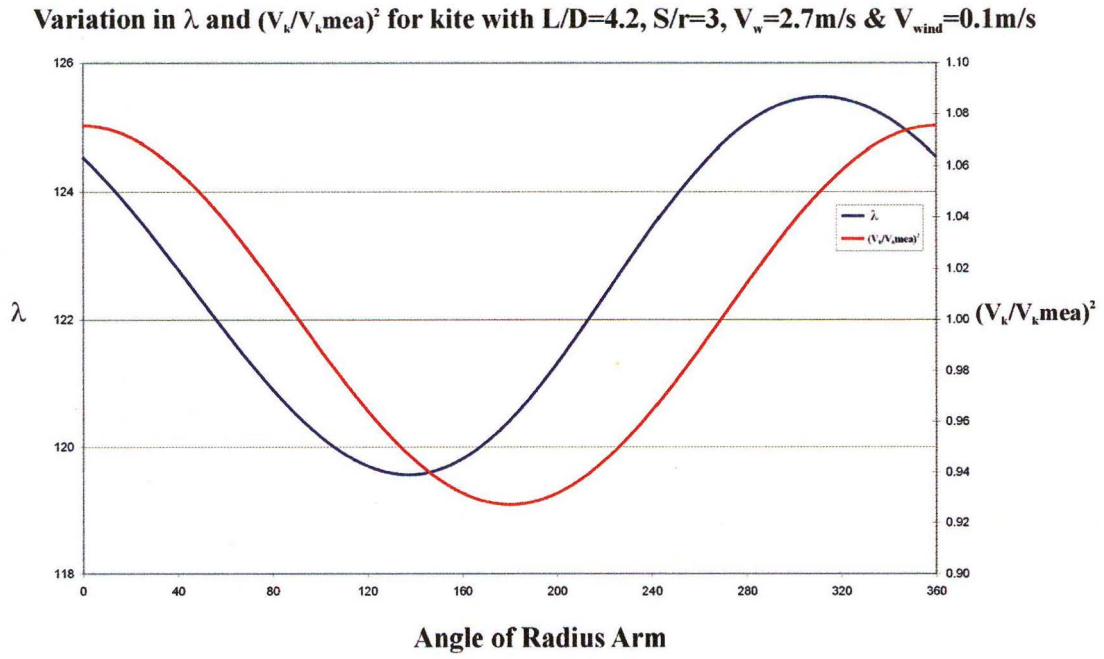

Figure 7:4 Variation in λ as radius follows its path in the presence of natural wind

There are a few key points about this graph. First, the average value of L_t/D_t as the kite surges is not the same as the kite's L_t/D_t, although the difference is not great. Secondly, the curves are not sinusoidal. This is because the maximum and minimum points are not 180^o apart. The maximum and minimum points occur when the angle ψ, shown in Figure 7:3, is 90^o and -90^0 respectively. This is because at these points R is tangential to an arc formed by r_{wind}. When this happens λ will be at its maximum and minimum points. Assuming that σ_1 is the angle of r and $\sigma_1=0$ corresponds to when r and r_{wind} are end on end then the angular locations of these points are

$$\sigma_{1max} = 360 - \cos^{-1}\left(\frac{S\sin(\beta) - r_{wind}}{r}\right) \qquad \textbf{Eq 7:3}$$

and

$$\sigma_{1\min} = 180 - \cos^{-1}\left(\frac{S\sin(\beta) + r_{wind}}{r}\right) \qquad \textbf{Eq 7:4}$$

The corresponding angle λ to these points are

$$\lambda_{\max} = 450 - \beta - \sigma_{1\max} \qquad \textbf{Eq 7:5}$$

$$\lambda_{\min} = 270 - \beta - \sigma_{1\min} \qquad \textbf{Eq 7:6}$$

These angles are illustrated in Figure 7:5.

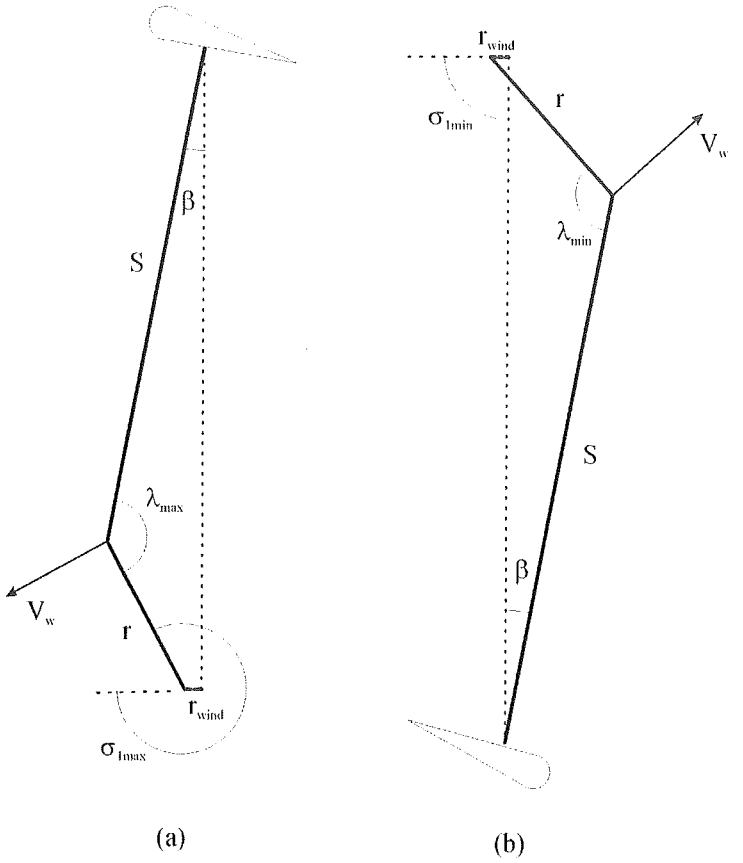

Figure 7:5 Location of peak points in wind affected data.

Thirdly, although not shown in either Figure 7:4 or Figure 7:5, if r_{wind} is large enough so that λ_{min} is not reached before θ_{min} reaches 180° then the kite will not complete a full circle. As shown in section 5.4.1 (Chapter 5) for each setup ratio, S/r, there is a minimum kite performance that can be tested. This minimum value is found when ψ equals 90° and θ_1=180°. Since r_{wind} changes the S/r ratio, the maximum r_{wind} that can be present is

$$r_w \max = r - S\sin(\beta) \qquad \textbf{Eq 7:7}$$

and from Eq 7:1

$$V_{wind} \max = \frac{(r - S\sin(\beta)) \cdot V_w}{r} = \left(1 - S/r \sin(\beta)\right) \cdot V_w \qquad \textbf{Eq 7:8}$$

If the wind speed is greater than this value the kite will be unable to fly and testing will be impossible. Eq 7:8 also shows that V_{wind}max increases for kites with high Lift to Drag ratios but can also be increased by reducing the ratio S/r. However, this is still a significant limitation on outdoor testing. For example, assuming that V_w=3m/s, S/r=3 and L/D = 4 (β=14°) then V_{wind}max=0.82m/s. Days with natural wind speeds this slow are infrequent limiting the viability of outdoor testing.

The proceeding analysis identifies some of the key characteristics of circular testing in the presence of natural wind. However, its accuracy is limited as it does not allow for the motion of the kite as it surges. To accurately model the kite a dynamic model is required.

7.3.2 Dynamic Analysis

Taking into account the movement of the kite adds a level of complexity to the model. The major difference between the static model and a dynamic model is that $V_\perp$ is no longer tied to V_w and the geometry of the test setup. Instead, the magnitude of $V_\perp$ is

dependent on $F_\perp$ which exists as the kite responds to the varying direction of the natural wind throughout the test.

Figure 7:6 shows all the relevant geometry of this model while Figure 7:7 is a flow diagram of the program of the dynamic model

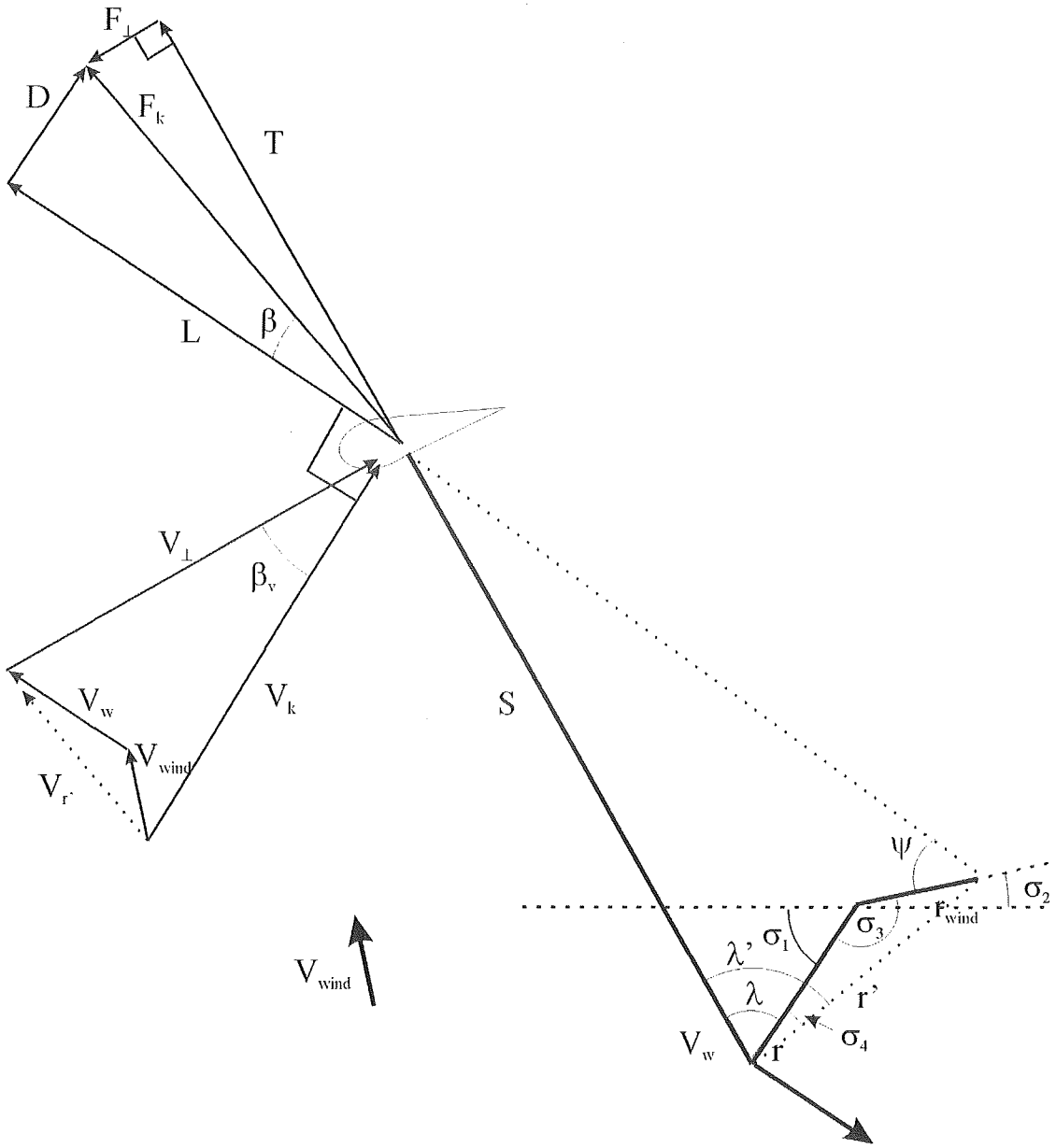

Figure 7:6 Dynamic model vector diagram

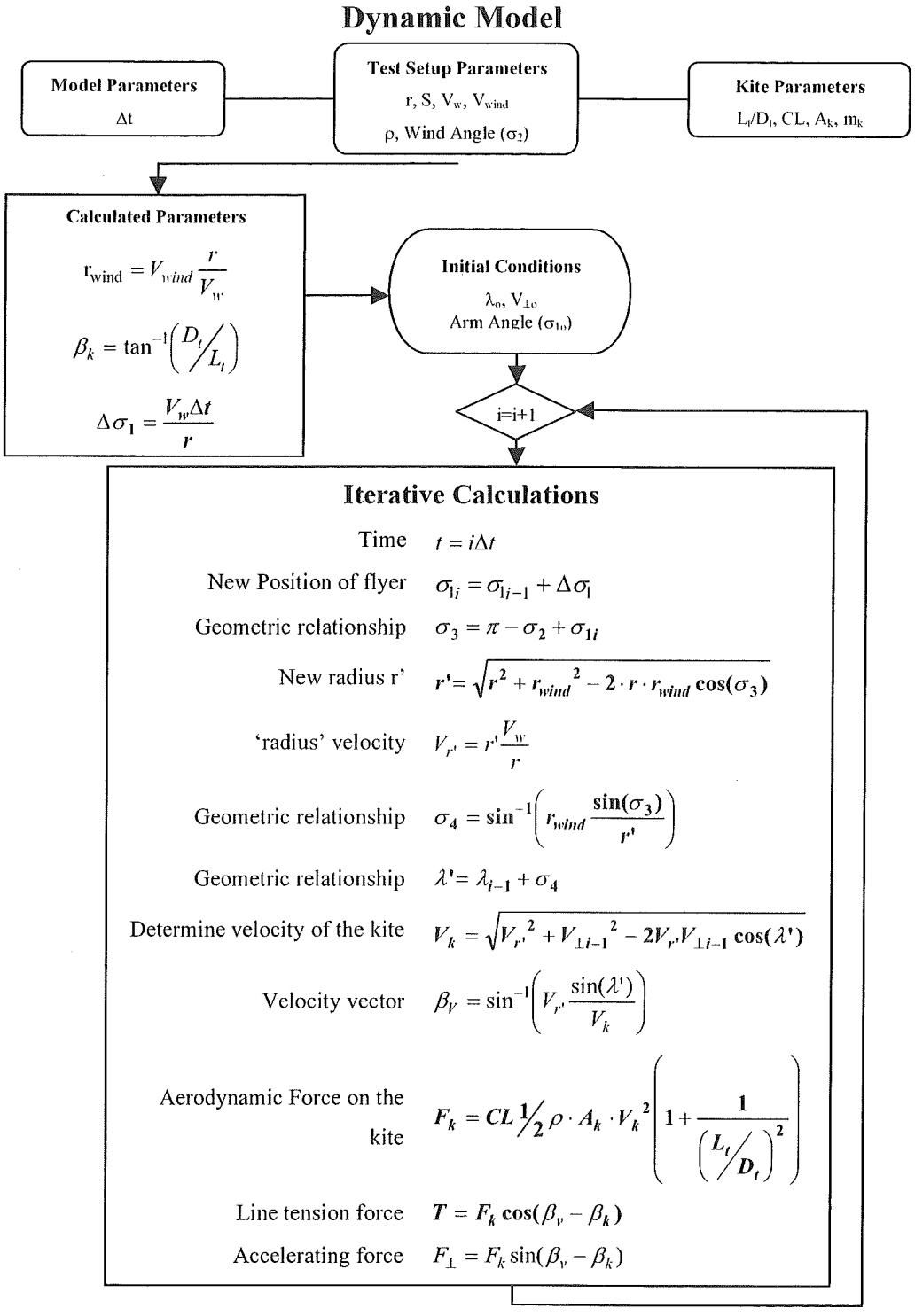

Figure 7:7 Dynamic model Programme format

Figure 7:8 shows the comparison between the dynamic model and the static model after the dynamic model has done three revolutions to eliminate the effect of the starting conditions.

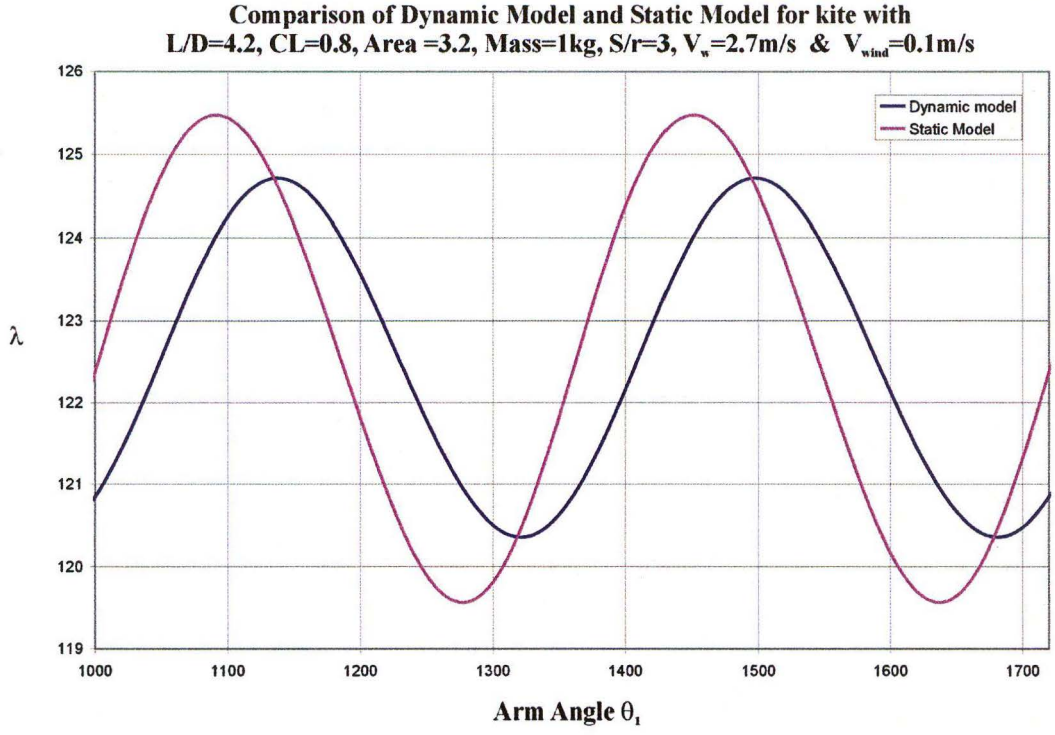

Figure 7:8 Comparison between static and dynamic model

The major difference between these two models is the size of the peaks and the angular location (θ_1) where these peaks occur. In the dynamic model the peaks occur later and are not as large. Both of these differences are due to the mass of the kite causing a lag in the response time of the kite. Ideally this model would also consider the added mass of the kite as it this will cause a greater variation in the two curves.

7.4 Applying Models to Data

As already explained it would be good to be able to extract the kite performance from the data obtained on a windy day. The following techniques have been attempted to try and achieve this goal.

7.4.1 Averaging the values

Perhaps the best method for extracting data from wind-affected results is to average the data throughout the course of a complete cycle. As already indicated the average data is not quite the same as the kite performance but the error is generally within ±5%. Compared to the other methods attempted this is a good degree of accuracy. It was found that averaging the data was the easiest and most effective means of obtaining usable and realistic kite performance information from wind-affected data.

7.4.2 Full Dynamic Reduction of Data

Given a series of data points for λ it should be possible to determine what the angular velocity and acceleration are of λ. From these values the kite's actual Lift to Drag data during the test should be able to be extracted from the wind-affected results.

Unfortunately at this point this technique has been unsuccessful. The major difficulty occurred when determining the angular acceleration of λ, as a double derivative of a location tends to be very noisy. Even after aggressive filtering the problem was not adequately solved so this type of data analysis was abandoned. In the future it may be possible to analyse experiments this way but it would require a faster sampling rate and more accurate readings. Even then there is no guarantee that this method will provide more accurate results than simply averaging the data or the other methods specified further.

7.4.3 Partial Dynamic Reduction of Data

Due to the difficulties obtaining stable data from wind-affected results using a full dynamic data reduction it is worth considering a partial dynamic reduction. In this technique the input parameters of the dynamic model described in section 7.3.2 are adjusted until the data matches the results that were obtained during the test.

This method still requires some of the data gained in the test to be used in the model. In particular the speed of the buggy must be used to determine the angle of the arm (σ_1) for each data point.

Figure 7:9 shows this technique applied to a data set. Despite the fact that a reasonable match can be made, the results are less than desirable. The main problem is that adjusting the parameters to fit the data is largely a matter of feel. This particular match was made with a reasonable idea of the kite's performance. Trying to achieve a blind match would be more difficult. The model is also relatively insensitive to the kite inputs so it is often difficult to determine if changing the input parameters is improving the correlation or not.

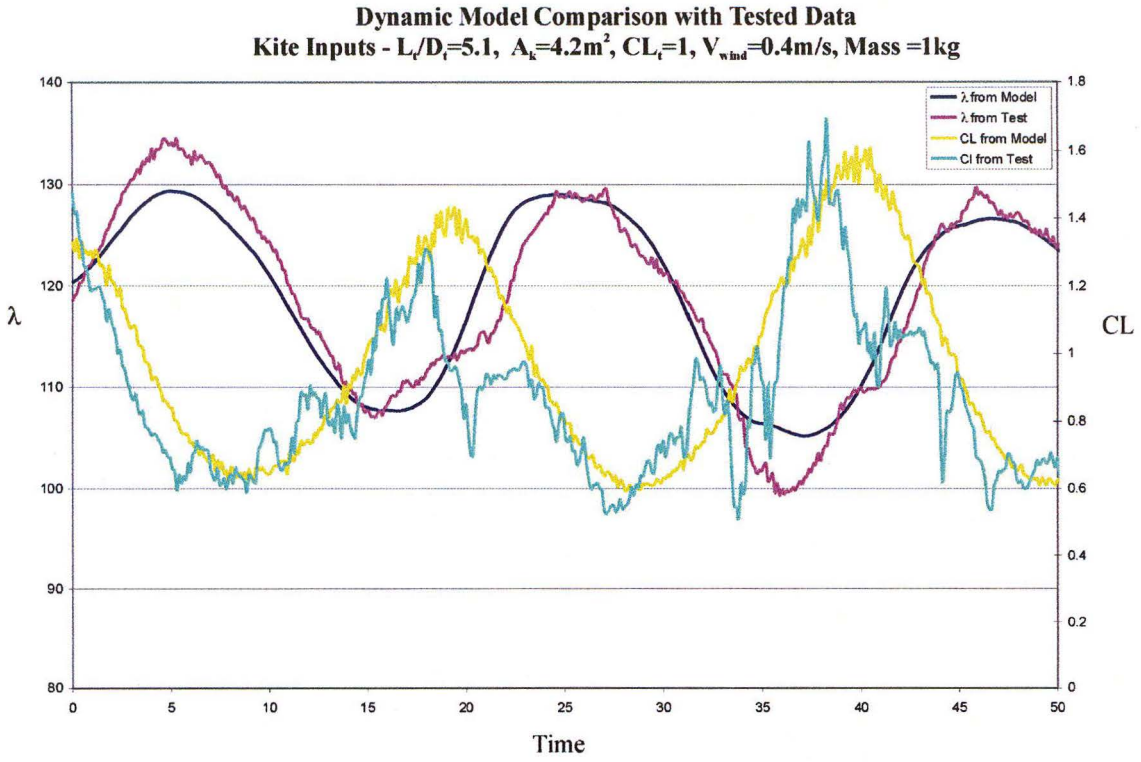

Figure 7:9 Partial dynamic data comparison

7.4.4 Static Analysis

Rather than applying a dynamic model and attempting to reduce the data it is worth considering applying a static model to the data. This is simply reversing the analysis outlined in section 7.3.1 to obtain a uniform set of results.

From the results the arm angle λ is known. By reversing the mathematical manipulation described in section 7.3.1 the dimensions r', λ' and R can be determined from the physical geometry. The only variables that need to be adjusted are the wind angle and wind speed. By doing this a more uniform Lift to Drag profile can be obtained. Figure 7:10 shows an example of this.

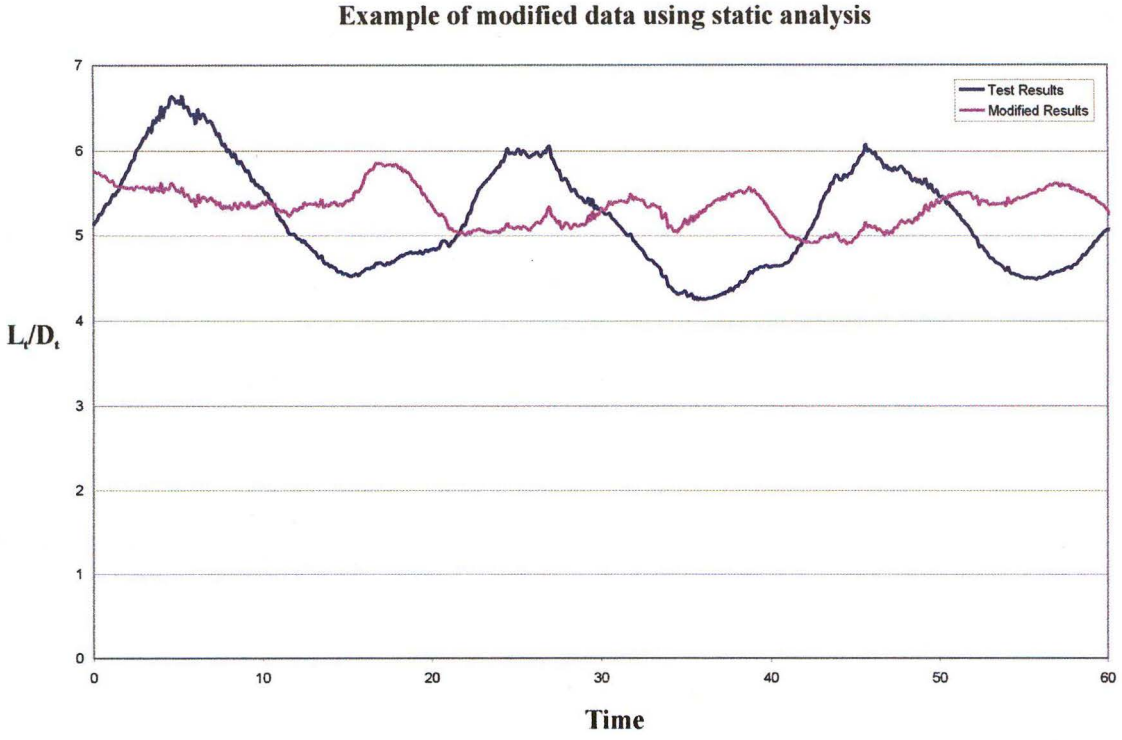

Figure 7:10 Static analysis of data

Although this technique had some success it has a few key problems. First, due to the offset between the dynamic and static model (See Figure 7:8), the wind direction that is used in the data reduction needs to be offset from its true direction. Secondly, the peaks in a static model are different to those in a dynamic model so a different wind speed is required. Thirdly, it is difficult to justify the application of a model to data when the model is known to be incorrect.

7.5 Walking Tests in Natural Wind.

Most people do not have access to a fixed arm circular test rig so would have to resort to walking tests done outdoors. To do a walking test the flyer walks backwards keeping the kite directly in front of them. With the kite in front of the flyer the angle λ will be 90^{o} throughout the test. As shown in Chapter 5 with $\lambda=90^{o}$ there is a direct relationship between the Lift to Drag ratio, the line length S and the walking radius r.

Since there is always some wind present outdoors, this will have an effect on the walking test. The following is a description of two numerical methods to analyse what happens. Both methods produce virtually the same answer.

Each method makes some assumptions. However, common to both methods is the assumption that the flyer varies their walking speed to keep the tension in the kite line constant.

7.5.1 Fixed Geometry Method

This first method is the simpler of the two. It is comparable to the static analysis performed in section 7.3.1. Figure 7:12(a) shows the geometry for this analysis. To determine the walking path the following steps need to be performed

1. In a spreadsheet or suitable program define the Lift to Drag ratio of the kite
2. Define the point (X,Y) where the flyer starts from and the angle of the line relative to the Y-axis (γ).
3. Using these dimensions and the line length (S) determine the location of the kite (X,Y)
4. Using these locations, find the appropriate walking speed (V_w) and the velocity perpendicular to the line ($V_\perp$) for each angle γ. In both methods the tension in the line, and therefore V_k, are assumed to be constant. The added assumption in this method is that the angle between V_k and $V_\perp$ is the same as the performance angle β. This is not strictly correct but is a useful approximation. With these assumptions the following equations apply.

$$V_k \sin(\beta) = const = V_W + V_{wind}\cos(\gamma)$$
$$\therefore V_w = V_k \sin(\beta) - V_{wind}\cos(\gamma) \qquad \textbf{Eq 7:9}$$

and

$$V_k \cos(\beta) = const = V_\perp + V_{wind} \sin(\gamma) \qquad \textbf{Eq 7:10}$$
$$\therefore V_\perp = V_k \cos(\beta) - V_{wind} \sin(\gamma)$$

5. Using $V_\perp$ the new angle γ is found by

$$\gamma_i = \gamma_{i-1} + \frac{V_\perp}{S}\Delta t \qquad \textbf{Eq 7:11}$$

6. Using this angle, the location of the flyer's location at the next time step is found by

$$(X_i \quad Y_i) = (X_{i-1} + V_W \sin(\gamma_i)\Delta t \quad Y_{i-1} - V_W \cos(\gamma_i)\Delta t) \qquad \textbf{Eq 7:12}$$

7. Return to step 2 and repeat for desired number of interval.

The results are shown in Figure 7:12.

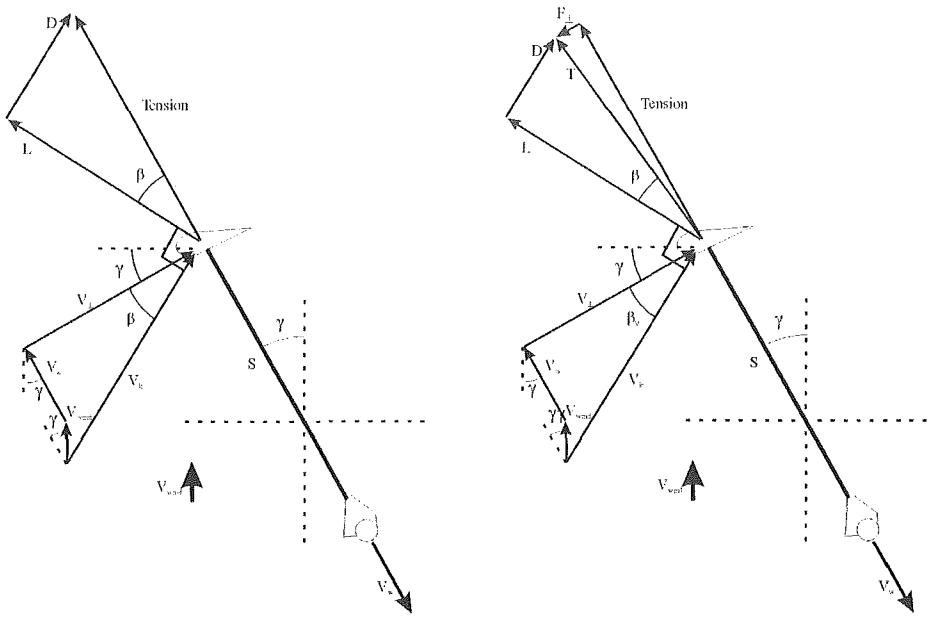

(a) Fixed Geometry Method (b) Dynamic Method

Figure 7:11 Fixed geometry and dynamic model for determining walking paths

7.5.2 Dynamic Method

The above method is only a first approximation which does not take into account the force required to change $V_\perp$. This Dynamic method allows $V_\perp$ to vary, due to the forces acting on the system as shown in Figure 7:11(b). The numerical method described below is slightly more complicated than for the fixed geometry method.

1. Define the kite's properties i.e., Lift to Drag ratio, CL, ρ, Area, Mass
2. Define the point (X,Y) where the flyer starts from and the angle of the line relative to the Y-axis (γ).
3. Using these dimensions and the line length (S) determine the location of the kite (X,Y)
4. Define an initial $V_\perp$. The closer this value is to the initial speed from the fixed geometry method the closer the results will be.
5. The next step is to define V_w. In reality this is not a complete dynamic model as the flyer is assumed to respond immediately to maintain a constant line tension. V_w is found by assuming that the magnitude of V_k is constant. Therefore using Pythagoras

$$(V_\perp + V_{wind}\sin(\gamma))^2 + (V_w + V_{wind}\cos(\gamma))^2 = V_k^{\,2}$$

$$\therefore V_w = \sqrt{V_k^{\,2} - (V_\perp + V_{wind}\sin(\gamma))^2} - V_{wind}\cos(\gamma) \qquad \textbf{Eq 7:13}$$

   This is a slight modification of the assumption that the line tension is constant. Keeping V_k constant this will make T (shown in Figure 7:11) constant instead of the line tension. However, the difference is relatively minor and doing the calculations this way is much simpler.
6. Find the new angle γ using Eq 7:11
7. Determine β_v using the following equation

$$\beta_v = \tan^{-1}\left(\frac{(V_w + V_{wind}\cos(\gamma))}{(V_\perp + V_{wind}\sin(\gamma))}\right)$$

Eq 7:14

8. β_d is then the difference between β_v and β.
9. Since V_k is known as well as the kite properties, the force T can be determined.
10. The driving force ($F_\perp$) is therefore

$$F_\perp = T\sin(\beta_d) \qquad \textbf{Eq 7:15}$$

11. The acceleration of the kite in the perpendicular direction is determined and the new $V_\perp$ found, assuming constant acceleration during the time step.
12. The new location of the flyer is found using Eq 7:12
13. Return to step 5 and repeat for the desired number of intervals.

7.5.3 Predicted Results and Performance Measurement

The results from the two models are shown in Figure 7:12. It can be seen that natural wind tends to make the walking path into a spiral. However, it is still possible to approximate the walking radius used in the performance equation by measuring the dimension shown in the figure.

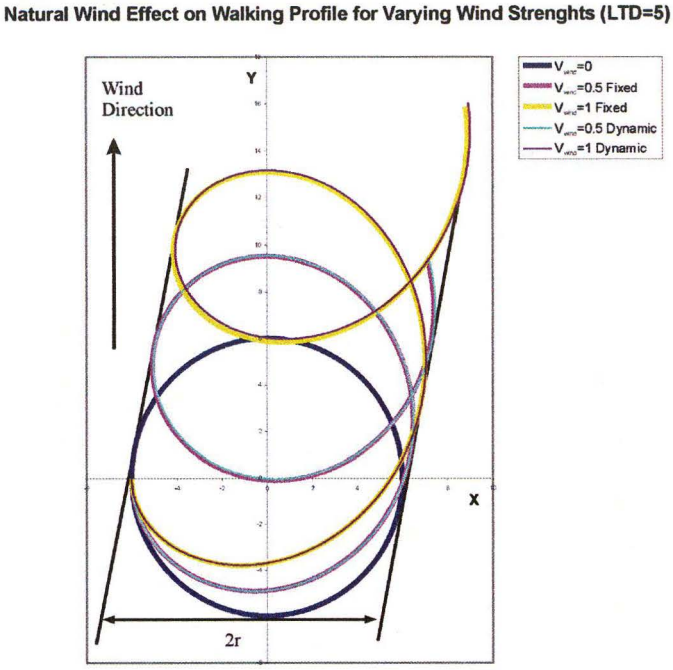

Figure 7:12 Variation in walking path with natural wind

Figure 7:12 also shows the results from the two models. Both kites had a Lift to Drag ratio of 5, a line length of 30m and the same starting point. The kite used in the dynamic model also had a CL=1, Area=4m^2 and mass of 1kg. The V_k used in both models was 10m/s and the initial starting velocity of the dynamic model was similar to that of the fixed model. With all these inputs there is only a slight difference in the walking paths predicted by each methods.

7.5.4 Practical Considerations For Walking Tests

Walking tests of this sort are best done on a markable surface so that the dimensions can be determined after the test is finished. In most cases this would be a beach or a dew covered field. The dimensions of the walking path can then be found later after the test has been performed. Figure 7:13 shows an example of these markings on a beach.

Although doing this method is less capital intensive than using an indoor test rig, the accuracy of the method is not as good. In the course of this project test runs were

performed which produced significantly different results. Increased measurement accuracy can be achieved by doing numerous runs but this exhausts whoever is doing the tests. However, despite the issues with this method it is still useful for obtaining an estimate of kite performance.

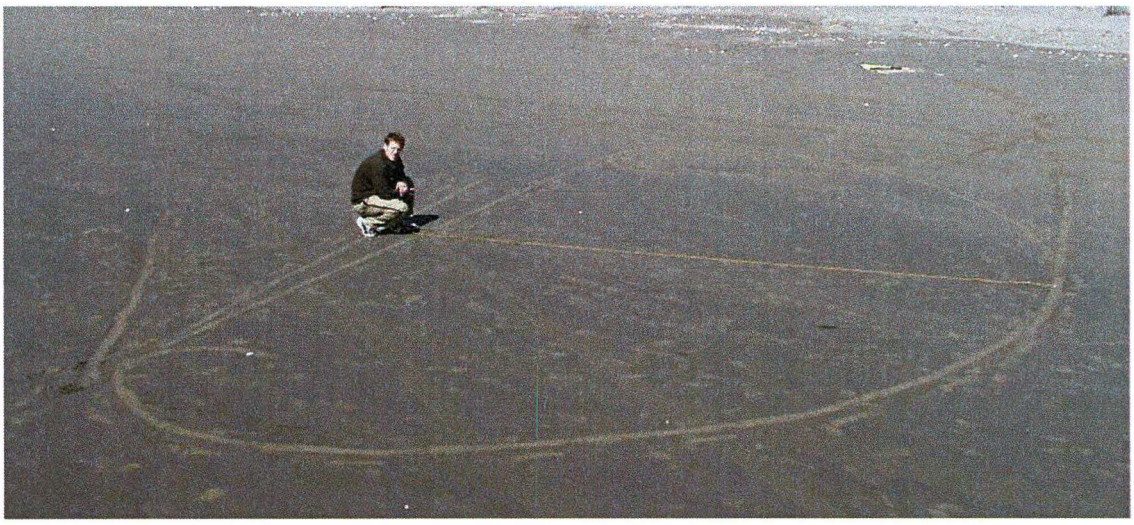

Figure 7:13 Wind effects circular walking test path

7.6 Conclusion

Natural wind has a significant effect on the results from circular testing. First, it causes large variations in the Lift to Drag measurement and the Lift Coefficient. Secondly, a small amount of wind can make the test impossible to do as it overly affects the velocity of the kite at some points around the flying circle.

Despite this it is possible to obtain usable data from natural wind-affected results. Although applying models to this data has an element of success, averaging the data is the most effective means of obtaining results.

Overall, these results show that it is not ideal to do circular tests outdoors. The major concern is not the effect on the data but the limited number of days when tests can actually be performed. In general outdoor tests should only be performed as a last resort.

8. Determining Kite Stability Points

8.1 Summary

This chapter outlines how the flying location of a kite can be determined based on the properties of the kite structure. The essential condition for kite stability is that the moment at the bridle point of the kite is equal to zero. To achieve this condition, the kite will change its angle of attack in flight. By adjusting the location of the bridle point, the kite can be made to fly at different angles of attack and therefore the performance of the kite can be varied.

An analytical model was developed to predict stability points and an experimental model was flown in the wind tunnel to confirm these predictions. The results from these tests closely correlated with the predicted results. It was also shown that under certain conditions multiple stability points exist in both the predictions and the experiments.

8.2 Introduction

8.2.1 What is a stability point?

A kite stability point is the angle of the line when a kite is flying in a settled position. Chapter 1 demonstrated that a kite's performance is directly related its Lift to Drag ratio, which in turn is related to the line angle. It is therefore a fundamental component of kite dynamics to be able to predict where a kite will settle and the angle of the line at this point. The focus of this chapter is to show how this is achieved when the properties different parts of a kite are known.

Understanding kite stability points is also important as it affects many other aspects of kite dynamics. It determines why kites can fly at different locations, is essential for

understanding kite turning and kite control and raises structural and design issues. Essentially most facets of kite behaviour rest on knowing where a kite will fly in a stable manner.

8.2.2 Past Research

Stability points have received very little attention in the brief amount of academic literature that exists on kites. Most authors have been more concerned with the kite line than with the interactions between the lifting surface and the line. Toshio Ito and Komura (1983) looked at the effect of moving the attachment point on the kite surface, but failed to recognise that the existence of a bridle point makes a kite behave differently than when the kite line is attached directly to the wing. In the later case there is only one possible angle for the line, while a bridle point introduces more possibilities. Hobbs (1986) also realised that there was a relationship between bridle position and kite line angle and went a long way to describing the interactions that are necessary for an analysis of kite stability points. Unfortunately, he did not identify some of the key characteristics of kite flight and consequently his conclusions missed key areas. In particular he failed to identify the existence of dual stability points and, by making the assumption that the line angle and the angle of attack were directly related, overlooked key components. Neither author did any experiments directly focussing on stability points.

8.2.3 Scope of Chapter

First, this chapter will outline the theory behind stability points showing two different analysis techniques. Secondly, it will outline the methodology used to determine the test kite's properties and the how stability points were measured. Thirdly, the program used to predict stability points will be outlined. Fourthly, the experimental results will be presented and compared to predicted values. Finally, there will be a discussion of the key findings from these experiments and their impact on kite design.

8.3 Theory

8.3.1 Conditions for a stability point to exist

Two things are required to define a stability point:

- First, the conditions required for a kite to maintain a constant angle of attack need to be found; and
- Secondly, the angle of the kite line under these conditions, and therefore the kite's Lift to Drag ratio, needs to be determined.

To illustrate how these two conditions are met, a simplified kite structure, with only the wing's aerodynamic loads, is shown in Figure 8:1.

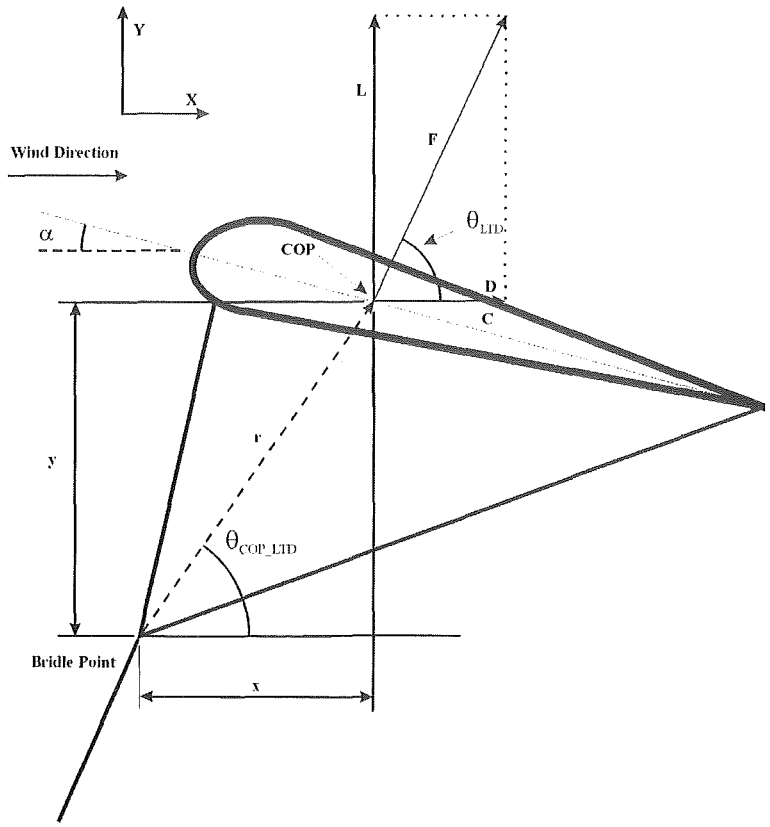

Figure 8:1 Simple kite force diagram

For the kite to maintain a constant angle of attack the moment about the bridle point must equal zero. In general the following equation must apply.

$$\sum_{i=1}^{n} \bar{r}_i \times \bar{F}_i = M = 0 \qquad \textbf{Eq 8:1}$$

where $\bar{r}_i$ is the radius from the bridle point to the location of the force $\bar{F}_i$. In the case of the kite shown in figure 1, this equation reduces to

$$L.x - D.y = M \qquad \textbf{Eq 8:2}$$

If the moment is equal to zero at a given angle of attack, then that point will be a stability point. If the moment is not equal to zero then the angle of attack will change until this condition is met.

If the wing's Lift and Drag coefficients, and centre of pressure migration are known for a range of angle of attacks, then the kite's stability points can be determined. Since the kite's lift and drag forces vary with wind speed, but the mass of the kite stays constant, it can be expected that the stability point will vary as the wind speed changes. Determining what the stability point is over a wide range of conditions is an iterative process.

Once the first condition is met, the second condition, determining the angle of the kite line, is relatively trivial. The angle of the line is determined by applying Eq 8:3.

$$\theta = \tan^{-1}\left(\frac{L}{D}\right) \qquad \textbf{Eq 8:3}$$

Although Figure 8:1 only includes two forces, Eq 8:1 will continue to apply when all the other forces acting on the structure are included.

8.3.2 Graphical method for determining stability points

Although the above analysis is effective for determining the stability points, some of the characteristics of kites are not easily identified using this method. In particular, although a plot of moment versus angle of attack will reveal the angle of attack where a stability point exists, it will not show the angle of the line at this point. Also, the above method does not show the interaction between the Lift to Drag ratio and the centre of pressure of the kite as the angle of attack varies.

One way to represent both the line angle at a stability point, and the change in kite properties, is to compare θ_{LTD} and θ_{COP_LTD} as the angle of attack of the kite varies. θ_{LTD} and θ_{COP_LTD} are both shown in Figure 8:1. θ_{LTD} is the angle that the force acts in and is defined in that same way as θ in Eq 8:3, while θ_{COP_LTD} is the angle of the line between the bridle point and the location of this force. Both angles are measured relative to the wind direction. If θ_{COP_LTD} is the same as θ_{LTD} at a given angle of attack then this point is a stability point. This result is expected, as at this point the resultant force will act though the bridle point, causing the moment to be zero.

When these two angles are plotted together against angle of attack they produce a graph similar to the one shown in Figure 8:2. Where the two lines intersect is a stability point and both the angle of attack and the line angle can be determined. It will be shown how varying the location of the bridle point and the wind speed affects these two curves and how they relate to each other.

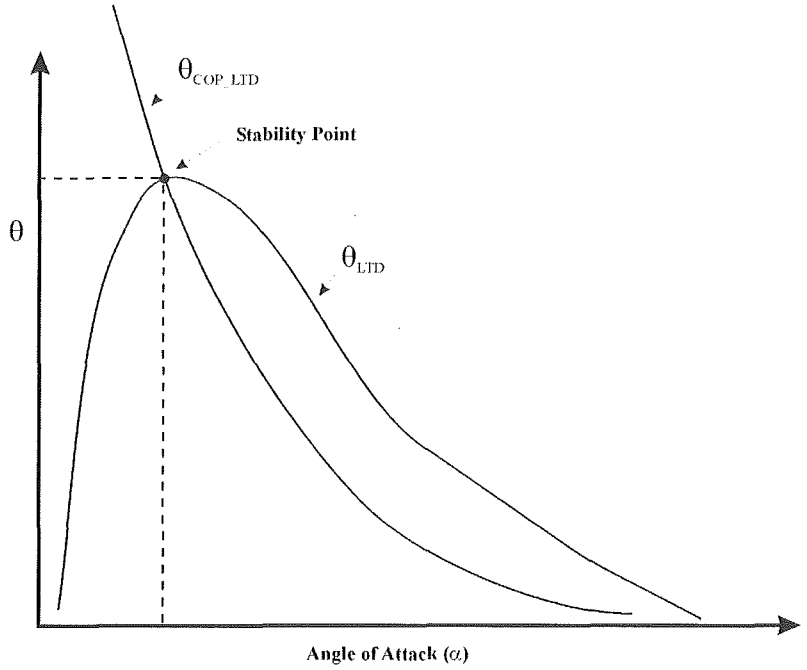

Figure 8:2 Stability point determined by intercept of COP_LTD and LTD line

Even the most simple kite structures have more forces acting on them than are shown in Figure 8:1. At the very least the mass of the wing should be included. Figure 8:3(a) shows the forces acting on a kite similar to that used in the tests performed in the following experiments. It includes both the weight and the aerodynamic forces acting on the kite and bridle. To simplify the diagram, distributed loads are shown as single forces acting through a point.

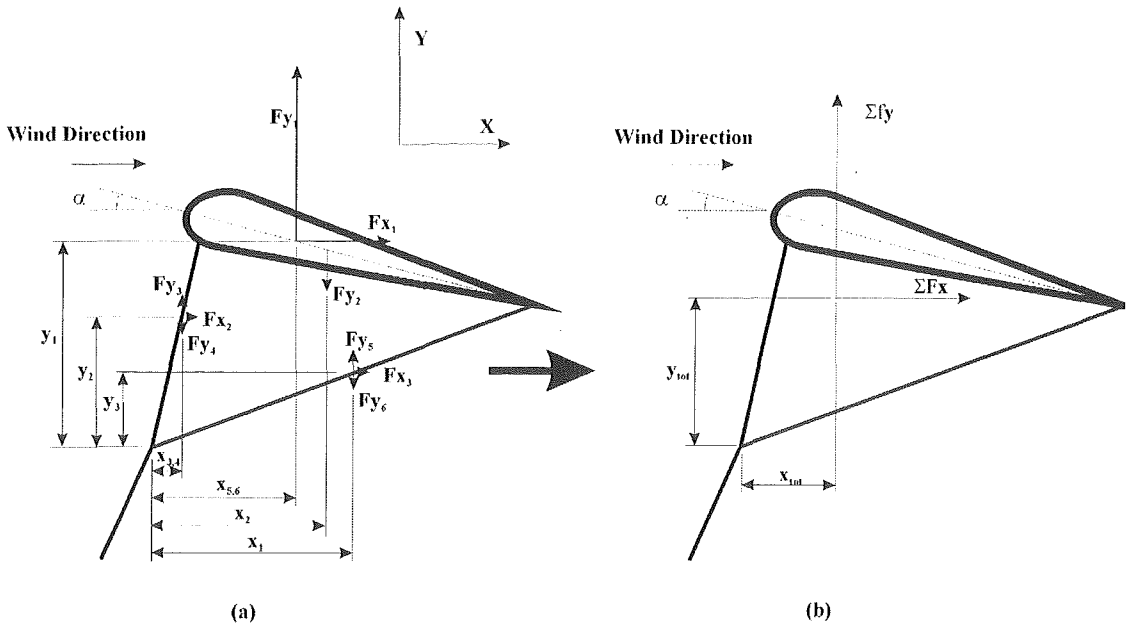

Figure 8:3 Kite with multiple different forces

With these more complicated models, determining θ_{COP_LTD} is more difficult as there are lots of individual forces. To find θ_{COP_LTD}, all the forces have to act at a single point. However, by combining the forces into a single force acting at a point (x_{tot},y_{tot}), as in Figure 8:3(b), θ_{COP_LTD} can be determined. Finding the point (x_{tot},y_{tot}) requires that the following equation to be solved.

$$\sum_{i=1}^{n} Fy_i x_i - \sum_{i=1}^{n} Fx_i y_i = x_{tot} \sum_{i=1}^{n} Fy_i - y_{tot} \sum_{i=1}^{n} Fx_i \qquad \textbf{Eq 8:4}$$

Since there are two unknowns (x_{tot} and y_{tot}) and one equation, the solution to this equation is a line. Any point along this line can be used to determine θ_{COP_LTD} but for this analysis to be relevant there should be some relationship between the location of (x_{tot},y_{tot}) and different angles of attack. A suitable restraint to apply is that the point (x_{tot},y_{tot}) is located on the chord line of the wing of the kite. Once this is done it is possible to plot both θ_{COP_LTD} and θ_{LTD} against one another and get meaningful results.

8.3.3 Potential Results

From Figure 8:2 it is apparent that under certain conditions the θ_{LTD} and θ_{COP_LTD} curves can intersect at more than one point. If this is the case it can be expected that a kite can sit at two or more different locations. It is expected that this will show up in experiments.

8.4 Aims of Experiment

The purpose of this experiment is two fold. The first purpose is to show that stability points can be predicted. When the aerodynamic properties, dimensions and the bridle position of the kite are known, the stability points should be able to be determined over a range of speeds. Secondly, the experiments aim to show the existence of multiple stability points in given conditions.

8.5 Determining Wing Properties and Kite Stability Points

To achieve the goals of this experiment a number of steps had to be performed. These are outlined below.

8.5.1 Kite structure used

The first step was to find a simple kite design that was rigid, strong and would fly stably in the wind tunnel. After many attempts the wing shape shown in Figure 8:4 was used. Two wings were made for these experiments. The first was made out of balsa wood, as this material is light enough to be used for a kite. An identical kite was made out of carbon so that the aerodynamic performance of the wing could be obtained without the risk of it breaking.

It was found that the having a dihedral angle was important for maintaining stability in flight. Stability was also aided by having curvature along the chord. This also increased the strength of the model.

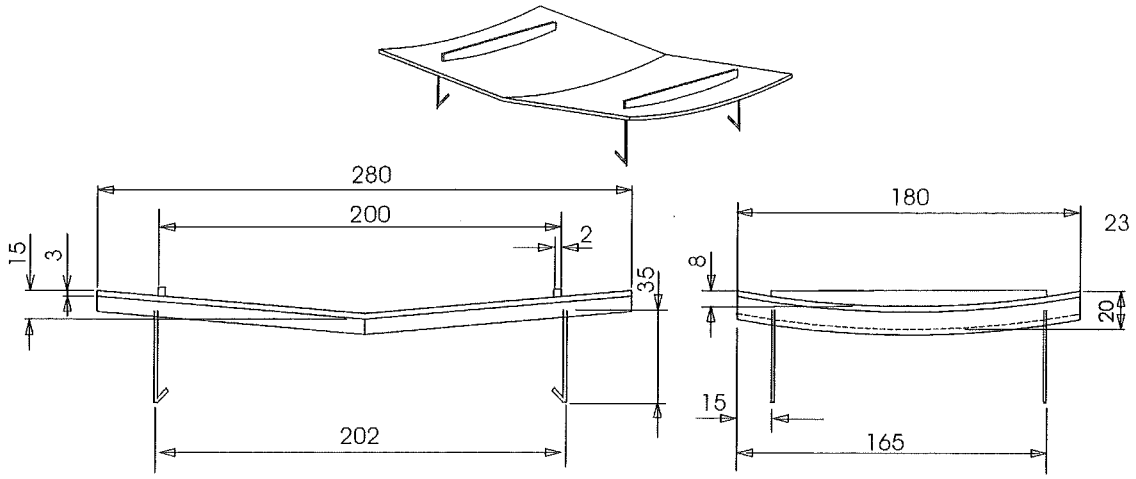

Figure 8:4 Dimensions of wing used in tests

The aspect ratio of this wing is approximately 1.5, which is relatively low. Although this restricted the performance of the wing, it was an aid to stability as it increased the angle of attack where stall occurs.

To perform multiple tests with different bridle positions, attachment points were fitted into the surface of the kite to simplify the change over process. The total weight of the balsa wing was 26g.

It was important that the bridle point was well defined, so the bridles were made of aluminium welding wire. This has a weight of 5g/m and a diameter of 1mm. Using aluminium was convenient as, with the help of a jig, numerous accurate bridle arrangements could be made. Because the aluminium was reasonably stiff it located the bridle point accurately.

8.5.2 Determine wing properties

Once this kite structure was built it was necessary to work out the aerodynamic characteristics of each part. The wing was tested in the wind tunnel on the three-axis force balance (see Figure 8:5). From this the Lift and Drag coefficients were obtained for angles of attack over a range of 0-60°.

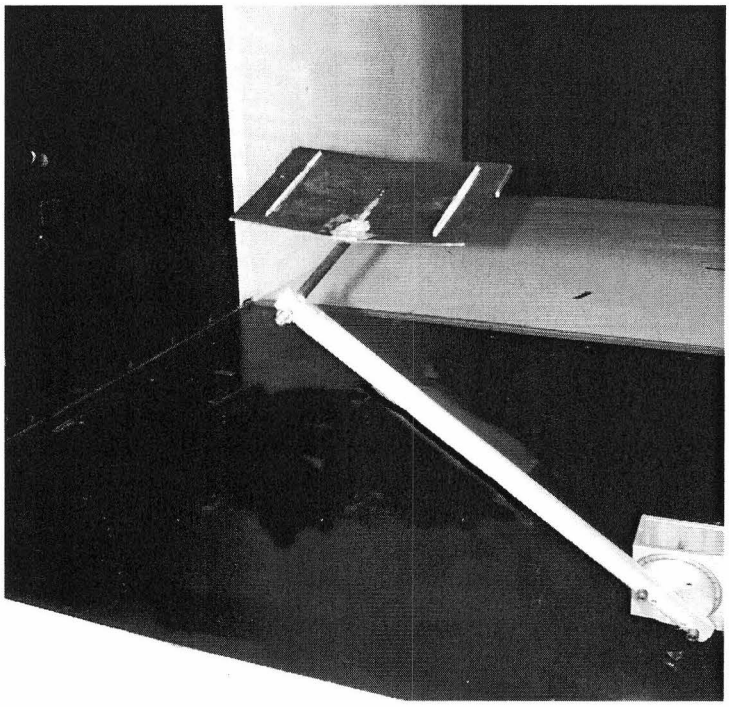

Figure 8:5 Wing mounted on sting in the wind tunnel

The centre of pressure data from the 3-axis balance was found to be unreliable so a different method was used to obtain this data. The wing was suspended between two pivot points on brackets attached to the sides of the kite (See Figure 8:6). These brackets had accurately drilled indents along the side so that the location of the pivot (and therefore the centre of pressure) could be varied. The angle of the wing at each pivot point was then determined and a plot of the migration of COP with angle of attack was created. The chord line was located on the line where the attachments point join the main body of the wing.

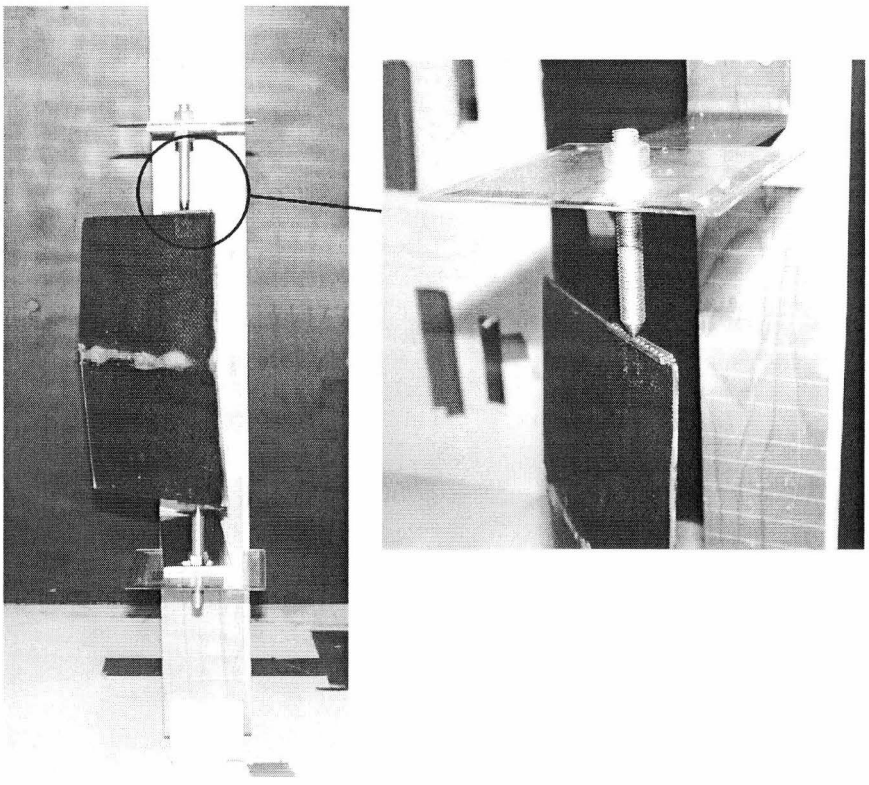

Figure 8:6 Apparatus used to find wing's centre of pressure migration curve

Bridle data was taken from Hoerner (1965) which details the lift and drag coefficients for tubes at an angle as

$$Cd = 1.1\sin^3(\omega) + .02 \qquad \textbf{Eq 8:5}$$

$$Cl = 1.1\sin^2(\omega)\cos(\omega) \qquad \textbf{Eq 8:6}$$

where ω is the angle of the tube to the wind .

The data from each component was then combined to determine the wings overall Lift and Drag coefficients, and the COP migration, at different angles of attack.

8.5.3 Stability Point Tests

A range of stability point data was obtained in the following way.

- First, a bridle of known dimensions was attached to the kite.
- The kite was placed in the wind tunnel and the kite flown at different wind speeds.
- While the kite was flying the angle of the line was measured. This was done by sighting across the kite line and reading the angle off a protractor.
- To find the dual stability points, measurements were taken at a number of wind speeds where there was a sudden jump in the height of the kite.

8.6 Program Format

Predicting stability points requires an iterative programme that varies wind speed and angle of attack. In this case a prediction programme was written in MATLAB and a graphical visualisation program was written in EXCEL. The following is an outline of the iterative programme.

1. The parameters of the chosen setup i.e., kite dimensions and weight, bridle setup, air density etc, were defined. The bridle point was located in relation to the leading edge of the wing. A positive 'x' direction was towards the trailing edge of the wing while a positive 'y' direction was away from the surface of the wing towards the ground.
2. The aerodynamic characteristics of the wing were defined.
3. A wind speed was selected
4. For each angle of attack all the forces were calculated, along with their location on the kite structure. To increase the accuracy of the prediction it was necessary to iterate between known data points.
5. The moment at the bridle point for each angle of attack was calculated.
6. The stability point was determined by finding the angle of attack where the moment was zero.

7. Based on these points, the resultant forces were calculated to find the line angle.
8. The results were recorded.
9. Steps 3-8 were repeated for the next wind speed interval.
10. The data was sorted and a plot of θ vs wind speed created.

8.7 Results

8.7.1 Wing Properties

The properties of the wing used for these tests, as determined using the 3-axis force balance, are shown in Figure 8:7. This data has not had a correction factor applied to eliminate wind tunnel blockage, as all further experiments using this wing have been performed in the wind tunnel[6].

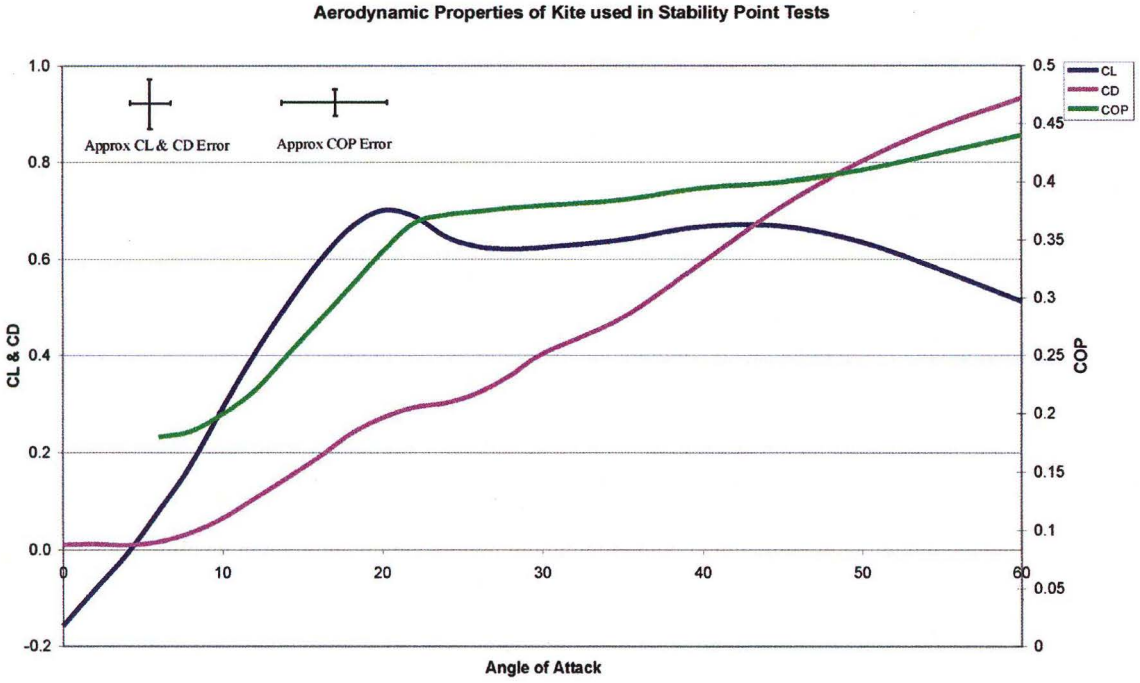

Figure 8:7 Properties of wing used in stability point tests

[6] If blockage corrected data is required, the wind tunnel cross-section has dimensions of 3' x 4'

The method used to determine the COP migration was unable to determine the COP of the wing at an angle of attack below 6°. However, it was unnecessary to have data below this point since the negative Lift Coefficient will ensure that the kite never flew in this region.

8.7.2 Errors in Wing Property Tests

- **Angle measurements** – The error in the angle measurements was ±1° for the Lift and Drag Coefficients and ±3° for the centre of pressure readings.
- **Lift and Drag Coefficients** – There was an overall error of ± 6% in the Lift and Drag Coefficients. 2% of this error was due to the load readings. Although the balance was accurate to ±0.5-1% two readings were required, one for the wing and one for the sting which the wing was attached to, roughly doubling the error. There was an error of ±1.5% due to the wind speed measurement, ±1% due to variations in the density and ±1.5% due area measurements of the wing.
- **Centre of Pressure** – There was an error of ±2% in the centre of pressure reading mainly due to the location of the pivot point bracket on the side of the wing.

8.7.3 Stability Point Results

Figure 8:8, Figure 8:9 and Figure 8:10 show the measured stability point results obtained compared with the predicted results. Nine bridle points were tested and these have been grouped into those with bridle points the same 'y' distance from the wing. This was done because these bridle arrangements have similar weights and therefore demonstrate the affect of varying the bridle point.

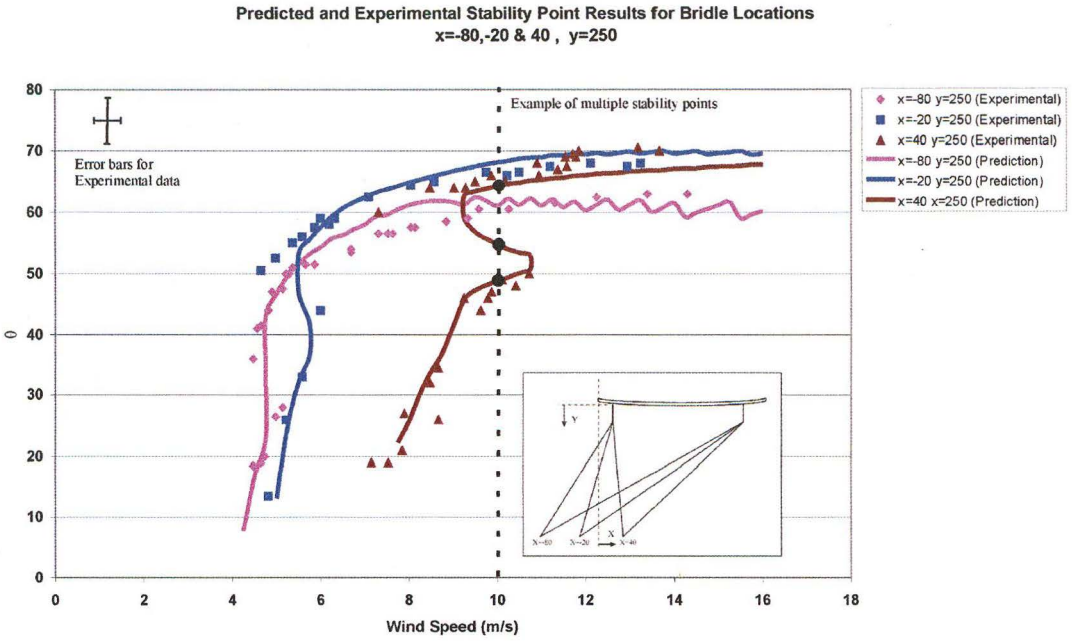

Figure 8:8 Predicted and experimental stability point results for y=250 (mm) bridle points

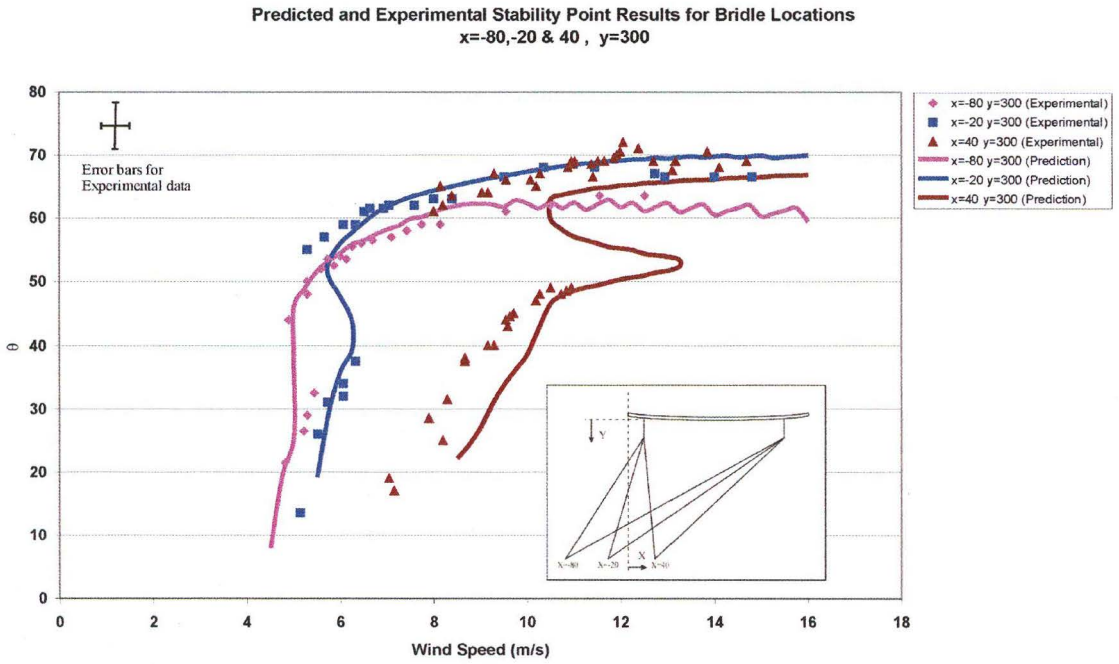

Figure 8:9 Predicted and experimental stability point results for y=300 (mm) bridle points

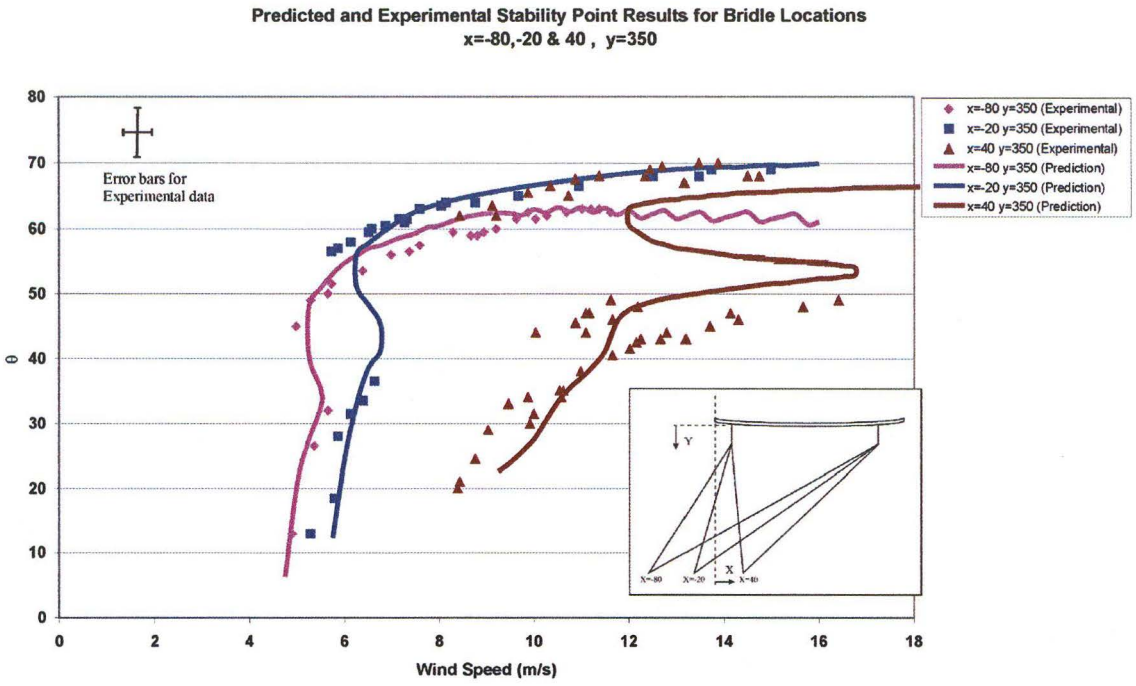

Figure 8:10 Predicted and experimental stability point results for y=350 (mm) bridle points

8.7.4 Error in Stability Point Tests

- **Wind Speed –** The error in the wind speed measurement was ±0.1 m/s
- **Angle Measurement** – The error in the angle measurement was ±3°. It was particularly hard to get accurate results at high θ angles as the kite line tended to oscillate very rapidly at these points.
- **Bridle Location** – The bridle location is accurate to within ±5mm in both the X and Y directions.

8.7.5 Prediction errors

It should be noted that the predicted data in Figure 8:8 to Figure 8:10 is also subject to measurement error, as they are based on the kite properties outlined in section 8.5.2. Unfortunately, these errors are very difficult to quantify. Some of the difficulties with the

predicted results are addressed in section 8.8.1. This section also demonstrates how varying the kite properties slightly can change the predicted stability point results.

8.8 Discussion

8.8.1 Theory vs Experimental Results

Allowing for experimental error, Figure 8:8, Figure 8:9 and Figure 8:10 show a fair correlation between the predicted stability points and the experimental results. Data sets (x=40,y=300) and (x=40, y=350) show a significant difference from the prediction but this can be attributed to limitations of the predicted data.

The major limitation is that stability points are predicted using data subject to experimental error. Given certain conditions these errors can have a large effect on the predicted results. Figure 8:11 shows the θ_{LTD} and θ_{COP_LTD} curves for the kite with a bridle point x=40 y=300 and wind of 10m/s. There are two areas where the prediction is very dependent on the accuracy of the wing performance data. The first is in the region where the two lines cross, at around an azimuth angle of 38^{o}. Any error in the experimental results of the wing properties will significantly vary the location of this stability point. Secondly, at lower angles of attack the two curves are very close together but do not cross. With the available data a stability point would not be predicted, but since the curves are so close one could actually exist. As will be shown, varying the data used in the stability point prediction within its error range can have a significant effect of the stability points that are predicted.

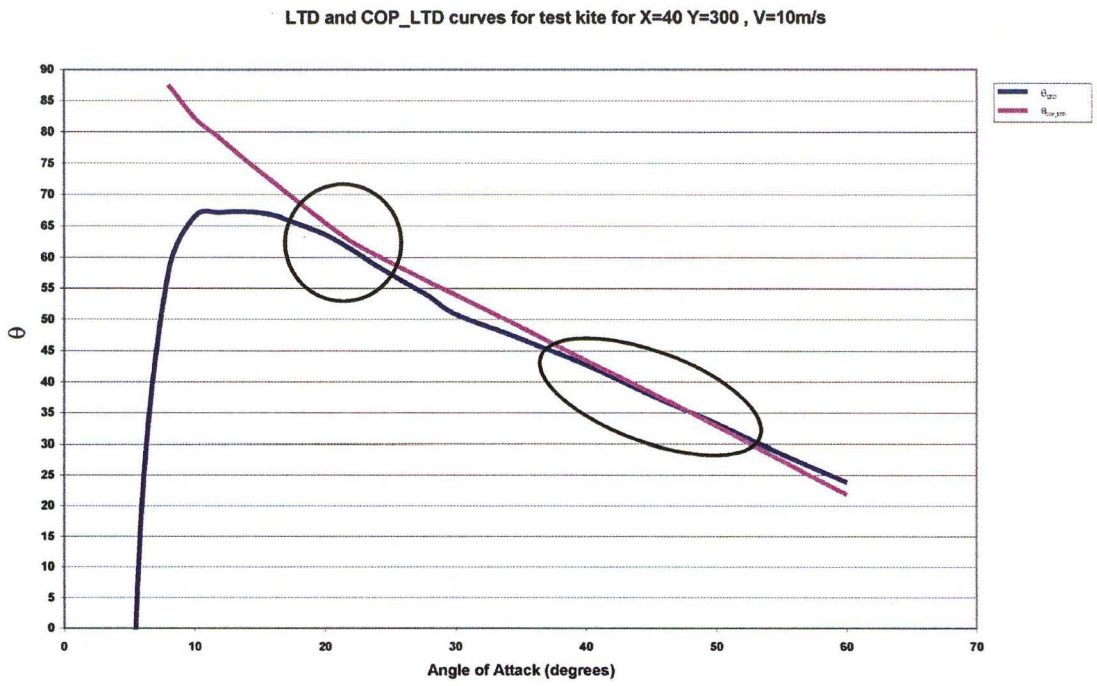

Figure 8:11 LTD and COP_LTD curves for X=40mm Y=300mm V=10m/s showing critical regions

Based on the stability point results, and in particular data sets (x=40,y=300) and (x=40, y=350), it was apparent that there was an error with the CL and CD measurements near the stall region of the wing between 18-24°. Obtaining accurate data around the stall point was difficult with the apparatus available, as the wind speed in the wind tunnel tended to surge when this wing was in the stall region, causing large load variations. Consequently the lift and drag values that were obtained were lower than expected, especially when compared to published data for a flat plate (ESDU, 1972) with the same aspect ratio. Since measurements near the stall are difficult ESDU publishes a range properties for a flat plate near the stall point. In this case, if the Lift and Drag Coefficients were modified in the stall region, as shown in Figure 8:12, a better correlation between the predicted stability points and the experimental results could obtained, as shown in Figure 8:13. These CL and CD values are estimations based on ESDU data, and experimental stability point results. Figure 8:13 demonstrates how changing these results in this way, significantly effects the correlation between the predicted and experimental stability

points. This problem is particularly significant with the two runs shown in Figure 8:12 because with these bridle points the kite flies in the stall region when flying at a higher line angle θ.

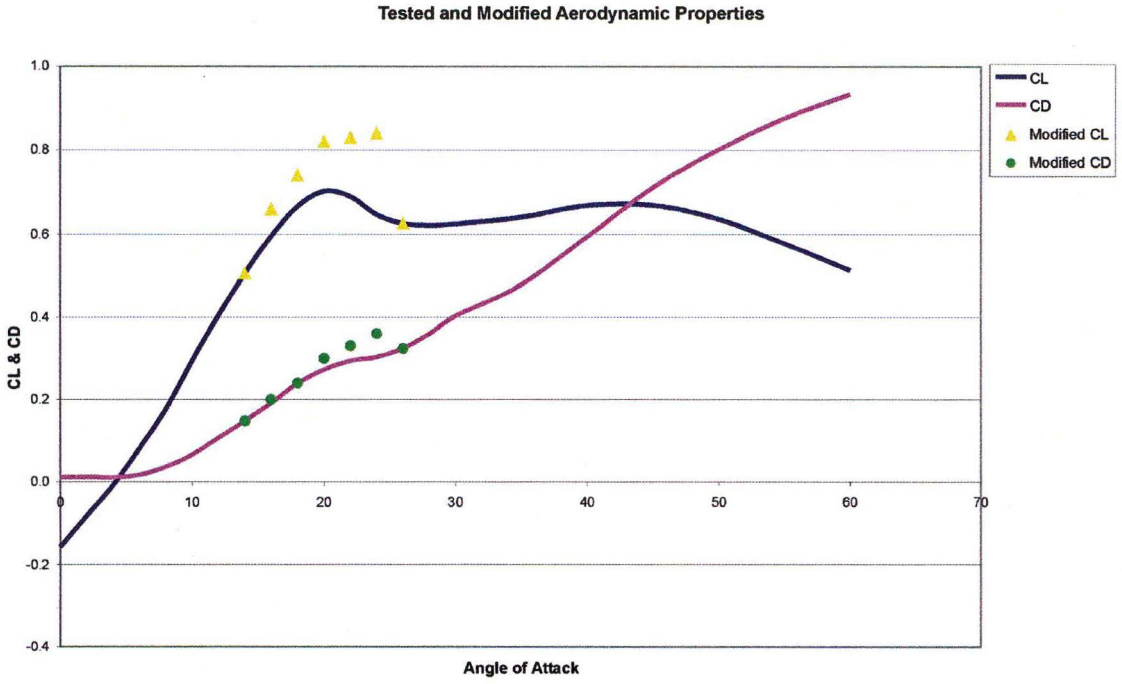

Figure 8:12 Kite performance data showing modified CL and CD in the stall region

Figure 8:13 Variation in stability point prediction with adjusted CL and CD Coefficients at the stall region.

Another difficulty with using experimental results for stability point predictions is shown in the x=-80 bridle points in Figure 8:8, Figure 8:9 and Figure 8:10. At high velocities (>8m/s) the azimuth angles prediction is not smooth. Although it is beyond the accuracy of this experiment, it is unlikely that the kite behaves in this way. The curve is not smooth because with this bridle point the kite flies at a low angle of attack. In this region the slopes of the θ_{LTD} and θ_{COP_LTD} curves are very steep. Therefore, the effects of any error in the experimental data will be magnified in this region.

8.8.2 Multiple stability Points

Based on the experimental data and the predicted values it is apparent that multiple stability points do exist under certain conditions. Figure 8:14 shows a kite with bridle point x=40 y=250 flying at two different locations at a wind speed of 10m/s.

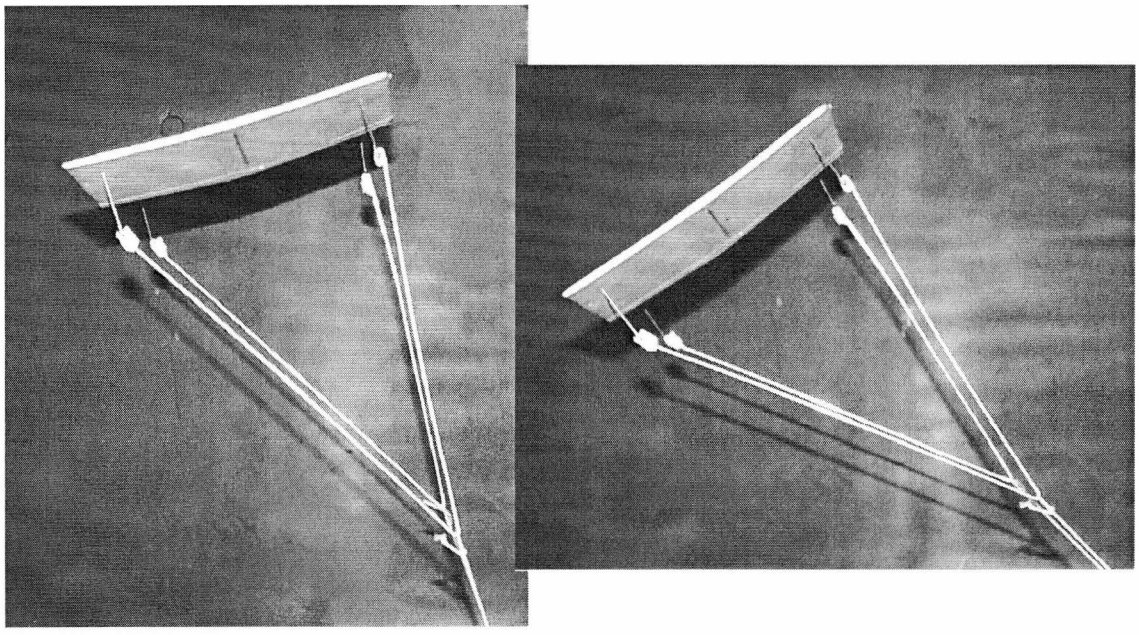

Figure 8:14 Kite with bridle of x=40 y=250 flying at two different points at a wind speed of 10m/s

According to Figure 8:8, the intersection of the dashed line and the predicted data indicates that three stability points should exist. In practice this third point never occurs, as it is dynamically unstable. It is dynamically unstable because if the angle of attack changes, the moment acting at the bridle will not return the kite to the stability point.

In Figure 8:13, the prediction curve when the stall values are modified is jagged in some areas. This is because the prediction program indicates that five stability points exist rather that the more usual three. Only three of these five are dynamically stable. However, the third stability point was not found during the experiments because as the tunnel speed increases the kite prefers to stay at the lower stability point and if it goes to the highest stability point it will stay there until the wind speed drops down again.

8.8.3 What Causes Multiple Stability Points?

There are two reasons for the existence of multiple stability points.

First, at low wind speeds the mass of the kite will have a large effect on the Lift to Drag curve (θ_{LTD}). The low Lift Coefficient at high angles of attack tends to give the θ_{LTD} curve a hump at low wind speeds (see Figure 8:15). Because of this it is easy for the θ_{COP_LTD} curve to cross the θ_{LTD} curve at multiple points. As the wind speed increases the mass of the kite becomes less significant and the θ_{LTD} curve flattens out.

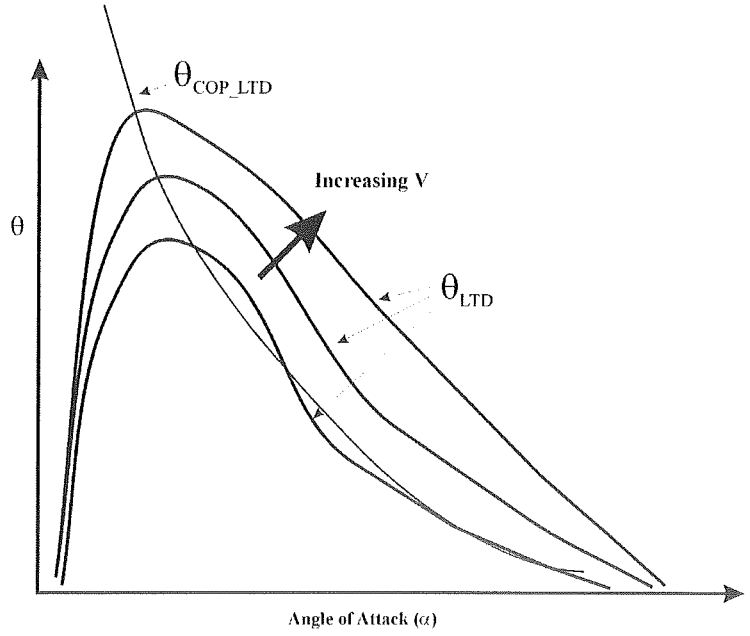

Figure 8:15 Effect of increasing wind speed on θ_{LTD} curve

Secondly, the bridle location has a large affect on the kite's stability points. From Figure 8:8, Figure 8:9 and Figure 8:10 it an be seen that the speed range where multiple stability points exist gets larger as the bridle point moves towards the rear of the kite and further away from the surface. This are two causes for this.

- First, for multiple stability points to occur the bridle must be located away from the surface of the kite. If the kite line was attached directly to the wing surface it would fly at an angle of attack where the centre of pressure corresponds with the attachment point. Since there is usually only one centre of pressure for each angle of attack, only one stability point will exist. As the bridle is located further away

from the kite the possibility of dual stability points exists. The further the bridle point is from the kite surface, the closer the variation in θ_{COP_LTD} with angle of attack gets to a straight line. This is shown as in Figure 8:16(a) with the θ_{COP_LTD} curve getting flatter as the bridle moves away from the wing.

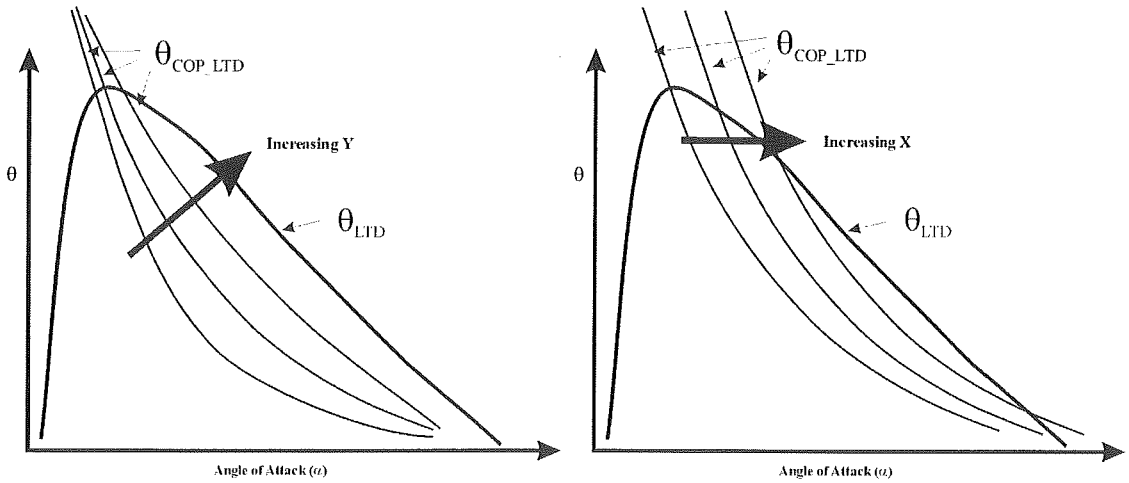

Figure 8:16 Effect of varying bridle location on θ_{COP_LTD} curve

- Secondly, by moving the location of the bridle in relation to the surface of the wing (i.e., in the x direction) the θ_{COP_LTD} curve moves left or right as shown in Figure 8:16(b).

By varying the bridle point, the θ_{COP_LTD} curve can be located so that it runs on top of the θ_{LTD} curve. In this way multiple stability points can be achieved. Figure 8:17 shows the predicted stability points for x=60 y=300 using stall corrected wing results. It can be seen that dual stability points will exist at all speeds for this configuration.

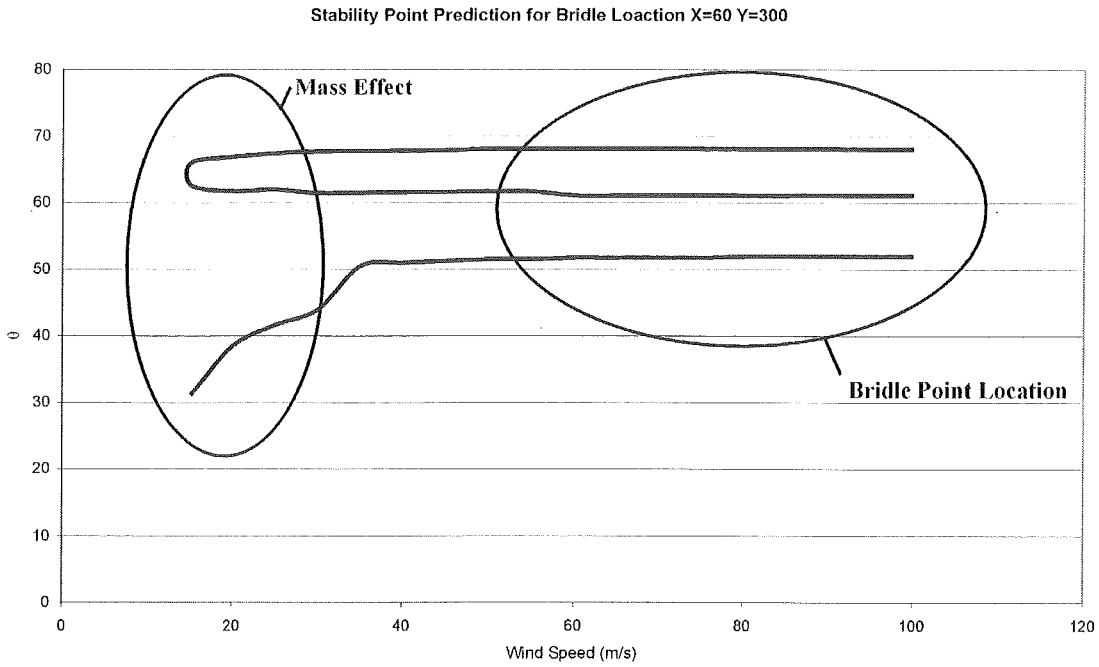

Figure 8:17 Bridle location where multiple stability points always exist.

8.8.4 Varying Angle of Attack to vary CL

In Traction kite based sports it is very important to be able to vary the Lift Coefficient to achieve some degree of 'power control'. By varying the length of the back-lines some degree of control can be achieved over the kite's angle of attack, and therefore Lift Coefficient. This affect has usually been explained by assuming that the back-lines pull the back edge of the kite down, increasing the angle of attack. The above analysis provides a more likely explanation of how varying the back-line length affects the angle of attack of the kite.

If there is any tension on the back-line, the bridle point moves from up near the kite to the flyer's control mechanism. As the length of the back line is reduced the bridle point moves towards the rear of the kite as shown in Figure 8:18. As shown in Figure 8:16(b), moving the bridle point in this way will tend to push the θ_{COP_LTD} curve to the right. This will move the stability point to a higher angle of attack, increasing the Lift Coefficient.

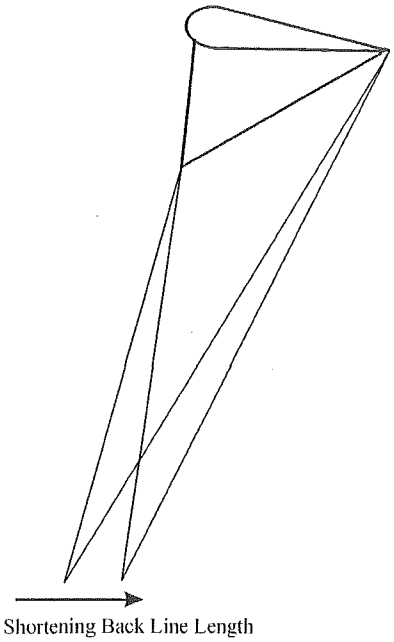

Figure 8:18 Effect of varying back-line length on bridle point

This perspective also explains the rapid loss of height that can occur when the back-line is shortened too far. As the θ_{COP_LTD} curve moves towards the right there will come a point where any further reduction in back-line length will mean that there is no intersection between the θ_{LTD} and θ_{COP_LTD} curves at low angles of attack. If there is a stability point at a higher angle of attack the kite will move to this point. If there is no stability point at all, the kite will not be able to fly.

Considering Figure 8:16(a) it is also apparent that significant variations in the Lift Coefficient through changes in the angle of attack can only be achieved with four-line kites, where the back line goes directly to the flyer. This is because the bridle is then located along way from the surface of the kite. If the bridle is near the kite surface the θ_{COP_LTD} will be too steep to achieve large changes in angle of attack.

8.8.5 Structural Considerations

As the design of kite structures moves away from the use of bridle lines to restrain the forces on the wing, knowledge about stability points becomes more important. To

maintain flight stability, kites that do not have bridles depend on the interactions between different parts of the kite. By varying the shape of the surface and the location of the airfoils in relation to each other, different sections of the kite can sit at different angles of attack giving the kite different flying characteristics. Determining the optimal location of each section is effectively a stability point problem as the aim is to ensure each section of the kite flies in its preferred stable location.

8.9 Conclusion

It is apparent from this analysis that a kite's stability points can be determined if enough detail is known about the properties and geometry of the kite structure. Being able to predict these stability points is fundamental to understanding kite dynamics as it affects the behaviour of the kite in many other areas. This analysis has shown that stability points can be predicted and has proved that multiple flying points are possible for a kite. Using the interactions between the θ_{LTD} and θ_{COP_LTD} it has been shown how multiple stability points exist and how the geometry of the kite can affect the flying behaviour. This analysis has also laid the foundations for further analysis of kite dynamics such as kite take off and kite turning.

9. Disk Wing Analysis

9.1 Summary

This chapter outlines the methodology for predicting the performance of a wing structure made up of multiple disks. Since the shape of a disk's leading edge relative to the wind is constant at all orientations, the aerodynamic performance of a disk around one axis of rotation is enough to predict the performance at all orientations. Using disks to create a wing enables the performance of complicated wing structures to be estimated without extensive wind tunnel testing.

Wind tunnel experiments on a wing made up of disks indicate that the performance of this type of structure can be predicted. However, if the disks are close then once one disk stalls, the wake produced interferes with the properties of the rest of the structure. However, as long as a disk kite is flown at an angle of attack below the stall point, the predicted wing performance is valid. The further apart disks are spaced, the more accurate the predictions will be beyond the stall point.

9.2 Introduction

The previous chapter demonstrated that if the aerodynamic properties of a wing and its appendages could be determined, then it is possible to predict its static flying position when flown as a kite. An extension to this concept was the ability to predict the static position of a wing in all orientations, which in turn leads towards a prediction model for how a kite turns. This section outlines how the process of predicting a wings performance can be simplified by using disks as the wing components.

To model a kite's motion in three dimensions it is necessary to determine the aerodynamic properties of the kite wing structure in all orientations. However, finding the

properties for every type of wing structure requires a lot of testing. If the performance of a wing could be predicted based on the knowledge of individual parts the testing process would be simplified, as the properties of one part would be sufficient to predict the properties of the whole structure. The testing process can be further simplified if the wing is made up of disks. Since the shape of the leading edge, and chord length, of a disk are constant irrespective of its location in space, the properties of a disk around one axis of rotation can be used to find the properties of a disk at any orientation.

The following sections show the steps required to determine the properties of a wing made up of well spaced multiple disks. It outlines: the necessary mathematical calculations to determine the properties of a disk at any orientation; how to determine the properties of a wing structure made up of multiple disks and its structural elements; the properties of a disk from wind tunnel tests; and a comparison between theoretical and experimental results for a specific disk wing structure. Due to structural considerations the disks were not as widely spaced in this wing structure as would have been liked.

9.3 Mathematical Derivation

The following calculations are used to predict the performance of a disk and disk wing structure. These predictions are based on data for a disk around one axis of rotation (see Section 9.4). The main goal in this section is to be able to determine the aerodynamic forces and moments at a known point on the wing. The properties are usually required at the centre of mass of the object, but any point can be chosen. Using vector geometry to find the required wing properties simplifies the mathematics considerably.

The following sections describe how to obtain the forces at the origin in a Cartesian coordinates system. The wing structure will be rotated by angles $(\theta_x,\theta_y,\theta_z)$ as defined by the right hand rule as shown in Figure 9:1.

9.3.1 Determining the forces on a disk in space.

The first step to determining a disk wing's performance is to consider the forces acting on a single disk orientated in space. To aid this description, Figure 9:1 shows the geometry of a disk in space along with the necessary construction vectors and forces.

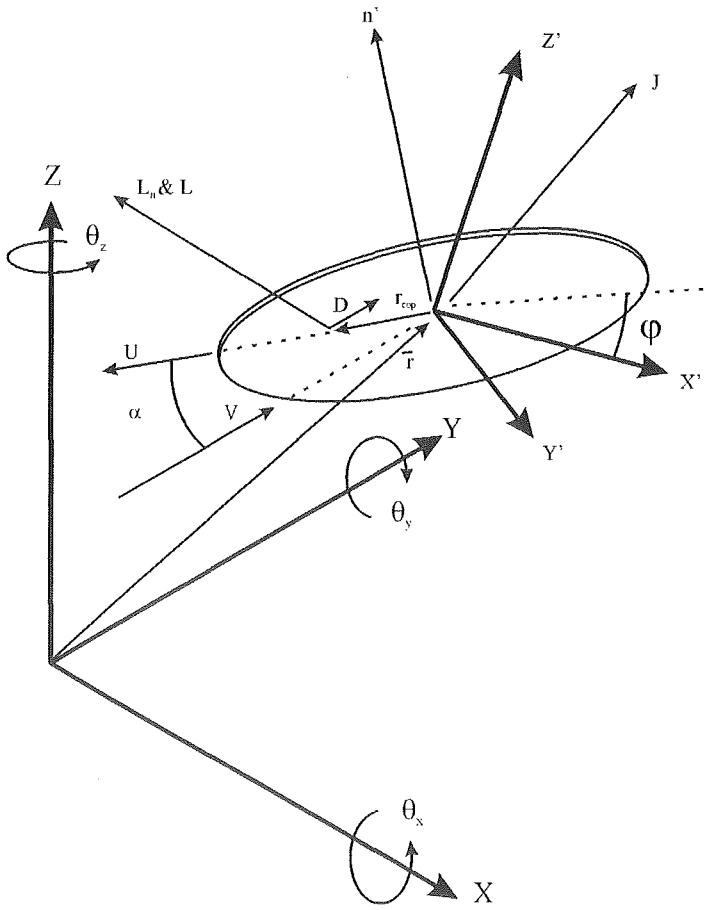

Figure 9:1 Coordinate geometry of a rotated disk

First, it is necessary to define a vector normal to the disk's surface before any rotation takes place. The disk is assumed to originally lie in the X-Y plane. For the benefit of future wing models, the disk is given a dihedral angle (φ). A dihedral angle is effectively an initial rotation around the Y-axis. The initial normal vector of the disk is therefore

$$n = [-\sin(\varphi) \quad 0 \quad \cos(\varphi)] \qquad \textbf{Eq 9:1}$$

Secondly, a vector is required to define the magnitude and direction of the wind. For simplicity this is defined as

$$V = V[0 \quad 1 \quad 0] \qquad \textbf{Eq 9:2}$$

Thirdly, once these vectors are defined the wing needs to be re-orientated by the three rotation angles θ_x, θ_y and θ_z. To do this a rotation matrix based on Euler angles is used. In this case

$$r = \begin{bmatrix} \cos(\theta_y)\cos(\theta_z), & \cos(\theta_y)\sin(\theta_z), & \sin(\theta_y) \\ \sin(\theta_x)\sin(\theta_y)\cos(\theta_z)+\cos(\theta_x)\sin(\theta_z) & -\sin(\theta_x)\sin(\theta_y)\sin(\theta_z)+\cos(\theta_x)\cos(\theta_z) & -\sin(\theta_x)\cos(\theta_y) \\ -\cos(\theta_x)\sin(\theta_y)\cos(\theta_z)+\sin(\theta_x)\sin(\theta_z) & \cos(\theta_x)\sin(\theta_y)\sin(\theta_z)+\sin(\theta_x)\cos(\theta_z) & \cos(\theta_x)\cos(\theta_y) \end{bmatrix}$$

Eq 9:3

The normal vector to describe the orientation of the disk is then found by

$$n' = rn^T \qquad \textbf{Eq 9:4}$$

Fourthly, using this new orientation of the disk, the angle of attack (α) of the disk can be found by

$$\alpha = \frac{\pi}{2} - \cos^{-1}\left(\frac{n' \bullet V}{\|V\|}\right) \qquad \textbf{Eq 9:5}$$

Based on experimental data, the Lift and Drag Coefficients and the Centre of Pressure of the disk can then be calculated.

Fifthly, the location and direction of the forces in Cartesian coordinates need to be determined. As an intermediate step a vector perpendicular to V and n' is defined as

$$J = \frac{n' \times V}{\|V\|} \qquad \textbf{Eq 9:6}$$

Using this vector a chord line vector can be found as

$$U = -\frac{J \times n'}{\|J \times n'\|} \qquad \textbf{Eq 9:7}$$

while the direction the lift force acts in is defined as

$$L_n = -\frac{J \times V}{\|J \times V\|} \qquad \textbf{Eq 9:8}$$

The distance from the centre of the disk to the Centre of Pressure is equal to

$$r_{cop} = (0.5 - COP) \cdot U \cdot chord \qquad \textbf{Eq 9:9}$$

while the vectors for the Lift and Drag forces are

$$L = Lift \cdot L_n \qquad \textbf{Eq 9:10}$$

and

$$D = Drag \cdot \frac{V}{\|V\|} \qquad \textbf{Eq 9:11}$$

Assuming that the forces at the centre of the disk are required then the moment vector at the centre of the disk is

$$M = r_{cop} \times (L + D) \qquad \textbf{Eq 9:12}$$

If the disk is at a radius r from the origin then to determine the moments at the origin Eq 9:12 becomes

$$M = (r_{cop} + r) \times (L + D) \qquad \textbf{Eq 9:13}$$

By applying these calculations, the aerodynamic properties of a disk at any orientation can be determined.

9.3.2 Complete kite properties

Using the previous calculations it is possible to predict the properties of a wing structure made up of a number of different disks. This prediction simply requires that the initial orientations of each disk within the wind structure be defined. The properties of the disks at each wing orientation rotation are then combined to determine the overall properties of the wing.

An accurate model of a disk wing must include the structural elements that hold the disks together. Determining the aerodynamic properties of these structural members requires similar calculations to those used for disks.

The first step is to define a vector for each structural element. In this model all the structural elements are rods or strings running between two points (P). These two points can be used to define the structural member (S) by

$$S_j = P_n - P_i \qquad \textbf{Eq 9:14}$$

Secondly, it is necessary to determine the location of the centre of these structural members by

$$r_j = \frac{(P_i + P_n)}{2} \qquad \textbf{Eq 9:15}$$

When the wing is re-orientated both S_j and r_j need to be modified using Eq 9:4 to get S_j' and r_j'.

The angle of the structural member relative to the wind can then be found by

$$\alpha_{s_j} = a\cos\left(\frac{V \bullet S'_j}{\|V\|}\right) \qquad \textbf{Eq 9:16}$$

The Lift and Drag Coefficients, and therefore the forces on the structural members, can then be determined by applying the following equations from Hoerner (1965).

$$Drag_{S_j} = \frac{1}{2}\rho\phi\|V\|^2\|S_j\|\left(1.1\sin^3\left(\alpha_{s_j}\right) + .02\right) \qquad \textbf{Eq 9:17}$$

$$Lift_{S_j} = \frac{1}{2}\rho\phi\|V\|^2\|S_j\|1.1\sin^2\left(\alpha_{s_j}\right)\cos\left(\alpha_{s_j}\right) \qquad \textbf{Eq 9:18}$$

The Drag force acts in the direction of the wind but to find the orientation of the Lift force two more vectors are required. Like for Eq 9:6 we need to define a vector perpendicular to the structural members and the wind by

$$J_{S_j} = \frac{V \times S'_j}{\|V\|} \qquad \textbf{Eq 9:19}$$

By taking the cross product between this vector and the velocity vector the direction of the Lift force becomes

$$L_{nS_j} = \frac{J_j \times V}{\|J_j \times V\|} \qquad \textbf{Eq 9:20}$$

Once this vector is determined, the forces and moments caused by the structural members at the origin can be found by applying Eq 9:10 to Eq 9:13. By including all the different components that make up the wing the overall performance can be predicted.

9.4 Disk Properties

9.4.1 Testing Method

The properties of a disk were determined using the same testing apparatus and method as outlined in Chapter 8. The test disk had a diameter of 250mm and a thickness of 1.5mm. The edges of the disk were rounded. The tests were performed in the departmental wind tunnel, which has a cross-section of 3' x 4'. Since all further tests using disk wings were performed in this wind tunnel, the result have not been corrected for blockage effects.

9.4.2 Results

Figure 9:2 shows the aerodynamic properties of a disk for angles of attack between 0^{o} and 60^{o}. Since a disk has a low aspect ratio the stall point occurs at a relatively large angle of attack.

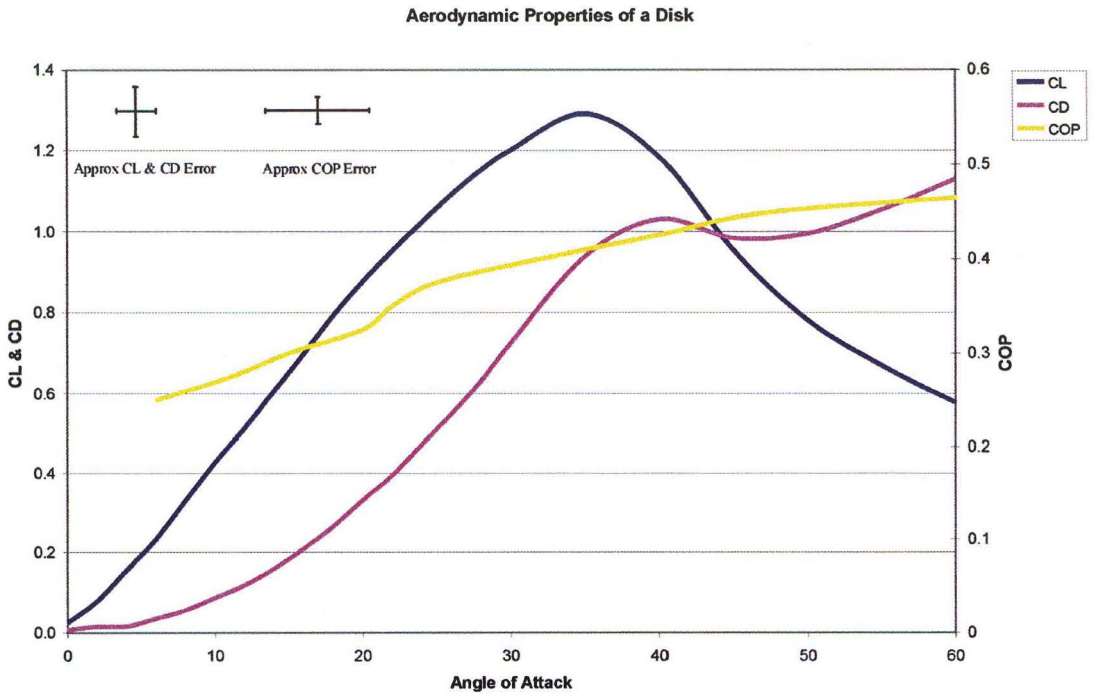

Figure 9:2 Aerodynamic properties of a disk for angles of attack between 0-60°

9.4.3 Experimental Errors

In general the experimental errors are the same as those for the wing tested in Chapter 8. However, there is a larger error in the angle of attack measurement while measuring CL and CD as it was difficult to stop the wing flexing. This total angle of attack error was estimated at ±1.5°.

9.4.4 Disk properties at different orientations

To confirm that the theory outlined in Section 9.3.1 was correct, wind tunnel tests were performed on a disk at different orientations. The disk was rotated around the y-axis and the aerodynamic properties found for a range of angles of attack. Unfortunately, only the 3-axis force balance was available for these tests, as the departmental 6-axis force balance was not completed in time for this project. By using the 3-axis balance only the vertical (Lift) and Drag coefficients could be determined. Due to the unreliable moment

results (see Chapter 8) a verification of the Centre of Pressure migration could not be performed.

Figure 9:3 and Figure 9:4 show the theoretical and experimental results for a disk at θ_y angles of 20°, 40°, and 60°.

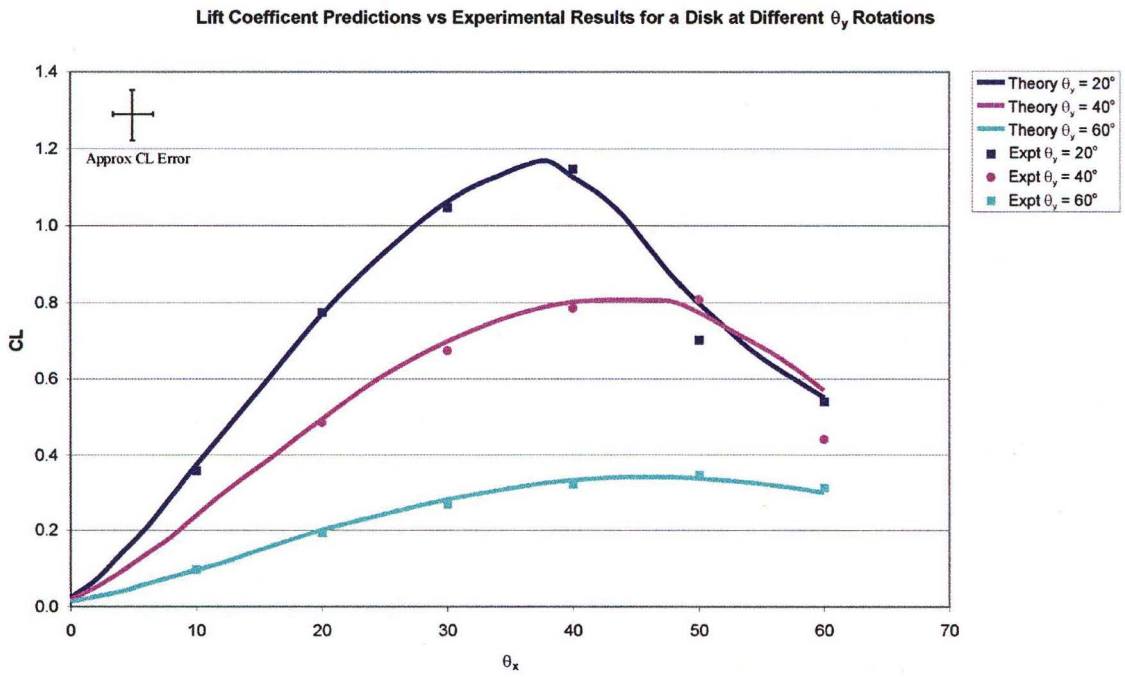

Figure 9:3 Predicted Lift Coefficient vs experimental results for a disk at different θ_y rotations

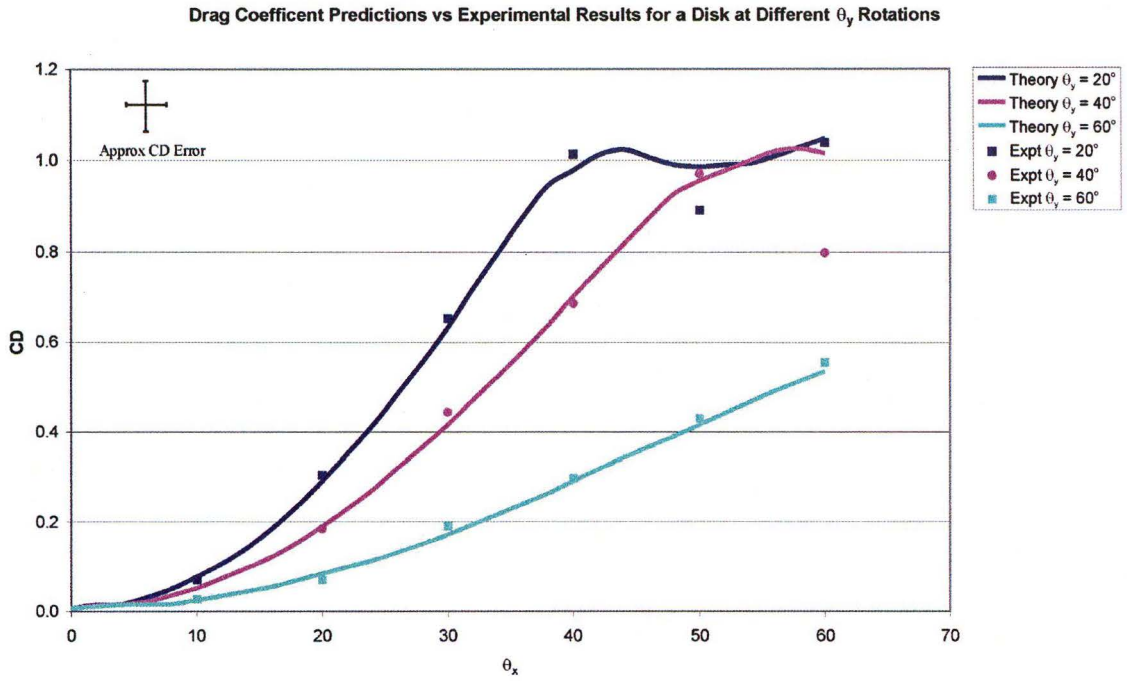

Figure 9:4 Predicted Drag Coefficient vs experimental results for a disk at different θ_y rotations

The close correlation between the predicted and experimental results indicates that the performance of a disk at different orientations can be determined from the data shown in Figure 9:2. The only significant difference between the predicted and experimental results occurred when the disk was rotated at θ_x=50°, θ_y=20°, and at θ_x=60°, θ_y=40°. Chapter 8 outlined the difficulties in obtaining readings near the wing's stall region. Since both these results occur near the stall this is the most likely explanation for the difference between the experimental and theoretical results.

9.5 Disk Kite Properties

Based on the previous results the properties of a wing structure made up of two or more disks should be able to be predicted. This section outlines the wing structure built to verify that this can be done. This structure was tested in the wind tunnel and the results compared to the theoretical performance.

9.5.1 Wing model

Figure 9:5 shows the dimensions of the disk wing used in the following experiments.

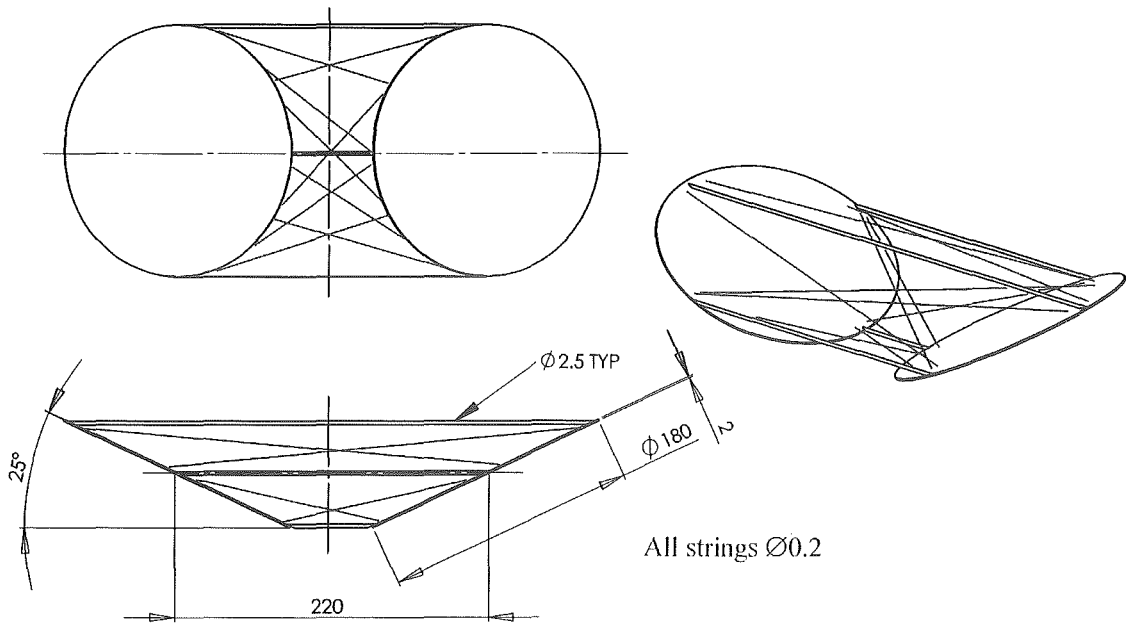

Figure 9:5 Disk wing model

9.5.2 Testing Method

The wing was tested on the same apparatus used in Section 9.4. To attach the wing to the sting a separate attachment had to be used as shown in Figure 9:6.

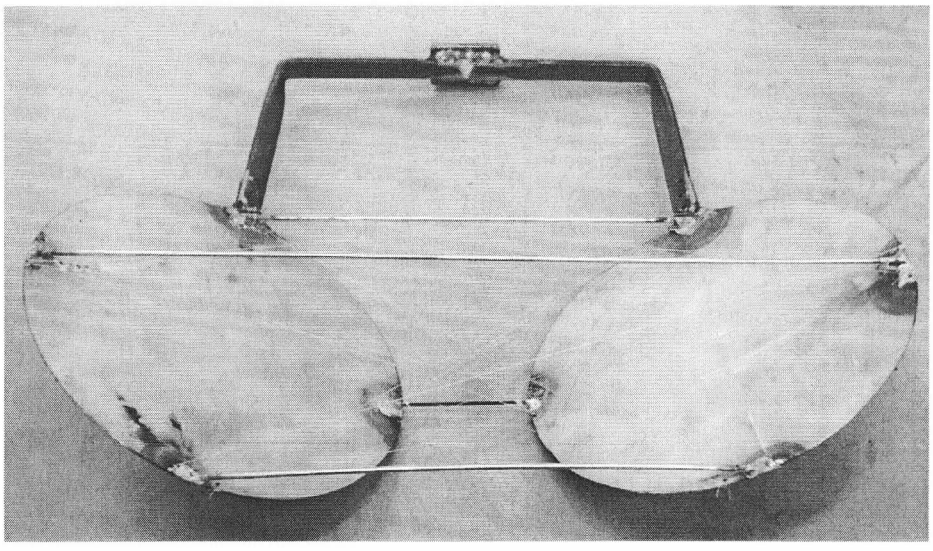

Figure 9:6 Disk wing model with sting attachment

9.5.3 Results

Figure 9:7 and Figure 9:8 show the experimental and predicted Lift and Drag Coefficients at a range of θ_x and θ_y rotations.

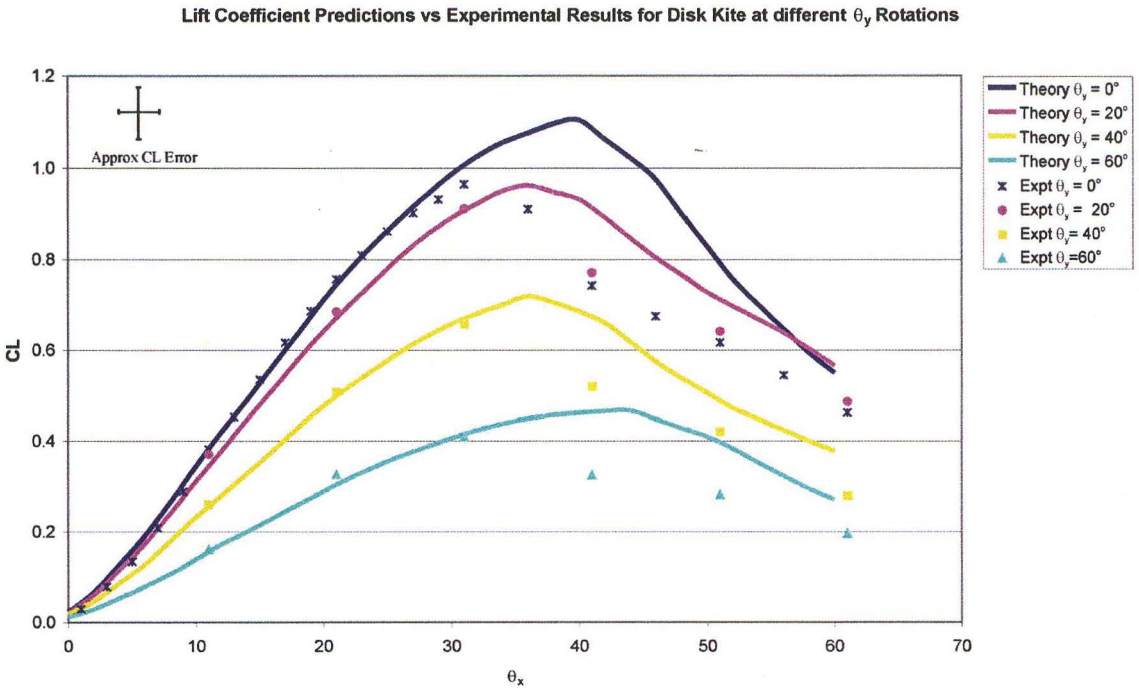

Figure 9:7 Predicted Lift Coefficient vs experimental results for the disk kite at different θ_y rotations.

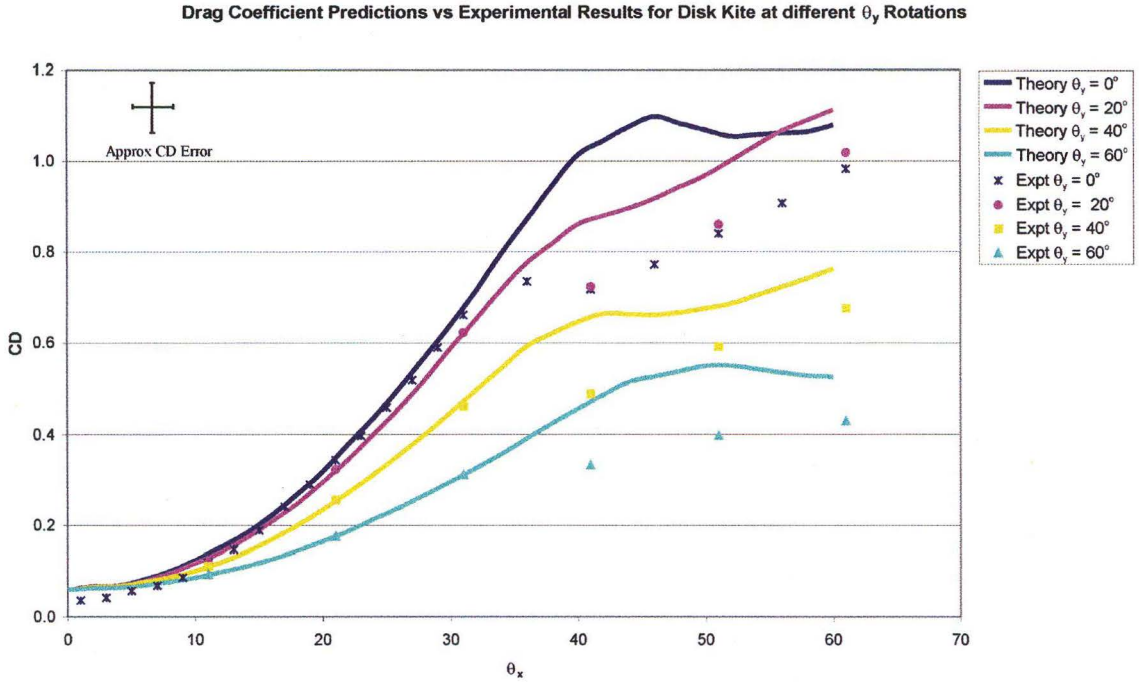

Figure 9:8 Predicted Drag Coefficient vs experimental results for the disk kite at different θ_y rotations.

9.5.4 Experimental Errors

In general the experimental errors are the same as those outlined for the wing tested in Chapter 8. Since the kite's structure was more rigid than for an individual disk the difficulties with flexing were not encountered. However, it was difficult to line the structure up accurately in its initial location. This caused an error of $\pm 1.5^{o}$ in the angle of attack readings. Since the theoretical performance results are based on experimental disk properties, they are subject to the same measurement errors as outlined in Section 9.4.3.

9.6 Discussion

Figure 9:7 and Figure 9:8 indicate that up until an angle of attack of $30\text{-}35^{o}$ there is a close correlation between the predicted performance and the actual performance of the wing. The deviation of the experimental results from the predicted performance occurs as the stall point of the structure is reached. The formation of a large wake on one or both disks has a large effect on the performance of each part. However, as long as the kite is flying at an angle of attack below the stall region, a reasonable prediction of the performance of a wing made up of disks should be able to be obtained.

Ideally, the disks should have been placed far enough apart so that they had no effect on each other. However, there are structural restraints on the distance between disks. The further apart the disks are the harder it is to make a rigid wing structure. If the structure is not rigid the wing will flex, varying the angle of attack of the disks, making a performance prediction impossible. Inevitably, a compromise has to be reached between structural requirements and the range of angles of attack for which data is required.

9.7 Conclusion

If the aerodynamic performance of a disk is known for angular rotations in one plane it is possible to determine the performance of the disk at all orientations. By constructing a

wing out of multiple disks the aerodynamic performance of the structure can be predicted. The predicted performance for this type of wing was valid up until the stall point. Once a large wake is produced there are significant differences between the predicted and experimental results. Based on these findings the performance of a wing flying at an angle of attack below the stall should be able to be predicted and the results used in further research.

10. Kite Turning Fundamentals

10.1 Summary

Kite turning and control are poorly understood areas of kite dynamics. Despite the fact that controllability is an essential component of Traction kite performance, very little attention has been given to the mechanisms involved. This section provides an initial analysis of how the dynamics of a kite are affected by varying the line length to the wing surface.

By varying the line length, the orientation of the wing and the location of net tension from the line are changed. It was found that these two things tend to have opposite effects on the movement of the kite. The final motion of the kite depends on the relative magnitudes of the wing rotation compared to the movement of the line tension.

This section is seen as only as a beginning to understanding kite turning. Only the most preliminary experimental work has been done to confirm the kite turning predictions made. Further work is required to model, and experimentally prove, the mechanisms of kite turning.

10.2 Introduction

A key characteristic of Traction kites is that their flight position can be controlled by the flyer. However, the mechanisms for achieving kite control are poorly understood. Even kite makers, with extensive knowledge of physics, declare that kite control is a 'miracle'. It is also apparent that luck is largely responsible for their kites turning, rather than deliberate design.

10.2.1 Defining kite turning

What does kite control or kite turning mean? Figure 10:1 show the geometry of a kite while it is flying. The kite wing is orientated so that its axes point in the X', Y' and Z' directions. While flying, there is an interaction between the wing and line forces, around the centre of mass of the wing. Depending on the magnitude and location of these forces the wing will be stationary, or move and/or rotate around the X', Y' or Z' axis. For a kite to turn and be controllable the key motions are: a rotation around the Z' axis, and a movement in the X' direction.

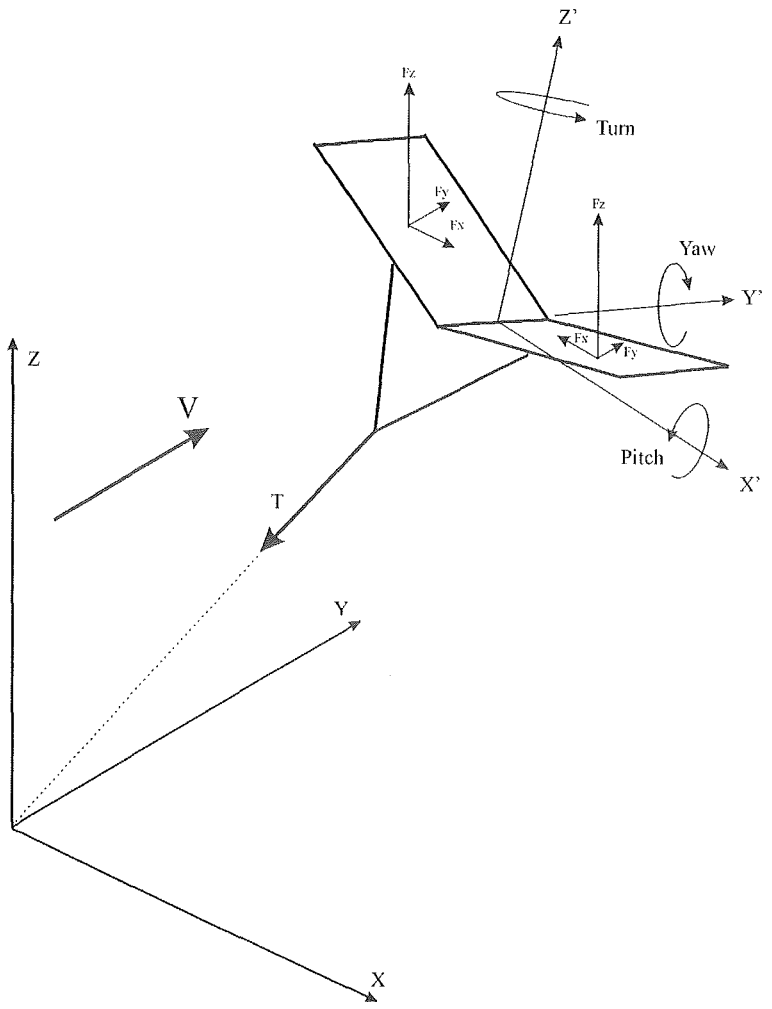

Figure 10:1 Kite rotations and movements

10.2.2 Past Research

Past research on maintaining kite stability has inadvertently addressed the issue of kite control. Ito and Komura (1983) spent considerable time trying to stop kites from spinning (rotating around the Z' axis). In doing so they outlined many mechanisms that could cause a kite to spin including: twist in the wing structure, different areas on either side of the wing, uneven tension in wing construction material, and changes in the bridle point location. In addressing these issues Ito and Komura applied physical principles so that they could more effectively **stop** kites from turning. Although this text is essential reading when considering kite turning, its principal objective is kite stability rather than kite control.

Likewise, other authors who have analysed kites mathematically (e.g., Hobbs, 1986. De Laurier, 1972 a,b. Bryant, Brown & Sweeting, 1942) have been primarily concerned with stability. Consequently, no study has considered a kite's response to deliberate inputs from the flyer to vary and/or control its flying location.

10.2.3 Scope of this chapter

This chapter considers the effect of flyer inputs on a kite with a rigid wing. Using the results for wings constructed out of disks (as outlined in chapter 9) a numerical analysis has been performed.

Varying the line length to either side of the kite is the main control a flyer has over its behaviour. To achieve this type of input the line can be physically shortened, or the flyer can adjust the relative lengths of the lines using their arms. Both techniques have the same effect.

Using a disk kite the effect of varying the kite line lengths can be analysed, and the initial response of the kite investigated. Once the kite has moved, the interactions between the line and the wing become complicated and further analysis would require a three-dimensional model that solves the kite's equations of motion. The main focus of this

chapter is to determine how varying the line length affects the wing of the kite and the initial kite motions that this produces.

10.3 Basic Kite Turning Mechanisms

10.3.1 Tether interactions and kite performance

The performance of the wing has an impact on how a kite will respond to different inputs. Hypothetically, there are two categories of wing performance to be considered, as illustrated in Figure 10:2. In the first case, the force on the kite (F_{tot}) acts so that there is a component of the force acting towards the trailing edge of the wing in the Y' direction ($F_{Y'}$). In the second case, where the performance of the wing is better, there is a force acting towards the leading edge of the kite. Note that these are not forces parallel and perpendicular to the wind (V), but rather the forces in the direction of the kite axis.

The second case is extremely unlikely with kites, as their wings have large angles of attack and low performance. Therefore this discussion will focus on the first case only.

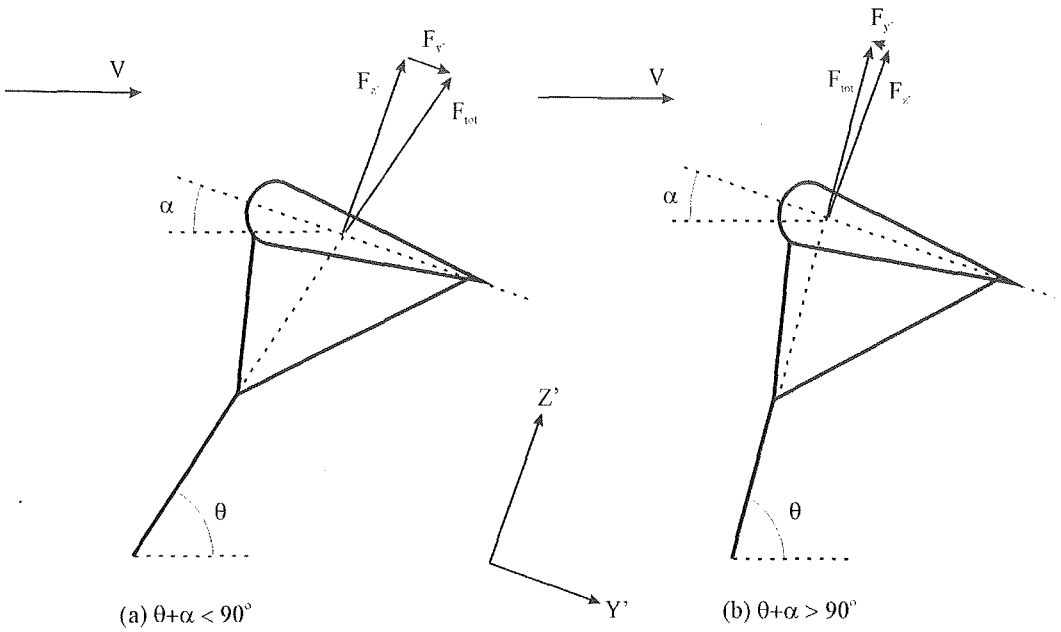

Figure 10:2 Two categories of kite performance

10.3.2 Dihedral and anhedral angles

A distinction needs to be made when describing the orientation of the kite wing. The wing can either have a dihedral or an anhedral angle as shown in Figure 10:3. This angle has a significant impact on the forces of the wing at different orientations. Traditionally, kites have been given a dihedral angle, as this shape tends to be more stable. However, modern Traction kites are ARC shaped, and therefore have an anhedral angle.

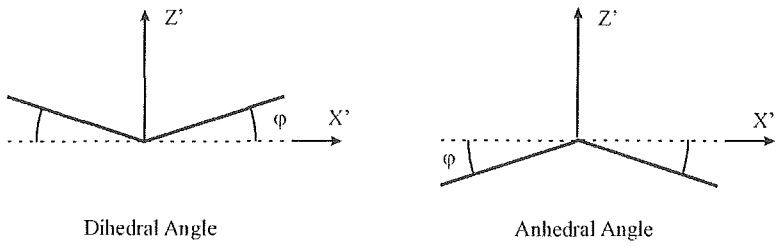

Figure 10:3 Dihedral and anhedral angles in a kite structure

10.3.3 Flyer Inputs

Kite turning can be distinguished from general kite motion in that it is a response to a deliberate input from the flyer. For kites with two or more lines, the primary control that a flyer has is the ability to vary the length of the lines attached to the kite. This is done either by shortening one line or varying the position of their arms relative to each other. With a flexible wing surface there are a number of different interactions that can take place in response to this input, most of which are beyond this chapter. By assuming that the wing is rigid, determining the initial response of the kite is simplified.

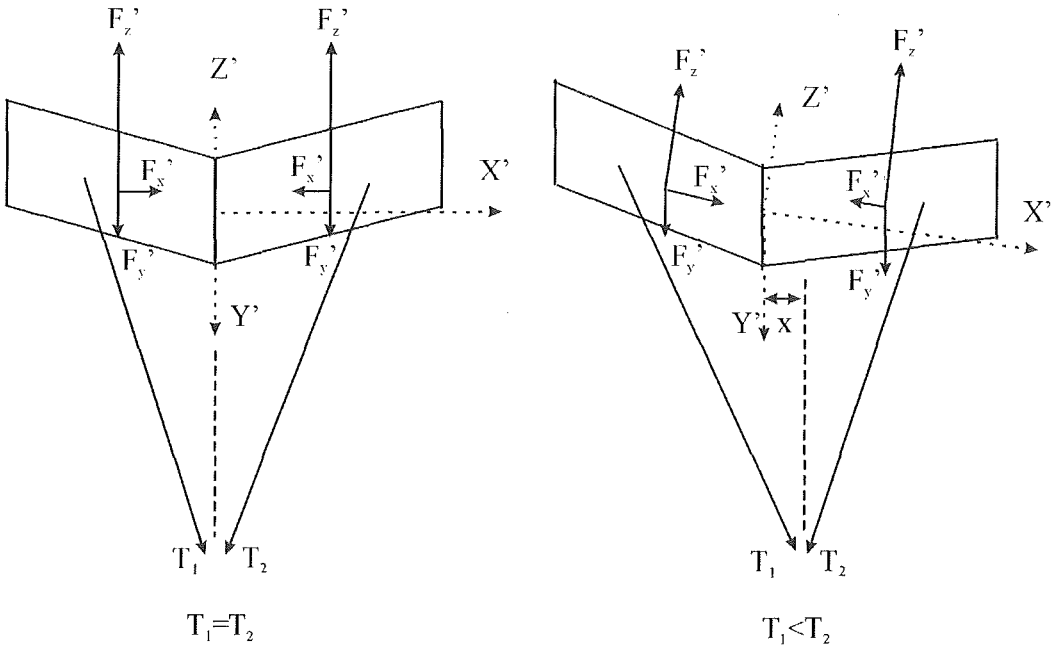

Figure 10:4 Wing rotation and bridle point movement in response to a line length change

Figure 10:4 shows the geometry of the kite from the perspective of the flyer. Two kites lines, represented by the line tensions T_1 and T_2, point inwards from the kite towards the flyer. In the first diagram the kite is flying stably, and the forces on the wing are balanced by the line tension. No turning of the kite will occur, because the moments around the kite's centre of mass, from the wing and line forces, are balanced. If the line length to the right hand side of the kite is then shortened two things occur.

First, varying the line length will cause a rotation of the wing around the X', Y' and Z' axis. The primary rotation will be in the Y' axis, as the lines are primarily pulling away from the surface of the kite. Depending on the nature of the bridle arrangement and the number of kite lines the wing may also rotate around the Z' axis as well. If a wing is flying in a stable manner there will be limited rotation in the X' axis. However, if the line is given a rapid tug, a significant rotation in the X' axis can occur.

Varying the angular location of the wing will change the forces acting on either side of the structure. This can introduce unbalanced moments and forces at the kite's centre of mass. The size of the turning moments and forces depends on the direction, and the amount of rotation.

The second effect of varying the line length is that the location of the net tension force from the lines will move away from its stable location at the centre of the kite. Usually this movements is in the X' direction (to the side of the kite). This movement can be significant and the interaction between the forces on the wing and the line tension will cause unbalanced moments at the centre of mass. If there is a force acting towards the trailing edge of the wing (section 10.3.1) a movement of the bridle in the positive X' direction will cause a negative turning moment around the Z' axis.

The motion for a rigid wing will be in response to these two interactions. In some cases the two effects are complementary and in others they oppose one another. Which one dominates depends on the particular wing and bridle arrangement.

10.3.4 Mass of the kite

The mass of the kite has an effect on how a kite moves. First, the mass of the kite impacts on how rapidly the kite will move in response to the forces acting on it. Secondly, the mass of the kite interacts with the line tension to turn the kite. How the mass will rotate the kite depends on the kite's angle of attack, the location of the bridle point and the forces in the line. If the kite is flying at a low angle of attack with the net tension to one side of the wing, then the mass will primarily rotate the kite around the Y' axis. If the kite is at a large angle of attack with the net tension force to one side of the wing, the kite will primarily rotate around the Z' axis. In both cases the mass of the kite will cause a slight rotation around the other axes. However, for a light kite structure flown in a reasonably large wind, the aerodynamic forces will be considerably larger than the mass, reducing the effect of mass on the motion of the kite.

10.4 Mathematical Predictions

10.4.1 Net line tension movement

The turning moments arising from a change in the position of the line tension depend on the characteristics of the wing, how far the line tension moves and the performance of the kite. Assuming the tension force has no X' component[7], and the kite was previously balanced, the unbalanced moments caused by a line tension movement in the X' direction are

$$MZ' = -CY' \cdot x \qquad \textbf{Eq 10:1}$$

and

$$MY' = CZ' \cdot x \qquad \textbf{Eq 10:2}$$

where MY' and MZ' are the moments around the Z' and Y' axis, CY' and CZ' are the force coefficients in these same directions, and x is the distance of the net line tension from the central axis of the wing.

Depending on the nature of the bridle arrangement the motion of the kite will be restrained around one or more axes. For two-line kites, the wing will be largely free to rotate around the Z' axis, but the rotation around the Y' axis will be restrained in at least one direction. With four-line kites the rotation about the Z' axis can also be restrained to a certain degree.

It can be assumed that the kite performance is such that there is a force acting in the Y' direction towards the trailing edge of the wing. In this case a movement in the line

---

[7] As an initial approximation this is adequate. With long lines in particular there is only a small sideways component to the line tension.

tension to the right of the wing will tend to turn the kite in the negative Z' direction (left turn).

10.4.2 Wing rotation

For a numerical analysis of a wing at different orientations, the disk wing model, as outlined in Chapter 9, was utilised. Using this model, the forces on the wing could be predicted without extensive testing. Although the findings from this analysis can be applied to other kite structures, there primary application is for predicting the behaviour of disk wing kites.

The kite structure outlined in Chapter 9 was rotated to set angles around the X', Y' and Z' axis and the forces and moments at the centre of mass determined. Graphs of the moments and forces have been included in Appendix III for reference. These results, along with others for different wing shapes, can be summarised in a graph like that shown in Figure 10:5. This figure shows the moment around the Z' axis for a wing, in response to a set rotation around the Y' axis of 4^{o}. A suitable X' rotation of 15^{o} was chosen, assuming that the kite would be tuned to fly near the wing's peak Lift to Drag ratio. On the bottom axis of Figure 10:5 is the dihedral angle of the wing, ranging from 50^{o} to -50^{o} (anhedral), while Z' axis moments are shown on the vertical axis. As the wing's dihedral angle was varied, the central width of the wing (220mm - see figure 9:5) remained the same. Included in Figure 10:5 are curves showing the effect of moving the line tension to the right of the wing in addition to a wing rotation. The line tension movement is specified as a proportion of the wing's width (w).

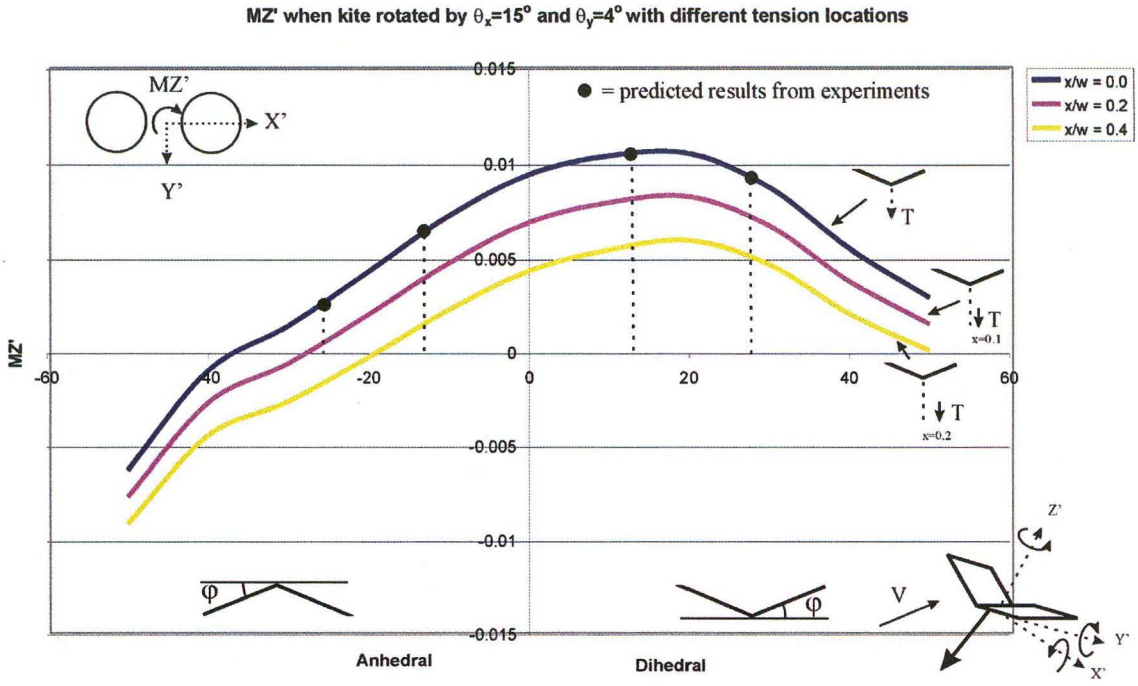

Figure 10:5 Moments around a wings Z' axis due to a rotation of θ_x=15° and θ_y=4° with different net tension locations

Figure 10:5 shows that for a disk wing the kite will tend to steer in the positive direction unless the anhedral angle becomes large. As the bridle point moves further to the side the wing will be more inclined to turn in the negative Z' direction.

10.4.3 Secondary Motions

Once the kite has started to respond to its initial input, the forces on the wing will change and there will be more complicated interactions with the line tension. However, by considering the graphs shown in Appendix III, after the initial movement has occurred the disk wing will tend to behave in the following ways.

In response to a shortening of the line length on the right hand side of the kite causing a positive rotation around the Y' axis, a kite will:

A dihedral kite – A dihedral kite will tend to rotate in a positive direction around the Z' axis. However, as shown in figures 15:2 – 15:4, for a small positive rotation around the Z' axis a moment exists to turn the kite in negative Z' direction. Unless the kite has significant turning momentum it will not continue to turn.

An anhedral kite – As long as the wing is not aggressively anhedral, or the bridle point too far from the centre of the wing, this wing will also tend to turn in a positive Z' direction. However, unlike a dihedral kite, once the wing starts to turn there is no restoring moment so the wing will continue to turn.

In both cases if the net line tension for is moved without significant wing rotation there will be a tendency for the kite to turn in the opposite direction to the line tension movement.

10.5 Experimental Findings

10.5.1 Kites used in experiments

Models of two kites suitable for wind tunnel testing were built to verify the above predictions. These kites were the same size as those used in Chapter 9 and had dihedral angles of 15^{o} and 25^{o}. They could also be turned over so that they were anhedral kites.

Unfortunately, it was difficult to fly the wings unaided, and the frequency of their response to inputs was very rapid. However, if the wings were gently held in place, the interactions between the wing and the line at different orientations could be identified.

10.5.2 Experimental predictions

The different wings were orientated in two ways.

- First, the wings were given a positive rotation around the Y' axis with the line tension acting through the central plane of the wing. The moment predictions for

this orientations are shown in Figure 10:5. It is expected that all the wings will turn in a positive Z' direction.

- Secondly, the wings were moved so that the net line tension was to the right of the wing. This is performed in such a way that there was no rotation of the wing around the Y' axis. Based on Eq 10:1 all kites should turn in the negative Z' direction in response to this input.

10.5.3 Findings

The following sections outline the results from these tests

15^0 Dihedral Wing

- If the bridle point is shifted without any rotation the wing spins in the negative Z' direction.
- If the wing is rotated around the Y' axis the wing spins in the positive Z' direction
- A restoring negative moment exists for small rotations in the Z' axis but eventually becomes positive after large Z' axis rotations.

25^0 Dihedral Wing

- Motion same as for 15^0 dihedral wing

15^0 Anhedral Wing

- If the bridle point is shifted without any rotation the wing spins in the negative Z' direction as above
- If the wing is rotated around the Y' axis the wing spins in the positive Z' direction but the moment is much less than for the dihedral wing. At the beginning the wing tends to move sideways rather than turn. However, once a significant amount of rotation in the Z' axis has occurred the wing continues to spin.

25° Anhedral Wing

- Motion same as for 15° anhedral wing

Although these tests are in no way a comprehensive, they indicate that the initial movements of the wing can be predicted.

10.6 Discussion

10.6.1 Wing rotations and bridle point movements

A wing rotation and a movement of the line tension cannot be treated as separate events when considering the response of a wing to a varying line length. It is very difficult to do one without the other. However, depending on the bridle arrangement one effect can dominate. For example, some kites have extensive cross bridling, with lines running from each bridle point to each side of the kite. A kite with this sort of bridle arrangement can achieve a net line tension movement without significant rotation far better than a kite with very little cross bridling. Likewise it is possible to arrange the lines so that a wing rotation is the primary response to varying line length. The kite can therefore be tuned by the maker to give the desired effect.

10.6.2 Z' axis rotations

This analysis has primarily considered the effect of an input rotation around the Y' axis. However, as can be seen in the graphs shown in Appendix III, rotating the wing around the Z' axis can have a significant effect on the moments at the kite's centre of mass. In particular the turning motion of the wing can be affected. Kites that have lots of back-line control will be able to utilise this effect. Varying the back-line load on either side of the wing will effectively turn the wing around the Z' axis. This occurs because varying the back line load to one side of the kite pulls the back edge of the wing down, causing a twist in the structure. The effect can be dramatic. For example, the C-Quad design from

Peter Lynn Kites Ltd is able to spin around the Z' axis by varying the back-line tension, with very little sideways movement. This is something other kites cannot achieve.

10.7 Conclusion

The mechanisms by which a kite turns are surprisingly complex. By assuming that a kite wing is a rigid structure, an initial prediction of how a kite will behave in response to flyer input, can be obtained. The primary method to control multiple-line kites is to vary the line length to either side of the kite. This input causes a rotation of the wing and a movement of the net line tension to the side of the wing. It was found that a positive rotation around the kite's Y' axis produces a positive rotation around the Z' axis. It was also found that a positive line tension movement in the X' direction tends to causes a negative rotation around the Z' axis.

As the kite moves, the interactions between the wing and the line become more complex. Analysing the full motion of a kite would require a full three dimensional model. This is beyond the scope of this research project, but it is hoped that the work that has been done will benefit any attempts to obtain a complete understanding of kite motion.

11. Conclusion and Recommendations for Future Research

This research project was successful in extending the understanding of kites in general, and Traction kites in particular. In recent years Traction kite-based sports have become very popular, and a lot of research and development effort has been spent in developing high performance structures. This project has focused on two major areas. First, developing methods to test Traction kites, so that design improvements can be identified. Secondly, ensuring that fundamental kite flying theory was keeping pace with kite development and laying the groundwork for further kite research. The key findings in these two areas are outlined in the following sections along with possible research directions.

11.1 Kite Testing

Finding methods for testing Traction kites was the major focus of this research project. The original goal was to build a test rig to aid the design processes of Traction kites at Peter Lynn Kites Ltd. A car-based test rig was the result of this work, but with the experience obtained, a new circular testing method was developed. The major findings from these two testing methods, and possible avenues for research, are outlined below.

11.1.1 Car based test rig

As outlined in Chapters 2 and 3, the car-based test rig was only partially successful in determining the performance of Traction kites. The major limitations of this method are: it is difficult to obtain accurate kite performance measurements due to the tangent relationship between line angle and Lift to Drag ratio; multiple tests are required for confidence in the measurements to be obtained; tests are weather dependent, so a complete test of a kite could take weeks, or even months, to perform; performing tests on a beach with the variable wind conditions, put limits on the accuracy of the rig and reduced the value of any design improvements.

In the end, the time required to adequately test each kite was the major limitation of this method. Due to their simple construction, kite designs change very rapidly. This testing method could not provide good results quickly enough to aid the design process. However, as each design became settled, the test rig was able to provide useful results for marketing purposes.

Although further design changes to the test rig may be beneficial they are unlikely to provide significantly better results than have currently being obtained.

11.1.2 Circular kite testing

Indoor circular testing, as outlined in Chapters 5, 6 and 7, shows considerable potential to be an effective method to test Traction kites. There are two reasons for this. First, the kite performance measurements are far more repeatable than those from the car test rig. This is primarily because the test setup can be tuned to suit each kite so that it insensitive to measurement error. Secondly, because the tests are more accurate, and performed inside, it takes far less time to perform kite tests than with the car-based test rig.

The major limitation of this testing method is the availability of adequately sized facilities. Large Traction kites require a test radius greater than 40m for results to be accurate. A building this size is currently beyond the financial resources of most Traction kite manufacturers. However, if facilities can be obtained, this method would be appropriate for testing kites.

Permanent facilities would also allow modifications to the testing apparatus. The test rig used in this research had many compromises in its design as it had to be movable to and from the test site. A more permanent test site would allow a robust rig to be built capable of providing better results than those currently obtainable.

11.2 Kite Theory and Modelling

This research project outlined the basics of kite theory and laid the groundwork for further research. In particular it determined: how the flying location of a kite can be determined based on the aerodynamic properties of the structure; how the bridle point influences the flying properties of a kite; how the performance of disk wing structures can be predicted; and the fundamentals of kite turning and control. As a result of this analysis, areas for further research became apparent.

The investigation of stability points, and the findings produced, are particularly beneficial for understanding kites. The dynamics of a kite is based on the interactions between the kite line and the forces on the wing structure. Having this theory in place allows further research into kite structures and allows more complicated wings to be investigated.

11.2.1 Simple performance predictions

Chapter 9 outlined how the properties of a complicated structure, made out of multiple disks, could be predicted from the properties of a single disk. Using this knowledge the performance of other kite structures can be investigated. One particular area where this can be applied is in investigating the behaviour of ARC-style kites. These kites have complicated surface structures and no bridles, but can be modelled by an arc of different sized disks. The angle of attack of different parts of the wing, and therefore the performance of the structure, should be able to be predicted based on the knowledge of stability points (outlined in Chapter 8). It should also be possible to investigate other performance attributes of ARC-style kites such as de-power and luff resistance.

11.2.2 Two-dimensional modelling

A two-dimensional model of a kite taking off to a stable flying location was attempted in the course of this project. The mathematics for the model and the difficulties faced when applying it to real kites are in Appendix IV. This work was not included in the body of the text as it was largely unsuccessful in modelling the movements of a kite. It was found

that the properties of a stable kite were substantially different to that of an accelerating kite. Further work is needed to adequately model kite take-off.

11.2.3 Three-dimensional modelling

Kite turning and control are essential for flying Traction kites, and the mechanisms by which they are achieved need to be fully understood. The fundamental theory for this area has been outlined in Chapter 10, but a full analysis will require a three-dimensional model that solves the equations of motion. The mathematics for a three-dimensional model are more complicated than for the two-dimensional case and, as with a two-dimensional model, it will be necessary to determine the appropriate kite properties. A model of this type will be needed for further research into kites, as the dynamic properties of a kite will always need to be considered when kite performance is investigated.

11.2.4 Comments on computational modelling

it has been suggested that computational modelling will be needed in order to improve the performance of Traction kites. Should this be done the kite model will need to take into account the response of a dynamic wing to changes in loadings and wind direction. Building a full model of this type will be a considerable challenge.

Designing a model of this type is a multi stage process. The first level is likely to involve analysing a solid kite structure in a fluid modelling programme, like FLUENT. Obtaining the correct shape of an existing kite, and meshing this, will be a significant challenge in its own right. If the wing shape is then modified based on the results from this programme, stability point movements will need to be taken into account. Changing the wing shape will require an iterative process to ensure that each part of the wing is balanced by the forces in the kite line. At present this is a lengthy process and would take too long for most kite designers.

11.3 Final Comments

The work outlined in this report has been very challenging. Kites are often viewed solely as a recreational activity, but it is continually surprising how complicated they are. As an example, kite testing was initially envisaged to be a straightforward exercise, but obtaining accurate results proved difficult. Understanding kite dynamics, especially in three dimensions, poses its own challenges, and there is enormous scope for further work in this area. It is hoped that the invention of Traction kite based sports will encourage further research efforts, and that this work will be useful in the development of successful, high performance kites that have a wide variety of applications.

THE END

12. References and Bibliography

References

Babinsky. H. (1999). The aerodynamic performance of paragliders. *The Aeronautical Journal*. Sept 1999, 421-428.

Baker, R.W., Whitney, R.L., Hewson, E.W. (1979). A low level wind measurement techniques for wind turbine generator siting. *Wind Engineering*, Vol. 3, No. 2: 107-114.

Bryant, L.W., Brown. W.S., Sweeting. N.E. (1942). Collected researches on the Stability of Kites and Towed Gliders. *Aeronautical Research Council reports and Memoranda No. 2303*. Feb.

Cochrane, J.A. (date unknown). The Dunfield aerial photographic system. *Aerial Archaelogy* 4: 8-11.

Cook, M.V., Kilkenny, E.A. (date unknown). *An Experimental Investigation of the Aerodynamics of the Hang Glider*. Cranfield Institute of Technology, Bedford.

Daniels, P.A. (1982(a)). *Kanuku Kite wind study: III. Turbulence analysis.* Department of Meteorology, University of Hawii, Nov.

Daniels, P.A., Oshiro, N.E. (1982(b)). *Kanuku Kite wind study: I. Kahuka beach boundary layer*. Department of Meteorology, University of Hawii, Sept.

Daniels, P.A., Oshiro, N.E. (1982(c)). *Kanuku Kite wind study: II. Kahuka foothills*. Department of Meteorology, University of Hawii, Sept.

Day, I.C., (1982). Jacob's Ladder. *Yachts and yachting*, Dec 17: 67-72.

De laurier, J.D. (1972(a)). *Stability Analysis of a Cable-Body Systems Totally Immersed in a Fluid Stream*. NASEA Contractor Report NASE CR-2021, Washington, April.

De laurier, J.D. (1972(b)). Stability Analysis for Tethered Aerodynamically Shaped Balloons. *Journal of Aircraft*, Vol 9, No 9: 646-651.

Duckworth. (1985). Reference not provided by Hobbs (1986). See Appendix I

Dusariez, M. (1985). *Kite Aerial Photography Worldwide Association newsletter*. Bruxelles, Belgique. ISSN 0773 6207

ESDU. (1972). Fluid Forces and Moments of flat plates. *Engineering Sciences Data Item No. 70015*. Oct.

Farrow, R.A., Dowse, J.E. (1984). Methods of using kites to carry tow net in the upper air for sampling migrating insects and its application to radar entomology. *Bulletin of Entomological Research*, Vol 74: 87-95.

Fletcher, C.A.J. (1983). On the Rotary wing Concept for Jet Stream Electricity Generation. *Journal of Energy*, Vol. 7, No. 1: 90-92.

Fletcher, C.A.J., Honan, A.J., Supuppo, J.S. (1983). Aerodynamic Platform Comparison for Jet-Stream Electricity Generation. *Journal of Energy*, Vol. 7, No. 1: 17-23.

Fletcher, C.A.J., Roberts, B.W. (1979). Electricity Generation from Jet Stream Winds. *Journal of Energy*, Vol. 3, No. 4: 241-249.

Geola, J.S. (1979). Wind Power Through Kites. *Mechanical Engineering.*

Geola, J.S., Somu, N., Abedinzadeh, R., VijayKumar, R. (1985). Wind Loading effects on a caternary. *Journal of Wind Engineering and Industrial Aerodynamics*, Vol. 21: 235-249.

Hardy, A.C., Milne, P.S. (1938). Studies in the distribution of insects by aerial currents, experiments in aerial tow-netting from kites. *Journal of Animal Ecology, Vol 7, No 2, Nov 1938.*

Hart, C. (1967*). Kites, A Historical Survey.* Faber and Faber, London, 1967.

Hobbs, S.E. (1986). *A Quantitative Study of Kite Performance in Natural Wind with Application to Kite Anemometry.* Cranfield Institute of Technology. (Thesis: PhD).

Hobbs, S.E. (1989). Kite Measurements in the Boundary Layer. *Wind Engineering*, Vol. 13, no. 2: 50-60.

Hollingdale, S.H., Richards, G.J. (1939). *First report on the development of a kite barrage.* RAE Farnborough, ref. D.I. 150 R / 39, item no 56 A/5/38, D.I. 101, Jan.

Hoerner, S.F. (1965). *Fluid Dynamic Drag.* S.F. Hoerner. USA.

Ito, T., Komura, H. (1983). *Kites – the Science and the Wonder.* Japan Publications, Inc.

Jackson, S.B. (1942). *Free flight tests on kites in the 24ft wind tunnel.* RAE Farnbourough, March 1942, ARC R&M 2599.

Jenkins, G.J. (1981). Kites and meteorology, *Weather*. October, Vol. 4, No. 10: 294-300.

Kunkel, K.E. (1981). *Evaluation of a tethered kite anemometer.* US Army Electronics Research and Development Command, Atmospheric Sciences Laboratory, White Sands Missile Range, New Mexico, USA. AD A 097 082. Feb

Kaimal, J.C., Baynton, H.W., Gaynor, J.E. (Editors). (1980). The Boulder Low-Level Intercomparison Experiment. Preprint of WMO report, report no. 2, June. Published by NOAA/NCAR, Boulder atmospheric observatory.

Kalikov, V.N., Nekrasov, I.V. and Ordanovich, A.E. (1974) Investigation of Plane Parallel Motion of a Kite. *Vestnik Moskovskogo Universiteta*. Mekhanika, Vol. 29, No. 5: 66-73.

La Burth, C. (1979). *Experimental study of the flight envelope and research of safety requirements for Hang – Gliders*. NASE CP 2085, Part II. Science and technology of Low Speed and Motorless Flight, NASA Langley Research Centre, 29-30, Mar,

Lloyd, A., Thomas, N. (1978). *Kites and kite flying*. Hamlyn, London.

Lloyd, M.L. (1980). Crosswind Kite Power. *Journal of Energy*, Vol. 4, No. 3: 106 – 111.

Marchaj, C.A. (1979). *Aero-hydrodynamics of Sailing*. Dodd, Mead and Company. NY.

Marvin, C.F. (1897). The Mechanics and Equilibrium of Kites. *Monthly Weather Review*, April 1897:136-161.

Met Office. (1961). *Handbook of meteorological instruments, Part II, Instruments for upper air observations.* Meteorological Office, HMSO.

Napier Shaw. (1926). *Manual of Meteorology*. Vol I. Meteorology in History. Cambridge University Press.

Naylor, C.H. (1940). *Roof balance tests on a B type Cody Kite in the 24ft wind tunnel.* BA Departmental Note, Large Wind Tunnel No 37. June.

New Scientist. (1978). *Wonderful flying machines for farmers*. 3, Aug: 344.

Nicolaides, J.D., Speelman, R.J., Menard, G.L.C. (1970) A review of parafoil application. *Journal of Aircraft*, Vol 7, No 5: 423-431.

Nicolaides, J.D., and Tragarz, M.A. (1971). *Parafoil Flight Performance*. Technical report AFFDL-TR_71-38, AD 731 143. June 1971.

Nowell, J. (1984). *The performance of kites with reference to bird scaring*. Canfield Institute of Technology. (Thesis: MSC).

Pelham, D. (1976). *The Penguin Book of Kites*. Penguin Books Ltd., London.

Pocock, G. (1827). *The Aeropleustic Art , or Navigation in the Air by the use of Kites, or Bouyant Sails.* 1827, Second edition 1851.

Powley, M., Wild, N.E. (1940). *The influence of kite characteristics on the performance of a kite barrage unit.* RAE research Department, Exeter, General kite problems; RAE ref D.I. 150, D.I.109, April.

Richards, G.J., Smith, T.L. (1942). *Report on Kite Duration Flight.* RAE Research Department Exeter, report Exe/121, Mar.

Riegler, G., Riedler, W., Horvath, E. (1983). Transformation of Wind Energy by a High Altitude Power Plant. *Journal of Energy*. Vol. 7, No. 1: 92-94.

Rogallo, F.M., et al . (1960). *Preliminary investigation of a paraglider.* NASA TN D443.

Schaefer, G.W., Allsopp, K. (1980). Kite sails for wind assisted wind assisted ship propulsion. *Royal Institute of Naval Architects, Symposium on Wind Propulsion of Commercial Ships,* paper no 9, Nov 4-6, London.

Schmidt, T. (1981). Kite sailing – a survey. *Boat technology international.* July 1981: 11-14

Shaw, C.T. (1980). *The Aerodynamics of kites.* Third year aerodynamics project, lent term 1980. Peterhouse College, Cambridge.

Stewart. (1985). Reference not provided by Hobbs (1986). See Appendix I

Sweeting, J.T. (1981). *An experimental investigation of Hang Glider Stability.* Canfield Institute of Technology. (Thesis: MSC).

Van Veen, H. (1996) *The Tao of Kiteflying.* Aeolus Press Inc. 1996.

Wllicome, J.F, Wilkinson, S. (1984). *Ship Propulsive Kites – an Initial Study.* University of Southampton. Department of Ship Science, Faculty of Engineering and Applied science, Dec.

Wiley, J. (1984). T*he kite building and kite flying handbook.* TAB books Inc.

Bibliography

Balsley, B.B., Williams, J.B., Tyrrell, G.W., Balsley, C.L. (1992). Atmospheric Research Using Kites: Here We Go Again! *Bulletin American Meteorological Society*, Vol. 73, No.1: 16-29.

Geola, J.S., Jain, M. (1982). How does a kite fly? *Science today*, Jan: 44-50.

Geola, J.S., Vijaykumar, R., Zimmermann, R.H. (1986). Performance Characteristics of a Kite-Powered Pump. *Transaction of the ASME. Journal of Energy Resources Technology*, Vol. 108: 188-193.

Kochkarev, M.V., Makarov, S.V. (1991) A study of the start and speeding up of an F-1-A glider on a towline with the use of a mathematical model. *Report of the Twenty-Fourth Annual Symposium of the NFFS:* 49-66.

13. Appendix I-Background Research

The following section is taken directly from Hobbs (1986), as it is a reasonably comprehensive outline of past research involving kites. A summary of the key points have been included in the main body of this work. References within this section have been included in the main reference list.

.....

....this thesis is concerned with measurements of kite performance, and treats the kite as a scientific tool. To give a useful perspective to the whole study, Table 1 (see Chapter 1) lists the main recorded uses of kites as research tools This is not meant to be a complete history, but merely lists some of the main events. Most kite hobby books include a brief history of the kite (see for example Pelham, 1976 and Wiley, 1984). Probably the most authoritative history of the kite is given in Hart (1967), which traces kite history back to its origins in the Far East, and also includes a separate chapter on Meteorological Kites. Several review articles have been concerned particularly with the meteorological use of kites, for example Jenkins(1981) and a chapter of Napier Shaw (1926) and Met Office (1961)

It can be seen that kites have a long history, and their most intensive period of development until recent years was that leading up to the invention of the aeroplane, i.e., 1885...1905. Since then, aeronautical knowledge has increased dramatically, but comparatively little work has been done to understand kites. The Royal Aircraft Establishment experiments in 1938..1942 and more resent research into the Rogallo Parawing and Jalbert's Parafoil are the main exceptions.

Research 1885..1905

In the period 1885..1905, kites were seen mainly as a useful aerial platform, and the main task was to develop the steadiest, most efficient design, and the most reliable system for launching and controlling them. Aerodynamics was comparatively poorly understood so that detailed fluid-dynamic studies were not made. However, the qualitative understanding was not necessarily weak; Marvin (1897) is an excellent account of the mechanics of Kites, and indicates the level of understanding in some quarters. Hargrave's Box Kite is an important design from this period and was one of the main kites used, due to its strength and steadiness. Another important design is the Eddy bow-kite (similar to the Malay used here). These are the two designs used by the US Weather Bureau for their kite work, which continued into the 1930's. These kites were used as aerial platforms, at heights of up to several thousand feet (5000 – 10 000 ft was not unusual), but as the aeroplane became more developed, it was obvious that it could extend the range of measurements quite easily, and was more convenient. Balloons too began to take over from kites since they too could carry small instrument packages, and by the end of the 1930's radio sondes were being built and used to transmit information from the sonde to the ground. Kites ceased to be used for meteorological measurements then because of the practical difficulties (and dangers) of the steel lines used which were usually several miles long) and the fact that balloons and aeroplanes allowed measurements to be made to greater heights more easily and conveniently. The main contributions from this period to the present work are the vast amount of practical experience gained, the new designs developed, and the first solid qualitative understanding of kite flight.

Royal Aircraft Establishment, 1938-1942

During the period 1938-1942 the Royal Aircraft Establishment (RAE) considered using kites for anti-aircraft barrages. A variety of kites were tested, but most work concentrated on designs similar to Cody's War Kites of around 1906. The research included wind tunnel test, field trials and attempts at kite design and theory.

The wind tunnel tests are of most interest here. A large wind tunnel (24 ft diameter) was used for a variety of kites. Most tests used a Cody kite (either the standard with a 3ft box (area = 9.8 m^2), or the 2 ft "storm kite" or "type A"), or one of several modification aimed at improving performance. The other tests tried related designs and new kites designed at RAE. The results were published in a series of reports over the period 1938-1942 of which the most complete is Jackson (1942). Other reports include BA Departmental Notes – Long Wind Tunnel – numbers 17, 33, 37, 39, 42 and 43: Naylor (1940) includes results which are used a s a comparison with the Cody tested at Cranfield. The kites tested were generally larger and heavier than those used at Cranfield since an important part of the study concerned strong wind performance. In strong winds the balloon barrage was unusable, and it was hoped that kites would be able to maintain an aerial barrage into such conditions.

One new design tried was a monoplane kite intended to achieve a much higher lift to drag ratio than the Codys. This is reported by Hollingdale and Richards (1939). The wind tunnel tests were generally disappointing due to the poor lateral stability and the weight of the kite. A Pterodactyl design (i.e., with one main wing swept backwards and no tail) is mentioned as "in progress", but no performance results are given. The report also considers a kite barrage more generally, including useful information concerning the frequency of surface wind speeds, and thus estimate the proportion of time for which kites may be usable. Powley and Wild (1940) continue the kite barrage study, and report that the Pterodactyl kite has been tested in a wind tunnel, achieving a lift to drag ratio of about 10. It is no considered stable enough for "free flight" (i.e., as a normal kite) but is to be used to help support the weight of balloon mooring cables. Richards and Smith (1942) describe an experimental kite barrage maintained from June 1940 to February 1941, using mainly Codys in trains. The practical experience is valuable, and they include the comment that "kites could be put to a real use for meteorological purposes especially in conditions of high wind and poor visibility, the tension in the wire giving a continuous indication of wind speed at height." Kite anemometry is not a new idea.

Independent of the RAE work, the Aerodynamics Division of the National Physical Laboratory (NPL) was working on the stability of kites and towed gliders. The research was mainly theoretical, although some trials were made in wind tunnels, and is brought together in the report of Bryant, Brown and Sweeting (1942). A major focus of the NPL work was to consider the stability of towed gliders. The mathematics is the same as for kite stability, although assumptions such as the use of short lines are not always valid for kites. NPL also attempted to design a kite of high efficiency (i.e., a high lift to drag ratio), and one model was built. It flew successfully in a wind tunnel, but was heavy and required winds above 15 mph (6.7 m/s) even to launch. It crashed during field trials. The foreword to the report comments: "The development of a satisfactory kite of high efficiency was however reckoned to be so formidable a problem that interest in the subject inevitably declined."

The main contributors from this period of research are the wind tunnel results (providing a valuable reference), the documented practical experience and attempts at improved designs or modifications, and the beginnings of a study of kite stability.

Recent Research

This section reviews post-war research into kite performance, i.e., since the late 1940's: a period which has been surprisingly fruitful for new kite designs.

Soon after the Second World War, Francis Rogallo developed his Flexible Kite, or Parawing, as the general design is known. A minimal rigid structure is used, with the kite surface able to conform to the wind. The design has been studied particularly with regard to the US space programme, who were interested in using these parawings for controlled landing of returned space capsules. In other directions, the parawing has led to the Delta kite family and the sport of Hang Gliding. Rogallo et al (1960) is the original report of this work: more recent accounts can be found in La Burthe (1979) and Sweeting (1981).

Another new kite design, the Sled, was patented in 1950 by William Allison. In 1964, Frank Scott introduced a valuable modification by using vents in the sled's lifting surface, and it is this form which is probably most common now. This kite has so far been restricted to mostly hobby use, and little research has taken the sled as its subject.

The third significant original design is the Parafoil, introduced by Domina Jalbert in 1964. Like Rogallo's parawing, the Parafoil was soon the subject of research since it provided an easily collapsible lifting surface. Many applications have been tried, including air dropping cargo, manned and unmanned powered flight, as well as tethered flight, i.e., use as a kite. Perhaps the most familiar use now is as the efficient and steerable rectangular parachutes used by many display teams. Two useful references are Nicolaides, Speelman and Menard (1970) and Nicolaides and Tragarz (1971). The first is a review of Parafoil applications; the second reports on Parafoil flight performance.

These three designs are the main recent developments and have spawned a wide range of new kites. Another important new design, although one which stands by itself, is the Flexifoil – a very efficient steerable kite which ahs been used successfully for kite sailing. Shaw (1980) is a short report studying the aerodynamics of the Flexifoil, and includes measurements of pressure distributions.

A difficulty with collecting details of previous kite research is that many separate areas of study are involved. Since there is no continuing research programme, what research has been done tends to be linked to other areas of study, so that drawing together all the relevant information can be a rather haphazard process.

This recent work contributes some valuable aerodynamic data for the various kite types allowing useful comparisons to be made between previous results (often from wind tunnels) and the current research (in natural wind), e.g., the Parafoil comparison.... The level of current understanding has also helped refine kite designs, so that it is slightly less hit-and-miss (but still as much art as technology).

Kiteline and stability theory

In parallel with work on kites, there has been research continuing into the properties of the kite line , and, as a natural part of this , the stability of a tethered object ....the work of Bryant, brown and Sweeting (1942) has already been mentioned. Perhaps the most important recent works is that of De Laurier (De Laurier, 1972 a,b). Since the problem has wide applications (any tethered object in a a fluid), the techniques have become fairly sophisticated ... A more useful physical understanding is provided by much simpler models... [in the research].

Kite Anemometry

Apart from the research taking kite or lines as their primary subject, there has been recent work in several areas, using kite or specific applications the two main areas of current interest are kite anemometry and kite sailing.

Kite anemometry, which is one of the main interests of this thesis, is an area which has been developed so far largely through the TALA system (Tethered Aerodynamically Lifting Anemometer, Tala Inc., Kite Anemometers, Ringgold, VA, USA). This uses a kite as the wind sensor to measure wind velocity at altitudes of up to several hundred metres, as anticipated by Richards and Smith (1942), A number of reports have been produced using TALA system as a tool (e.g., Daniels and Oshiro, 1982 b,c; Daniels, 1982; Baker, Whitney and Hewson, 1979), and comparing it with other types of anemometer (eg. Kunkel, 1981; Kaimal et al, 1980). ....The kite used for the TALA system is a plain sled with a tail, but no other designs appear to have been evaluated. Neither has a detailed study of kite response to natural wind been made. The goal of this thesis is to answer both these questions, so that kite anemometry is placed on a firmer footing.

Kite Sailing

Kite sailing (or more generally, kite traction) is a recently discovered use of kites. Pocock (1827) gives a colorful account of his experiences, mainly towing carriages on land. Other kite sailors have included Portuguese fishermen, who use kites to leave port using upper winds when the sea-level winds were too light (Lloyd and Thomas, 1978), and S.F.Cody who crossed the English Channel in 1903 using kites to tow a small dingy (Pelham, 1976). The first recent paper on kite traction is that by Schaefer and Allsopp (1980), who describe the basic principals and provide simple estimates of performance. The potential for improved performance over conventional sail is large, as has already been demonstrated by the kite-powered boat Jacobs Ladder, which captured a world speed sailing record (C-class, 25.03 kt) in 1982. Research since 1980 has been either largely empirical (as reported by Schmidt, 1981 and Day, 1982) or purely theoretical (Wellicome and Wilkinson, 1984). The conference Windtech '85 included two other report of recent kite traction work: Duckworth (1985) discusses a conservative use of (parachute) kite to tow oil tankers; Stewart (1985) is a strong anecdote, but has no firm performance measurements to offer (the inflatable kites are interesting however). The greatest opportunity for kite sailing seems to be in a sport, or perhaps rescue, application. there is great need for through experiments...

Other kite applications

Over the last century, kites have been put to all sort of other tasks, apart from anemometry and sailing. Most of these use kites as an aerial platform. Examples include insect netting at altitude (Hardy and Mine, 1938; Farrow and Dowse, 1984), aerial photography (Cochrane, n.d.; Dusariez, 1985), bird scaring (Nowell, 1984), crop spraying (New scientist, 1978), distress beacons,, radar target,...and many others. There is also significant amateur interest in kites, providing a fertile source of new ideas, designs and applications. Although many of these other uses of kites do not provided "hard" information concerning kite performance, their contribution is communicated through several magazines and newsletters produced regularly by various kite clubs....

14. Appendix II – Derivation of Circular Testing Modifying factors

The following sections detail the mathematics used to determine the modifying factors for Chapter 5 – Circular Testing Theory.

14.1 Derivation of modifying factors for kites centrifugal force

$$\frac{L_h}{L_c} = \frac{T_c \cos(\beta) - {m_k V_k}^2 / T_c \cos(\beta)}{T_c \cos(\beta)} = 1 - \frac{{m_k V_k}^2}{R T_c \cos(\beta)}$$

$$\frac{T_h}{T_c} = \sqrt{\frac{\left(T_c \cos(\beta) - {m_k V_k}^2 / R\right)^2 + {T_c}^2 \sin^2(\beta)}{{T_c}^2}}$$

$$\Rightarrow \sqrt{\frac{{T_c}^2 \cos^2(\beta) + {T_c}^2 \sin^2(\beta) - 2T_c \cos(\beta) {m_k V_k}^2 / R + \left({m_k V_k}^2 / R\right)^2}{{T_c}^2}}$$

$$\Rightarrow \sqrt{1 - \frac{2 m_k {V_k}^2 \cos(\beta)}{T_c R} + \frac{{m_k}^2 {V_k}^2}{{T_c}^2 R^2}}$$

14.2 Derivation of modifying factors for mass of kite

$$\frac{L}{L_h} = \sqrt{\frac{{T_h}^2 \cos^2(\beta) + (m_k + k m_l)^2}{{T_h}^2 \cos^2(\beta)}} = \sqrt{1 + \frac{(m_k + k m_l)^2 g^2}{{T_h}^2 \cos^2(\beta)}}$$

$$\frac{L - Mg}{L_h} = \frac{\sqrt{{T_h}^2 \cos^2(\beta) + \left((m_k + k m_l) g\right)^2} - (m_k + k m_l) g}{T_h \cos(\beta)} = \sqrt{1 + \frac{(m_k + k m_l)^2 g^2}{{T_h}^2 \cos^2(\beta)}} - \frac{(m_k + k m_l) g}{T_h \cos(\beta)}$$

$$\frac{T}{T_h} = \sqrt{\frac{T_h^{\,2} + ((m_k + km_l)g)^2}{T_h^{\,2}}} = \sqrt{1 + \frac{\left((m_k + km_l)g\right)^2}{T_h^{\,2}}}$$

$$\frac{T_k}{T_h} = \frac{\sqrt{\left(L - (m_k + km_l)g\right)^2 + D^2}}{T_h}$$

$$L = \sqrt{L_h^{\,2} + ((m_k + km_l)g)^2} = \sqrt{T_h^{\,2}\cos^2(\beta) + ((m_k + km_l)g)^2}$$

$$\therefore \frac{T_k}{T_h} = \frac{\sqrt{\left(\sqrt{T_h^{\,2}\cos^2(\beta) + ((m_k + km_l)g)^2} - (m_k + km_l)g\right)^2 + T_h^{\,2}\sin^2(\beta)}}{T_h}$$

$$\Rightarrow \frac{\sqrt{T_h^{\,2}\cos^2(\beta) + T_h^{\,2}\sin^2(\beta) + 2(Mg)^2 - 2Mg\sqrt{T_h^{\,2}\cos^2(\beta) + (Mg)^2}}}{T_h}$$

$$\Rightarrow \sqrt{1 + \frac{2((m_k + km_l)g)^2}{T_h^{\,2}} - \frac{2(m_k + km_l)g}{T_h^{\,2}}\sqrt{T_h^{\,2}\cos^2(\beta) + \left((m_k + km_l)g\right)^2}}$$

15. Appendix III – Kite Rotation Results

The following figures are the forces and moments at the centre of mass, for a disk wing rotated around its three axes. The wing used to generate these curves is the same as that outlined in Chapter 9. It has been oriented in dihedral and anhedral directions, and given a θ_x rotation around the X-axis from 0-60°. Along with this rotation, each figure shows the moments and forces at 0°, 4°, 8° and 12° rotations around the Y-axis[8]. Each figure is for a θ_z rotation around the Z-axis ranging from –12° to 12°. With these figures, forces and moments on the wing can be determined at all orientations within this range.

The values presented in these figures are dimensionless coefficients. The force coefficients, CX', CY', and CZ' represent the forces acting on the wings centre of mass in the X', Y' and Z' directions. These are based on the area of two disks. The moment coefficients, MX', MY', and MZ' are based on the area of two disks and the chord length.

Although the data is presented from 0-60° around the X-axis, data above the stall should be treated with caution. As outlined in chapter 9, disk kite predictions are not accurate when the wing has stalled.

These graphs do not include the tether forces. As outlined in chapter 10, interactions between the tether and the wing become more complex as a kite moves. However, for initial movements the location of the line and the forces on the line will be virtually the same as when the kite was flying in a stable manner. Therefore the moments around the X' axis will be largely balanced, and the forces in the Y' and Z' directions will be balanced.

---

[8] For graphs of θ_z=0°, the MZ', MY' and CX' values at θ_y= 0° are not included, as they are equal to 0.

15.1 Sample Calculation

Assume that a dihedral kite is flying at a stable location with an angle of attack of 20^{o}. It is then given a θ_y rotation of 8^{o} and a θ_z rotation of 4^{o}. Based on Figure 15:2 the following moments and force coefficients will occur at the kites centre of mass.

MX' = -0.14
MY' = 0.02
MZ' = 0.022
CX' = 0.12
CY' = 0.3
CZ' = 0.65

Assuming that MX', CY' and CZ' are largely balanced by the line tension, the wing can be expected to rotate in the positive direction around the Y' axis, rotate in the positive direction around the Z' axis (right turn), and move in the positive X' direction (right). How much rotation there is around the Y'-axis will depend on the bridle restraint on the kite.

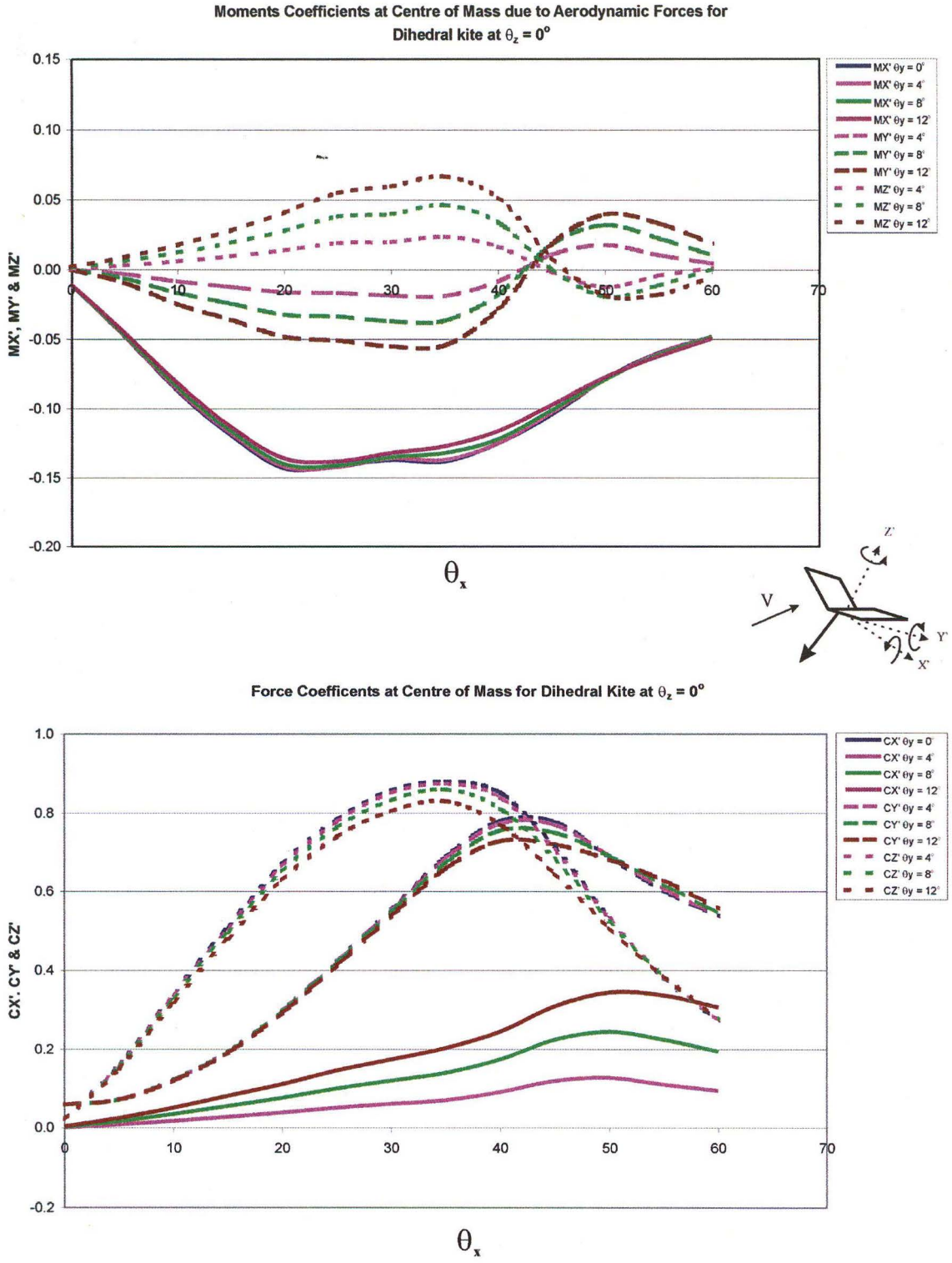

Figure 15:1 Moment and Force Coefficients at the centre of mass of a dihedral kite for $\theta_z=0^o$

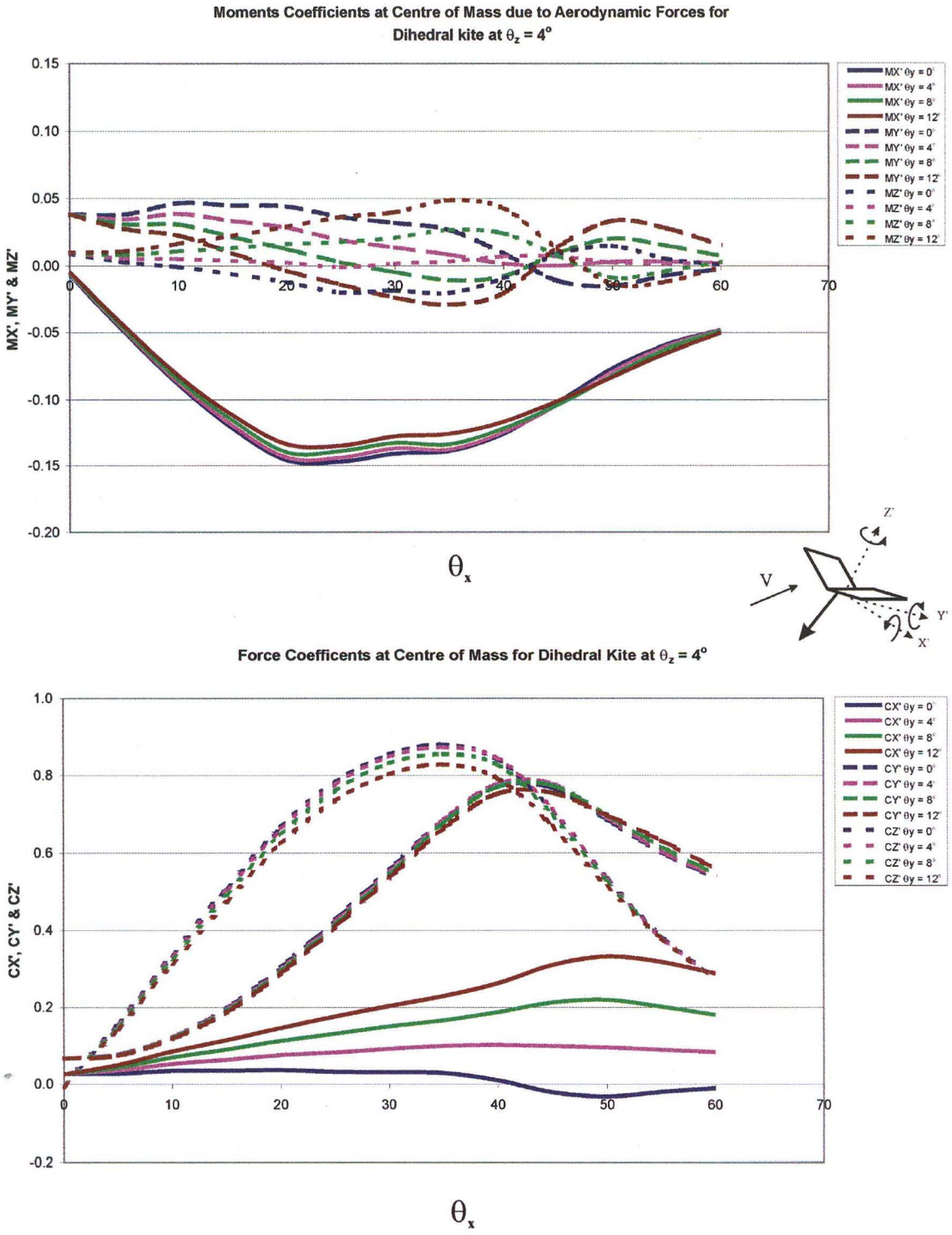

Figure 15:2 Moment and Force Coefficients at the centre of mass of a dihedral kite for θ_z=4°

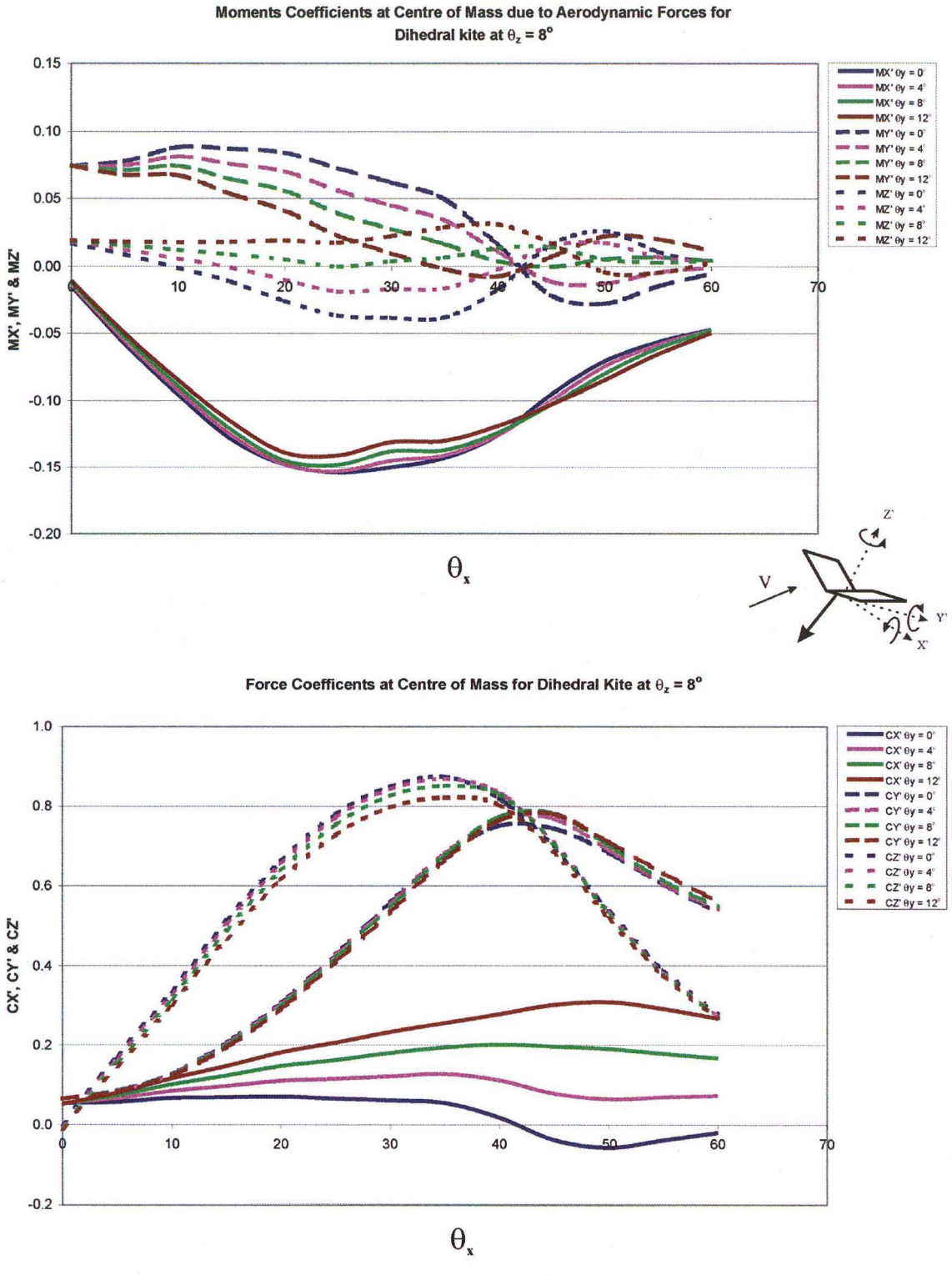

Figure 15:3 Moment and Force Coefficients at the centre of mass of a dihedral kite for θ_z=8°

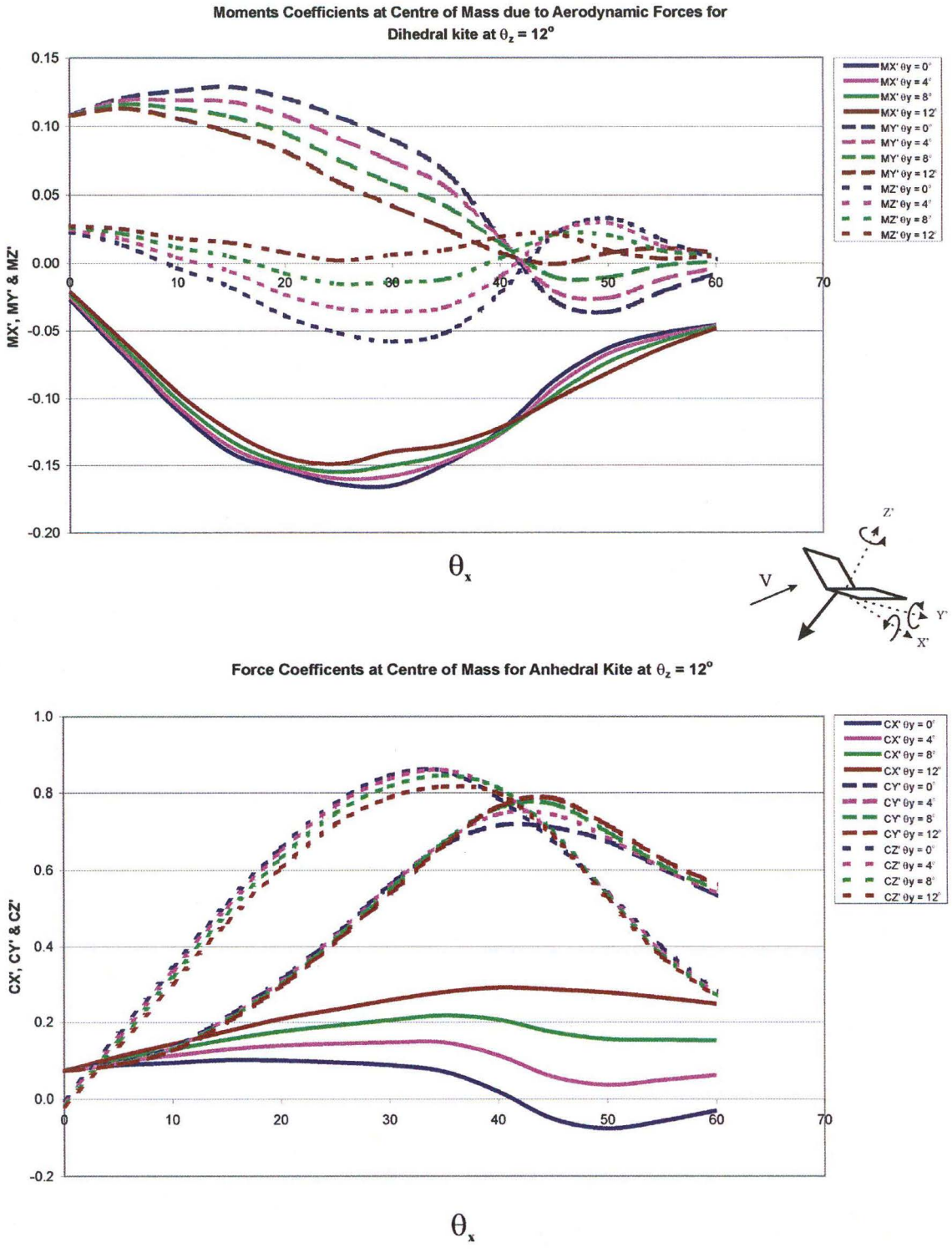

Figure 15:4 Moment and Force Coefficients at the centre of mass of a dihedral kite for θ_z=12°

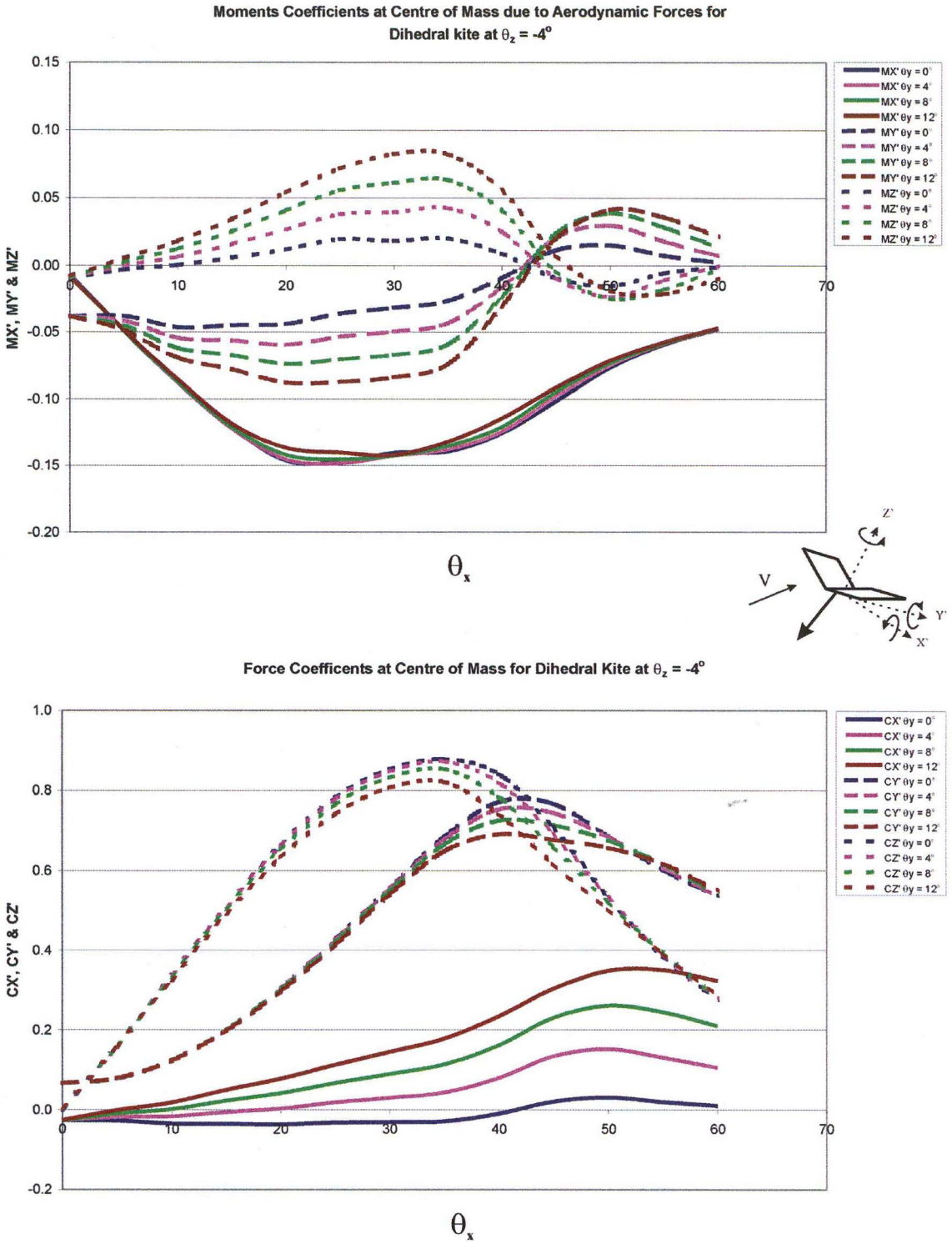

Figure 15:5 Moment and Force Coefficients at the centre of mass of a dihedral kite for θ_z=-4°

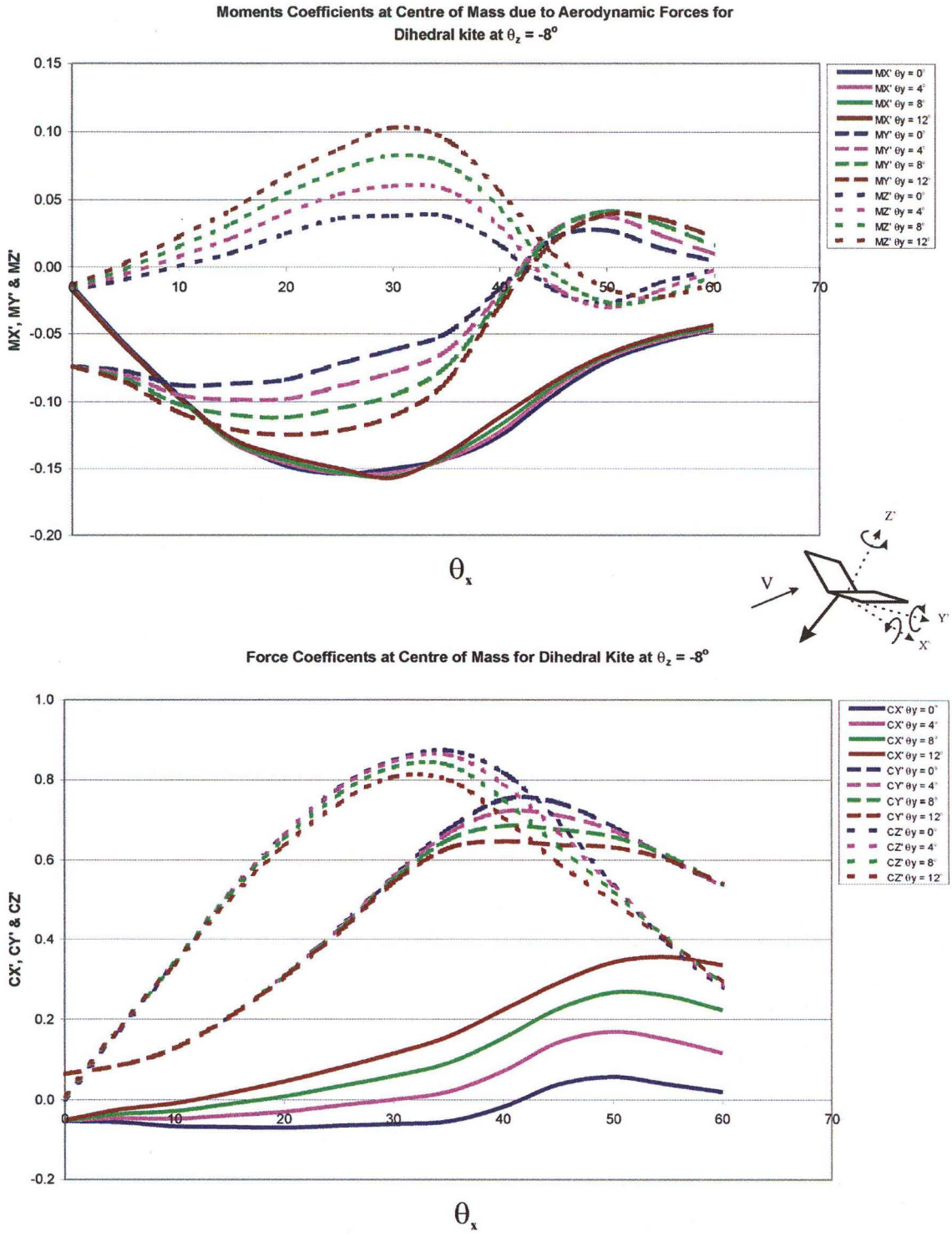

Figure 15:6 Moment and Force Coefficients at the centre of mass of a dihedral kite for θ_z=-8°

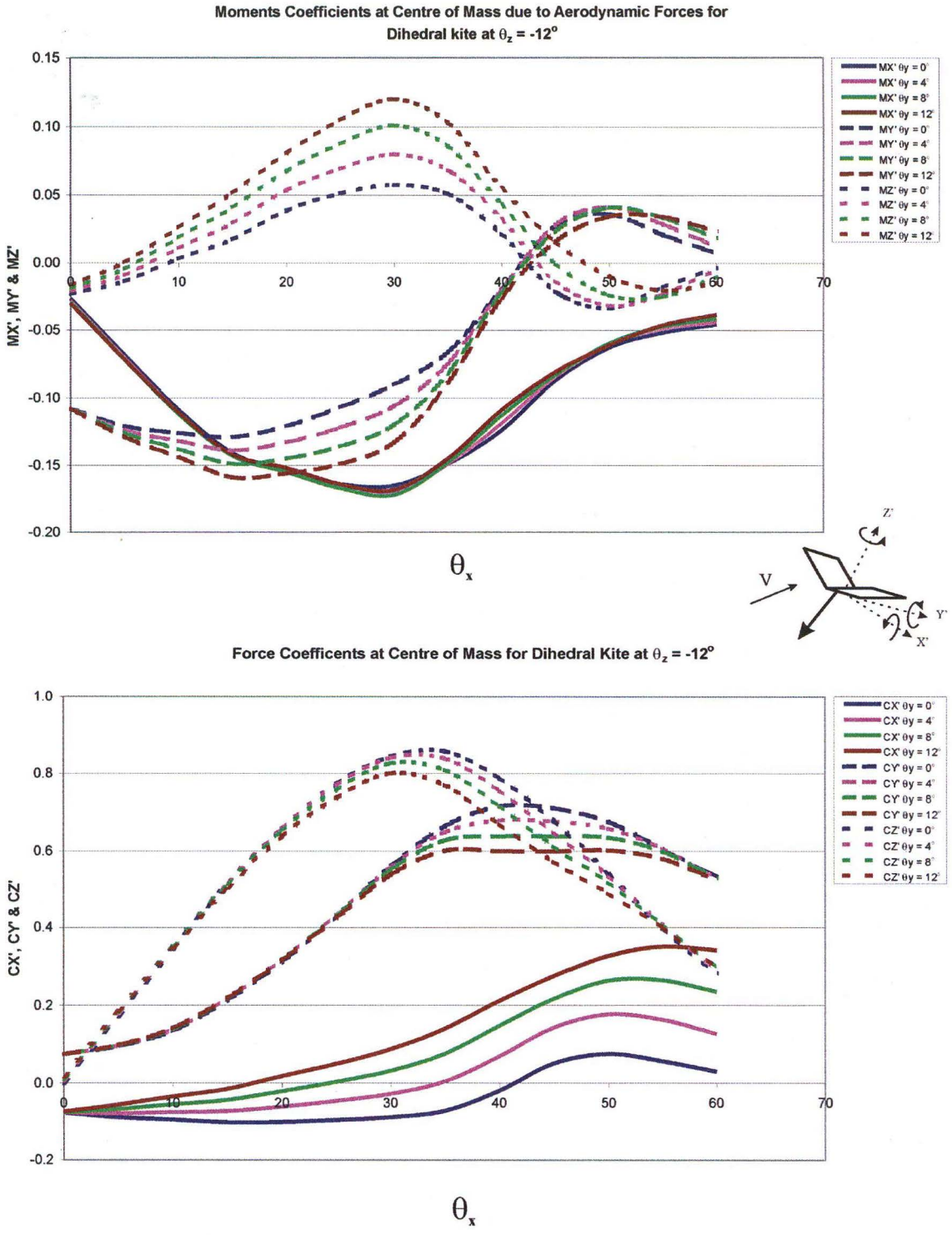

Figure 15:7 Moment and Force Coefficients at the centre of mass of a dihedral kite for θ_z=-12°

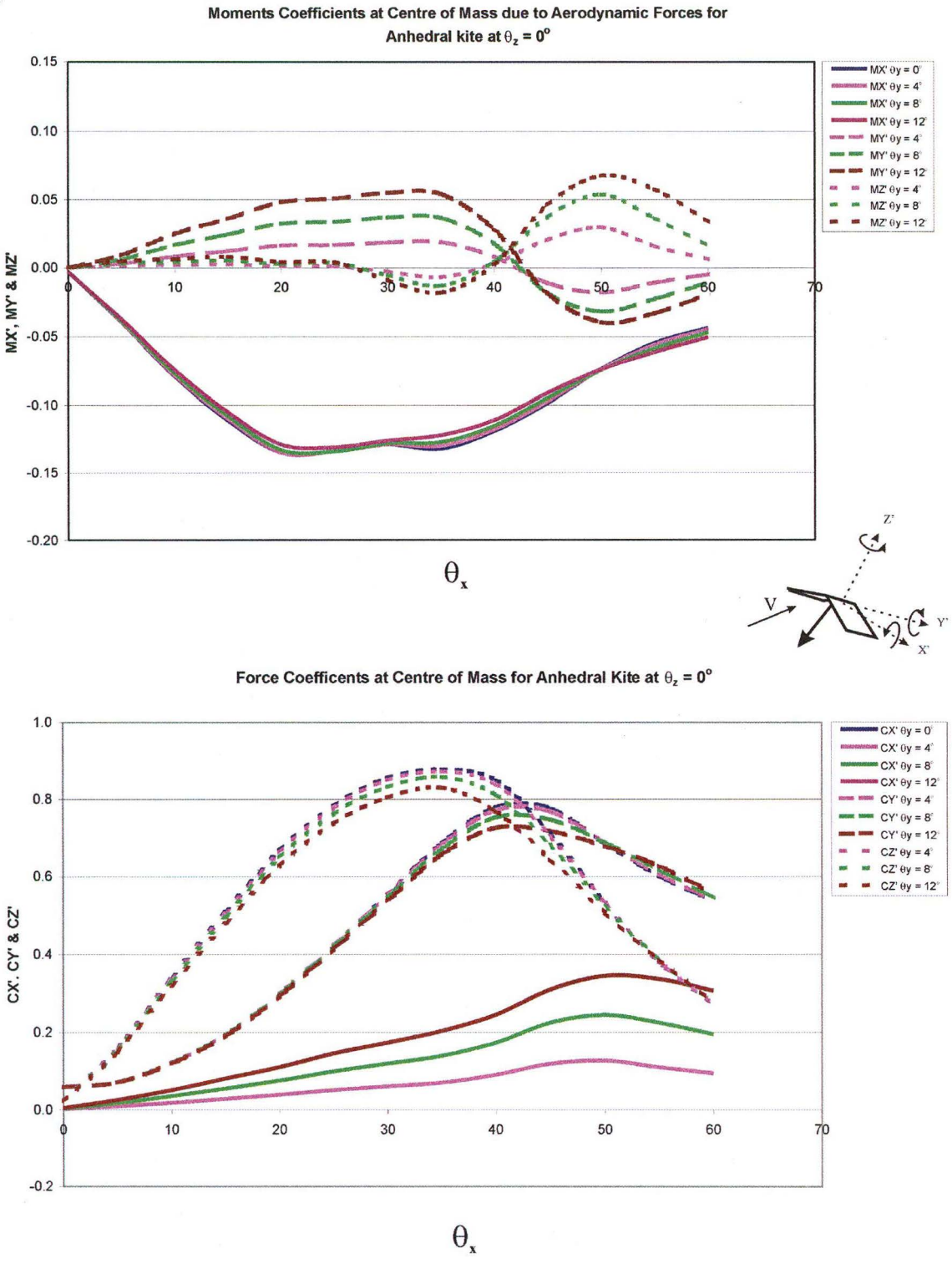

Figure 15:8 Moment and Force Coefficients at the centre of mass of an anhedral kite for $\theta_z=0^o$

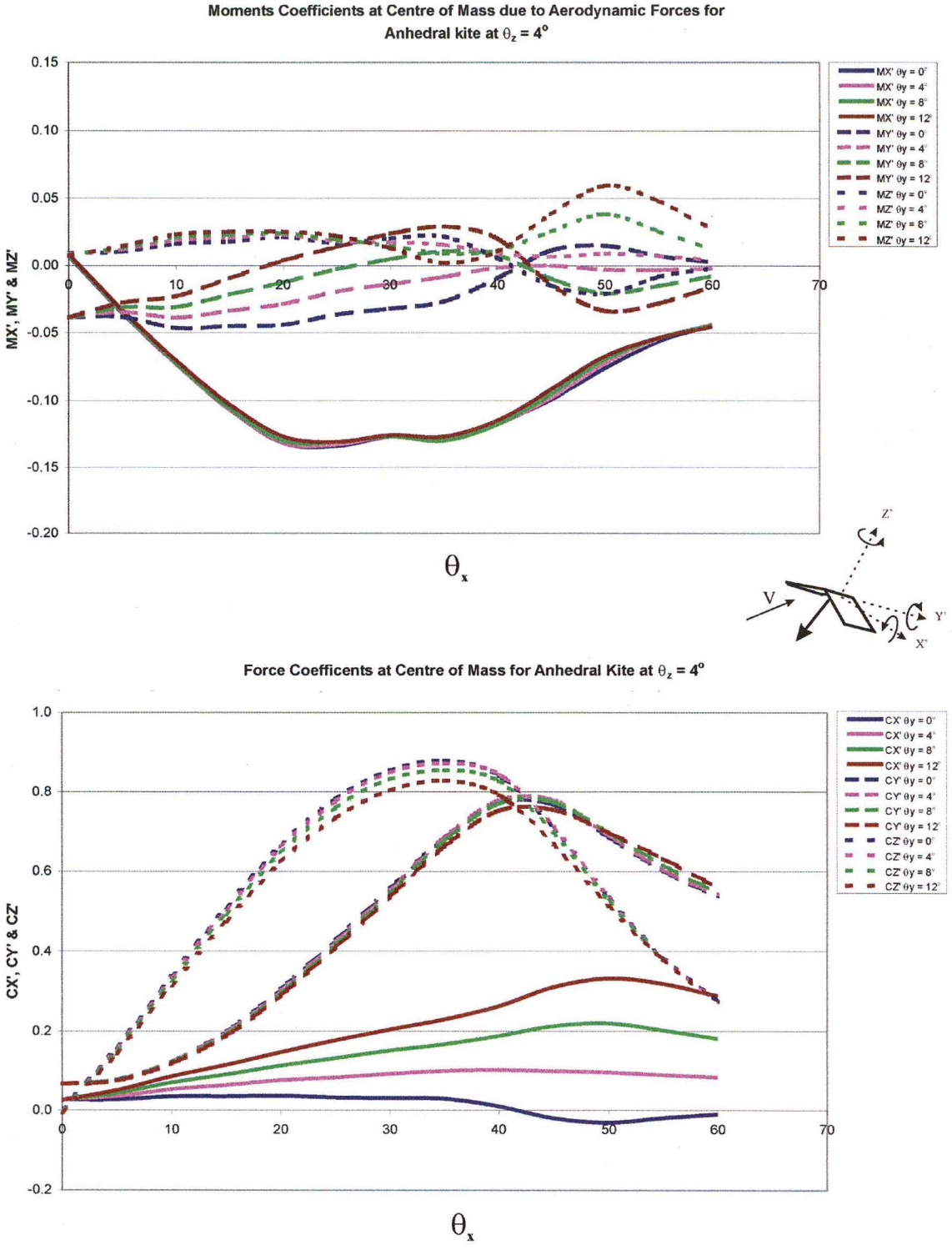

Figure 15:9 Moment and Force Coefficients at the centre of mass of an anhedral kite for θ_z=4°

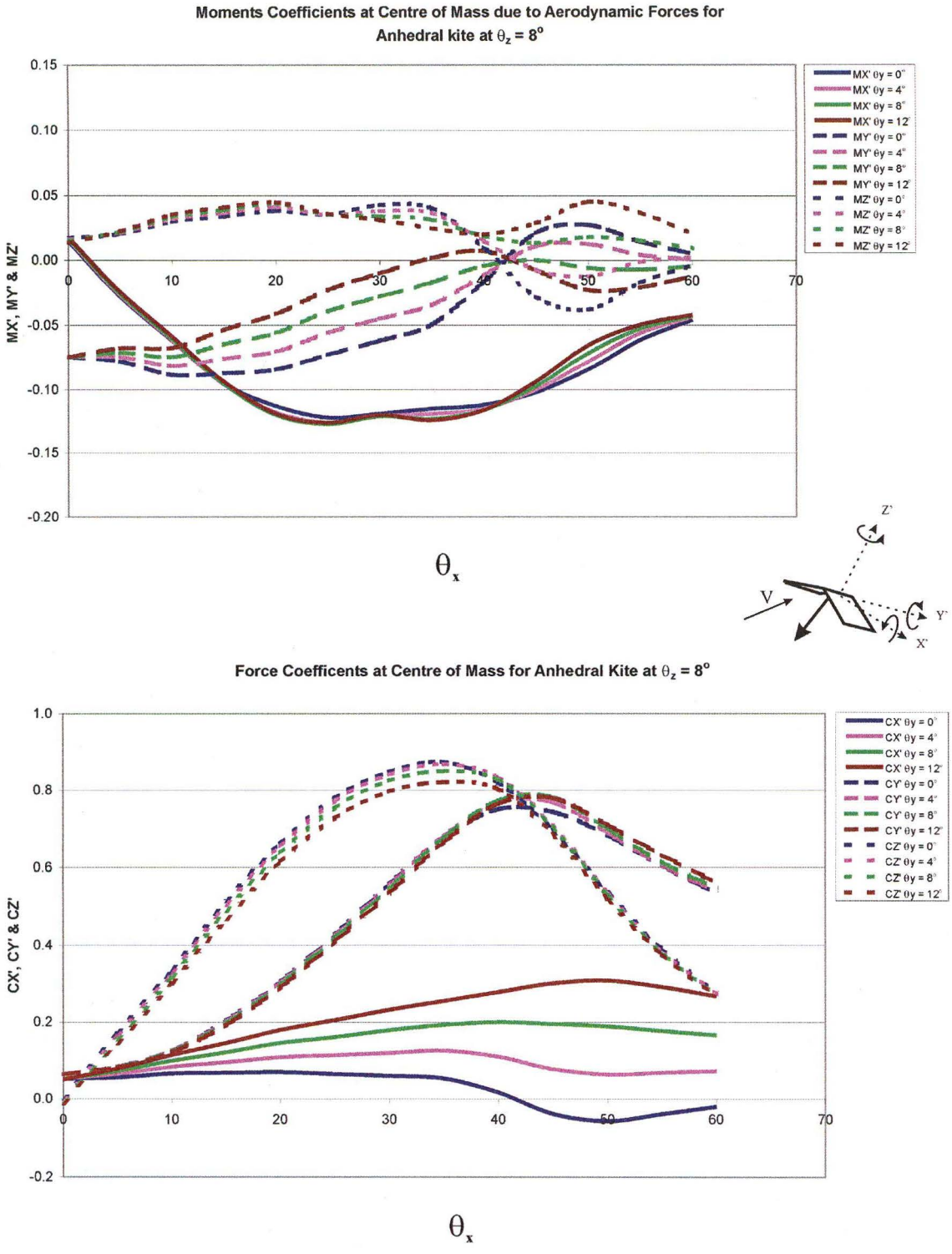

Figure 15:10 Moment and Force Coefficients at the centre of mass of an anhedral kite for θ_z=8°

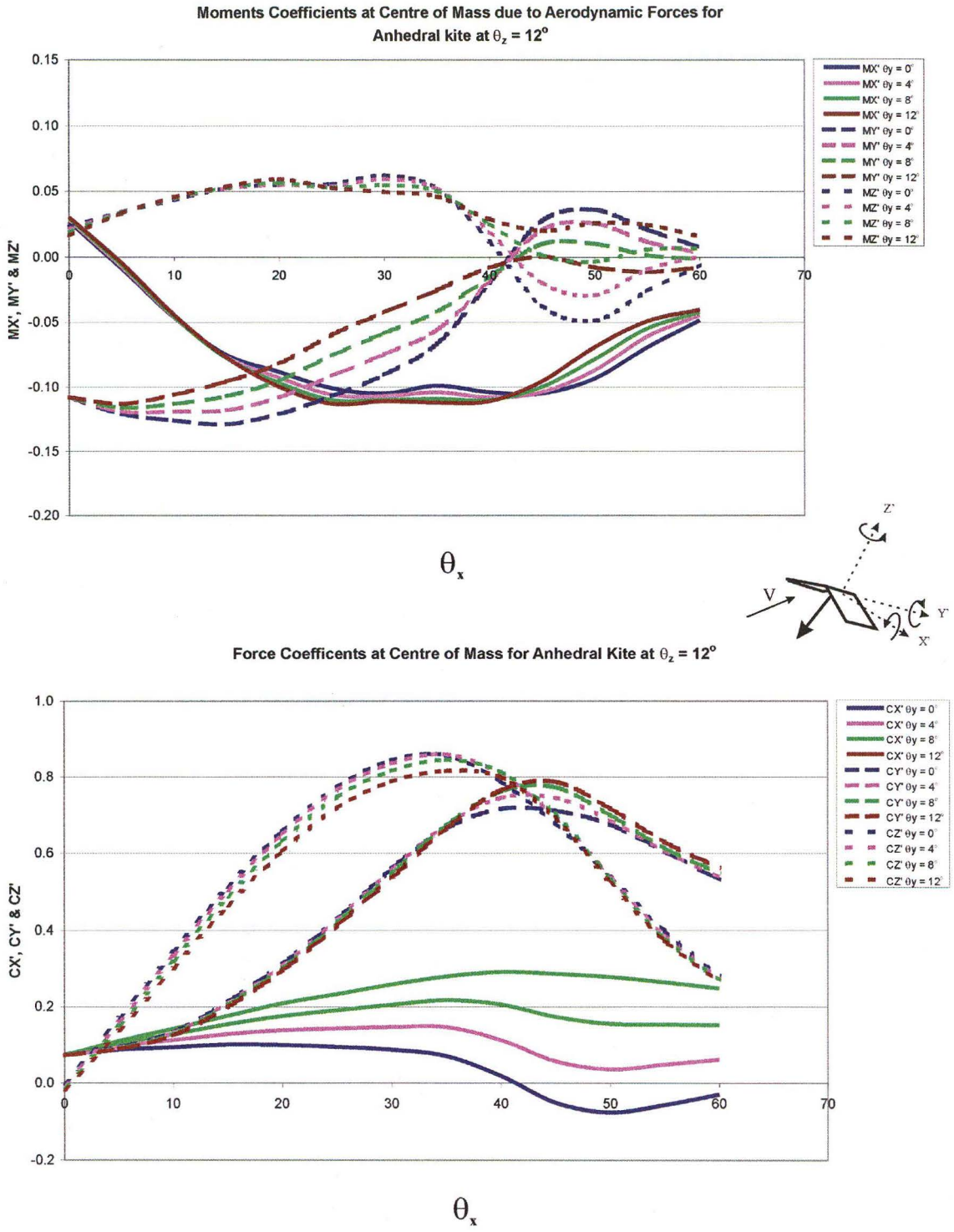

Figure 15:11 Moment and Force Coefficients at the centre of mass of an anhedral kite for θ_z=12°

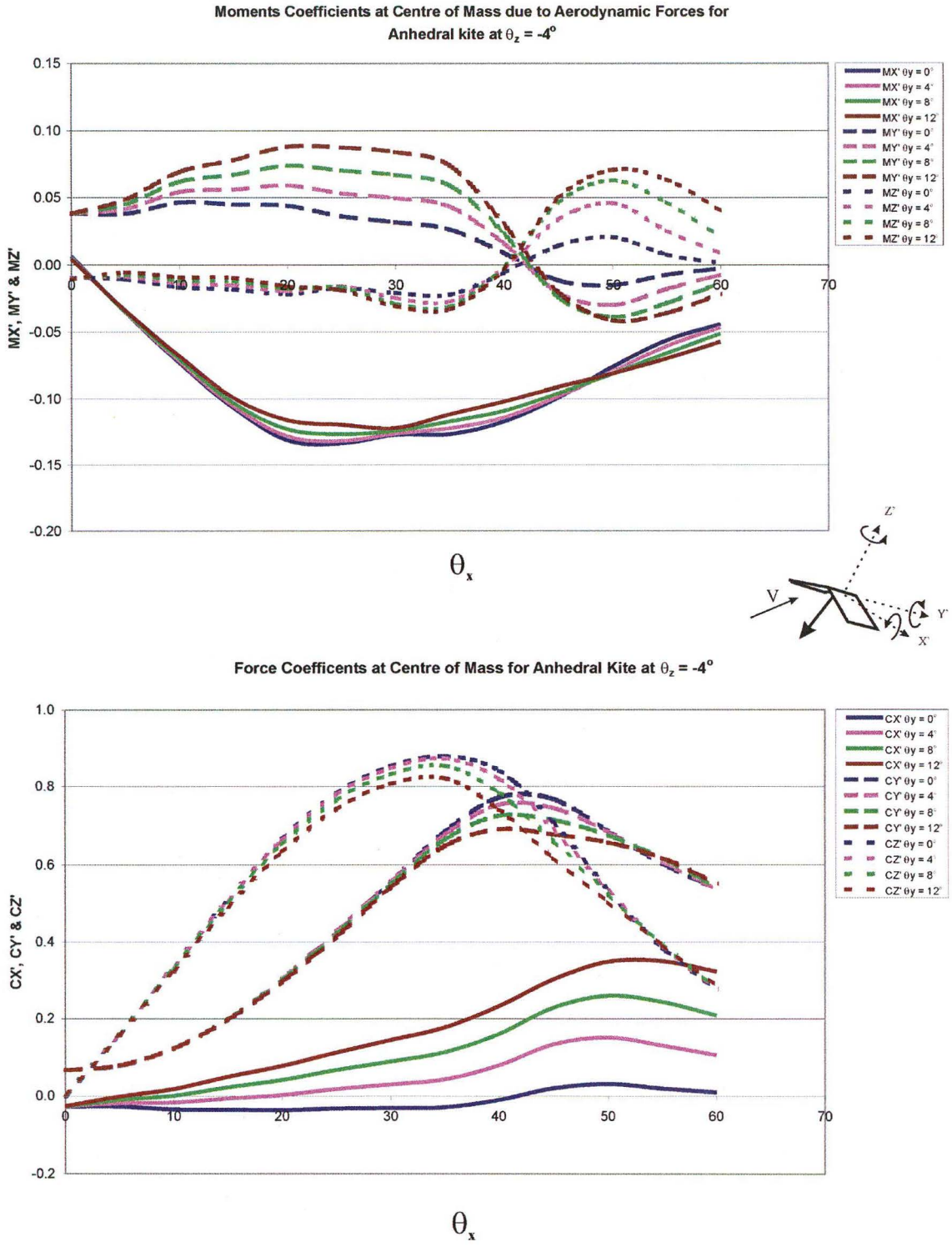

Figure 15:12 Moment and Force Coefficients at the centre of mass of an anhedral kite for θ_z=-4°

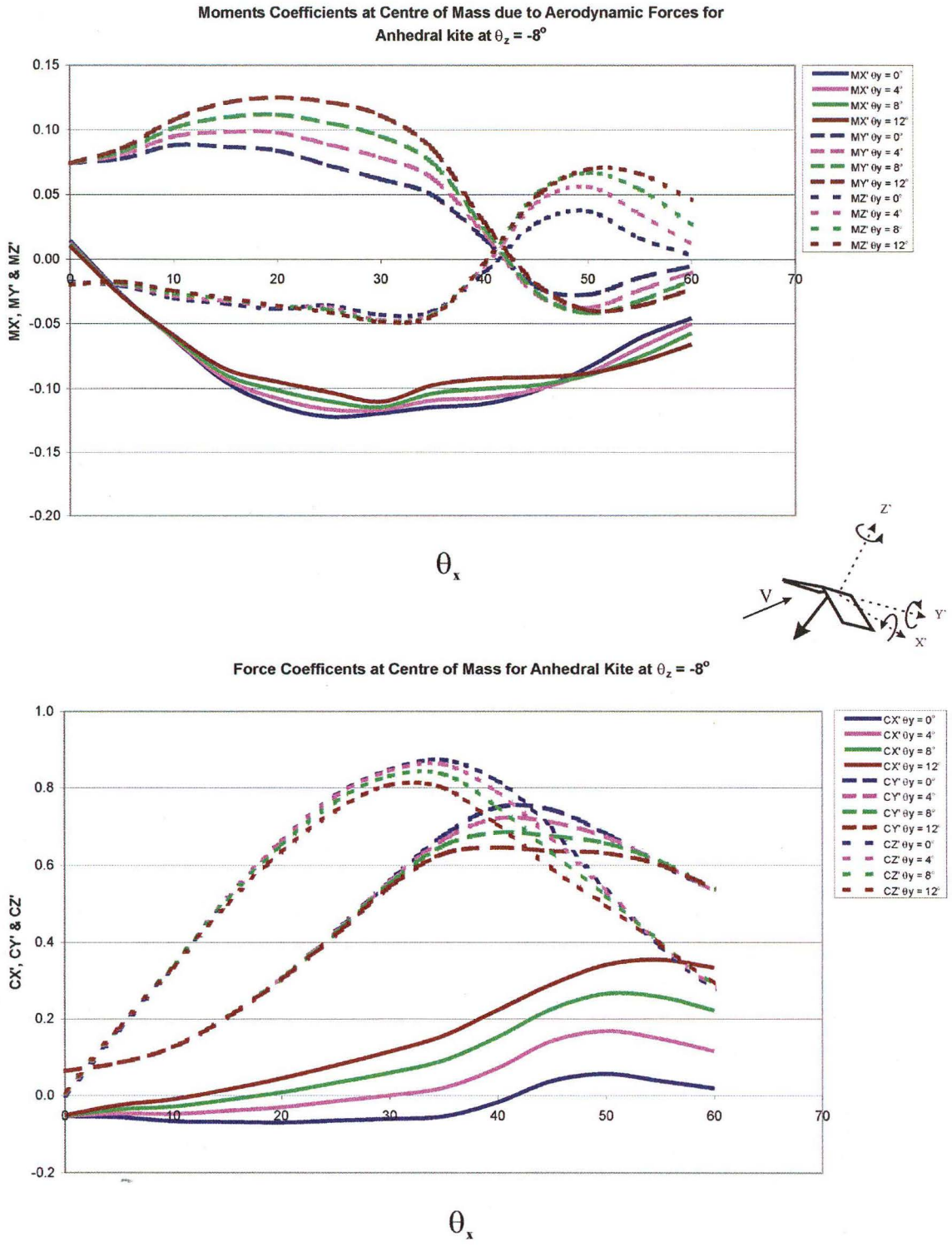

Figure 15:13 Moment and Force Coefficients at the centre of mass of an anhedral kite for θ_z=-8°

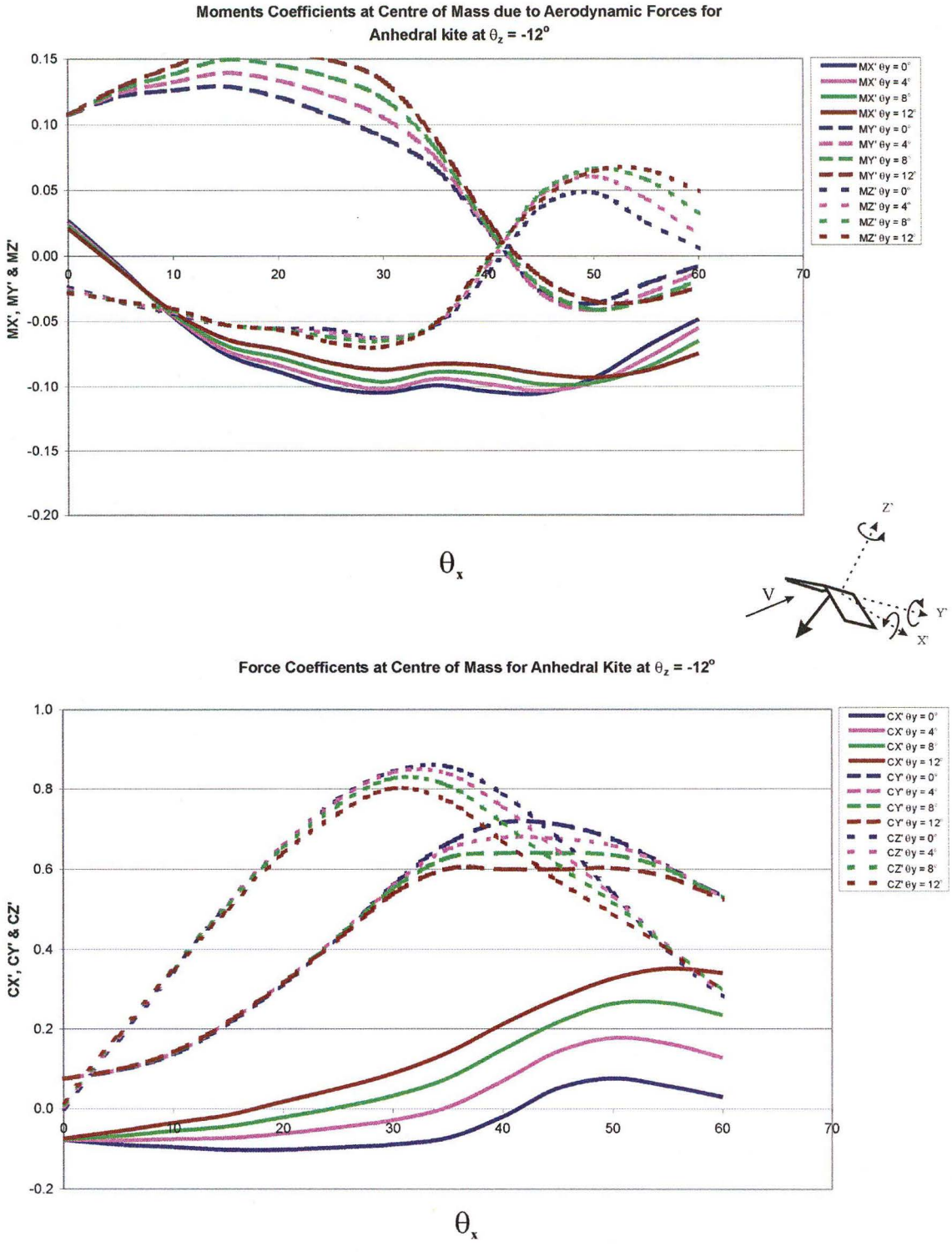

Figure 15:14 Moment and Force Coefficients at the centre of mass of an anhedral kite for θ_z=-12°

16. Appendix IV – Kite take-off mathematics

16.1 Introduction

In the course of this project considerable effort was made to model the motion of a kite. The first stage was to create a two-dimensional model of a kite as it took off from the ground towards its stable flying location. Unfortunately, finding the required inputs for the programme proved to be very difficult, and the model was largely unsuccessful in predicting the motion of a kite. However, the mathematics used in the take-off model has been presented here so that they can be utilised for future work.

16.2 Mathematical Model

Figure 16:1 shows the model used to mathematically describe a kite taking off. A key assumption is that the line (S) is a rigid member. Based on the discussion of line drag models, presented in Chapter 4, this assumption is valid when applied to Traction kites. It was also assumed that the line does not have any forces acting on it. This is only valid when short lines are used, as they are for a kite in a wind tunnel. A slightly more complicated model will be required if the forces acting on a long line are to be taken in account.

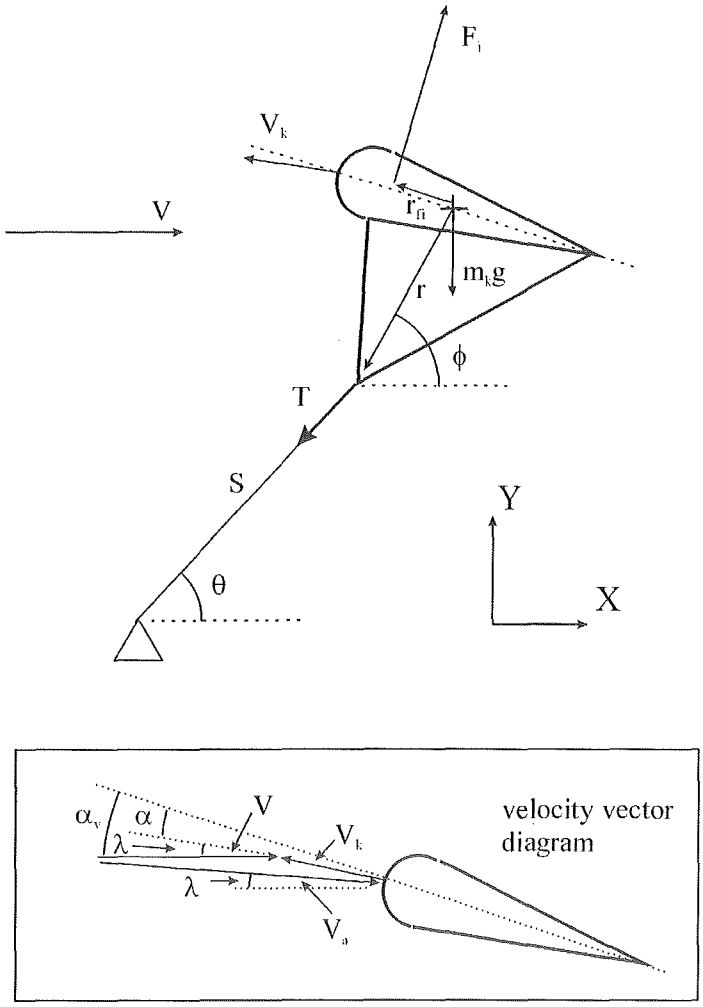

Figure 16:1 Model used in kite take-off programme

16.2.1 Equations of motion

The equations of motion for the wing structure are

$$\sum_{i=1}^{j} \boldsymbol{F}_i \cdot \hat{\boldsymbol{i}} - \boldsymbol{T}\cos(\theta) = m_k \ddot{X} \qquad \textbf{Eq 16:1}$$

$$\sum_{i=1}^{j} \boldsymbol{F}_i \cdot \hat{\boldsymbol{j}} - m_k \boldsymbol{g} - \boldsymbol{T}\sin(\theta) = m_k \ddot{Y} \qquad \textbf{Eq 16:2}$$

$$\sum_{i-1}^{j} \boldsymbol{F}_i \times \boldsymbol{r}_i + \boldsymbol{T}.\boldsymbol{j} = I_o \ddot{\phi} \qquad \textbf{Eq 16:3}$$

where

$$J = r_x \sin(\theta) - r_y \cos(\theta) \qquad \textbf{Eq 16:4}$$

From the geometry of the system

$$X = S\cos(\theta) + |r|\cos(\phi) \qquad \textbf{Eq 16:5}$$

$$Y = S\sin(\theta) + |r|\sin(\phi) \qquad \textbf{Eq 16:6}$$

and therefore

$$\dot{X} = -S\dot{\theta}\sin(\theta) - |r|\dot{\phi}\sin(\phi) \qquad \textbf{Eq 16:7}$$

$$\dot{Y} = S\dot{\theta}\cos(\theta) + |r|\dot{\phi}\cos(\phi) \qquad \textbf{Eq 16:8}$$

and

$$\ddot{X} = -S\dot{\theta}^2\cos(\theta) - S\ddot{\theta}\sin(\theta) - |r|\dot{\phi}^2\cos(\phi) - |r|\ddot{\phi}\sin(\phi) \qquad \textbf{Eq 16:9}$$

$$\ddot{Y} = -S\dot{\theta}^2\sin(\theta) + S\ddot{\theta}\cos(\theta) - |r|\dot{\phi}^2\sin(\phi) + |r|\ddot{\phi}\cos(\phi) \qquad \textbf{Eq 16:10}$$

Substituting Eq 16:9 into Eq 16:1

$$T = \frac{\sum_{i=1}^{j} F_i \cdot \hat{i}}{\cos(\theta)} + m_k S\dot{\theta}^2 + m_k S\ddot{\theta}\tan(\theta) + m_k|r|\dot{\phi}^2\frac{\cos(\phi)}{\cos(\theta)} + m_k|r|\ddot{\phi}\frac{\sin(\phi)}{\sin(\theta)} \qquad \textbf{Eq 16:11}$$

Substituting Eq 16:11 and Eq 16:10 into Eq 16:2

$$\ddot{\phi}\left[m_k|r|(\cos(\phi)+\sin(\phi)\tan(\theta))\right]+\theta\left[m_k S(\cos(\theta)+\sin(\theta)\tan(\theta))\right] \qquad \textbf{Eq 16:12}$$
$$=\phi^2 m_k|r|(\sin(\phi)-\cos(\phi)\tan(\phi))+\sum_{i=1}^{j}F_i\cdot J-\left(\sum_{i=1}^{j}F_i\cdot i\right)\tan(\theta)-m_k g$$

and substituting Eq 16:11 into Eq 16:3

$$\ddot{\phi}\left[I_o-m_k|r|J\frac{\sin(\phi)}{\cos(\theta)}\right]+\ddot{\theta}\left[-m_k SJ\tan(\theta)\right]=\dot{\phi}^2 m_k|r|J\frac{\cos(\phi)}{\cos(\theta)}+\dot{\theta}^2 m_k SJ+\sum_{i=1}^{j}F_i\times r_i+J\frac{\sum_{i=1}^{j}F_i\cdot i}{\cos(\theta)} \qquad \textbf{Eq 16:13}$$

The angular accelerations, $\ddot{\theta}$ and $\ddot{\phi}$, can be determined by solving Eq 16:12 and Eq 16:13 simultaneously. This can be done with matrices by using

$$\begin{bmatrix}P_{11} & P_{12}\\ P_{21} & P_{22}\end{bmatrix}\begin{bmatrix}\ddot{\phi}\\ \ddot{\theta}\end{bmatrix}=\begin{bmatrix}f(\dot{\theta},\dot{\phi},\theta,\phi,F_i,r,m_k g)\\ f(\dot{\theta},\dot{\phi},\theta,\phi,F_i,r)\end{bmatrix} \qquad \textbf{Eq 16:14}$$

where the P values correspond with the angular accelerations in Eq 16:12 and Eq 16:13. To solve Eq 16:14 the values on the right hand side of the equation need to be determined. The steps to do this are outlined in sections 16.2.2 and 16.2.3

16.2.2 Kite inputs

The kite parameters need to be defined in the programme. These are

- The size of the wing and its aerodynamic properties
- The bridle point location.
- The mass of the wing and the location of the centre of mass.
- Dimensions of the bridle lines.
- Line length and dimensions.
- The rotational inertia of the wing (I_o).
- The added mass of the wing.

16.2.3 Determining the forces on the wing

Within the model the angles θ and ϕ are known at each time step, along with the corresponding angular velocities. Once these are defined the following steps are required to determine the aerodynamic forces acting on the wing.

1. The velocity vector of the wing (V_k) needs to be determined. This can be found by using Eq 16:7 and Eq 16:8
2. The apparent velocity vector of the wing needs to be found by applying

$$V_a = V - V_k \qquad \textbf{Eq 16:15}$$

3. The angle of attack relative to V (α_v) is directly related to ϕ. Once this is found the angle of attack of the wing in relation to the apparent wind (α) can be calculated. To find this angle it is necessary to calculate the angle between V and V_a (λ) by

$$\lambda = \cos^{-1}\left(\frac{V \cdot V_a}{|V||V_a|}\right) \qquad \textbf{Eq 16:16}$$

and therefore

$$\alpha = \alpha_v - \lambda \qquad \textbf{Eq 16:17}$$

When the kite is moving backwards the programme must make λ negative.

4. Based on α, the aerodynamic properties of the wing can be found. More detail of this process is outlined in Chapter 8.

16.2.4 Programme format

Once the kite wing properties and forces determined, the P matrix and the RHS of Eq 16:14 can be calculated. This equation can then be used to find the angular accelerations. To determine the movement of the kite these equations need to be solved for a set time period. This can be done by using a time-step model, where the acceleration in each time step is assumed to be constant. Alternatively, ODE solvers, conveniently defined in MATLAB, can be used. These ODE functions are relatively easy to use and solve the problem quickly.

Table 2 shows an example programme using an ODE solver from MATLAB. A separate file (kite) is called from this programme which calculates the kite properties and forces and solves Eq 16:14. This programme then returns the angular acceleration values.

Table 2 Example ODE solver to solve kite take-off programme

```
function [T,Y,lift] = fd
clc
clear all;
% global XOut TOut
format compact

options = odeset('MaxStep',1e-0);%,'OutputFcn',@myfun);%'RelTol',1e-4,'AbsTol',[1e-4 1e-4 1e-4], % parameters for ODE solver

tspan = 0:0.01:7; % time interval over which the problem is solved
xo=[30*pi/180 0 30*pi/180 0]; initial state vector [ theta, theta_dt. phi. Phi_dt]

[T,Y] = ode45(@funcrigid,tspan,xo,options);  %ODE Solver
plot(T,Y(:,1)*180/pi,'b-') %plotting theta
hold on
plot(T,Y(:,3)*180/pi,'r-') %plotting phi


        function [dy,lift] = funcrigid(t,y)  % function call ed by ODE solver
        dy = zeros(4,1);    % a column vector

        theta = y(1);
        dtheta_dt = damp*y(2);
        phi=y(3);
        dphi_dt=damp*y(4);
```

```
[d2theta_dt2,d2phi_dt2,lift]=kite(theta,dtheta_dt,phi,dphi_dt,t); %calling a file which determines kite properties and forces at state vector

% defiing the differential of the state vector
dy(1) = dtheta_dt;
dy(2) = d2theta_dt2;
dy(3)=dphi_dt;
dy(4)=d2phi_dt2;
```

The key step in this programme is that the ODE solver is given an initial state vector containing the angular positions and velocities of the kite. The ODE solver then calls a function (funcrigid) that differentiates this vector to get the angular velocities and accelerations. The angular velocities were already defined in the initial state vector, while the angular accelerations are calculated using Eq 16:14 in the program called 'kite'. The program then returns this vector back to the ODE solver, which determines the new state vector at the next time-step.

16.3 Difficulties with model

Attempting to model the motion of a real kite using this programme was unsuccessful. A number of reasons were identified for this

1. The aerodynamic properties of a stable wing are different to a wing rapidly changing angle of attack. At this point no information is available on how these properties are affected.
2. Due to their low mass, kites are significantly affected by added mass. Added mass is an extra effect included if a body is accelerating in a fluid. As an object accelerates it must also accelerate the streamlines around it, requiring extra energy. When the weight of the disturbed fluid in relation to the weight of the object is significant, this extra energy must be taken into account in the programme model. Determining the added mass of objects is difficult. In this case the added mass will be required at a number of angles of attack. Since kites fly

near the stall point, the size of the wake will change significantly with angle of attack and have a large effect on the added mass component.

3. No data was available about how the aerodynamic properties of the wing are affected as it accelerates. Due to the streamlines not being stable as the kite accelerates, the properties of the kite will be affected.

With the inputs used in the model, it was difficult to stop the kite from over-flying to a negative angle of attack. This did not happen with a real kite. The model was only stable if the kite was initially located near to its stability point. it seems likely that the model does not adequately predict the motion of the kite because the input properties have not been adequately determined.

16.4 Sample Results

Figure 16:2 shows an example of the rare occasions when the programme model did not become unstable, and the results roughly approximated a real kite's behaviour. In this experiment, the kite used to determine stability points (Chapter 9), was held by its bridle points near the base of the tunnel. The kite was then released and allowed to take off to its stable flying location. The kite was held by its bridle points so that it started out flying at its stable angle of attack. This reduced the change in angle of attack of the wing as it took off.

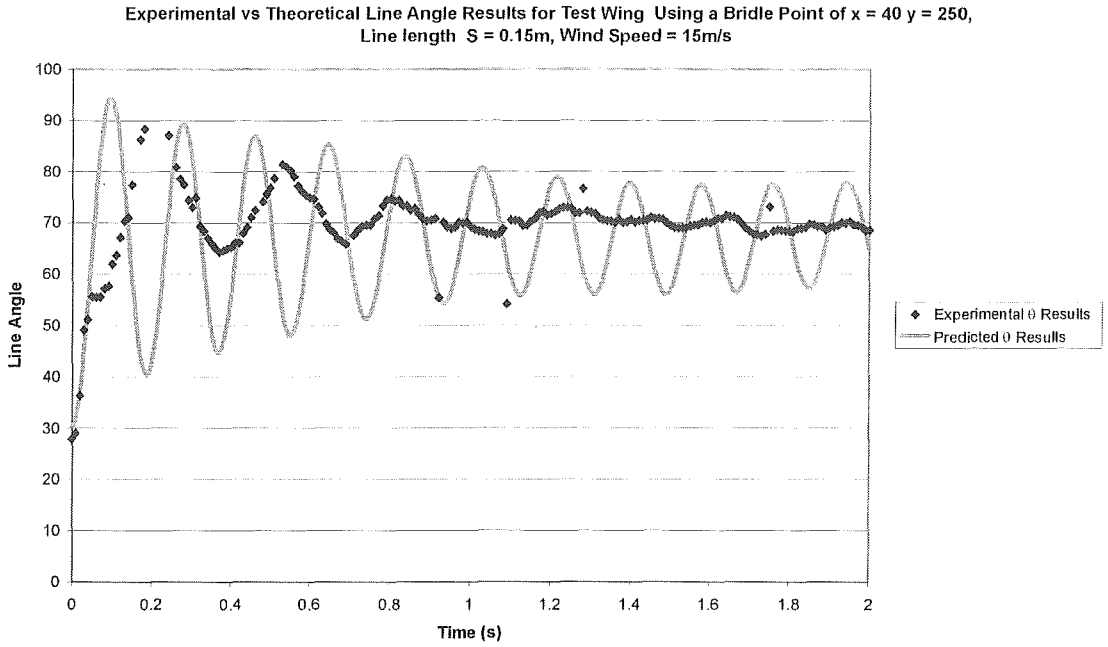

Figure 16:2 Experimental vs theoretical take-off results for wing in the wind tunnel. Bridle point X=40, Y=250, S=0.15m, V=15m/s

It can be seen that the theoretical model takes off more quickly, but does not settle down as fast, as the actual kite. This indicates a few things. First, the fast frequency of the programme model indicates that the real kite has to accelerate more mass. This is either the result of the kites extra added mass or because the aerodynamic forces on an accelerating kite are less than a stationary kite. Secondly, there is less damping in the programme model than for a real kite. In some manner, energy is lost from the real kite system so that it settles faster than the programme model.

16.5 Discussion

From the experience gained with modelling the motion of kites it is apparent that carefully determining the kite properties is very important. It was originally felt that the aerodynamic properties of a wing at a large range of angles of attack would be sufficient for the programme model. This was not the case. It was found that there were unexpected

effects on the properties of the wing as it accelerated in the flow. To succeed in kite modelling, these effects need to be taken into account.

16.6 Conclusion

Attempts at modelling kite movements during this project were unsuccessful due to a lack of information of the aerodynamic properties of an accelerating wing. Static properties were found to be inadequate to account for the behaviour of a moving kite. However, once these properties are known the implementation of the mathematical model presented in this chapter should be successful.